ANALYSIS OF THE ROLE OF GLUTATHIONE AND STRESS RESISTANCE IN *Staphylococcus aureus*

A THESIS SUBMITTED FOR THE DEGREE OF

DOCTOR OF PHILOSOPHY

BY

ROSLINAH MOHAMAD HUSSAIN

(UNIVERSITY TECHNOLOGY MARA, SHAH ALAM, MALAYSIA)

JANUARY 2008

DEPARTMENT OF MOLECULAR BIOLOGY AND BIOTECHNOLOGY,

UNIVERSITY OF SHEFFIELD

FIRTH COURT, WESTERN BANK, SHEFFIELD S10 2TN.

Abstract

Staphylococcus aureus is a major pathogen causing both community and hospital-acquired infections. The diversity of diseases caused by this organism can be attributed to its ability to colonize a range of niches and to adapt to the stressful environments of the host. As part of this, successful utilization of host nutrients is crucial for pathogenesis.

Sulfur is an essential element required for many cellular components. *S.aureus* can use glutathione as sole sulfur source and as it cannot synthesize this molecule, it must acquire it from the host. Glutathione utilization is facilitated by gammaglutamyltranspeptidase (GGT) in many organisms. To analyse the role of GGT in *S.aureus*, the putative *ggt* gene was identified and insertionally inactivated. The *ggt* mutant was still able to grow on glutathione, which suggests a novel alternative pathway for catabolism. The role of a putative glutathione transporter was also investigated. Mutant strains, although still able to grow on glutathione showed a stress defect, in particular to tellurite. *S.aureus* is well known as having high level tellurite resistance. Resistance occurs via reduction leading to cytoplasmic deposits of tellurium. Purification of tellurite reductase activities resulted in the identification of alkylhydroperoxidase subunit F (AhpF) and thioredoxin reductase (TrxB). The relative roles of these two enzymes in tellurite reduction was examined.

Acknowledgements

To my supervisor, Prof Simon Foster for your guidance, dedication and patience and for giving me the confidence to complete this work, thank you.

My gratitude to University Technology MARA (UiTM) for my scholarship and study leave.

To all the members of F18, past and present, those who I have shared this journey with and helped me overcome many hurdles, thank you. I would also like to thank Dr. Arthur Moir and Chris J. Hill for their help in this study.

To my family, especially Hajira Bee Abdul Rahman, Zaleha Bee Abdul Rahman and Farah Khalid, for your love, encouragement and believing in me, thank you.

I dedicate this work to my children, Mohd Aliff Mohd Razif and Dahlia Mohd Razif. For all your sacrifices, for bearing with me through the most troubled times and for just being here with me, thank you and I hope that someday you will understand.

Abbreviations

A	Absorbance
ABC	ATP-binding cassette
Ahp	Alkyl hydroperoxide reductase
AhpCF	Alkylhydroperoxide reductase subunits C and F
AIP	Auto-inducing peptide
Amp	Ampicillin
AP	Alkaline phosphatase
APS	Ammonium persulphate
Asp	Asparagine
ATP	Adenosine triphosphate
BAC	Bacterial artificial chromosome
BCIP	5-bromo-4-chloro-3-indolyl phosphate
β-gal	β-galactosidase
BHI	Brain heart infusion
bp	Base pair
BSA	Bovine serum albumin
C	Cytosine
Cad	Cadmium
CAPS	3 – (cyclohexylamino) – 1 – propanesulphonic acid
CDM	Chemically defined media
Cfe	Cell free extract
cfu	Colony forming units
CGD	Chronic granulomatous disease
CIAP	Calf Intestinal Alkaline Phosphatase
cm	Centimetres
Cm	Chloramphenicol
CoADR	Coenzyme A disulphide reductase
°C	Degrees Celsius
dH_2O	Distilled water
DIG	Digoxigenin
DMF	N,N-dimethylformamide
DMSO	Dimethyl sulphoxide
DNA	Deoxyribonucleic acid
Dnase	Deoxyribonuclease
dNTPs	Deoxyribonucleoside-5'-triphosphate
ECM	Extracellular matrix
EDTA	Ethylenediamine tetra-acetic acid
Ery	Erythromycin
Fc	Fragment crystallisable domain of immunoglobulin molecules
Fg	Fibrinogen
Fn	Fibronectin
g	Grams
x g	x Gravity
G	Guanine
GGT	Gammaglutamyltransferase
Gln	Glutamine
Glu	Glutamic acid
Gpx	Glutathione peroxidase

GSH	Glutathione
GSSG	Oxidised form of glutathione
GS-Se-SG	Selenoglutathione
hr	Hours
H_2O_2	Hydrogen peroxide
His	Histidine
HIV	Human Immunodeficiency Virus
HOCl	Hypochlorous acid
HRP	Horseradish peroxidase
IgG	Immunoglobulin G
Inc	Incompatibility
IPTG	Isopropyl-β-D-thiogalactopyranoside
K_2TeO_3	Potassium tellurite
Kat	Catalase
Kan	Kanamycin
kb	Kilobase pairs
kDa	Kilodaltons
kV	Kilovolts
l	Litre
LB	Luria-Bertani medium
Lin	Lincomycin
Lys	Lysine
M	Molar
mA	Milliamps
Mb	Megabase
mbar	Millibars
Met	Methionine
mg	Milligrams
MHC	Major histocompatibility comples
min	Minutes
MIC	Minimum inhibitory concentration
mJ	Milli Joules
ml	Millilitres
mm	millimetres
mM	Millimolar
mol	moles
mRNA	Messenger RNA
MRSA	Methicillin-resistant *Staphylococcus aureus*
MSCRAMM	Microbial surface components recognising adhesive matrix molecules
MSSA	Methicillin-sensitive *Staphylococcus aureus*
MU	4-Methyl umbelliferone
MUG	4-Methyl umbelliferyl-β-D-galactopyranoside
n	Nano
NADH	reduced form of nicotinamide adenine dinucleotide hydrogenase
NADPH	reduced form of nicotinamide adenine dinucleotide phosphate
NBT	Nitroblue tetrazolium
NCBI	National Centre for Biotechnology Information
NMR	Nuclear magnetic resonance
NO	Nitric oxide

$NO_2\cdot$	Nitric oxide radical
NO_2^-	Nitrite
NO_3^-	Nitrate
Nramp	Natural resistance associated macrophage protein
O_2^-	Superoxide
OD_X	Optical density at Xnm
$OH\cdot$	Hydroxyl radical
$OONO^-$	Peroxynitrite
ORF	Open reading frame
PAGE	Polyacrylamide gel electrophoresis
PBS	Phosphate buffered saline
PCR	Polymerase chain reaction
PerR	Peroxide response regulator
p	pico
pfu	Plaque forming units
PMSF	Phenylmethylsulfonyl fluoride
PVDF	Polyvinylidene diflouride
PVL	Panton-Valentine Leukocidin
Pwo woesei	Thermostable DNA polymerase derived from *Pyrococcus*
RAP	RNAIII activating protein
RNA	Ribonucleic acid
Rnase	Ribonuclease
RNS	Reactive nitrogen species
$RO\cdot$	Alkoxyl radical
ROS	Reactive oxygen species
rpm	Revolutions per min
RSH	Free sulfhydryl group
r-TrxB	Recombinant thioredoxin reductase
RT	Room temperature
SAG	Superantigen
SDS	Sodium dodecyl sulphate
sec	Seconds
SNP	Sodium nitroprusside
SOD	Superoxide dismutase
Sup	Supernatant
SPB	Sodium phosphate buffer
spec	Spectrophotometric
SSC	Saline sodium citrate buffer
SSF	Staphylococcal scarlet fever
SSSS	Staphylococcal scalded skin syndrome
t	Time
TAE	Tris-acetate EDTA (buffer)
Taq	Thermostable DNA polymerase derived from *Thermus aquaticus*
T-cell	Subset of lymphocytes; developed in the thymus
TCA	Tricarboxylic acid
TCS	Two-component system
TE	Tris-EDTA (buffer)
Te^R	Tellurite resistance determinant
TEMED	N,N,N'N'-tetramethyl-ethylenediamine

Tet	Tetracycline
Tf	Transferrin
TIGR	The Institute of Genomic Research
Tn	Transposon
Tris	Tris(hydroxymethyl)aminomethane
Trx	Thioredoxin
TrxB	Thioredoxin reductase
TSB	Tryptic soya broth
TSS	Toxic shock syndrome
TSST-1	Toxic shock syndrome toxin-1
Tyr	Tyrosine
UCFE	Undialysed cell free extract
μF	Microfarad
μg	Micrograms
μl	Microlitres
U/L	Units per liter
μM	Micromolar
UV	Ultra violet
VRSA	Vancomycin-resistant *Staphylococcus aureus*
v/v	Volume for volume
w/v	Weight for volume
x	Times
X-Gal	5-bromo-4-chloro-3-indolyl-β-D-galactoside
σ	Sigma factor
~	Approximately
ϕ	Phage

Table of contents

Chapter Three   **Analysis of the role of glutathione**
                                 in *Staphylococcus aureus*

List of figures

List of tables

CHAPTER ONE

INTRODUCTION

1.1   The staphylococci

The staphylococci are gram-positive cocci measuring approx 1 μm in diameter

and because they divide perpendicular to the preceeding plane

of division they characteristically grow in grape-like clusters. Members of

the genus *Staphylococcus* are ubiquitous in the environment , are facultative

anaerobes which are non-motile, non-spore forming and typically oxidase-

negative and catalase-positive.

The genus *Staphylococcus* has a low G + C content (Baba *et al.*, 2008) and is

separated from the genus *Micrococcus* based on Hsp60 (heat shock protein) and

16s RNA sequence analysis (Kwok and Chow, 2003; Kwok *et al.*, 1999; Goh *et*

al., 1996). There are 36 species and nine subspecies designated and the

staphylococci are separated into two main groups based on the presence of

coagulase, a plasma clotting enzyme. The human pathogens in this genus are

S.aureus which is coagulase-positive while *S.epidermidis, S.saprophyticus* and

others are coagulase-negative (Kloos and Schleifer, 1975; Kloos and Wolfshohl,

1982).

1.2   *Staphylococcus aureus*

S.aureus characteristically produces pigmented golden yellow colonies thus its

given name which originates from the Latin word *"aureus"* meaning golden. The

pigment staphyloxanthin that is derived from caroteinoids is responsible for its

coloration and has been implicated as a virulent factor (Liu *et al.*, 2005). *S.aureus*

was first isolated in pus from surgical abscesses by the surgeon Sir Alexander Ogston in 1880 and is differentiated from other staphylococci on the basis of positive results of coagulase, mannitol fermentation and deoxyribonuclase test (Forsgren, 1970).

1.2.1 Diseases and pathogenesis of *S.aureus*

S.aureus is a successful human pathogen that is a cause of both community and hospital-acquired infections. Its ability to survive within the host as well as the emergence of multi-drug resistant strains makes it an increasing problem thus qualifying it as one of the major medical pathogens. *S.aureus* is an opportunist pathogen which can be found commonly in the anterior nares, on the skin, and mucus membranes of 11-32% of the population (Tolan, 2007). These healthy carriers may potentially be the source of spread of infection especially in hospital environments. There is no significant difference in nasal carriage of *S.aureus* between medical and non-medical personnel in the hospital environment. However, medical personnel have a higher hand carriage and are more colonized with antibiotic resistant strains (Cespedes, 2002). Patients with diabetes mellitus are more likely to carry *S.aureus* as part of the conjunctival flora and it is one of the organisms that are more often recovered from postoperative endophthalmitis compared to nondiabetic patients (Bilen *et al.*, 2007).

S.aureus can cause disease either by invasion of tissues or by toxin production. Characteristically *S.aureus* causes abscesses, which are suppurative with walled-off lesions encased by fibrin. The organisms exist in the central core of

this focus of infection and may spread hematogenously causing bacteremia and become disseminated to other areas of the body (Fig 1.2).

Diseases produced by virulent strains of *S.aureus* can range from mild superficial skin infections of the hair follicles and glands such as bullous impetigo, folliculitis, to more severe cutaneous infections such as furuncles and carbuncles (Lowy, 1998). Scalded skin syndrome or Ritters disease is a rare disease in infants caused by the exfoliative toxins that causes epidermal splitting resulting in peeling of the skin. *S.aureus* is also the causative agent of staphylococcal scarlet fever (Jarraud *et al.*, 2001), bone and joint infections (osteomyelitis) (Bocchini *et al.*, 2006) and acute septic arthritis (Fihman *et al.*, 2007).

The more serious and life-threatening *S.aureus* infections include sepsis (Piechowicz *et al.*, 2007), endocarditis (Myolnakis and Calderwood, 2001; Fowler *et al.*, 2006), toxic shock syndrome (Mehrotra *et al.*, 2000) and meningitis (Benca *et al.*, 2007). A study of community acquired severe *S.aureus* sepsis (SAS) amongst children in New Zealand showed increased prevalence of methicillin resistant *S.aureus* (MRSA) (Miles *et al.*, 2007). Endocarditis is normally associated with long-term indwelling prosthesis such as cathethers in patients with preexisting heart disease. It is a complication of staphylococcal bacteremia that involves infection of the heart valves and can include both damaged and undamaged cardiac valves. *S.aureus* adheres to cardiac endothelial cells possibly by MSCRAMM-mediated mechanisms or adhesin-receptor interactions. The MSCRAMMS (microbial surface components recognizing adhesive matrix

3

molecule<u>s</u>) are a class of surface proteins that promote attachment of bacteria to all types of extracellular matrices (Projan and Novick, 1997, Foster and Hook, 1998). Once attached, S.aureus is phagocytized by these endothelial cells causing cellular alterations that promote fibrin deposition and formation of vegetations (Lowy, 1998). This contributes to the establishment of metastatic foci of infection and the pathogenesis of endocarditis.

Staphylococcal toxic shock syndrome (TSS) is generally associated with the use of superabsorbent tampons during menstruation and is caused by the production of the exotoxin TSST-1 (toxic shock syndrome toxin 1). TSST belongs to the family of pyrogenic toxin superantigens (Schlievert, 1993) that bind directly to MHC II receptors on antigen presenting cells and the variable portion of T-cell receptor β-chain (Marrack and Kappler, 1990) causing activation and clonal expansion with subsequent release of cytokines that result in symptoms mimicking endotoxic shock (Lowy, 1998). Based on serological classification, staphylococcal enterotoxin groups are recognized as SEA through SEE and SEG through SEJ (Balaban and Rasooly, 2000; Mehrotra et al., 2000). Enterotoxins are small proteins which are potent gastrointestinal toxins causing food poisoning and diarrhea with rapid onset (2-6 hours) after ingestion. The acute symptoms, which include vomiting and watery diarrhea are however self-limiting. SEA (entA) is the common toxin causing staphylococcal food poisoning (Balaban et al., 2000) and is associated with septic shock in patients with S.aureus bloodstream infection (Tristan et al., 2007). Enterotoxins are also superantigens.

Non-menstrual TSS can also be caused by other superantigens such as the staphylococcal enterotoxin serotype B (SEB) or staphylococcal enterotoxin serotype C (SEC). *S.aureus* strains possessing both genes for enterotoxins and toxic shock syndrome toxin are associated with phagetype 187 (Piechowicz *et al.*, 2007). *S.aureus* also causes staphylococcal scarlet fever (SSF) which is associated with production of TSST-1, SEB and SEC (Jarraud *et al.*, 2001) and is an emerging pathogen in causing postsurgical or nosocomial meningitis as well as community acquired meningitis (Lesnahova *et al*, 2007).

Other infections caused by *S.aureus* include necrotizing pneumonia commonly seen in infants, children and debilitated patients, thrombophlebitis that is associated with infected catheter insertion sites (Lowy, 1998) and purpura fulminans (Kravitz *et al.*, 2005).

1.2.2 Antibiotic resistance and treatment of diseases caused by *S.aureus*

Infections caused by gram-positive cocci were traditionally treated with penicillin G but since the emergence and prevalence of resistant strains, the penicillinase-resistant penicillins (eg. oxacillin, nafcillin) or cephalosporins (eg cephalexin, cefuroxime) are commonly the drugs of choice. Penicillin is inactivated by a beta-lactamase which hydrolyses the beta-lactam ring (Lowy, 1998). Over the recent years *S.aureus* has alarmingly evolved multi-drug resistance to the penicillins including the β-lactamase-resistant penicillins, as well as the cephalosporins and carbapenems. The challenge of treatment of infections caused by this organism is heightened with the increased incidence of methicillin-resistant *S.aureus* (MRSA) in both hospital (HA-MRSA) and

community-acquired infections (CA-MRSA) (Johnson and Saravolatz, 2005).

Resistance to methicillin renders resistance to all penicillinase-resistant

penicillins and cephalosporins.The drugs of choice for treating MRSA or other

potentially life-threatening infections or intoxication are intravenous or oral (CA-

MRSA) trimethoprim-sulfamethoxazole (TMP-SMX). In addition, daptomycin,

linezolid and quinopristin-dalfopristin may be used for CA-MRSA (Johnson and

Saravolatz, 2005). For many multiple resistant strains vancomycin has been the

drug of last resort. No vancomycin-resistant strains were evident in the first 20

years of the use of the drug. Naturally the isolation of MRSA strains with

intermediate-resistance to vancomycin (VISA) in 1996 and vancomycin-resistant

S.aureus (VRSA) in 2002 (Sievert et al., 2002) generated a great deal of

attention and concern. Limited treatment alternatives are available for treating

vancomycin-resistant MRSA infections and these include, rifampin, gentamicin,

imipenem, chloramphenicol, TMP-SMX and tetracycline (Cinel and Dellinger,

2007). Superficial localized skin infections such as impetigo are generally treated

with muciprocin. To prevent spread of this organism, strict isolation procedures

and stringent control measures must be observed.

1.3   Virulence factors of S.aureus

Attributes of S.aureus that contribute to its pathogenecity include

production of virulence factors such as host-binding adhesins, pyrogenic toxins,

enterotoxins and enzymes such as hemolysins, catalase, superoxide dismutase

and peroxidase that circumvent the host phagocytic mechanism and enable it to

flourish. Virulence factors are produced during the growth cycle only when

6

needed and their production is coordinately controlled in response to cell density,

energy availability, environmental signals and superantigens (Fig. 1.1, Novick,

2003).

Virulence determinant	Gene	Growth phase of expression
Clumping factor A & B	*clfA & clfB*	Early-exponential
Fibrinogen-binding protein	*fbpA*	Early-exponential
Fibronectin-binding protein A	*fnbA*	Early-exponential
Fibronectin-binding protein B	*fnbB*	Early-exponential
Collagen-binding protein	*cna*	Post-exponential
Catalase	*katA*	
Coagulase	*cga / coa*	Log phase
Polysaccharide/adhesin (PS/A)	-	-
Polysaccharide intracellular adhesin	-	-
Enterotoxin A	*sea*	Constitutive
Enterotoxins B, C1-3, D, E, H	*seb-h*	Post-exponential
Toxic shock syndrome toxin-1 (TSST-1)	*tst*	Post-exponential
Staphylococcal exotoxin-like proteins	*set* 1-5	-
Exfoliative toxins A, B	*eta, etb*	Post-exponential
Protein A	*spa*	Early-exponential
Lipase	*lip*	Post-exponential
V8 protease (serine protease)	*sspA*	Post-exponential
Fatty acid modifying enzyme (FAME)	*fme*	Post-exponential
Panton-Valentine leukocidin	*lukPV, lukS-PV*	Post-exponential
Capsular polysaccharide types 1	*cap1 locus*	Post-exponential
Capsular polysaccharide type 5	*cap5 locus*	Post-exponential
Capsular polysaccharide type 8	*cap8 locus*	Post-exponential
Staphylokinase	*sak*	Post-exponential
Glycerol ester hydrolase	*geh*	Post-exponential
α-haemolysin (α-toxin)	*hla*	Post-exponential
β-haemolysin (β-toxin)	*hlb*	Post-exponential
δ-haemolysin (δ-toxin)	*hld*	Log-phase
γ–haemolysin (γ-toxin)	*hlgA, B, C*	Post-exponential
Metalloprotease (aureolysin)	*aurA*	Post-exponential
Cysteine protease	*sspB*	Post-exponential
Phospholipase C	*plc*	Post-exponential
Hyaluronidase (hyaluronate lyase)	*hysA*	Log-phase

Table 1.1

Virulence factors of *S.aureus*. Adapted from Novick 2003.

Known virulence factors of *S.aureus* are listed in Table 1.1 and can generally be categorized into three groups, that is those that have roles in 1) attachment of *S. aureus* to the host; 2) evasion of the host immune system; and 3) invasion and tissue penetration of the host cell (Projan and Novick, 1997). The cause and development of pathogenesis of *S.aureus* is not solely attributed to a single virulence determinant but is rather multifactorial whereby the interplay of the virulent factors as well as the host response generally determines the severity and outcome of the disease.

1.3.1   Cell surface adhesins - Attachment

Before *S.aureus* is able to colonize and initiate an infection it must first successfully attach to the host cell surface. Several surface proteins, collectively called adhesins or MSCRAMMs, aid in this attachment process. Several of these adhesive proteins are as shown in Table 1.1. They all share structural similarities in having the common LPXTG motif in their amino acids sequence, in the C-terminal region between the cell-wall spanning domain and just before the membrane spanning domain. This conserved LPXTG motif is anchored at a conserved pentaglycine residue in the peptidoglycan (Foster and Hook, 1998, Schneewind *et al.*, 1995). Protein A (SpA) is an MSCRAMM and a constituent of the cell wall as well as an extracellular product (Forsgren, 1970). It is present in approximately 95% of all pathogenic strains of *S.aureus*. (Greenberg *et al.*, 1990).

Other virulence factors that are involved in attachment include the collagen binding protein (Cna) and the enzyme coagulase (Cga/Coa). Cna binds with collagenous tissues and may play a role in mediating attachment to cartilage (Patti *et al.*, 1994). The role of coagulase in virulence is unclear although its ability to bind fibrinogen and cause the formation of a fibrin clot in host plasma may facilitate in the evasion of the immune system by *S.aureus* (Foster, 2005). *S.aureus* strains possessing the most prevalent coagulase genotypes (A1 and A4) were found to be refractory to phagocytosis and/or killing by bovine neutrophils (Aarestrup *et al.*, 1994). The fibronectin-binding proteins (FNBPs) FnBPA and FnBPB bind immobilized fibronectin *in vitro* and mediate adherence of *S. aureus* to plasma clots and are factors that contribute to the initiation infections associated with foreign implants (Foster and Hook, 1998). FNBPs also mediates bacterial invasion through formation of a fibronectin bridge to integrin (fibronectin-binding protein) that is present on the host cell surface (Palmqvist *et al.*, 2005). The *clfA* and clfB genes also encode for fibrinogen binding protein called the clumping factors (McDevitt *et al.*, 1994, Ni Edhin *et al.*, 1998). ClfA and the related ClfB facilitate fibrinogen-mediated adhesion and promote clumping of *S. aureus* cells (Palmqvist *et al.*, 2005) and adherence to plastic biomaterials (Foster and Hook, 1998). IsdA is produced by *S. aureus* under iron-limiting conditions and was shown to bind fibronectin, fibrinogen , promote cell clumping and be involved in evasion of host innate defences (Clarke *et al.*, 2004, 2007). It was also shown to be involved in nasal cell binding and colonization by *S.aureus* (Clarke 2004, 2006). In addition, the *S.aureus* surface protein G (SasG) is an

adhesin that is also involved in colonization of the anterior nares. Expression of SasG was shown to mask the binding of *S.aureus* MSCRAMMs to their ligands and promote biofilm formation (Corrigan *et al.*, 2007).

1.3.2 Toxins and invasins - How *S.aureus* overcomes the immune system

Once attachment has ensued, *S.aureus* has to overcome the host immune system before it can establish itself. *S.aureus* produces many cell wall-associated proteins and several extracellular proteins including hemolysins, toxins, and proteases that enable it evade and overcome the host immune system (Uziel *et al.*, 2004). Phagocytosis is the major mode of elimination of *S.aureus* in the host and this organism possesses several antiphagocytic mechanisms to resist phagolysosome killing. The ability of *S.aureus* to survive within polymorphonuclear neutrophils (PMN) is a virulence mechanism regulated by the global regulator, *sar*, that aids in the pathogenesis the organism (Gresham *et al.*, 2000).

The *dlt* operon which encodes DltA, DltB, DltC and DltD confers resistance to antimicrobial peptides (defensins) that are stored in PMN granules. The Dlt proteins catalyze the introduction of D-alanine into teichoic acids (staphylococcal cell wall polymers) (Collins *et al.*, 2002) and the dlt- strain was more efficiently killed by neutrophils compared to the wildtype strain. Protein A (*spa*), a protein found on the surface of *S.aureus* allows nonspecific attachment to the Fc portion of IgG (Dossett *et al.*, 1969) thereby preventing opsonization and phagocytosis (Dossett *et al.*, 1969, Peterson *et al.*, 1977).

11

S.aureus also produces pore forming toxins (PFT) consisting of 2 families, the single-component α-hemolysin and the bicomponent leukocidins and γ-hemolysins. These toxins act to damage target cells by forming oligomeric pores in their plasma membrane, thus killing leukocytes and weakening the hosts immune defense (Menestrina et al., 2003). The α-hemolysin (hla) is secreted as a monomer and associates to form a heptamer on the membrane of target cells. The α-toxin is a major virulence factor during S.aureus keratitis causing corneal epithelial erosions and iritis (O'Callaghan et al., 1997). The γ-hemolysins comprise of three proteins HlgA, HlgB and HlgC that combine to generate two toxins HlgA + HlgB and HlgC + HlgB (Menestrina et al., 2003). Panton-Valentine leukocidin (PVL) is directly lethal to polymorphonuclear neutrophils (PMN) and is found in approximately 50% of S.aureus isolated from abscesses. Leukocidins are the products of genes designated lukS-PV, lukF-PV, hlgA, hlgB and hlgC which form different combinations with the γ-hemolysin to generate different toxins. The LukF-PV/LukS-PV combination is most leukocytolytic, the LukF/LukS and LukF/HlgA combinations are dermonecrotic while the two γ-hemolysin combinations and the LukF/HlgA combinations are hemolytic (Projan and Novick, 1997). Labadeira-Rey et al. (2007) found that PVL-positive S.aureus strains were more virulent than PVL-negative strains and cause necrotizing pneumonia in a mouse model with manifestations similar to that seen in human disease. In addition, the PVL-positive S.aureus strains showed an altered transcription profile with repression of agr transcripts (agr A-C) and the exoproteins, hla (alpha toxin), hlg (gamma toxin), ssp (serine protease), spl (splA-F protease). Genes

encoding for cell wall-anchored proteins (*sdrC, sdrD* and *clfB*) and *sarS* as well as *spA* (Protein A) was upregulated (Labadeira-Rey *et al.*, 2007). The development of multiple furuncle with intense erythema in healthy young adults is associated with PVL positive strains (Yamasaki *et al.*, 2005). In addition, PVL positive strains from osteomyelitis in children presented a more severe local disease with higher systemic inflammatory response (Bocchini *et al.*, 2006).

A majority of the clinical strains of *S.aureus* produce capsular polysaccharides which possibly have a role in virulence by preventing attachment of the organism to antibodies. There are eleven capsular polysaccharide types in *S.aureus* of which types 5 and 8 have been shown to cause the majority of human infections (*Roghmann et al.*, 2005). Capsular polysaccharide type 5 predominates among methicillin-resistant *S.aureus* (MRSA) strains whereas MSSA isolates possessed mostly type 8 (Verdier *et al.*, 2007). Type 5 was shown to be more virulent and possesses a higher resistance to *in vitro* opsonophagocytic killing by neutrophils than type 8 (Watts *et al.*, 2005). *S.aureus* produces several extracellular proteolytic enzymes or proteinases that degrade human protease inhibitors and modulate the activity of other proteins that are secreted by the pathogen (Shaw *et al.*, 2004). SspA (*sspA*) is a serine protease (serine glutamyl endopeptidase; V8 protease) that cleaves fibrinogen-binding protein and surface protein A (Spa) (Karlsson *et al.*, 2001). It also cleaves the heavy chains of all classes of human immunoglobulins (Prokesova *et al.*, 1992). Mutations in both the *sspA* and *sspB* (SspB, cysteine protease) showed attenuation in a mouse abscess model of infection (Shaw *et al.*, 2004). It

was shown that *sspB* but not *sspA* is important in infection by *S.aureus* (Rice *et al.*, 2001) and that the maturation of SspB requires SspA. SspA is secreted in an inactive precursor form and is processed by the metalloprotease aureolysin (Aur) to the mature serine protease form. Aur cleaves the surface-associated clumping factor ClfB (McAleese *et al.*, 2001) and modulates immunogenic reactions by stimulating T and B lymphocytes and inhibiting immunoglobulin production (Prokesova *et al*, 1992). Staphopain (ScpA) is a cysteine proteinase that also possesses elastinolytic activity and may possibly be involved in tissue invasion and destruction that is associated with staphylococcal ulceration (Shaw *et al.*, 2004). Proteases may also protect against neutrophil defensins or platelet microbiocidal proteins (PMPs) which are antimicrobial peptides (Projan and Novick, 1997). In addition, proteases may have housekeeping roles in scavenging of usable nutrients from their environment (Lowy, 1998). Staphylococci produce superantigens such as enterotoxins A to E, TSST-1 and the exfoliative toxins A and B that bind directly and activate a subpopulation of T-cells resulting in the release of cytokines/lymphokines and ultimately resulting in T-cell death. Enterotoxin causes staphylococcal food poisoning by binding to specific receptors in the gut. It has also been suggested that the staphylococcal superantigens may act in synergy with peptidoglycan and lipoteichoic acids to produce septic shock through release of cytokines from T-cells (Projan and Novick, 1997). Peptidoglycan (PG), lipoteichoic acid (LTA) and TSST-1 from *S.aureus* are found to induce the TF (tissue factor) in human umbilical vein endothelial cells in the presence of monocytes. This results in a proinflammatory

endothelial cells in the presence of monocytes. This results in a proinflammatory and procoagulant state and increased vascular leakage (Mattson *et al.*, 2007) which causes TF dependent fibrin formation in intravascular *S.aureus* infection.

Three exfoliative toxins ETA (*eta*), ETB (*etb*) and ETC (*etc*) cause loosening of the skin as observed in staphylococcal scalded skin syndrome (SSSS) that is often associated with neonates (Gemmell *et al.*, 1995). These exfoliative toxins act as epidermolytic proteases that cleave desmoglein 1, a protein that connects epidermal cells in the granular layer of epidermis. They are also serine proteases and show 25% similarity with the V8 protease (Dancer *et al.*, 1990) and have been associated with community-acquired MRSA strains causing bullous impetigo and impetigo (Tristan *et al.*, 2007). A higher percentage of *S.aureus* isolated from infected skin lesions are found to produce ETA and/or ETB and Panton-Valentine leukocidin (Mertz *et al.,* 2007).

The host produces several bactericidal fatty acids and other lipid molecules in response to infection. Staphylococcal lipases and FAME (fatty acid metabolizing enzymes) may metabolize these fatty acids and lipids and harvest them as nutrients (Gortz *et al.*, 1985, Mortensen *et al.*, 1992).

Biofilm formation in *S.aureus* and *S.epidermidis* is another factor which enables the bacteria to resist the host immune responses as well as antimicrobial agents (Chuard *et al.*, 1991, Rohde *et al.*, 2005). Biofilm formation begins with adherence to the cell surface followed by formation of glycocalyx (Mack *et al.*, 2004), which in *S.aureus* is supported by the polysaccharide intercellular adhesion (PIA) (Mack, 1999) encoded by the *icaADBC* locus.

Bacterial communities within this biofilm are generally protected from the effects of antibiotics and host immune reponses.

IsdA is a surface protein that decreases the hydrophobicity of *S.aureus* thus making it resistant to the bactericidal effect of skin fatty-acids and sebum (Clarke *et al.*, 2007). In addition it was shown that the presence of IsdA enhances survival of *S.aureus* on live human skin (Clarke *et al.*, 2007).

1.3.3   Enzymes involved in tissue invasion and penetration

In order to establish an infection it is necessary for *S.aureus* to invade and penetrate cells. This it accomplishes in part by the production of hemolysins which are cytotoxic agents that basically act on and disrupt the components in the host cell membrane. The α-toxin (*hla*) forms pores in cell membranes resulting in cell lysis (Bhakdi and Tranum-Jensen, 1991) and has been suggested to cause apoptosis in lymphocytes (Jonas *et al.*, 1994). β-toxin (*hlb*) is a sphingomyelinase and is thus potentially cytolytic to cell membranes containing sphingomyelin for instance in red blood cells resulting in the observed hemolytic effects and in corneal and scleral tissues resulting in inflammation, edema and ocular damage in the rabbit eyes model of infection (O'Callaghan *et al.*, 1997). The γ-toxin expresses three proteins, two class S components (HlgA and HlgC) and one class F component (HlgB). Both the α-toxin and γ-toxin together are shown to promote virulence in a murine septic arthritis model (Nilsson *et al.*, 1999). In addition, γ-toxin was suggested to play a role in the pathogenesis of toxic shock syndrome together with TSST-1 (Clyne *et al.*, 1988). The δ-hemolysin

was found to enhance the hemolytic action of β-hemolysin and lyses bacteria that lack cell walls (Bernheimer and Rudy, 1986).

Hyaluronic acid is found in connective tissues and acts as biological cement that holds tissues together. It is digested by hyaluronate lyase that is produced by staphylococci causing tissue degradation and thus aiding in the spread of the organism. Hyaluronate lyase (*hysA*) is a virulent factor that is important in the early stage of subcutaneous infections and is regulated by both *agr* and *sar* (Makris *et al.*, 2004). Introduction of the *hysA* gene into the non-pathogenic *S.cornosus* resulted in production and secretion of hyaluronate lyase as evident by a large zone of clearing in media containing hyaluronic acid (Williams *et al.*, 2002). Metalloproteases also degrade connective tissues thereby contributing to the invasiveness of the organism.

1.4   Regulation of virulence determinant production

Pathogenecity of *S.aureus* is largely determined by the coordinated production and action of virulence factors that are controlled by genes referred to as global regulators (Tegmark *et al.*, 2000). Expression of the genes for these virulence factors are temporally controlled and geared to the demands of the infection and whose transcription is either stimulated or repressed by several gene regulators (Fig. 1.1). Novick (2003) categorized these gene regulators into three groups; the two component systems (TCS) (which includes the Agr system, Sae, ArRLS and SrrAB), alternative sigma factors, and transcription factors (such as the SarA family and superantigens). Expression of target genes is controlled

by virulence gene regulators that bind directly to their promoters or indirectly to their regulators (Said-Salim *et al.*, 2003).

The temporal controlled expression of virulence factors is illustrated in a hypothetical model of infection in Figure 1.2 (Projan and Novick, 1997). Infection is initiated by bacteria in the lag phase followed by entry into the exponential phase which is accompanied by logarithmic multiplication and synthesis of surface proteins. In the post-exponential phase (PXP), crowding activates a density dependent sensing mechanism which triggers the production of exoproteins such as cytotoxins, superantigens, enzymes and capsular polysaccharides (Novick 2003). These facilitate escape of the organism during stationary phase (STA) from the localized site of infection to spread to and colonize new niches in the host where the cycle is repeated. Cell wall associated proteins that mediate attachment processes are generally produced during early
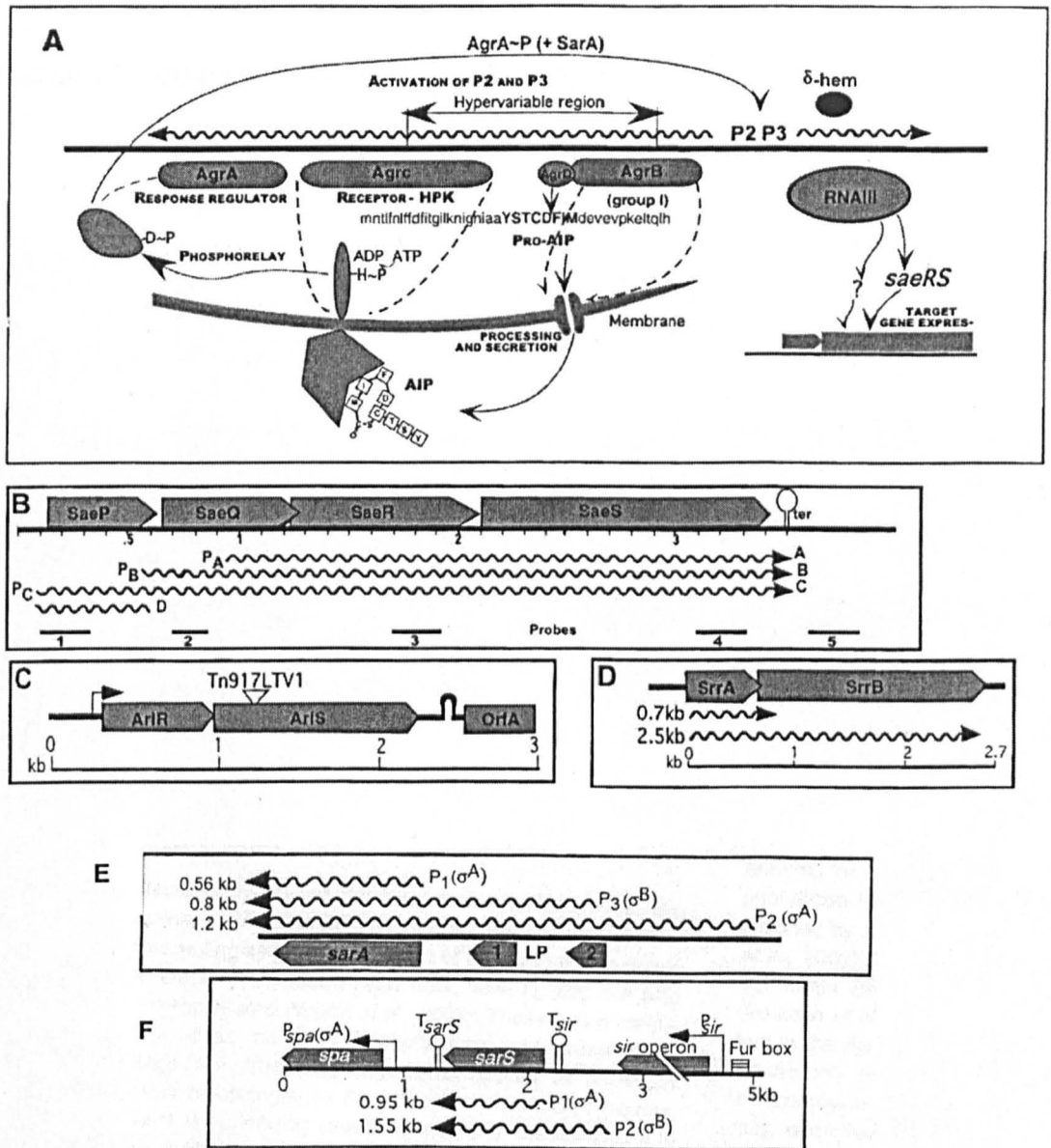
Figure 1.1

Regulatory systems of *S.aureus*. A, *agr*; B, *sae*, C, *arlRS* (adapted from Fournier *et al.*, 2001); D, *srrAB* (adapted from Yarwood *et al.*, 2001); E and F, *sarA* and *sarS* (adapted from Manna and Cheung, 1998 and Tegmark *et al.* 2000). *SarHI* (Tegmark et al., 2000) is redesignated as *sarS* (Arvidson and Tegmark, 2001).

Transcripts are indicated by wavy lines, terminators by stem-loops; P, promoter;

T, terminator; LP, leader peptide. Adapted from Novick (2003).

10

Log Bacteria

Synthesis of
Surface-Associated
Virulence Determinants

Synthesis of
Extracellular
Virulence
Determinants

9

8   Lag   Exponential   Post-exponential   Stationary

PMNs

Abcess

Spread to
new sites
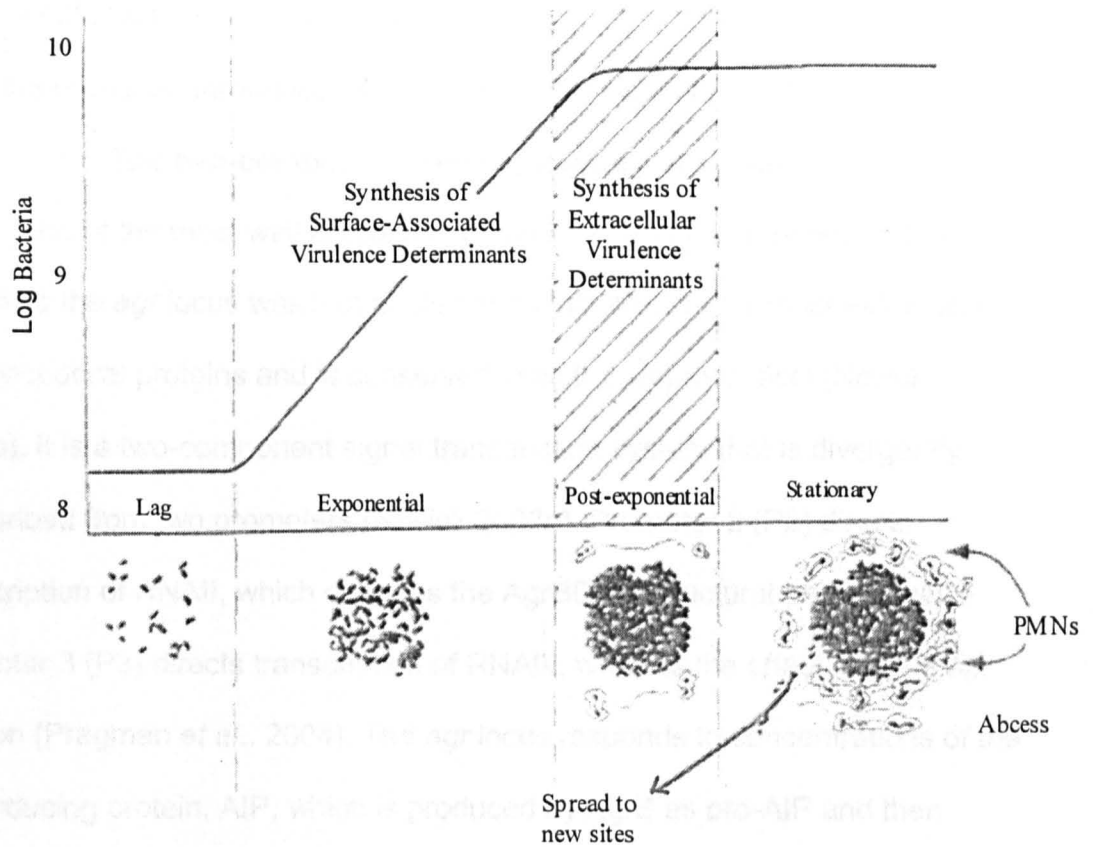
Figure 1.2

Control of virulence determinant production in *S.aureus*.

The temporal control of surface-associated and extracellular virulence
determinants. Adapted from Projan and Novick (1997).

exponential phase followed by the production of most exoproteins in the post-exponential phase. Enterotoxin A (*sea*), δ-hemolysin (*hld*) and hyaluronidase (*hys*) are produced throughout the exponential phase (Novick, 2003).

1.4.1   The two-component gene regulatory systems

One of the most well characterized two-component gene regulatory system is the *agr* locus which controls genes that encode for most extracellular staphylococcal proteins and is conserved in all the staphylococci (Novick, 2003b). It is a two-component signal transduction system that is divergently transcribed from two promoters (Novick 2003a). Promoter 2 (P2) directs transcription of RNAII, which encodes the AgrBDCA structural proteins while Promoter 3 (P3) directs transcription of RNAIII, which is the effector of the *agr*-regulon (Pragman *et al.*, 2004). The *agr* locus responds to concentrations of the autoinducing protein, AIP, which is produced by AgrB as pro-AIP and then processed and secreted by AgrD (Novick, 2003a). AIP binds and activates AgrC which in turn activates AgrA and together with SarA enhances expression of the *agr* locus via P2 and P3 (Novick *et al.*, 1995, Ji *et al.*, 1997). Activation of P3 leads to the production of RNAIII which has a direct effect on transcription of target genes via one or more intracellular regulatory mediators including SaeRS (Novick, 2003b). RNAIII upregulates transcription of extracellular gene products and downregulates the expression of genes encoding surface-associated virulence factors (Janson and Arvidson, 1990; Novick, 1993) although the precise mechanism of action at target promoters is unclear. RNAIII has been shown to

22

activate transcription of *hla* (alpha toxin), and *ssp* (serine protease) and inhibit transcription of *spa* (Protein A) and *coa* (coagulase).

The *sae* (*S.aureus* exoprotein expression) locus (Novick, 2003a & b) consists of two genes *saeR* and *saeS* and encodes a second major two-component signal transduction system that consists of four ORFs, SaeP, SaeQ, SaeR and SaeS. The *sae* locus is transcribed from three promoters to produce three major transcripts and disruption of the *sae* locus results in decreased expression of alpha-toxin (*hla*), beta-hemolysin (*hlb*), and coagulase(*coa*) (Giraudo *et al.*, 1997). It also upregulates DNase and Protein A (Pragman and Schlievert, 2004). Transcription of *sae* is affected by *agr*, σ^B and *sarA* but it however does not affect transcription of any of these genes (Novick, 2003b). In addition, its transcription is affected by environmental stimuli such as 1M NaCl, pH below 6 or subinhibitory concentrations of clindamycin.

Another two-component signal transduction system is ArlRS that controls autolysis, adhesion and extracellular proteolytic activity in *S.aureus* (Fournier *et al.*, 2000). The *arlRS* locus encodes a receptor–HPK (*arlS*) and a response regulator (*arlR*). It acts as a global transcriptional regulator and directly and/or indirectly modulates the expression of genes involved in autolysis, cell growth and pathogenesis (Liang *et al.*, 2005). ArlRS downregulates the expression of *hla, ssp* and *spa*. (Pragman and Schlievert, 2004).

SrrAB (or SrhSR) is a two-component system that controls expression of staphylococcal virulence genes under microaerobic conditions (Novick, 2003). The *srrAB* (staphylococcal respiratory response) locus encodes a receptor-HPK

(*srrB*) and a response regulator (*srrA*) and is driven by a single promoter that generates two transcripts. It functions to regulate many genes that are involved in energy metabolism under anaerobic conditions (Yarwood *et al*, 2001). Disruption of *srrB* results in increased levels of RNAIII and decreased production of TSST-1 in microaerobic conditions. Conversely, expression of *srrAB* represses transcription of both RNAIII and TSST-1 under microaerobic conditions (Yarwood *et al.*, 2001). *srrAB* therefore inhibits *agr* activation and is in turn downregulated by *agr*.

1.4.2 Alternative sigma factors (σ^B)

The alternative sigma factors are activated directly within the cell and not through signal transduction (Novick, 2003). *S.aureus* possesses σ^A and σ^B (Clements and Foster, 1999) but only σ^B is involved in stress resistance. It is involved in the recovery from heat shock at 54°C and in acid and hydrogen peroxide resistance but not in resistance to ethanol and osmotic shock or starvation-survival (Chan *et al.*, 1998c). RsbU is a positive regulator of σ^B and is required for its activation (Giachino et al, 2001). Activity of σ^B is also regulated by RsbW, RsbV and RsbP (Novick, 2003). SarA upregulates expression of σ^B (Chan *et al.*, 1998a) which in turn upregulates the expression of exoprotein genes such as *coa* and *fnbB* in the early stages of growth (Nicholas *et al.*, 1999). σ^B represses transcription of *aur* and *scp* operons (Shaw *et al.*, 2004) as well as the *ssp* (Horsburgh *et al.*, 2002). σ^A is involved in the transcription of *scpA*, *sspABC* and *aur* which is positively regulated by *agr* and negatively regulated by *sarA* (Shaw *et al.*, 2004).

1.4.3   Transcription factors

Intracellular transcription factors regulate target genes by transmission of environmental signals that are recognized by transmembrane and intracellular receptors (Novick, 2003). An example of this is the *sar* (staphylococcal accessory regulator) locus which encodes the 14.7kDa DNA-binding protein SarA that regulates several exoproteins as well as cell surface protein genes (Pragman and Schlievert, 2004; Bayer *et al.*, 1996; Morfeldt, 1996; Cheung and Projan, 1994). *S.aureus* possesses a family of proteins that are homologous to SarA which are classified into three subfamilies based on their domain structures (Cheung *et al.*, 2004) i.e. 1. the single domain structure, SarA, SarR, SarT, SarV and SarX; 2. the two-domain structures, SarS, SarU and SarY; and 3. single-domain structures that are highly homologous to the MarR family (gram-negative bacteria), SarZ, MrgA/Rat and two other homologs. SarA is necessary for the full transcription of *agr* RNAII and RNAIII (Heinrichs *et al.*, 1996) and is expressed from three promoters (P1, P2 and P3) that direct synthesis of three overlapping transcripts (Novick, 2003). The three *sarA* promoters are regulated as follows: sarP1 is positively regulated by SarA itself, sarP2 is silent and sarP3 is σ^B-dependent (Pragman *et al.*, 2004). *sarA* transcription from the sarP2 promoter is inhibited by another homolog, SarR (Manna and Cheung, 2001) which binds to all three promoters. Transcription of the *sar* locus is dependent on both the σ^A and σ^B -dependent promoters (Deora *et al.*, 1997; Manna *et al.*, 1998). The expression of *sarA* from the σ^A dependent promoter is growth phase dependent (Bayer *et al.*, 1996) and that from the σ^B is shown to be higher in the presence of

RsbU (anti anti-sigma factor) (Wolz *et al.*, 2000). *sarA* stimulates the transcription of *agr* (Lindsay and Foster, 1999; Cheung *et al.*, 1997a) and downregulates the expression of *hla* (alpha-toxin) by downregulating its repressor, SarT (Schmidt *et al.*, 2001) via SarU (Manna and Cheung, 2003). It however represses transcription of *cna* (collagen adhesin) and *spa* (Protein A) as well as several genes that encode for extracellular proteases in an *agr*-independent way (Cheung *et al.*, 1997b, Chan and Foster, 1998; Blevins *et al.*, 1999; Cheung *et al.*, 1999). An increase in transcription of *spa* was shown in *sarA* mutants whilst a decrease was shown in the transcription of genes coding for secreted toxins.

The ability of Agr and SarA to function as both activators and repressors of target genes is facilitated by the presence of SarS which is a homolog of SarA. The amino acid sequence of SarA shows identity to both the N-terminal and C-terminal halves of SarS, suggesting possibly a folding of this protein to assume a structure similar to that of SarA (Tegmark, 2000). SarS binds to *agr* P3, *hla* and *ssp* (serine protease) promoters. Agr downregulates *sarS* which is an activator for *spa* (Protein A) expression, resulting in downregulation of Protein A. SarS binds directly to the *spa* promoter thus activating transcription of *spa* with maximum levels attained postexponentially suggesting the involvement of other factors such as catabolite repression in the regulation of *spa* (Tegmark *et al.*, 2000). In contrast, SarS at high concentrations was found to repress transcription of *hla* in the presence of RNAIII.

MrgA (Rat) is the only member of the *mgr* (multiple gene regulator) locus and is homologous to the MarR family. It is a global regulator of autolysis and

virulence (Cheung *et al.*, 2004). It activates type 8 capsular polysaccharide and nuclease and represses α-hemolysin, coagulase, protease and protein A (Pragman and Schlievert, 2004).

Other transcription factors that are also global repressors of the exoprotein genes in *S.aureus* are TSST-1 and SEB which are superantigens. These proteins directly bind and inhibit the promoters of target genes via an intermediate transcription factor (Novick, 2003). TSST-1 affects production of cytokines and the synthesis of some exoproteins eg. lipase which is possibly inhibited by this protein.

Rot (repressor of toxins), a SarA homolog (Cheung *et al.*, 2004) is a repressor and a global regulator with both positive and negative effects on *S.aureus* gene expression (Said-Salim *et al.*, 2003). It positively regulates the expression of *sarS* (Cheung *et al*, 2001, Tegmark *et al.*, 2000) and acts together with SarS to activate *spa* (Protein A). Other factors that are positively modulated by Rot include *clfB* (clumping factor B) and *sdrC* which are cell surface adhesions, *dltD*, a member of the *dlt* operon that encodes proteins involved in D-alanine incorporation into teichoic acid in the *S.aureus* cell wall (Said-Salim *et al.*, 2003). Rot negatively regulates proteases and represses synthesis of *hla* (α-hemolysin) and *hlb* (β-hemolysin). Rot and *agr* have opposing effects on the expression of virulence genes and Rot is likely inhibited by RNAIII posttranscriptionally.

1.4.4 Regulation by environmental/host signals

Studies performed by Chan and Foster (1998b) demonstrate that environmental conditions impact the regulation of virulence determinants. The presence of 1M NaCl and 20mM sucrose were shown to strongly repress the expression of *hla*, *tst* and *spa* but had no effect on *sarA* expression. σ^B was also repressed by 1M NaCl during stationary phase (Chan *et al.*, 1998). Neither salt nor sucrose repression was demonstrated to be due to the *agr* global regulator. Low concentrations of divalent cations such as Ca^{2+} and Mg^{2+} significantly stimulated expression of *tst* in an *agr*-independent manner but no effect was observed with novobiocin, a DNA gyrase inhibitor. The expression of *spa* was significantly reduced by EGTA.

1.5 Stress resistance in *S.aureus*

The host naturally presents a stressful, even hostile, environment to which *S.aureus* has developed and demonstrates a high level of resistance. *S.aureus* possesses several components that make it highly adaptable to the stress presented by the host both intracellularly and outside cells.

Upon entry into the host, *S.aureus* encounters the first line of attack from the host that is the non-immune defense mechanism involving phagocytes especially neutrophils (PMNs) and macrophages (Ocana *et al.*, 2007). This initial phagocytic killing is essential to prevent spread and colonization of the organism in the host. Clements and Foster (1999) described the putative resistance mechanisms of *S aureus* to host attack within the phagolysosome where it is confronted by several degradative components and enzymes that eventually lead

to its demise. Reactive oxygen species such as the superoxide anion (O_2^-), hydrogen peroxide (H_2O_2), peroxynitrite ($OONO^-$) and hypochlorous acid ($HOCl$) that are generated by the host can damage DNA, proteins, and lipids (Clements and Foster, 1999, Farr and Kogoma, 1991).

S.aureus has developed several resistance mechanisms in order to survive in the phagolysosome. It possesses two superoxide dismutases, SodA and SodM (encoded for by *sodA* and *sodM* respectively) that convert superoxide to hydrogen peroxide. The presence of O_2^- (both intra and extracellular) increases transcription of both *sodA* and *sodM* although SodA is mainly responsible for the elimination of internally generated O_2 (Karavolos *et al.*, 2003), which is growth phase and Mn-dependent. H_2O_2 damages proteins by oxidizing cysteine and methionine residues and is especially toxic to DNA when reduced to the hydroxyl radical by Fe (II) via the Fenton reaction (Imlay, 2003). Catalase (KatA) detoxifies H_2O_2 and *katA* together with *ahpC* are members of the regulon which consists of genes that encode antioxidants and whose expression is controlled by PerR. Cosgrove *et al.* (2007) showed that a mutation in *ahpC* relieves the repression of PerR on *katA* thereby increasing its expression resulting in increased H_2O_2 resistance. In addition AhpC was shown to provide residual catalase activity in the *katA* mutant indicating their compensatory roles in peroxide stress resistance (Cosgrove *et al.*, 2007).

The formation of hypochlorous acid (HOCl) by myeloperoxidase within the phagolysosome maintains an acidic environment that is necessary for bactericidal activity. Although *S.aureus* is killed at pH2, it portrays an adaptive

response whereby it acquires acid resistance if first exposed to a higher non-lethal pH (Chan and Foster, 1998b). This acid adaptation response in *S.aureus* induces *sodA* suggesting a connection between acid and oxidative stress (Clements and Foster, 1999).

Both AhpC and KatA are required for nasal colonization and resistance to dessication (Cosgrove *et al.*, 2007). The ability of *S.aureus* to withstand dessication over a prolonged period allows survival and persistence in the hospital setting. Although the mechanism of tolerance dessication in *S.aureus* has not been established, it is correlated with pigmentation (Clements and Foster, 1999). Upon aging *S.aureus* produces the classic golden yellow coloration due to accumulation of staphyloxanthin which has been implicated as a virulent factor associated with reduced killing by neutrophils (Liu *et al.*, 2005) and protection against oxidative stress (Clauditz *et al.*, 2006).

S.aureus also exhibits a high tolerance for osmotic stress whereby at high NaCl concentrations its cell-wall peptidoglycan forms shorter interpeptide bridges for increased mechanical strength to resist implosion caused by the turgor pressure (Vijarankul *et al.*, 1995). In addition, since osmotic stress induces expression of *ahpC* (Armstrong-Buisserat, 1995) a connection between oxidative and osmotic stress is suggested.

In response to nutrient limiting conditions (outside the host), *S.aureus* enters the starvation-survival response mode and produces smaller colonies, divides infrequently and show increased resistance to acid and oxidative stress and lytic enzyme challenge (Watson *et al.*, 1998a). Several loci are important in

the starvation-survival state including sodA, heme A synthase (*ctaA*) and umuC which is a component of the SOS response (Watson *et al.*, 1998b). A rapid recovery response is observed in the starved cells upon availability of nutrients which trigger immediate RNA and protein synthesis (Clements and Foster, 1998).

1.6   *S.aureus* metabolism during pathogenesis

The virulence factors discussed previously are mainly those that enable *S.aureus* to colonize, invade and initiate infection within the host. Several regulatory mechanisms that control expression of the virulence factors that are involved in adhesion and the production of toxins were also discussed. These regulatory systems comprise of not only the interactions between Agr, SarA, SaeR and sigma B but also other regulators that are encoded in the genome (Becker *et al.*, 2007). A genomic comparison study of *S.carnosus* (non-pathogenic) against different strains *S.aureus* and *S.epidermidis* revealed that approximately 25% of the conserved gene products in staphylococci belong to proteins involved in basic metabolic pathways such as substrate transport and metabolism, coenzymes, energy production, transcription, translation or replication (Becker *et al.*, 2007).

Pathogenesis requires a complex interaction between the invading organism and its host. To exert a pathogenic effect, *S.aureus* like other pathogens must persist in significant numbers within the host and be continually producing different virulent factors which is energetically demanding. Metabolism of the pathogen must therefore be highly tuned to efficiently use the available nutrients.

Two global screens for genes required for infection by *S.aureus* both identified multiple metabolic components. Signature tagged mutagenesis (STM) using transposon Tn*917* identified several mutants that were attenuated in a mouse model of bacteremia (Mei *et al.*, 1997). DNA sequence analysis of these mutants showed that apart from those associated with genes of unknown function, a majority of them represent genes involved in nutrient biosynthesis, cell surface metabolism, cellular repair processes, and genes encoding the TCA cycle. Similarly, a study conducted by Coulter *et al.* (1997) using STM in three different *in vivo* mouse model of infection (abscess, bacteremia and wound) identified highly attenuated mutants in genes that encode for, amongst others, transport binding proteins (*Opp* and *dtp* (di-tripeptide transporter)), cell wall metabolism (*femA* and *femB*), amino acid uptake (*alsT*-alanine) and biosynthesis (*trp*- tryptophan, *putP*-amino acid permease) and DNA replication. Proline is an essential amino acid and *S.aureus* relies on transporters to acquire proline for survival in the host. Two transporters for proline uptake have been identified i.e. PutP, a high affinity proline permease encoded by *putP* (Wengender and Miller, 1995) and ProP, a low affinity proline transporters encoded by a *proP* gene homolog (*E.coli*) (Schwan *et al.*, 2006). The low affinity proline transporters may be the same as the low-affinity glycine betaine transporter which in *S.aureus* is possibly involved in osmoregulation (Pourkomailian and Booth, 1992). The expression of *putP* was increased at low concentrations of proline (as low as 17.4 μM) and high NaCl (up to 2M) concentrations which occur at the transcriptional level both in growth medium and in animal models of infection

(Schwan *et al.*, 2006). In addition, *putP* expression was shown to be decreased in the presence of the alternative factor sigma B. Mutation of *putP* in *S.aureus* was found to be significantly attenuating in mouse models bacteremia, endocarditis and wound infections suggesting a role of the gene in virulence of the organism (Schwan *et al.*, 1998, Bayer *et al.*, 1999,). Another amino-acid gene component which has been shown to be involved in pathogenesis of *S.aureus* is PheP, a putative amino acid permease in *S.aureus* which was shown to be involved in growth and starvation survival (Horsburgh *et al.*, 2004). A mutation in *pheP* in *S.aureus* resulted in poor growth under microaerobic or anaerobic conditions on pig serum agar and reduced virulence in a murine abscess model of infection (Horsburgh *et al.*, 2004). Further, the *pheP* mutant was found to be less pathogenic in the *Drosophila melanogaster* model of infection with three times more death observed compared to the flies infected with the wild-type strain (Needham *et al.*, 2004).

1.6.1 Sulfur source uptake and utilization in *S.aureus*

1.6.1.1   Sulfur

Cysteine is an essential amino acid component of proteins and is the major source for the synthesis of most sulfur-containing compounds in bacteria. (Wilkinson,1997). Lithgow *et al.* (2004) showed that *S.aureus* is able to utilize various sulfur sources such as thiosulphate, glutathione, sulfite, cysteine and cystine.

1.6.1.2   Genes involved in sulfur source utilization in *S.aureus*

In addition to being a sulfur source, cysteine is also found in catalytic sites in redox proteins for formation, isomerization, and reduction of disulfide bonds and for other redox functions (Fomenko and Gladvshev, 2003). Cysteine is synthesized in two pathways; the first by incorporation of thiosulfate or sulfide into serine which occurs in bacteria and by the transsulfuration pathway in animals which produces cysteine from methionine and serine (Borup and Ferry, 2000, Kitabatake *et al.*, 2000).

The *cysE, cysK,* and *cysM* genes in *E.coli* encode for the serine transacetylase, O-acetylserine(thiol)-lyase-A and O-acetylserine (thiol)-lyase-B respectively which catalyze the production of cysteine from serine (Kitabatake *et al,* 2000). In this assimilation pathway, serine and acetyl-CoA is first converted to O-acetylserine by serine transacetylase (*cysE*). The sulfide or thiosulphate is incorporated into O-acetylserine by either O-acetylserine (thiol)-lyase-A (*cysK*) or O-acetylserine (thiol)-lyase-B (*cysM*) to produce cysteine.

Lithgow *et al* (2004) developed a flow diagram (Fig.1.3) that shows the genes involved in the uptake and utilization of different sulfur sources for cysteine (Cys) biosynthesis in *S.aureus*. As indicated on the diagram, *S.aureus* possesses gene homologues for uptake of cysteine, cystine and glutathione but not for sulphate and sulfite. The gene *cysM* in *S.aureus* encodes a cysteine synthase that is functionally homologous to *E.coli* CysM (Lithgow *et al.*, 2004) and is the O-acetylserine (thiol) lyase B type protein. In addition, *S.aureus* possesses homologs of *cysE, cysK* and *cysM* that allows for the utilization of sulfide and

permease together with CysP, a thiosulphate binding protein whereas sulfate uptake is enabled by *cysT* (Hryniewicz, 1990). Utilization of thiosulphate by *S.aureus* is dependant on *cysM* but as there are no *cysP* homologs in *S.aureus*, thiosulphate uptake probably occurs by a different mechanism. The gene *cysT* or its homolog is absent in *S.aureus* which is unable to use sulfate as a sole sulfur source. Lithgow *et al.,* (2004) showed that chemically defined media containing only methionine and sulfate as the sulfur source does not support growth of *S.aureus* SH1000. The trans-sulfuration reaction therefore does not occur in this organism. *S.aureus* is able to acquire extracellular cysteine and cystine for use as sulfur sources although the mechanism(s) for their uptake is not established. The presence of a *ggt* homolog in *S.aureus* presumably enables the utilization of glutathione.

THIOSULFATE SULFATE R-SULFONATE CYSTEINE /
$(S_2O_3^{2-})$ ex (SO_4^{2-}) ex $(R\text{-}SO_3^-)$ ex CYSTINE GLUTATHIONE
ex ex

| cysP* | cysPTWAM | cysP* | cysTWAM | ssuBAC | tauABC |
| | | | sbp | | |

$S_2O_3^{2-}$ SO_4^{2-} $R\text{-}SO_3^{2-}$ Cys / Glu-Cys-Gly
Cys-Cys

ATP
sulfurylase
| ylnB | cysND |

APS

APS kinase ggt ggt
| ylnC | cysC |

PAPS

PAPS sulfo-
transferase
| cysH | ssuD | tauD |

SULFITE (SO_3^{2-})

Sulfite reductase
cysI	cysI (haemoprotein)
cysJ	cysJ (flavoprotein)
ylnDEF	cysG (siroheme synthase)

SERINE

| cysE | SULFIDE (S^{2-}) |

OAS

cysK
cysM
cysM

S-SULFO- ?
CYSTEINE CYSTEINE

Figure 1.3

S.aureus sulfur sources. Homologues in *S.aureus* of genes involved in uptake and utilization of different sulfur source for cysteine biosynthesis in *E.coli* and *B.subtilis* are shown. Shaded region shows genes in which no homologues are presumed present in *S.aureus*. Adapted from Lithgow *et al.*, 2004.

1.6.2 Gene involved in glutathione uptake and utilization- *ggt* (GGT).

S.aureus is unable to synthesize glutathione as evident by the lack of

gene homologs within its genome coding for the enzymes γ-glutamyl cysteine

synthetase and glutathione synthase and its low intracellular glutathione content

(Fahey *et al.*, 1978) . However, it possesses the gene *ggt*, which codes for the

gammaglutamyltransferase (GGT) which is an important enzyme in glutathione

degradation and metabolism.

Meister and Anderson (1983) categorized the GGT catalytic functions into

three groups i.e. 1) transpeptidation which involves transfer of the γ-glutamyl

moiety to an acceptor; 2) autotranspeptidation which involves transfer of the γ-

glutamyl moiety to GSH to form γ-glutamyl-GSH; and 3) hydrolysis where the γ-

glutamyl moiety is tranferred to water.

The GGT from *E.coli* is subject to many studies and is similar to

mammalian GGTs in its primary structure and enzyme characteristics except for

two main differences. GGT from *E.coli* possesses a signal peptide at its N-

terminus suggesting that it is a soluble periplasmic enzyme whereas the

mammalian GGTs are membrane bound enzymes. A signal peptide sequence is

also present at the N-terminus of the *B.subtilis* GGT (Xu *et al*, 1996).The

presumed γ-glutamyl binding site in the highly conserved putative active site is

threonine in *B.subtilis* (Xu *et al.*, 1996), serine in *E.coli* and other bacterial GGTs

(Suzuki *et al*, 1989) and cysteine in mammalian GGTs (Sakamuro *et al.*, 1988).

In addition, *E.coli* GGT is nonglycosylated whereas mammalian GGT are

heterologously glycosylated (Suzuki *et al.*, 2002). GGT, in *E.coli* is a periplasmic

enzyme which is approximately 59kD and like the human GGT consists of one large subunit and one small subunit (Suzuki, 1989). It is produced as a single inactive precursor unit which undergoes autocatalytic processing to form a large (α) subunit (MW approx. 40,000) and a small (β) subunit (MW approx. 20000) (Suzuki and Kumagai, 2002). The human kidney GGT is also a dimer comprising of a large peptide subunit (MW 65,000) and a small peptide subunit (MW 25,000) (Tate and Meister, 1976). In the *E.coli* GGT, the threonine (Thr391) residue in the small subunit acts as a nucleophile in this autocatalytic cleavage (Suzuki and Kumagai, 2002).

Bacillus subtilis GGT shows a high degree of amino acid homology with that of *E.coli*, is expressed after onset of stationary phase and its expression is not temperature dependent (Xu *et al.*, 1996). The *E.coli* GGT however is expressed during logarithmic growth with greater expression at 20 than 37°C (Suzuki *et al.*, 1986). Glutathione content was found to be significantly higher in the transition between exponential and stationary phase (Fahey *et al.*, 1978).

Other proteins that show sequence identities with GGT have been identified but their involvement in glutathione metabolism have not been elucidated. The YwrD protein in *Bacillus subtilis* is predicted to have GGT-like activity based on its sequence identity with the amino acid sequence of *E.coli* GGT (31%) (Suzuki *et al.*, 1989) and *Bacillus subtilis* GGT (27%) but was reportedly not involved in glutathione utilization in the organism (Minami *et al.*, 2004). A structurally related but distinct mouse enzyme, γ-glutamylleukotrienase,

showed γ-glutamyltranspeptidase-like activities but was unable to hydrolyse glutathione (Ikeda and Tanaguchi, 2005).

1.7   Glutathione and thiol metabolism

Glutathione is a tripeptide (N-L-γ-glutamyl-L-cysteinylglycine) consisting of glutamic acid, cysteine and glycine and is the most abundant intracellular low molecular non-protein thiol antioxidant in most living cells (Penninckx, 2000). The glutamic acid moiety is attached to cysteine via the carboxyl group on the side chain of the glutamic acid thereby creating the γ-glutamyl bond (Hanigan and Ricketts, 1993). This bond is resistant to most proteases but can be cleaved by GGT. The sulfhydryl group on the cysteinyl component confers on glutathione a strong electron-donating ability.

Glutathione synthesis occurs by consecutive actions of two ATP requiring enzymes, γ-glutamyl cysteinyl synthetase and GSH synthetase (Meister and Anderson, 1983). The former initiates glutathione synthesis by conjugating cysteine with glutamate to form γ-glutamyl cysteine which is then added to glycine to produce glutathione by the latter enzyme (Ikeda and Taniguchi, 2005). Glutathione synthesis is more predominant amongst the gram-negative bacteria including *E.coli* but is only present in *Lactococcus lactis* and *Streptococcus agalactiae, Streptococcus thermophilus and Enterococcus fecalis* amongst the gram positives (Fahey *et al.*, 1978; Newton *et al.*, 1996). Other gram-positive bacteria including *S.aureus, Bacilus subtilis* and *S.epidermidis* do not synthesize glutathione.

Meister and Anderson, 1983 summarizes glutathione metabolism in a pathway refered to as the γ-glutamyl cycle. In the transpeptidation reaction the γ-glutamyl moiety of glutathione is tranferred to an acceptor amino acid resulting in cysteinyl-glycine (cys-gly) dipeptide. A peptidase (aminopeptidase N and cysteinylglycine dipeptidase) then cleaves the cys-gly thereby releasing the glycine and cysteine moieties for use as a sulfur source as well as other cellular functions (Hanigan and Ricketts, 1993). The GGT enzyme, in *E.coli*, hydrolyzes the γ-glutamyl linkage of the γ-glutamyl amino acid which releases the amino-acid for utilization by the organism (Suzuki, 1993). Shibayama *et al.*, (2007) report a pathological role of GGT in the metabolism of extracellular glutamine and glutathione to glutamate in *Helicobacter pylori*. The resulting depletion of the two components and the production of NH_3 are suggested to contribute toward the demise of infected mammalian cells.

In a highly reduced environment within the cell, glutathione exists mostly in the reduced form, GSH, and undergoes oxidation to form disulphide bonds with either another glutathione to form glutathione disulphide (GSSG, oxidized form) or with sulfhydryl groups on cysteine moieties in proteins or other low molecular weight thiols. Glutathione is regenerated by reduction of GSSG with NADPH through the glutathione reductase reaction (Rieber *et al.*, 1968) and *de novo* synthesis (Dickinson and Forman, 2002).

In mammalian tissues reduced glutathione (GSH) is the metabolically active form with concentrations ranging from 0.5 to 10mM (Meister and Anderson, 1983). Glutathione concentration is highest in the liver (up to 10mM) where it is exported

and transported to the intestine via the bile duct. It is present in the spleen, kidney, lens, erythrocytes and leukocytes and lower concentrations of approximately 4.5 µM, are found in the plasma.

1.7.1 Role of glutathione as a sulfur source

Glutathione is a transport and storage source for cysteine (Meister and Anderson, 1983) and glutamate (Shibayama *et al.*, 2007). The cysteine moiety liberated from hydrolysis of extracellular glutathone was utilized by glutathione depleted GGT-positive mouse fibroblasts cells for growth and to replenish intracellular glutathione (Hanigan and Ricketts, 1993). Utilization of extracellular glutathione has also been demonstrated in *Streptococcus mutans* (Sherrill *et al.*, 1998), *Bacillus subtilis* (Minami *et al.*, 2004) and *Lactococcus lactis* (Li *et al.*, 2003). Suzuki *et al.* (1993) showed that *E.coli* could utilize exogenous glutathione as a cysteine source and a glycine source. *Haemophilus influenzae* does not synthesize glutathione but is able to import it from the growth medium (Vergauwen *et al.*, 2003). In addition, export of intracellular glutathione was reported in strains of *Salmonella typhimurium* and *E.coli* (Owens *et al.*, 1986).

S.aureus is also able to use glutathione as the sole sulfur source as suggested by the presence of the *ggt* gene homolog (Lithgow *et al.*, 2004). It however does not possess the genes for glutathione synthesis therefore glutathione has to be acquired from an external source that is the host. The exact mechanism of glutathione uptake and utilization in *S.aureus* remains to be elucidated.

1.7.2 Protective roles of glutathione

In addition to being a sulfur source, glutathione also possesses multiple protective roles within the cell which include maintaining a reducing environment, involvement in detoxification processes and redox signaling (Sen, 1998). Aerobic repiration generates harmful reactive oxygen species (ROS) such as superoxide (O_2^-), hydrogen peroxide ($H_2O_{2)}$, hydroxyl (OH), and organoperoxide radicals in bacteria. These reactive oxygen species are biological oxidants that bind to cellular elements (DNA, proteins, and lipids) and cause damage. Many bacteria including *S.aureus* have antioxidant enzymes such as catalases , peroxidases and superoxide dismutases and antioxidants such as cysteine, glutathione and other thiols that detoxify and eliminate these toxic oxygen species.(Karavalos *et al.*, 2003; Izawa 1996). Both thioredoxin and glutathione maintain a reducing environment intracellularly and provide overlapping protection against oxidative stress (Penninckx, 1993, Uziel *et al.*, 2003).

Numerous protein and genomic sequencing studies have revealed that *S.aureus* possesses survival mechanisms against toxic oxygen species generated in aerobic environments that may contribute to its virulence (Clements *et al.*, 1999, Horsburgh *et al.*, 2002). Studies suggest that in many microorganisms including *S.aureus*, glutathione may possess direct roles as an antioxidant and plays an important role in the reductive elimination of H_2O_2 and organoperoxides that result from activation of

42

oxygen during respiration. Gluthathione (GSH) is used as a substrate for glutathione peroxidase (GSHPx) and peroxiredoxins for reduction of H_2O_2 and lipid hydroperoxides (Dickinson, 2002). It acts together with superoxide dismutase by reacting with carbon-centered radicals, R·, to prevent oxidative damage. (Dickinson 2002). Studies by Vergauwen *et al.*, (2003) showed that glutathione is able to overcome the toxic effects of hydrogen peroxide (H_2O_2) generated in catalase deficient mutants of *Haemophilus influenzae*. In addition, the authors showed that the presence of imported gluthathione conferred protection against methylglyoxal, *tert*-butyl hydroperoxide (t-BuOOH) and S-nitrosoglutathione toxicity. Glutathione is also suggested to be involved in regulation of catalase and its activity against H_2O_2 in *E.coli* (Oktyabrsky, *et al.* 2001). Cellular glutathione was shown to protect *Streptococcus mutans* against growth inhibition by the thiol-oxidizing agent diamide (Sherill and Fahey, 1998). In *E.coli* glutathione has a role in reversing the growth inhibiting effect of this thiol oxidant (Hibberd, 1978). Within the cell, glutathione exists mainly in the reduced form (GSH) and the GSH:GSSG ratio is an indicator of the level of oxidative stress (Hurd *et al.*, 2005). Reduction in the GSH:GSSG ratio in *E.coli* may possibly activate the transcription factor OxyR leading to the induction and activation of antioxidant genes *trxA* (thioredoxin), *grxA* (glutaredoxin1), *gorA* (glutathione reductase), *gshA* (glutathione synthethase) and *trxB* (thioredoxin reductase) (Zheng, 1998). Furthermore glutathione may have roles in resistance to stress agents such as methyl viologen (oxidative stress) and tellurite.

1.8 Aims of the project

The overall aim of the research project was to determine the role of glutathione as a sulfur source and in stress resistance in *S.aureus*. Glutathione utilization in other organisms has been previously shown to be facilitated by gammaglutamyltranspeptidase (*ggt*). The *S.aureus* GGT homolog and a putative glutathione transporter were characterized. The role of glutathione in tellurite resistance was also studied and the major proteins involved in the tellurite resistance were identified.

CHAPTER TWO

MATERIALS AND METHODS

2.1 Media and antibiotics
2.1.1 Media

Unless otherwise stated all media were prepared using distilled water (dH_2O) and were sterilised by autoclaving for 20 min at 121 °C (15 pounds per square inch).

2.1.1.1 B2

Casein acid hydrolysate (Oxoid)	10 g l^{-1}
Yeast extract (Oxoid)	25 g l^{-1}
K_2HPO_4	1 g l^{-1}
NaCl	5 g l^{-1}

The pH was adjusted to 7.5. Once autoclaved and cooled, sterile glucose was added to 1 mM (final concentration).

2.1.1.2 Brain heart infusion (BHI) (Oxoid)

Brain heart infusion (BHI)	37 g l^{-1}

Oxoid agar No. 1 (1 % (w/v)) was used for BHI agar.

2.1.1.3 Chemically Defined Media (CDM) – without cysteine.

CDM, which consists of five components (CDM1-5) as shown was mixed in the following quantities to form the CDM liquid media with 0.1% glucose (w/v). For CDM agar media, 7.5g of bacteriological agar was added for every 600 ml of CDM liquid media.

CDM 1(10X)	140 ml
CDM 2(5X)	40 ml
CDM 3	100 ml
CDM 4(10X)	2 ml

To this mixture, 1518 ml of distilled water was added and then autoclaved. When cooled, 200 ml of sterile CDM 5 was added for every 1800 ml of CDM liquid media.

CDM-1 (10X)   Made up to 1.4 L with dH_2O and autoclaved to dissolve.

Chemical	Weight (g)	Chemical	Weight (g)
L-aspartic acid	3	L-phenylalanine	2
L-alanine	2	L-proline	3
L-arginine	2	L-serine	2
Glycine	2	L-threonine	3
L-glutamic acid	3	L-tryptophan	2
L-histidine	2	L-tyrosine	2
L-isoleucine	3	L-valine	3
L-lysine HCl	2	Na_2HPO_4	140
L-leucine	3	KH_2PO4	60
L-methionine	2		

CDM-2 (5X)   Made up to 400 ml with dH_2O, filter sterilized.

Chemical	Weight (mg)	Chemical	Weight (mg)
Biotin	2	Riboflavin	40
D-panthothenic acid	40	Nicotinic acid	40
Pyridoxal	80	Thiamine HCl	40
Pyridoxamine	80		

HCl			

CDM 3   Made up to 2 L with 0.1M HCl, and autoclaved.

Chemical	Weight (mg)	Chemical	Weight (mg)
Adenine sulphate	800	Guanine HCl	800

CDM 4   Made up to 100 ml with 0.1M HCL.

Chemical	Weight	Chemical	Weight
$CaCl_26H_2O$	1 g	$MnCl_2$	500 mg
Ferric ammonium sulphate	600 mg		

CDM-5   Made up to 2 L with dH_2O and autoclaved.

Chemical	Weight (g)	Chemical	Weight (g)
Glucose	200	$MnSO_47H_2O$	10

The appropriate sulfur source (Chapter 2.2.13.1-2.2.13.4) was added as required for growth of bacterial cultures.

2.1.1.4   Glucose- yeast extract-tryptone medium (GYT)

Glucose	10 % v/v
Yeast extract	0.125 % w/v
Tryptone	0.25 % w/v

2.1.1.5   Luria-Bertani (LB) (Miller, 1972)

Tryptone (Oxoid)	10 g l^{-1}
Yeast extract (Oxoid)	5 g l^{-1}
NaCl	10 g l^{-1}

The pH was adjusted to 7.2 using NaOH. Oxoid Agar No. 1 (1.0 % w/v) was added for LB agar.

2.1.1.6   **LK**

Tryptone (Oxoid)	10 g l^{-1}
Yeast extract (Oxoid)	5 g l^{-1}
KCl	7 g l^{-1}

Oxoid Agar No. 1 (1.0 % w/v) was added for LK bottom agar.

Oxoid Agar No. 1 (0.7 % w/v) was added for LK top agar.

2.1.1.7   **Phage agar**

Casamino acids (Oxoid)	3 g l^{-1}
Yeast extract (Oxoid)	3 g l^{-1}
NaCl	5.9 g l^{-1}

Oxoid Agar No. 1 (1.0 % w/v) was added for phage bottom agar.

Oxoid Agar No. 1 (0.33 % w/v) was added for phage top agar.

2.1.1.8   **Super optimal broth (SOB)(Sambrook *et al.*, 1989)**

Tryptone (Oxoid)	2 % w/v
Yeast extract (Oxoid)	0.5 % w/v
NaCl	10 mM
KCl	2.5 mM

Once autoclaved and cooled, sterile supplements of $MgCl_2$ and $MgSO_4$ were added, each to 10 mM (final concentration).

2.1.1.9 Super optimal broth with catabolite repression (SOC) (Sambrook *et al.*, 1989)

2.1.1.9.1 SOC. Medium (TOPO TA Cloning Kit - Invitrogen)

Tryptone	2% w/v
Yeast extract	0.5% w/v
NaCl	10 mM
KCl	2.5 mM
$MgCl_2$	10 mM
$MgSO_4$	10 mM
Glucose	10 mM

2.1.1.9.2 SOC was prepared by the addition of sterile glucose (20 mM) to SOB

2.1.1.10 Terrific Broth (TB)

Tryptone	12 g l^{-1}
Yeast	24 g l^{-1}
Glycerol	4 ml

Made up to 900 ml and autoclaved.

Salts

KH_2PO_4	2.31 g
K_2HPO_4	12.54g

Salts were dissolved in 100 ml distilled water and autoclaved.

The media and salts were combined when cooled after autoclaving.

2.1.1.11 Tryptic Soya Broth (Oxoid)

Tryptic soya broth (TSB)	30 g l^{-1}

2.1.2 Antibiotics

All antibiotics used in this study are listed in Table 2.1 The stock solutions were filter-sterilised (0.2 μm pore size) and stored at -20 °C. For use in agar plates, the antibiotic stock solutions were added to the media once they had cooled to below 55 °C. For use in liquid media, the antibiotic stock solutions were added just before use. Concentrations of antibiotics used for selection were as in Table 2.1, unless otherwise stated.

Antibiotic	Stock Concentration (mg ml^{-1})	Working Concentration in *S. aureus* (μg ml^{-1})	Working Concentration in *E. coli* (μg ml^{-1})
Ampicillin (Amp)	50[a]	-	50
Erythromycin (Ery)	5 or 75[b]	5	300
Lincomycin (Lin)	25[c]	25	-
Kanamycin (Kan)	50[a]	50	50
Tetracycline (Tet)	5[c]	5	12.5
Chloramphenicol (Cm)	5[b]	5	-
Cadmium chloride (CdCl$_2$)	100[a]	250	-

Table 2.1 Antibiotics used in this study

Stock concentrations of antibiotics were dissolved in dH$_2$0[a], 95% v/v ethanol[b], or 50 % v/v ethanol [c], filter-sterilised and stored at -20 °C. The inducing concentration of Ery was 0.15 μg ml^{-1}.

2.2 Buffers and stock solutions

All buffers were prepared in dH$_2$O and stored at room temperature. Solutions for use in microbiological work and in vitro DNA manipulations were sterilised

by autoclaving. All of the methods in this chapter are as in Sambrook *et al.* (1989), unless otherwise stated.

2.2.1 β-galactosidase assay solutions

2.2.1.1   ABT

NaCl	5.884 g
K_2HPO_4	10.51 g
KH_2PO_4	5.44 g
TritonX-100	1 ml
dH_2O	1 litre

2.2.1.2   Stopping solution

Na_2CO_3	42 g
dH_2O	1 L

2.2.1.3   ABTN

ABT	500 ml
Na_2CO_3	500 ml

2.2.2   β-mercaptoethanol (100 mM)

β-mercaptoethanol	70 µl
dH_2O	9.93 ml

2.2.3   DNA loading buffer (6X)

Bromophenol blue	0.25 % w/v
Xylene cyanol FF	0.25 % w/v
Glycerol	30 % v/v

2.2.4   Frozen storage buffer (FSB)

KCl	7.4 g
$MnCl_2.4H_2O$	8.9 g
$CaCl_2.2H_2O$	1.5 g
$Co(NH_3)Cl_3$	0.8 g

| Potassium acetate (1 M, pH 7.5) | 10 ml |
| Glycerol | 100 ml |

The constituents were made up to 1 l with sterile dH_2O and the pH adjusted to 6.4 using 0.1 M HCl. The solution was divided into 100 ml aliquots and stored at -20°C. Aliquots were defrosted as required and filter-sterilized (0.45 μM pore size) before use.

2.2.5 GGT assay (Diagnostics Chemicals)

2.2.5.1 Assay reagent

| Glycylglycine | 125 mM |
| L-γ-glutamyl-p-nitroanilide (GPNA) | 4.2 mM |

Buffer pH 8.0 at 25°C

Stabilizer (supplied in the reagent, details not provided)

Preservative (supplied in the reagent, details not provided)

2.2.5.2 DC-TROL (Diagnostic Chemicals)

DC-TROL is a control serum prepared from human serum containing human and nonhuman enzymes, nonprotein constituents and bacteriostatic agents.

2.2.6 Phosphate buffered saline (PBS)

NaCl	8 g l^{-1}
Na_2HPO_4	1.4 g l^{-1}
KCl	0.2 g l^{-1}
KH_2PO_4	0.2 g l^{-1}

The pH of PBS was adjusted to 7.4 using NaOH.

2.2.7　　　　Phage buffer

MgSO$_4$	1 mM
CaCl$_2$	4 mM
Tris-HCl pH 7.8	50 mM
NaCl	0.59% w/v
Gelatin	0.1% w/v

2.2.8　　　　Potassium tellurite (K$_2$TeO$_3$) (50 mM)

K$_2$TeO$_3$	0.127 g
dH2O	10 ml

2.2.9　　　　QIAGEN buffers

The composition of QIAGEN buffers is detailed in the manufacturer's instructions provided with the kits.

2.2.9.1　　　　QIAGEN Buffer P1

Tris-HCl, pH 8	50 mM
EDTA	10 mM
RNase A	100 ug ml^{-1}

2.2.9.2　　　　QIAGEN Buffer P2

NaOH	200 mM
SDS	1% w/v

2.2.9.3　　　　QIAGEN Buffer P3

Potassium acetate, pH 5.5	3.0 M

2.2.9.4　　　　QIAGEN Buffer EB

Tris-HCl, pH 8.5	10 mM

2.2.9.5　　　　QIAGEN Buffer QG, PB and PE

Supplied in the QIAquick kit, details not provided

2.2.10 Alkaline phosphatase (AP) buffer

Tris-HCl (pH 9.5)   100 ml l^{-1}

NaCl   5.8 g l^{-1}

MgCl$_2$.6H$_2$0   10.2 g l^{-1}

2.2.10.1 Colour substrate solution

10 ml AP buffer containing 200 µl NBT/BCIP solution (Roche).

2.2.11 SDS-PAGE solutions

2.2.11.1 5x Laemmli SDS-PAGE sample buffer

1M Tris-HCl (ph 6.8)   2.5 ml

SDS   1.0 g

Glycerol (100% v/v)   5.0 ml

Bromophenol blue   0.05 g

The components were made up to 10 ml with dH$_2$O. 5% v/v β-mercaptoethanol was added just before use. 1x sample buffer was made by diluting the 5x stock solution with dH$_2$O.

2.2.11.2 SDS-PAGE gel formulations and construction of gel

The following components were added together in a 30 ml plastic universal;

12.5 % w/v Resolving gel (2X)

30 % w/v Acrylamide/Bis (37.5:1)   4.1 ml

1.5M Tris-HCl (pH 8.8)   2.5 ml

dH$_2$O   3.4 ml

10 % w/v SDS   100 µl

10 % w/v Ammonium persulphate   100 µl

TEMED (N,N,N'N'-tetramethyl-ethylenediamine)   10 ul

The components were mixed by gentle swirling so as not to introduce air bubbles and loaded into the gel casting apparatus using a plastic 10 ml syringe. A layer of isopropanol was carefully pippeted on top of the gel to isolate it from the air. After the gel has solidified, the stacking gel was made up as follows;

4 % w/v stacking gel (2X)

30 % w/v Acrylamide/Bis (37.5:1)	0.75 ml
0.5M Tris-HCl (pH 6.8)	1.25 ml
dH$_2$O	3.0 ml
10 % w/v SDS	100 µl
10 % w/v Ammonium persulphate	50 µl
TEMED (N,N,N'N'-tetramethyl-ethylenediamine)	5 µl

The components were mixed by gentle swirling and dispensed on top of the resolving gel. A plastic comb was inserted into the gel to create wells and to separate the gel from air. After the gel had solidified, it was transferred to the gel-running tank and submerged in 1x SDS-PAGE electrophoresis buffer.

2.2.11.3 10x SDS-PAGE electrophoresis buffer

Glycine	144 g l^{-1}
Tris base	30.3 g l^{-1}
SDS	10 g l^{-1}

1x SDS-PAGE buffer was made by diluting 10x SDS-PAGE buffer 1:10 with dH$_2$O.

2.2.11.4 Coomassie Blue staining solutions

Coomassie Blue R-250	0.25 % w/v
Acetic acid	10 % w/v
Methanol	50 % w/v

Coomassie stain is light sensitive and was stored in a foil-wrapped Duran bottle.

2.2.11.5 Destain solution

Acetic acid	10 % w/v
Methanol	5 % w/v

2.2.12 Southern blotting buffers and solutions

2.2.12.1 Depurination solution

HCl	250 mM

2.2.12.2 Denaturing buffer

NaOH	0.5 M
NaCl	1.5 M

2.2.12.3 Neutralising buffer

Tris-HCl (pH 7.5)	0.5 M
NaCl	3 M

2.2.12.4 SSC (20X)

NaCl	3 M
Tri-sodium citrate·2H_2O	300 mM

The pH was adjusted to 7.0 with 1 M NaOH. 20X SSC was diluted with water to make 10X, 5X, 2X and 0.5X SSC.

2.2.12.5 Pre-hybridisation solution

SSC	5X
Blocking reagent (Roche)	1 % w/v
N-lauroylsarcosine, Na salt	0.1 % w/v

SDS	0.02 % w/v

2.2.12.6   Hybridisation solution

Digoxigenin-labelled DNA probes were diluted in prehybridisation buffer to 5 - 25 ng ml^{-1}.

2.2.12.7   Wash solution (2X)

SSC	2X
SDS	0.1 % w/v

2.2.12.8   Wash solution (0.5X)

SSC	0.5X
SDS	0.1 % w/v

2.2.12.9   Maleic acid buffer

Maleic acid	0.1 M
NaCl	0.15 M

The pH was adjusted to 7.5 with solid NaOH.

2.2.12.10   Washing buffer

Maleic acid buffer containing 3 % v/v Tween® 20.

2.2.12.11   Blocking solution

Maleic acid buffer containing 1 % w/v blocking reagent (Roche).

Blocking reagent was dissolved in maleic acid buffer by microwaving and stored at   -20 °C.

2.2.12.12   Antibody solution

Blocking solution containing 0.2 µg ml^{-1} anti-digoxigenin-AP conjugate (Roche).

2.2.12.13   Detection buffer

Tris-HCl (pH 9.5)	100 mM
NaCl	100 mM
$MgCl_2 \cdot 6H_2O$	50 mM

The pH was adjusted to 7.5 using 1 M NaOH.

2.2.12.14   Colour substrate solution
Detection buffer containing 2 % v/v NBT/BCIP (Roche).

2.2.12.15   Tris/Acetate/EDTA (TAE) buffer (50X)
Trisma base	242 g l^{-1}
Glacial acetic acid	57.1 ml l^{-1}
Na_2EDTA (0.5 M pH 8.0)	100 ml l^{-1}

Before use the buffer was diluted 1:50 to produce TAE.

2.2.12.16   Tris/EDTA (TE) buffer
| Tris-HCl | 1 mM |
| EDTA | 0.1 mM |

The pH was adjusted to 7.5 using 1 M HCl before autoclaving.

2.2.13   Sulfur sources
The following sulfur stock solutions were prepared in sterile dH_2O at a final concentration of 50 mM, filter sterilized (0.2 µm) and stored in 4°C.

2.2.13.1 Cysteine
2.2.13.2 Glutathione
2.2.13.3 Sulphate
2.2.13.4 Thiosulphate

2.2.14 Tris HCl buffer

Tris	0.485 g
dH$_2$O	200 ml

pH to 7.5 using 5M HCl

2.2.15 Western Blotting for N-terminal sequencing solutions

2.2.15.1 CAPS buffer (100 mM)

CAPS (3-(cyclohexylamino)-1-propanesulphonic acid)	22.13 g
dH$_2$O	800 ml

Adjusted to pH 11 with 2M NaOH and made up to 1 l.

2.2.15.2 Transfer buffer

100mM CAPS buffer	25 ml
methanol	25 ml

Add dH$_2$O to 250 ml.

2.2.15.3 Coomassie blue staining solution for N-terminal sequencing

Coomassie blue R-250	1 g
Methanol	400 ml
Acetic acid	10 ml

Coomassie blue was dissolved in methanol by stirring for 30 min. Acetic acid and dH$_2$O was added to 1 l and stirred for a further 30 min. The solution was filtered through a 0.45 µm filter.

2.2.16 Protein analysis buffers and reagents

2.2.16.1 Ammonium sulphate precipitation solution

Ammonium sulphate was added to cell free extracts accordingly to obtain a 55 % cut and a 75 % cut final concentration.

2.2.16.2   Cell free extract preparation buffers and stock solutions

2.2.16.2.1   Resuspension and dialysis buffer (pH 7.5)

Tris base	10 mM
2-mercaptoethanol	1 mM

pH to 7.5 with 5M HCl

2.2.17   Buffers for protein overexpression analysis

2.2.17.1   0.1M sodium phosphate buffer (SPB)

1M Na_2HPO_4	68.4 ml per liter
1M NaH_2PO_4	31.6 ml per liter

Add 900 ml dH2O.

2.2.17.2   Buffer A

0.1M SPB	200 ml
NaCl	29.22 g l^{-1}

dH_2O added to 1 l.

2.2.17.3   Buffer A with urea (8 M)

0.1M SPB	200 ml
NaCl	29.22 g l^{-1}

dH_2O added to 1 liter.

Urea	480.48 g l^{-1}

2.2.18   FPLC buffers and solutions

2.2.18.1   Ion exchange chromatography (Mono Q column)

Start Buffer	Tris-HCl pH 8.0	20 mM
Elution Buffer	Tris-HCl pH 8.0 +	20 mM
	NaCl	1.0 M

Buffers were degassed and vacuum filtered (0.45uM) before use.

2.2.18.2   Gel exclusion chromatography (Superdex 200 10/300GL)

Eluent	Sodium phosphate buffer pH 7.0	50 mM
	NaCl	0.15M

Buffers were degassed and vacuum filtered (0.45 µM) before use.

2.2.19   Native-PAGE stock solutions
2.2.19.1   Resolving gel buffer (Solution 1)
1.5 M Tris-HCl, pH 8.8.

2.2.19.2   Stacking buffer (Solution 2)
0.5 M Tris-HCl, pH 6.8

2.2.19.3   2X sample buffer (Solution 3)

Solution 2	2.5 ml
Glycerol	2 ml
Distilled water	5.5 ml

2.2.19.4   Native-PAGE gel formulations and construction of gel
The following components were added together in a 30 ml plastic universal;

7.5 % w/v Resolving gel (2X)

dH$_2$0	5.0 ml

Solution 2	2.5 ml
30 % (w/v) Acrylamide/Bis (37.5 : 1) (BioRad)	2.5 ml
10 % (w/v) Ammonium persulphate	100 µl
TEMED	10 µl

The components were mixed by gentle swirling, so as not to introduce air bubbles, and loaded into the gel casting apparatus using a plastic 10 ml syringe. A layer of water-saturated isopropanol was carefully pipetted on top of the gel to isolate it from the air. After the gel had solidified, the stacking gel was made up as follows;

4% w/v Stacking gel (2X)

dH$_2$0	3.0 ml
Solution 3	1.25 ml
30 % w/v Acrylamide/Bis (37.5 : 1) (BioRad)	0.75ml
10 % w/v Ammonium persulphate	50 µl
TEMED	5 µl

The contents were mixed by gentle swirling and pipetted on top of the resolving gel. A plastic comb was inserted into the gel to create wells and to separate the gel from the air. After the gel had solidified, it was transferred to the gel-running tank and submerged in 1X Native-PAGE buffer.

2.2.19.5   10X Native-PAGE electrophoresis buffer

| Glycine | 140 g l^{-1} |
| Tris HCl pH | 30 g l^{-1} |

A 1X Native-PAGE buffer was used for protein gel electrophoresis and was made by diluting 10X Native-PAGE buffer 1:10 with dH$_2$0.

2.2.19.6 Coomassie Blue stain

Coomassie Blue R-250	0.25% w/v
Acetic acid	10 % v/v
Methanol	50 % v/v

Coomassie stain is light-sensitive and was stored in a foil-wrapped Duran.

2.2.19.7 Destain solution

Acetic acid	10 % v/v
Methanol	5 % v/v

2.3 Enzymes and chemicals

All chemicals and enzymes were of analytical grade and purchased from Sigma, Merck (BDH) or Fisons unless otherwise stated. All restriction enzymes, RNase A, DNase, T4 ligase, polymerases and buffers for the modification of DNA were purchased from ABI Perkin-Elmer, Life Technologies (formally Gibco BRL), Northumbria Biologicals Limited (NBL), Promega, MBI Fermentas or Roche (formally Boehringer Mannheim).

Lysostaphin (Sigma) was dissolved in 20 mM sodium acetate to 5 mg ml^{-1} and stored at -20 °C. MUG (4-methylumbelliferyl-β-D-galactopyranoside) (Sigma) was dissolved in dimethyl sulfoxide to 4 mg ml^{-1} and stored at -20 °C. 4-MU (4-methylumbelliferone) (Sigma) was dissolved in DMSO to 1 mM and stored at -20 °C. Phenylmethylsulphonyl fluoride (PMSF) was dissolved to 0.25 M in 100 % v/v ethanol and stored at -20 °C. RNase A (DNase-free) (Sigma) was dissolved in dH$_2$O to 10 mg ml^{-1} and stored at -20 °C. DNase (Sigma) was dissolved in dH$_2$O to 2 mg ml^{-1} and stored at –20°C. Proteinase K was dissolved in 50 mM Tris HCl pH 7.5 to 10 mg ml^{-1} and stored at –20°C. X-Gal (Sigma) was dissolved in DMF to 20 – 100 mg ml^{-1} and stored at -20 °C in a foil-wrapped 30 ml universal tube. IPTG was dissolved in dH$_2$O to 100mM and stored at –20°C. NADH (Sigma) was dissolved in dH$_2$O to 20mM and stored at 4°C. Methyl viologen (Sigma) was dissolved in dH$_2$O to 1 M and stored at 4°C.

2.4 Bacterial strains, plasmids and bacteriophage

2.4.1 Bacterial maintenance, culture and storage conditions

Bacterial strains used in this study are listed in Table 2.2 - 2.3.

2.4.1.1 *Staphylococcus aureus* strains

Staphylococcus aureus strains (Table 2.2) were taken from glycerol stocks and grown on BHI agar plates containing antibiotics where appropriate to maintain selection of resistance markers. Plate cultures were stored for up to two weeks at 4 °C, after being re-streaked from glycerol stocks. For long-term storage, a single colony was spread onto a BHI agar plate containing relevant antibiotics and grown overnight at 37 °C. A loopful of cells was resuspended in 2 X 1 ml BHI containing 15 % v/v glycerol in a sterile 1.5 ml microfuge tube. These glycerol stocks were then snap-frozen in liquid nitrogen and stored at -20 °C and -70 °C.

Liquid cultures were normally prepared by inoculation of culture medium with a single isolated colony. Unless otherwise stated, cultures were grown overnight in conical flasks (culture:flask volume ratio 1:2.5), and were aerated on a rotary shaker at 250 rpm. All *S. aureus* plates or liquid medium cultures were grown at 37 °C unless otherwise stated. These conditions are referred to as standard conditions. For additional information on growth conditions for reporter gene fusion analysis and/or growth experiments (Chapter 2.7).

2.4.1.2 *Escherichia coli* strains

Escherichia coli strains (Table 2.3) were cultured, at 37 °C, using LB broth or LB agar containing antibiotics where necessary to ensure selection of plasmids. Plate cultures were stored at 4 °C for up to two weeks before re-streaking from glycerol stocks. Liquid cultures were prepared as for *S.aureus* (Chapter 2.4.1.1) using LB medium in place of BHI. For long-term storage, glycerol stocks of

E. coli strains were prepared as for *S. aureus* (Chapter 2.4.1.1), using LB medium rather than BHI.

Strain	Relevant Genotype / Markers	Source / Reference
8325-4	8325 cured of known prophages	Novick, 1963
SH1000	Functional rsbU$^+$ derivative of 8325-4	Horsburgh *et al.*, 2002
RN4220	Restriction deficient transformation recipient	Kreiswirth *et al.*, 1983
RMHggt	SH1000 *ggt::tet* (Tet^R)	This study
RMHggt3	RN4220 *ggt::tet* (Tet^R, Ery^R)	This study
RMHcol11	SH1000 *SACOL0185 :: lacZ* (Ery^R)	This study
RMHcol8	RN4220 *SACOL0185 :: lacZ* (Ery^R)	This study
RMH25	SH1000 *ggt::tet SACOL0185::lacZ* (Tet^R, Ery^R)	This study
RMH10	RN4220 *ggt::tet SACOL0185::lacZ* (Tet^R, Ery^R)	This study

Table 2.2

S. aureus strains used in this study.

Ery^R, erythromycin resistant; Tet^R, tetracycline resistant; Kan^R, kanamycin resistant; Cd^R, Cadmium resistant.

Strain	Relevant Genotype / Markers	Source / Reference
Top 10 electrocompetent cells	F⁻ mcrA Δ(mrr-hsdRMS-mcrBC) Φ 80 lacZ ΔM15 ΔlacX74 recA1 deoR araD139 Δ(ara-leu)7697 galU galK rpsL (Str^r) endA1 nupG Relevant Genotype / Markers	Invitrogen
TOP10 One Shot™ chemically competent cells	F⁻ mcrA Δ(mrr-hsdRMS-mcrBC) Φ 80 lacZ ΔM15 ΔlacX74 recA1 deoR araD139 Δ(ara-leu)7697 galK rpsL (Str^r) endA1 nupG	Invitrogen

TOP10F' One Shot electrocompetent cells	F' (lacI^q Tn10 (Tet^R)) mcrA Δ (mrr-hsdRMS-mcrBC) φ80lacZΔM15 ΔlacX74 recA1 araD139 Δ(ara-leu)7697 galU galK rspL(Str^R) endA1 nupG	Invitrogen
RMHt7	trxB in Tuner(DE3) placI	This study
RMHt7 col10	trxB in petBlue-1 in Tuner (E.coli Top 10)	This study

Table 2.3

E. coli strains used in this study.

2.4.2 Plasmids

The plasmids used in this study are listed in Table 2.4. Plasmid DNA was purified using QIAGEN plasmid kits (Chapters 2.12.2 and 2.12.3) according to the manufacturer's instructions. Purified plasmid DNA was stored in TE buffer at -20 °C.

Plasmid	Relevant Genotype / Markers	Source / Reference
pLTV1	Vector carrying Tn917 (promoterless lacZ) (Ery^R, Cm^R, Tet^R)	Camilli *et al.*, 1990
pAZtet	pAZ106 vector containing tet cassette	Ramlan Mohamad, personal communication
pMUTIN4	Promoterless transcriptional lacZ fusion vector (Amp^R, Ery^R)	Vagner *et al.*, 1998
PCR 2.1 - TOPO	Vector for cloning using TOPO TA cloning method (Amp^R, Kan^R)	Invitrogen
pMUTggt	2.9kB fragment from SH1000 containing the coding region of *ggt* in HindIII site of pMUTIN4	This study
pRMH01	1.5 kB *tet* cassette insertion in KpnI site of pMUTggt (Tet^R, Amp^R, Ery^R)	This study
pTopoRMH	866 bp fragment from SH1000 containing coding region of SACOL0185 in HindIII site of PCR 2.1 TOPO vector	This study

pTopoRMH	866 bp fragment from SH1000 containing coding region of SACOL0185 in HindIII site of PCR 2.1 TOPO vector	This study
pRMH02	866 bp fragment from SH1000 containing coding region of SACOL0185 in HindIII site of pMUTIN4	This study

Table 2.4

Plasmids used in this project.

2.4.3 Bacteriophage

Bacteriophage ϕ11 (Mani *et al.*, 1993) was used for phage transduction of *S. aureus* (Chapter 2.10.3). This phage is a *S.aureus*-specific, temperate, transducing phage of serological group B, and requires Ca^{2+} ions for maintenance of infection in bacterial cells. ϕ11 has an approximate genome size of 45 kb (Novick, 1991).

2.5 Centrifugation

Different types of centrifuges were used for harvesting cells and precipitating materials and these were: 1. Eppendorf microfuge 5415D; maximum volume - 2 ml, maximum speed 13,200 rpm (10,000 g); 2. Centaur 2 centrifuge (Sanyo); maximum volume - 50 ml, maximum speed 5,000 rpm; 3. Avanti™ J25I (Beckman), maximum volumes and speeds dependent on the rotor used: JA-20; maximum volume - 50 ml, maximum speed 20,000 rpm (48,384 g); 4. JA-14; maximum volume - 250 ml, maximum speed 14,000 rpm (30,074 g); and 5. JA-10.5; maximum volume - 500 ml, maximum speed 10,000 rpm (18,480 g).

All centrifugation was carried out at room temperature unless stated otherwise.

2.6 Determination of bacterial cell density

2.6.1 Spectrophotometric measurement (OD_{600})

A Jenway 6100 spectrophotometer was used to perform spectrophotometric measurements at 600 nm (OD_{600}) to quantify the bacterial yield of a culture. When the OD600 of a culture exceeded the linearity limit of the spectrophotometer (0.8) the cultures were diluted 1:10 in unused sterile culture medium to give a reading below 0.8. The final bacterial yield was calculated by multiplying the OD600 of the the diluted culture with the dilution factor.

2.6.2   Direct cell counts (cfu)

An alternative method for the quantification of cell numbers involved direct cell counts. Bacterial samples were serially diluted 1:10 in PBS in duplicate. 100 μl samples of each dilution were spread using sterile glass beads onto duplicate BHI agar plates containing antibiotics where necessary. After overnight incubation at 37 °C, the number of colony forming units (cfu) were determined.

2.7   Growth experiments

2.7.1 Sulfur source utilization

Strains were streaked from glycerol stocks onto chemically defined media (CDM) plates containing suitable antibiotics and sulfur sources (Chapters 2.1.2 and 2.2.14). After overnight incubation at 37°C, a single colony was inoculated into 5 ml CDM (no antibiotics) supplemented with the suitable sulfur source in a sterile 30 ml universal tube and grown overnight at 37 °C, with aeration on a rotary shaker at 250 rpm. The overnight preculture was used to inoculate 100 ml pre-warmed CDM (no antibiotics) in a 250 ml conical flask to an OD_{600} of 0.01. The 100 ml culture was grown at 37 °C in a Grant OLS 200 water-bath with linear shaking (equivalent to 250 rpm). For growth experiments without *lacZ* fusion analysis, culture OD_{600} was determined in duplicate over a period of 8-10 hours. For growth experiments with *lacZ* fusion analysis, the 100 ml culture was grown to an OD_{600} of approximately 1.0 and used to inoculate a second 250 ml conical flask containing 100 ml CDM (no antibiotics) to an OD_{600} of 0.01. The use of exponential-phase precultures prevented carry-over of preformed β-

galactosidase from stationary phase cultures, as this would affect *lacZ* fusion analysis results. The second 100 ml culture was then grown under the same conditions as the 100 ml preculture. At appropriate intervals over a 24 h period, culture OD_{600} was determined in duplicate and samples for β-galactosidase assays were taken (Chapter 2.8).

2.8   β-galactosidase assays using MUG as a substrate

Liquid culture samples were assayed for β-galactosidase (*lacZ*) production with MUG as substrate, using a method based on that developed by Youngman (1990).   100 µl culture samples were collected in 1.5 ml microfuge tubes at regular intervals from cultures grown as in Chapter 2.7. Following centrifugation (11,000 g, 3 min), supernatants were discarded, and cell-pellets were snap-frozen in liquid nitrogen and stored at -70 °C for later analysis. The cell pellets were thawed at room temperature for 5 min and resuspended in 0.5 ml ABT buffer. 50 ul of freshly prepared MUG (4 mg ml^{-1}) was added and the reactions were mixed by gently inverting the tubes. The reactions were immediately incubated at 25 °C in a water-bath for exactly 60 min. During the reaction, MUG is hydrolysed to β-D-galactopyranoside and 4-methylumbelliferone (MU) by the action of β-galactosidase. MU is a fluorescent compound and is therefore a quantifiable indicator of β-galactosidase activity. The reaction between β-galactosidase and MUG was stopped by adding 0.5 ml 0.4 M Na_2CO_3, and gently inverting the tubes to mix.

250 µl of each sample was pipetted into the top wells of a 96-well microtitre plate (Nunc). 225 µl of ABTN was added to each of the remaining wells to be used. 25 µl was removed from the 250 ul sample and diluted 1:10 by mixing with 225 µl ABTN. Serial 1:100 and 1:1,000 dilutions were then performed. 25 µl was removed from the 1:1,000 dilution well to allow a consistent well volume of 225 ul.

A fluorimeter (Victor^2™, Wallac) was used to measure the fluorescence of each sample (355 / 460 nm, 0.1 sec). The relationship between fluorescence and amount of MU was determined using a calibration curve (Chapter 2.8.1; Figure

69

using the equation shown in Chapter 2.8.1. The amount of MU was then related to β-galactosidase activity using the equation shown below and expressed in MUG units of β-galactosidase activity. 1 MUG unit of β-galactosidase activity is defined as the amount of enzyme that catalyzes the hydrolysis of 1 pmol of MUG per min, per ml of culture, per unit of optical density at 600nm (OD_{600}). The background level of β-galactosidase activity measured from 8325-4 and SH1000 control samples was deducted from the β-galactosidase activity of *lacZ* fusion strains.and the β-galactosidase activity (MUG units) was calculated as follows;

$$\text{pmoles} \times (A / B) / (60 \times OD_{600} \times 0.1) = \text{β-galactosidase activity, } min^{-1} \, ml^{-1} \, OD_{600}^{-1} \text{ (MUG Units)}$$

Where;

pmoles = pmoles MU (see Chapter 2.8.1 and Fig 2.1 for equation to determine amount of MU from calibration curve)

A = Volume of assay (1.05, where cell pellets were resuspended in 0.5 ml ABT buffer and had 50 ul MUG and 0.5 ml Na_2CO_3 added)

B = Volume of sample read in plate (ie. 0.225 where 225 µl sample read)

60 = No. min incubated at 25 °C

OD_{600} = OD_{600} of culture at given time-point

0.1 = Volume of culture sampled (ie. 0.1 ml)

2.8.1 β-galactosidase assay calibration curve

A calibration curve was prepared each time β-galactosidase assays were performed. These were created with the fluorescent product (MU) diluted to a range of concentrations such that the final amount of MU in the 225 µl samples was 625, 250, 125, 62.5, 25, 12.5 and 2.5 pmoles. An example of such a calibration curve is shown in Figure 2.1, for which the equation of the straight

line was y = 1494.4 + 111.74x. For this example, the following equation was used to convert fluorescence readings into pmoles MU.

$$\frac{[(Fluorescence*D) - Background\ fluorescence] - 1494.4}{111.74} = pmoles\ MU$$

D = dilution of samples in microtitre plate wells (eg. 10 for 1:10 dilution)
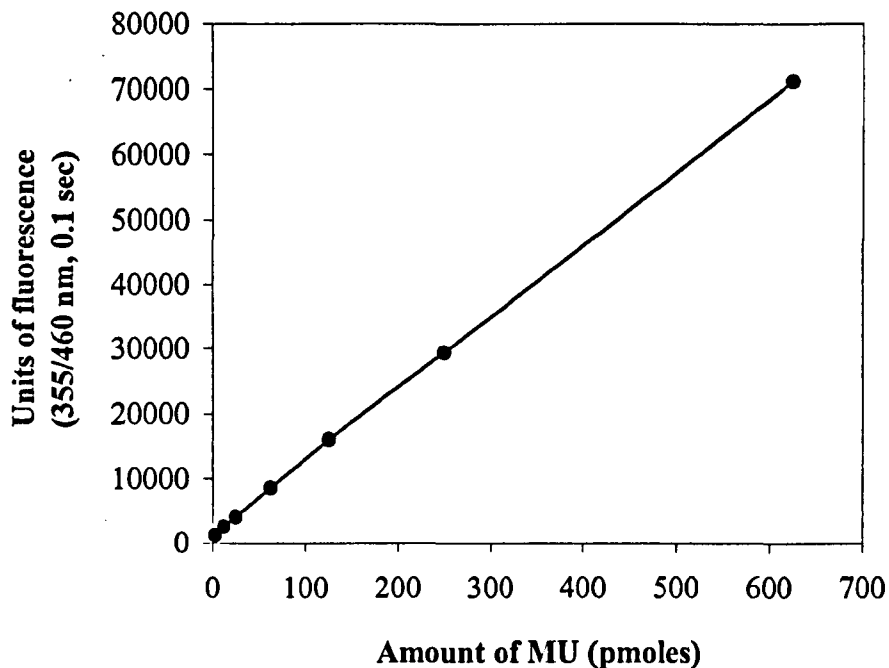
Figure 2.1

Calibration curve of amount of MU against units of fluorescence.

2.9   GGT activity assay using L-γ-glutamyl-p-nitroanilide (GPNA)-Diagnostic Chemicals

GPNA is used as a substrate for measurement of GGT activity because it allows a direct reaction rate measurement without deproteinization or any chemical treatment of the cleavage product, p-nitroaniline. The principle of the reaction is

71

conversion of GPNA and glycylglycine by the action of GGT to p-nitroaniline and L-γ-glutamylglycylglycine (Szasz, 1976). The rate of increase in absorbance at 405nm is due to the release of p-nitroaniline which is directly proportional to the GGT activity.

2.9.1 Preparation of cell free extract – small batch culture

One colony of the *S.aureus* strains was inoculated in 5 ml of CDM with 50 µM glutathione. Cells were harvested by centrifugation at 4,000 rpm, 10min, 4°C and supernatant was discarded. The pellet was washed twice in PBS and resuspended in 500 µl of PBS and transferred into 50 ml fresh CDM containing 50 µM glutathione and incubated at 37°C overnight with shaking (250rpm). Cells were harvested by centrifugation at 4000 rpm, 10min, 4°C and the supernatant was transferred to a sterile tube and frozen at –20°C. The pellet was washed twice in PBS and resuspended to 500 µl in PBS and the bacterial density was measured at 600 nm (OD_{600}). Cultures from all *S.aureus* strains were standardized to the same OD_{600} with PBS. 400 µl culture was transferred to an Eppendorf tube and 100 µl lysostaphin was added and the mixture incubated at 37°C for 2 hours. The mixture was centrifuged at 13 000rpm, 15 min., 4°C and the supernatant (CFE) removed and frozen at –20°C.

2.9.2 GGT activity assay

200 µl of thawed sample was added to 2 ml reagent, mixed and incubated for 3-5 min at 37°C. Absorbance readings were taken at 405nm every minute for the first 5 min. and the change in absorbance per minute was determined (ΔA/min). GGT

activity was calculated using the following equation and is expressed as U/L. In this study GGT activity is expressed as GGT Units (U/L x 100). The DC –TROL Level 1 (Diagnostic Chemicals) was included as a control.

$$GGT(U/L) = \frac{(\Delta A/min\ sample - \Delta A/min\ control) \times 2.2\ ml\ (assay\ volume) \times 1000}{9.9 \times 1\ cm\ (lightpath) \times 0.2\ ml\ (sample\ volume)}$$

$$= \Delta A/min \times 1111\ (factor\ derived\ from\ constants\ in\ the\ equation)$$

GGT Units = GGT (U/L) x 100

2.10   Phage techniques

2.10.1   Preparation of phage lysates

S. aureus strains were used to inoculate 5 ml BHI (containing   relevant antibiotics) in a 30 ml universal tube, and grown at 37 °C (unless otherwise stated) with 250 rpm rotary shaking until in log phase (OD_{600} 0.2 - 0.5). 2-5 ml of cells were recovered by centrifugation (4 000 rpm , 3 min) and resuspended in 5 ml sterile BHI. 5 ml phage buffer and 100 μl phage φ11 or φ85 stock lysate (propagated using *S. aureus* 8325-4 or SH1000 cells) were added to give a cell:phage ratio of approximately 20:1). The tubes were then incubated at 30 °C shaking slowly (50 rpm) for 2 - 4 h, until clear. If cells failed to lyse in this time, they were left overnight (static) at 25 °C. Lysates were filter sterilised (0.2 μm pore size) and stored at 4 °C. The resulting lysates contained between 10^9 and 10^{10} pfu ml^{-1}.

2.10.2   Determination of phage titres

S. aureus 8325-4 or SH1000 was grown in 5 ml BHI at 37 °C with 250 rpm rotary shaking until log phase (OD_{600} ~ 0.5).   Phage lysates were diluted in phage buffer to 10^{-7}. 100 μl of diluted phage was mixed with 50 μl of 1 M $CaCl_2$ and 400 μl of culture, and were incubated for 10 min at room temperature. 5 ml

of phage top agar (cooled to 50 °C), was added to the phage mixture and used to overlay a pre-warmed (~ 60 °C) phage bottom agar plate. After setting (10 min), plates were incubated overnight at 37 °C, after which time the number of pfu ml^{-1} was determined.

2.10.3   Phage transduction

The recipient *S. aureus* strain was inoculated into 100 ml LK broth and incubated overnight at 37 °C with shaking (250 rpm). The cells were harvested by centrifugation (4,000 rpm, 10 min), and resuspended in 5 ml sterile unused LK. 500 μl of cell culture was transferred to a sterile 30 ml universal tube. 500 μl of phage lysate and 1 ml LK (containing 10 mM CaCl$_2$) were then added. After gentle mixing the lysate/cell mixture was incubated statically for 25 min, followed by 15 min with shaking (250 rpm). The temperature used for incubation steps following addition of the lysate was 37 °C unless otherwise stated. 1 ml ice-cold 0.02 M sodium citrate was added and cells were harvested (5000 rpm, 10 min) and resuspended in 1 ml 0.02 M sodium citrate before being left on ice for 2 h.

Using sterile glass beads, 50 μl and 100 μl aliquots of the lysate/cell mixture were spread onto 25 ml LK bottom agar plates containing 0.05 % v/v sodium citrate and inducing levels of Ery (0.15 μg ml^{-1}) where necessary. Plates were incubated for 90 min, and overlaid with 5 ml LK top agar containing relevant antibiotics at 6X their normal selective concentration. After setting (10 min), plates were incubated for 24-72 h. Any resulting colonies were considered putative phage transductants, and were patched onto separate BHI plates containing relevant selective antibiotics to ensure that they possessed the correct resistance profile.

2.11   Transformation techniques

2.11.1   Transformation of _E. coli_

2.11.1.1   Preparation of _E. coli_ Top 10 competent cells (Hanahan, 1983)

A single colony of E. coli Top 10 cells from an overnight LB agar plate was inoculated into 1 ml of SOB and the cells were dispersed by vortexing. This was used to inoculate 100 ml of pre-warmed SOB in a 1 l conical flask. The culture was incubated at 37 °C, with shaking (250 rpm), until an OD_{600} of 0.5 - 0.6 was reached. The culture was divided into 2 X 50 ml centrifuge tubes and chilled on ice for 15 min. The cells were then harvested by centrifugation (5,000 rpm), 15 min, 4 °C), and the pellet was drained (removing all traces of supernatant with a pipette). After resuspension in 33 ml of FSB (16.5 ml per pellet), the two cell suspensions were pooled and incubated on ice for 15 min. The cells were pelleted and drained as before and resuspended in 8 ml FSB and placed on ice. 280 µl of DMSO was added and the sample was mixed by swirling and the tube was incubated on ice for 5 min. A second 280 volume of DMSO was added as before and the tube was incubated on ice for a further 15 min. 200 µl aliquots were pipetted into microfuge tubes, used immediately or snap-frozen using liquid nitrogen and stored at -70 °C. The level of competence of the cells was determined by transformation with a suitable control plasmid (Chapter 2.11.1.3).

2.11.1.2   Preparation of electrocompetent _E.coli_ cells

A single colony of E.coli Top 10 from an overnight LB agar plate was inoculated into 25 ml LB medium. The culture was incubated overnight at 37°C with shaking (250 rpm). This was used to inoculate 500 ml of prewarmed LB in a 2 l conical flask. The culture was incubated at 37°C with shaking (250 rpm) until an OD_{600} 0.4 was reached. The culture was then chilled on ice for 15-30 min and the cells were harvested by centrifugation (2 000 rpm, 15 min, 4°C). The pellet was drained (removing all traces of supernatant with a pipette) and resuspended in 500 ml of cold sterile deionised water. The cells were recovered by centrifugation (2 000 rpm, 15 min, 4°C) and resuspended in 250 ml cold sterile 10% v/v glycerol. The cells were washed in cold sterile 10% v/v glycerol

for at least two more times. Finally pelleted cells were resuspended in 1 ml of cold GYT medium and the OD_{600} was measured at a 1:100 dilution (1 OD600 = ~ 3.5 x 10^8 cells/ml). The suspension was diluted to $3x10^{10}$ cells/ml with GYT medium and 100 µl volumes were aliquoted in 1.5 ml microcentrifuge tubes. The competent cells were used immediately or snap frozen using liquid nitrogen and stored at –70°C. The level of competence of the cells was determined by electrotransformation with a suitable control plasmid.

2.11.1.3 Transformation of Hanahan competent *E. coli* cells by heat-shock

An aliquot of frozen Hanahan competent cells (200 ul) (Chapter 2.10.1.1) was thawed on ice in a pre-chilled microfuge tube. Up to 50 ng of DNA (in a volume of up to 20 µl) was added, and the mixture was incubated on ice for 45 min. The tube was then incubated at 42 °C for 90 sec and immediately returned to the ice for a further 2 min. 800 µl SOC was added to the cells, which were incubated for 1 hr at 37 °C with shaking at 250 rpm to allow expression of plasmid encoded antibiotic resistance markers. A 200 µl aliquot of transformed cells were spread using sterile glass beads onto an LB agar plate containing appropriate antibiotics. The remainder of the cells were recovered by centifugation at 4 000, 5 seconds and most of the supernatant was removed so that only approximately 200 µl remained. The pellet was then resuspended in the residual volume of supernatant and the whole of the sample was spread onto an LB agar plate as before. The plates were then incubated at 37 °C for 18 - 48 h.

2.11.1.4 Transformation of electrocompetent *E.coli* cells

An aliquot of electrocompetent cells (100 µl) (Chapter 2.11.1.2) was thawed on ice in a pre-chilled microcentrifuge tube. Up to 50 ng of DNA (in a volume of up to 20 µl) was added, mixed and transferred to a 0.1 cm gap cuvette (BioRad). The plasmid/cell mixture was electroporated at 100 ohms, 25 µF and 1.25kV using a BioRad Gene Pulser. The cells were recovered by adding to the cuvette 1 ml of prewarmed LB and transferred to a microcentrifuge tube before being incubated at 37°C with shaking for 1 hour. A 200 µl aliquot of recovered cells

was spread using sterile glass beads onto an LB plate containing appropriate antibiotics. The plate was then incubated at 37°C overnight.

2.11.2   Transformation of *S. aureus*
2.11.2.1   Preparation of *S. aureus* electrocompetent cells

A single colony of *S. aureus* RN4220 was used to inoculate 10 ml BHI medium and incubated overnight at 37 °C with shaking (250 rpm). 2 ml of culture was used to inoculate 1 l of fresh BHI in a 2 l conical flask and grown at 37 °C with shaking (250 rpm) until late log phase (OD_{600} 0.5 - 1.0). Cells were harvested by centrifugation at 5 000 rpm, 10 min, 4°C and washed on ice 3X with 300 ml prechilled sterile distilled water (4 °C). Cells were then concentrated in a series of harvesting 5 000 rpm 10 min, 4 °C, and gentle resuspension steps using the following volumes of 10 % v/v ice-cold glycerol: i) 100 ml; ii) 50 ml; and iii) 25 ml. All of the supernatant was removed after each spin. The cells were finally resuspended in 1.25 ml 10 % v/v ice-cold sterile glycerol. Cells were snap-frozen in liquid nitrogen and stored at -70 °C. The level of competence of the cells was determined by electroporation with a suitable control plasmid (Chapter 2.10.2.2).

2.11.2.2   Transformation of *S. aureus* by electroporation

5-20 μg of plasmid DNA was precipitated by isopropanol precipitation (Chapter 2.11.4), and washed twice with 70 % v/v ice-cold (-20 °C) ethanol, ensuring the complete removal of salt. The DNA was then resuspended in 100 μl of sterile dH_2O and transferred to a 0.1 cm gap cuvette (BioRad). 2×10^{10} - 2×10^{11} competent cells, which had been thawed for 5 min at room temperature were then added to the cuvette. The plasmid/cell mix was electroporated at room temperature at 100 ohms, 25 μF and 1.25 kV using a BioRad Gene Pulser. Cells were recovered by adding 1 ml of pre-warmed B2 (containing an inducing concentration of Ery, ie. 0.15 μg ml^{-1}, where appropriate) to the cuvette. Cells were then transferred to a sterile 2 ml microfuge tube and incubated at 37 °C

with shaking (250 rpm) for 2 h. A 200 µl aliquot of recovered cells was spread using sterile glass beads onto a BHI plate containing appropriate antibiotics. The remainder of the cells were recovered by centifugation at 4 000, 5 seconds and most of the supernatant was removed so that only approximately 200 µl remained.   The pellet was then resuspended in the residual volume of supernatant and the whole of the sample was spread onto a BHI plate as before. The plates were then incubated at 37 °C for 18 - 48 h.

2.12   DNA purification techniques

2.12.1   Genomic DNA preparation

Genomic DNA was isolated and purified from *S. aureus* using a QIAGEN DNeasy^{TM} kit using a method based on the manufacturer's instructions. A single colony of *S. aureus* was used to inoculate 5 ml of BHI in a 30 ml sterile universal tube and grown overnight at 37 °C with shaking at 250 rpm. 1.25 ml of cells was harvested by centrifugation 4,000 rpm, 15 min. 180 ul QIAGEN Buffer B1, 10 µl RNAse A (10 mg ml^{-1}) and 5 µl lysostaphin (5 mg ml^{-1}) were added and used to resuspend the cell pellet. After incubation at 37 °C for 30 min, the protocol was continued as per the manufacturer's instructions. Genomic DNA was eluted into clean 1.5 ml microfuge tubes using two 200 µl aliquots of buffer AE, and the two eluates were pooled. Genomic DNA was concentrated by isopropanol precipitation (Chapter 2.12.4). The DNA was dissolved in 20 µl QIAGEN Buffer EB overnight at 4 °C, and stored at this temperature.

2.12.2   Small scale plasmid preparation from *E. coli*

A single colony of the *E.coli* Top 10 plasmid-bearing cells was used to inoculate 5 ml LB containing appropriate antibiotics. The culture was incubated overnight at 37 °C with shaking at 250 rpm, and the cells were harvested (4 000 rpm, 5 min). Plasmid DNA (up to 20 µg) was isolated and purified using a QIAprep Spin Miniprep kit DNA purification system (QIAGEN) according to the manufacturer's instructions. Plasmid DNA was eluted using 50 µl of Buffer EB into a clean 1.5 ml microfuge tube and stored at -20 °C.

2.12.3 Large scale plasmid preparation from *E. coli*

Large amounts of plasmid DNA (up to 500 µg) were isolated from *E. coli* using a Plasmid Maxi kit DNA purification system (QIAGEN). A single colony of plasmid-containing cells of *E. coli* Top 10 from an overnight LB agar plate containing appropriate antibiotics was used to inoculate 5 ml LB broth containing antibiotics where necessary. The culture was grown for 8 h at 37 °C with shaking at 250 rpm. The whole culture was used to inoculate 500 ml LB (containing appropriate antibiotics), and grown overnight at 37 °C with shaking at 250 rpm. The cells were harvested by centrifugation at 6,000 g, 15 min, 4 °C. The protocol was then continued as per the manufacturer's instructions. Purified plasmid DNA was resuspended in an appropriate volume of TE and stored at -20 °C.

2.12.4 Isopropanol precipitation of DNA

DNA was precipitated by the addition of an equal volume of isopropanol and a 1/10 volume of 3 M sodium acetate (pH 5.2). The mixture was vortexed and incubated at room temperature for 2 min. The precipitated DNA was recovered by centrifugation at 11,000 g, 10 min and the pellet was washed with 500 µl ice-cold 70 % v/v ethanol. The DNA was harvested by centrifugation 11,000 g, 5 min, and the 70 % v/v ethanol wash step was repeated. The pellet was air-dried, and the DNA was dissolved in an appropriate volume of TE and stored at -20 °C.

2.12.5 Gel extraction of DNA using a QIAquick spin column

The DNA was excised from the 1% w/v agarose gel with a clean, sharp scalpel. The gel slice was weighed and 3x volume of Buffer QG (Qiogen kit) was added. The suspension was incubated at 50°C for 10 min (or until the gel had completely dissolved). The solution was applied to a QIAquick column and centrifuged (13 000 x g, 1 min). The flow through was discarded, and the column washed with 0.75 ml Buffer PE (Qiagen kit). The column was centrifuged as before, and the flow through discarded, and the column was

centrifuged again as before. The QIAquick column was placed in a clean 1.5 ml micro-centrifuge tube and the DNA was eluted with 30 µl buffer EB (Qiagen kit). The column was left to stand at RT for 1 min, and then centrifuged as before and the recovered DNA was stored at –20°C.

2.12.6 Purification of PCR products using a QIAquick spin column

5x volume of Buffer PB (Qiagen kit) was added to 1x volume of the PCR reaction, and mixed. A QIAquick spin column was placed in the provided 2 ml collection tube. The Buffer PB and PCR mixture was applied to the column and centrifuged at 13 000 rpm for 30 – 60 sec. The flow through was discarded and the column placed back in the same collection tube. The column was washed with 0.75 ml Buffer PE (Qiagen kit) by centrifugation (as before). The flow-through was discarded and the column placed back in the same collection tube and centrifuged (13 000 rpm) for 2 min. The QIAquick column was placed in a 1.5 ml clean microcentrifuge tube to elute the DNA by adding 30 µl buffer EB (Qiagen kit). The column was left to stand at RT for 1 min, and then centrifuged as before, and the eluate was stored at –20°C.

2.13 Quantification of DNA

To quantify the concentration of DNA in a solution, spectrophotometric measurements were performed at 260 nm. An OD_{260} of 1 corresponds to approximately 50 µg ml⁻¹ for double stranded DNA, and approximately 20 µg ml⁻¹ for single stranded oligonucleotides. OD_{260} measurements were taken using a Shimadzu UV-2401PC spectophotometer. Alternatively, the concentration of DNA could be estimated by agarose gel electrophoresis (Chapter 2.14.5). This involved comparing the intensity of ethidium bromide stained bands to bands of molecular weight markers containing known amounts of DNA (Table 2.5).

Standard mDNA size markers (bp)		
	1 kb DNA ladder	λ HindIII/EcoRI
	10,000	21,226
	8,000	5,148
	6,000	4,973
	5,000	4,268
	4,000	3,530
	3,500	2,027
	3,000*	1,904
	2,500	1,584
	2,000	1,375
	1,500	947
	1,000	831
	750	564
	500	
	250	

Table 2.5

The size of DNA fragments used as size markers for agarose gel electrophoresis.

*The 3,000 bp band of 1kb generuler contains ~ 147 ng DNA per 10 ul marker.

2.14   *In vitro* DNA manipulation techniques

2.14.1   Polymerase chain reaction (PCR) techniques

2.14.1.1   Primer design

The primers used for PCR amplification were short synthetic oligonucleotides (19 - 32 bp) that were based on DNA sequences from published studies or obtained from cloning vector information and *S. aureus* databases (http://www.ncbi.nlm.nih.gov/ and http://www.genome.ou.edu/staph.html). Suitable restriction sites were introduced where necessary at the 5' ends of primers to enable subsequent cloning. The primers used in this study are shown

2.6. Oligonucleotide primers for PCR and sequencing reactions were all synthesized at Sheffield University coordinated by Dr. Athur Moir.

Primer	Primer sequence (5' → 3')	Source / Reference
BAC RMH F	ACT TGT CGA CGA TAC TGG TAA CG	Garcia-Lara, J Personal communication
BAC RMH R	TAC TAC ACT CAA GCA TCA CTC	
loch λ 1F	TGG CAA CGC CAT GGA TGC CGT GAT TGC AAT TCA ACT GGC ATT GAA TTA CAT CCT ATT CAC AAT CG	This study
loch λ 2R	TTC CCT CGT ATC ATC AGC ACC TCC CGA CGC GTC ACG TGT ATT TTA GAA ATC CCT TTG AGA ATG	This study
loch λ 3F	TGG CAA CGC CAT GGA TGC CGT GAT TGC AAT TCA ACT GGC ATT GAA TTT TAT GAC CGA TGA AC	This study
loch 4 F with HINDIII	AGT AT<u>A AGC TT</u>G ATC CGA ATA ATG CAT TGT C	This study
loch 5F with Kpn I	AGT TA<u>G GTA CCC</u> ATG TCG ATT TAC CAT CTA TG	
loch 6R with BamHI	TAT AA<u>G GAT CCC</u> AGT AAT GCA TCA ACA AAG G	This study
loch 7R with Kpn I	GAT AT<u>G GTA CCC</u> ATA GAT GGT AAA TCG ACA TG	
loch 8F with EcoRI site	AGT AT<u>G AAT TCG</u> ATC CGA ATA ATG CAT TGT C	This study

82

loch 9F	TTG TAT CAC AAG GCA TTT TAC AAG TTT G	This study
loch 10R with BamHI	ATA TA<u>G</u> <u>GAT</u> <u>CC</u>T CTG GCA TAT AAG ATG G	
loch 11F	AAT TGT GAG CCG CTC ACA ATT AAG CTT GCC	This study
loch 12F	TTT TTT CCA TGG CGA TGA CTG AAA TAG ATT TTG AT	This study
loch 13R	TTT TTT CTC GAG AGC TTG ATC GTT TAA ATG TTC	This study
lochpB1(F)	ATGACTGAAAATAGATTTTGATATAGC	This study
lochpB1(R)	TTAAGCTTGATCGTTTAAATGTTC	This study

Table 2.6

Synthetic oligonucleotides used as primers for PCR amplification of DNA fragments in this project.

Relevant restriction sites are underlined.

2.14.1.2   DNA amplification

2.14.1.2.1   *Taq* polymerase

Where accurate amplification was not required, standard PCR amplification reactions were performed using *Taq* polymerase (Promega). The following components were added, on ice, to a 0.5 ml thin-walled PCR tube.

Template DNA	100 - 500 ng
Forward primer	300 nM*
Reverse primer	300 nM*
10X Taq PCR buffer (Promega)	10 µl
MgCl$_2$	1.5 - 4.5 mM*
dNTPs	0.2 mM*

Taq DNA polymerase	0.5 µl (2.5 Units)
dH$_2$O	to 100 µl

*final concentration.

PCR amplification was carried out using an Eppendorf 5330 Mastercycler. The lid was heated to 106 °C for the duration of the PCR amplification, and the block was pre-heated to 95 °C. The following thermal cycling programme of 30 cycles of steps 2 - 4 was used:

1) Denature	95 °C; 5 min
2) Denature	95 °C; 30 sec
3) Anneal	50-55 °C; 30 sec
4) Extension	72 °C; t min (t=1 min kb^{-1} + 10 %)
5) Extension	72 °C, 20 min

PCR products were stored at -20 °C.

2.14.1.2.2 *Pwo* polymerase

DNA amplifications of < 3 kb that required 3'-5' proof-reading activity were performed with Pwo polymerase (Roche).

The following Master mixes were made on ice:

Master mix 1:

Template DNA	0.1 - 0.75 µg
dNTPs	0.2 mM*
Forward primer	300 nM *
Reverse primer	300 nM *
dH$_2$O	to 50 µl

Master mix 2:

10X PCR buffer with 20 mM MgSO$_4$	10 µl
Pwo polymerase	0.5 µl (2.5 Units)
dH$_2$O	to 50 µl

*final concentration

Master mix 1 and 2 were combined on ice in a 0.5 ml thin-walled PCR tube and cycling immediately commenced.

PCR amplification was performed using an Eppendorf 5330 Mastercycler. The lid was heated to 106 °C for the duration of the PCR amplification, and the block was pre-heated to 94 °C. Once the tubes were added, the DNA was denatured at 94 °C for 2 min, followed by 10 cycles of programme A, then 20 cycles of programme B:

Programme A :

Denature	94 °C; 15 sec
Anneal	45-65 °C; 30 sec
Extension	72 °C; t min (t = 45 sec kb^{-1})

Programme B :

Denature	94 °C; 15 sec
Anneal	45-65 °C; 30 sec
Extension	72 °C; t min (t = (45 sec kb^{-1}) + 5 sec per cycle)

Once all the cycles were complete a final step of 72 °C for 7 min was added to allow complete extension of the primers. The PCR products were stored at -20 °C.

2.14.1.2.3 Expand™ Long Template PCR system

DNA amplifications of >3 kb, that required 3'-5' proof-reading activity were performed with the Expand™ Long Template PCR system (Roche). This system is composed of a unique enzyme mix containing the thermostable Taq and Pwo polymerases, and is optimised for amplifying fragments of up to 27 kb in length.

The following Master mixes were made on ice:

Master mix 1:

Template DNA	10 - 500 ng
dNTPs	350 uM*
Forward primer	300 nM*
Reverse primer	300 nM*
dH$_2$O	to 25 µl

Master mix 2:

10X PCR buffer with 1.75 mM MgCl$_2$	5 µl
Expand™ polymerase	0.75 µl
dH$_2$O	to 25 µl

*final concentration

Master mix 1 and 2 were combined on ice in a 0.5 ml thin-walled PCR tube and cycling immediately commenced.

PCR amplification was carried out using an Eppendorf 5330 Mastercycler. The lid was heated to 106 °C for the duration of the PCR amplification, and the block was pre-heated to 94 °C. Once the tubes were added, the DNA was denatured at 94 °C for 2 min, followed by 10 cycles of programme A, then 20 cycles of programme B:

Programme A :

Denature	94 °C; 10 sec
Anneal	65 °C; 30 sec
Extension	68 °C; t min (t = 40 sec kb^{-1})

Programme B:

Denature	94 °C; 10 sec
Anneal	50-55 °C; 30 sec
Extension	68 °C; t min (t = (40 sec kb^{-1}) + 20 sec per cycle)

Once all cycles were complete a final step of 68 °C for 7 min was added to allow complete extension of the primers. The PCR products were stored at -20 °C.

2.14.1.2.4   PCR screening of *E. coli* cells

Putative *E. coli* transformants were patched using sterile toothpicks onto LB agar plates containing appropriate antibiotics and grown overnight at 37 °C. A small amount of each patched positive clone was transferred to a PCR tube containing the PCR mix as in Chapter 2.14.1.2.1 (minus the DNA). The PCR programme followed was as in Chapter 2.14.1.2.1 with the tubes heated to 95 °C initially for 10 min to ensure lysis of the cells and release of DNA. The PCR products were visualised by agarose gel electrophoresis (Chapter 2.14.5) and putative positive clones were chosen for further screening using small scale plasmid preparations (Chapter 2.12.2) and restriction digestions (Chapter 2.14.2).

2.14.2   DNA restriction

DNA restriction digests were performed in volumes from 20 - 100 µl. They were prepared as follows:

Restriction enzyme buffer	10 % v/v

| Restriction enzyme(s) | up to 10 % v/v |
| DNA | up to 80 % v/v |

Where appropriate the reaction volume was made up with dH_2O. The restriction digests were incubated at 37 °C for between 2 h and 16 h. Before digested DNA was used for further manipulation, it was purified using a QIAGEN PCR purification kit (Chapter 2.12.6) or separated using agarose gel electrophoresis (Chapter 2.14.5) and purified using a QIAquick gel extraction kit (Chapter 2.12.5).

2.14.3   Alkaline phosphatase treatment of restriction-digested plasmids

The 5' ends of plasmids digested with only one restriction enzyme were dephosphorylated using Calf Intestinal Alkaline Phosphatase (CIAP) (Promega) to reduce vector re-ligation in subsequent cloning steps. The following were added on ice:

Digested plasmid DNA	up to 5 µg
10X reaction buffer (Promega)	10 µl
CIAP	0.01 U per pmol of ends*
dH_2O	to 100 µl

*the number of picomoles of ends for a given sample of digested plasmid was calculated using the following equation;

(µg DNA / kb size of DNA) X 3.04 = pmol of ends

The mixture was incubated for 30 mins at 37 °C. A second aliquot of CIAP (0.01 U per pmol of ends) was added and the sample was incubated for an additional 30 mins at 37 °C. To stop the reaction, 2 µl of 0.5 M EDTA was added and the mixture incubated at 65 °C for 20 min. The DNA was purified and

concentrated using a QIAquick PCR purification kit (Chapter 2.12.6) prior to use in a ligation reaction.

2.14.4   DNA ligation

The following were added on ice:

Digested plasmid DNA	100 ng
Digested DNA insert	x ng*
10X DNA ligase buffer (Promega)	2 µl
T4 DNA ligase (Promega)	1 µl

*the amount of insert added was calculated using the following equation to allow a 1:1 and 1:3 molar ratio of vector:insert to be used;

$$\frac{100 \text{ ng of plasmid} \quad X \quad \text{kb size of insert}}{\text{kb size of plasmid}} \quad X \quad \text{molar ratio of} \quad \frac{\text{insert}}{\text{plasmid}} = \frac{\text{ng of insert}}{\text{plasmid}}$$

The reaction was made up to 20 µl with dH_2O and incubated overnight at 14 °C. The completed ligation mix was then used to transform *E. coli* (Chapter 2.11.1.4).

2.14.5   Agarose gel electrophoresis

DNA fragments were separated by horizontal gel electrophoresis using various size electrophoresis tanks (Life Technologies). Appropriate volumes of agarose gel (0.8 - 4 % w/v dissolved in TAE by microwaving) were submerged in suitable volumes of TAE electrophoresis buffer. The gel contained 0.2 µg ml^{-1} ethidium bromide. DNA samples were mixed with 1/5th their volume of 6X DNA loading buffer and loaded into wells in the gel. The gel was run at 80 - 120 V for 1 - 2 h and visualised by means of a UV transilluminator at 260 nm. To estimate the sizes of DNA fragments, DNA markers were also loaded into the gel. These included pUC mix markers (MBI Fermentas), Generuler^{TM} 1 kb DNA ladder (MBI

Fermentas), or genomic DNA digested with *HindIII* and *EcoRI* (MBI Fermentas) (Table 2.6).

2.14.5.1   Agarose gel photography

A permanent record of agarose gels was obtained by photographing the ethidium bromide-stained gels illuminated from below with UV light at 260 nm. A Kodak 203 red-orange filter, and Polaroid 667 (ASA 3000) film were used. In addition, photographs were scanned using a UMAX Powerlook 1100 for a permanent electronic record.

2.15   DNA Hybridisation techniques

2.15.1   Labelling of DNA probes with digoxigenin

DNA fragments were labelled by a random priming method using a commercially available digoxigenin (DIG) DNA labelling and detection kit (Roche). DNA to be labelled (up to 3 µg in a maximum of 15 µl EB in a microfuge tube) was denatured at 100 °C for 10 min, then immediately chilled on ice for 10 min. The following components were added on ice;

Random hexanucleotide mixture	2 µl
dNTP labelling mixture (containing DIG-dUTP)	2 µl
Klenow enzyme (2 units)	1 µl

The volume of the reaction was made up to 20 µl with dH_2O. The reaction was incubated overnight at 37 °C, followed by purification using a QIAquick PCR purification kit (Chapter 2.12.6).   The purified probe was then quantified (Chapter 2.15.2).

2.15.2   Quantification of DIG-labelled DNA probes

The amount of DIG-labelled material in a volume of labelled DNA was determined by comparison to labelled control DNA of known concentration supplied in the DIG DNA labelling and detection kit (Roche). The sample DNA

and the control DNA were diluted according to the manufacturer's instructions, using a single pre-dilution step to obtain an estimated concentration of 1 ng ul^{-1}, followed by five serial 10-fold dilutions. 1 µl of each 10-fold dilution was spotted onto Hybond-N+ Extra (positively charged) nylon membrane (Amersham Life Sciences). The DNA was permanently bound to the membrane using a UV crosslinker (Chapter 2.15.3.1) and DIG-labelled DNA was then detected immunologically, using AP-linked anti-dioxygenin antibody (Chapter 2.15.3). The spot intensities of the control and probe dilutions were compared visually to estimate the concentration of the probe.

2.15.3   Southern blotting

Agarose gel electrophoresis of ~ 1 ug samples of digested genomic DNA was performed and photographed as described in Chapters 2.13.5 and 2.13.5.1 with a 0.8 % (w/v) agarose gel. DIG-labelled λ HindIII /EcoRI markers were loaded into the gel to estimate the size of DNA bands following development of the blot using AP-conjugated anti-DIG antibody. The gel was soaked in Southern depurination solution for 10 min and washed in dH_2O. The gel was soaked in Southern denaturation buffer twice for 15 min and rinsed in dH_2O. The gel was neutralised by soaking in Southern neutralisation buffer twice for 15 mins. The DNA was transferred from the gel to a Hybond-N+ Extra membrane by vacuum blotting at 60 mbar for 90 mins using transfer buffer.

2.15.3.1   Fixing the DNA to the membrane

DNA was fixed to the Hybond-N+ Extra nylon membrane with the use of a UV crosslinker (Amersham Life Sciences RPN 2500), 70 mJ / cm^2; 15 sec).

2.15.3.2   Prehybridisation and hybridisation

Membranes to be probed with the DIG-labelled DNA were prehybridised for 2 h at 68 °C in pre-hybridisation solution (20 ml per 100 cm^2 of membrane). Just prior to use, the labelled probe (Chapter 2.15.1) was denatured in a microfuge tube by placing the tube in a boiling water bath for 10 min. The labelled probe

was immediately chilled on ice for 10 min and added to pre-heated hybridisation solution to give a final probe concentration of 5 - 25 ng ml^{-1}. The membrane was then hybridised with the labelled probe overnight at 68 °C. After hybridisation the solution was retained for future use and stored at -20 °C. Unbound probe was removed by washing the membrane twice in 2X wash solution for 5 min at room temperature. The membrane was then washed twice in 0.5X wash solution for 5 min at 68 °C.

2.15.3.3 Colorimetric detection of DIG-labelled DNA

The hybridised and washed membranes were equilibrated with washing buffer for 1 min and then blocked for 30 min with gentle rocking in blocking solution. The membrane was then transferred to antibody solution containing a 1:5,000 dilution of stock anti-DIG-AP antibody (Roche). After 30 min incubation with gentle rocking, the membrane was washed twice for 15 min with washing buffer. The membrane was equilibrated for 2 min with detection buffer before 10 ml colour substrate solution was applied to the membrane. This was then incubated in the dark to allow the membrane to develop. The presence of anti-DIG-AP bound to DIG-labelled DNA was visualised by the appearance of purple bands or spots. After the colour had developed sufficiently, the membrane was washed in 1X TE for 5 min to stop the reaction. The membrane was then air-dried, scanned using a UMAX Powerlook 1100 and stored in the dark.

2.16 Analysis of lacZ fusion expression

2.16.1 *lacZ* expression on X-Gal plates

β-galactosidase activity was detected directly on solid media using the substrate X-Gal. X-Gal is hydrolysed by β-galactosidase resulting in β-D-galactopyranoside and 5-bromo-4-chloro-3-indolyl. The latter has a blue colouration and is thus a visible indicator of β-galactosidase activity. Unless

otherwise stated, 100 µl 20 mg ml⁻¹ X-Gal solution was pipetted onto agar plates and spread across the surface with sterile beads. The beads were then removed and the plates were dried at 50 °C for 20 min. Plates were used immediately or stored at -4 °C for up to one week.

2.17   Sequence and database analysis
2.17.1   Sequence for cloning

DNA sequences for cloning were obtained from the National Centre for Biotechnology Information (NCBI) database (http://ncbi.nlm.nih.gov/), or from manufacturer's instructions (ie. supplied by Invitrogen and Epicentre for use of PCR-II-TOPO and pMOD(MCS) respectively). Putative open reading frames (ORFs) and restriction sites were identified in DNA sequences using the Gene Jockey II program (Biosoft) or the program Visual Cloning 2000 (Redasoft). Diagrammatic representations of DNA fragments and plasmids were prepared using Visual Cloning 2000 (Redasoft).

2.18   Microscopy
2.18.1   Transmission electron microscopy (Robards et al., 1999)

S. aureus SH1000 were grown in 10 ml CDM with and without 50 µM K_2TeO_3 and incubated at 37°C with shaking (250rpm) overnight. Cells were harvested at 4 000 rpm for 15 min at 4°C, washed twice in PBS and cell pellets were fixed in Karnovsky's fixative in 100 mM sodium cacodylate buffer for 3 h at 4°C. The specimens were then washed 3 times (30 min intervals each) in 100 mM sodium cacodylate buffer containing 10 % w/v sucrose at 4°C. Secondary fixation was performed in 2 % w/v osmium tetroxide for 1 h at room temperature (Hayat, 1981). The specimens were then dehydrated through a graded series of ethanol (75 % v/v, 15 min; 95 % v/v, 15 min; 100 % v/v, 15 min; 100 % v/v, 15 min; 100 % v/v, 15 min), and dried over anhydrous copper sulphate for 15 min at room temperature. They were then placed in 2 changes (15 min each) of an intermediate solvent, propylene oxide followed by infiltration with propylene-oxide-Spurr resin (50:50) overnight at room temperature. The specimens were then placed in Spurr resin for 6-8 h at room temperature after which they were

embedded in fresh Spurr resin for 8 h at 70°C (Glauert, 1974). Ultrathin sections (approx. 70-90nm) were cut on a Reichert Ultracut E ultramicotome and stained for 15 min with 3 % w/v uranyl-acetate-50 % ethanol v/v ethanol followed by staining with Reynold's lead citrate for 2 min. The sections were examined using a Phillips CM10 Transmission Electron Microscope at an accelerating voltage of 80 kV. Electron micrographs were recorded on Kodak 4489 Electron Microscope Film.

2.19   Purification and identification of tellurite reductase protein.

2.19.1   Growth of cultures for protein production

S. aureus SH1000 was grown in 3 sterile 2 liter flasks each containing 500 ml TSB at 37 °C with rotary shaking (250 rpm) overnight. Cells were harvested by centrifugation using the Beckman (JA 10.5) at 5000 g for 10min at 4°C. The pellets were combined and resuspended in 15 ml of 20mM Tris HCl pH 7.5.

2.19.1.1   Preparation of cell free extract

2.19.1.2   Cell lysis using lysostaphin

30 µl of lysostaphin was added to 3 ml of the sample and incubated at RT for 15 min. 60 µl PMSF was added and the mixture was centrifuged at 20 000 x g, 20 min, 4°C. The supernatant (CFE) was carefully transferred to a clean tube, filtered through a 0.2 µm (Millipore) filter into a clean sterile tube and stored in – 20°C.

2.19.1.3   Cell breakage using the Braun Homogenizer

7 ml aliquots of the sample were the placed in Braun Homogenizer bottles each containing 50 g microglass beads(< 106 µm) which were precooled at 4°C. Cell breakage was performed using a Braun Homogenizer where each bottle was shaken 6 times at 30 seconds per bottle. Liquid CO_2 was used to cool the system during cell breakage and bottles were kept immersed in ice after cell breakage. Small aliquots of (1-2 ml) of 20mM Tris HCl were added to the microglass beads in a vacuum filter to remove the extract. RNase, DNase and PMSF were each

added to the extract to a final concentration of 1 mM and the mixture was incubated at 37°C for 30 minutes. The suspension was then centrifuged at 20 000 g for 15min at 4°C and the supernatant was then removed, filtered through a 0.2 μm filter and an aliquot was saved (uCFE). The remaining sample was dialyzed in 4 liters 10 mM Tris HCl pH 7.5 with 1 mM 2-mercaptoethanol at 4°C overnight. This dialysed crude cell free extract (CFE) was the frozen at –20°C.

2.19.2   Determination of tellurite reductase (TR) activity

2.19.2.1   Spectrophotometric assay

Reaction mixture

20mM Tris-HCl, pH 7.5	125 μl
20mM NADH	50 μl
100mM 2-mercaptoethanol	2.5 μl
50mM K_2TeO_3	5 μl
Cell free extract	200 μl

Reaction mixture was incubated at 37°C for 15minutes. The reaction was stopped with 382.5 μl 2M NaCL and 382.5 μl distilled water and absorbance read at 500nm against dH_2O. A_{500} reading was multipled by 3 (dilution factor). The NADH in the reaction mixture was replaced with equal volume of dH_2O in the control for each sample.

2.19.3   Protein determination

2.19.3.1   Bovine serum albumin standard (1.44mg/ml)

A protein standard curve using the protein standard (BSA) was performed with each sample analysis. Protein standards were prepared as in Table 2.7

Protein standard concentration (µg)	Volume of BSA (µl) + Volume of dH₂O (µl)
0 (Blank)	0 + 100
2	1.4 + 98.6
5	3.5 + 96.5
10	7.0 + 93.0
20	14.0 + 86.0

Table 2.7

Protein standards used in BioRad/Bradford assay. Bovine serum albumin (1.44 mg/ml) was diluted in dH₂O to final concentrations of 2, 5, 10 and 20 µg/µl and the absorbance measured at 595 nm (A_{595}). A standard protein curve was plotted using the readings and used to determine the protein concentration in sample.

2.19.3.2 BioRad protein assay

2.19.3.2.1 Protein determination

10 µl of sample was made up to 100 µl with dH₂O. 700 µl dH₂O was added to all tubes including the protein standards. This was gently mixed and 200 µl of BioRad reagent mix was added to all tubes and mixed gently. Absorbance measurements were taken at 595 nm (A_{595}) after 2 minutes incubation at room temperature against the blank. A standard protein graph was plotted and used to determine the protein concentration of the sample in the assay mixture that was multiplied by 10 (dilution factor) to obtain the final protein concentration in the sample (µg/µl).

2.19.3.3   Bradford protein assay

2.19.3.3.1   Protein determination

10 µl of sample was made up to 100 µl with dH₂O. 1.5 ml Bradford reagent was added to each 50 µl sample and 50 ul of each protein standard, mixed and absorbance measurements were taken at 595 nm (A_{595}) after 5 minutes incubation at room temperature against the blank. A standard protein graph was plotted and used to determine the protein concentration of the sample in the

assay mixture that was multiplied by 10 (dilution factor) to obtain the final protein concentration in the sample (µg/µl).

2.19.3.4   Calculation of specific activity (U/L)

The A_{500} and A_{595} readings obtained in 2.19.2.1 and 2.19.3. were used to calculate the specific tellurite reductase (TR) activity (Units) as follows:

1. $\Delta A_{500} = A_{500}\text{sample} - A_{500}\text{control}$
2. $\Delta A_{500} / 15\text{min} = \mathbf{A\ min^{-1}}$
3. Protein concentration in 1 µl sample = <u>$\mathbf{B\ \mu g \times 200\ (sample\ volume)}$</u>

$$\hspace{8cm} \mathbf{1000}$$

$$= \mathbf{C\ mg}$$

4. Specific Activity (U) $= \mathbf{A / C}$

$$= \mathbf{D\ min^{-1}\ mg^{-1} / 0.001^{a}}$$

$$= \mathbf{E}$$

[a] 1 Unit (U) of specific TR activity is defined as a 0.001 change in absorbance at 500 nm (A_{500}) per min per mg protein.

2.19.4 Gel submersion assay
2.19.4.1 TR reaction mixture

10mM Tris-HCl, pH 7.5	100 ml
2-mercaptoethanol	7.0 µl
NADH	0.071 g
K_2TeO_3	0.254 g

2.19.4.2   7.5% Native-PAGE protein analysis

Protein samples prepared from *S. aureus* strains were visualized using 7.5% native polyacrylamide gel electrophoresis (native-PAGE). The gels were cast using the BioRad Mini-Protean 3® cell system according to the manufacturer's instructions. 7.5 % v/v polyacrylamide gels were used for the resolving portion of

the gel and 4 % v/v polyacrylamide gels were used for the stacking portion of the gel (Chapter 2.2.19.4).

Protein samples were mixed with equal volume of native-PAGE sample buffer (1:2 ratio) and applied to the wells in the gel in duplicate using a micropipette as depicted in Figure 2.1. The gels were electrophoresed at 150 V for 50-60 min, or until the blue dye front of the sample buffer was at the base of the gel plates. The gels were carefully removed from the apparatus and cut in half for staining.

2.19.4.2.1 Coomassie Blue stain for protein identification

One half of the gel (Portion A) was placed in 30 ml Coomassie stain for 30 min at room temperature with gentle rocking. The Coomassie stain was then removed and the gel was washed 3X, 5 min with 50 ml of destaining solution at room temperature with gentle rocking. After the third wash the gels were left in 50 ml destaining solution until the blue bands of the proteins were apparent and the gel background was colourless. The destaining solution was discarded and the gels were washed twice (10 min) with dH_2O at room temperature with gentle rocking. The gel was then removed from the solution and placed between two DryEase™ minicellophane (Invitrogen) sheets which had been pre-soaked in 20 ml Gel-Dry™ gel drying solution (Invitrogen) for 5 min. The sandwich was then fastened into a gel drying frame (Novex) and left to stand on the bench overnight to dry. For a permanent electronic record, protein gels were scanned using an Epson Scanner.

2.19.4.2.2 Gel submersion assay for tellurite reductase (TR) activity

The other half of the gel (Portion B) was immersed in 100mL of tellurite reductase mixture (2.19.4.1) for the Gel Submersion Assay for 30 – 45 minutes at 37°C without rocking. The gel was then removed and placed between two DryEase™ minicellophane (Invitrogen) sheets which had been pre-soaked in gel drying solution for 5 min and then fastened into a gel drying frame (Novex), dried overnight and scanned as previously described.

2.19.5 Treatment of CFE

2.19.5.1 Heat

1ml aliquots of the CFE was heated at 100°C for 15 min, cooled and centrifuged at 13 000 rpm for 5 min. The supernatant was transferred to a clean micro-centrifuge tube and used to perform the tellurite reduction (Chapter 2.19.2.1), protein (BioRad) (Chapter 2.19.3.2) and gel submersion assays (Chapter 2.19.4). Specific activity was calculated as described in Chapter 2.19.3.4.

2.19.5.2 Proteinase K

3ml of CFE was mixed with 30 μl of Proteinase K and incubated at 37°C for 15 min. A control tube containing 3 ml CFE with dH_2O was also included. The tubes were cooled and centrifuged at 13 000 rpm for 5 min. Supernatant from each tube was transferred to a clean micro-centrifuge tube and used to perform the tellurite reduction (Chapter 2.19.2.1), protein (BioRad) (Chapter 2.19.3.2) and gel submersion assays (Chapter 2.19.4). Specific activity was calculated as described in Chapter 2.19.3.4.

2.19.6   Protein purification

2.19.6.1   Ammonium sulphate precipitation

12.23g of ammonium sulphate was added to 37.5 ml of CFE to a final concentration of 55 % w/v in a 1 liter flask that was immersed in ice slurry. After thorough mixing, the mixture was kept in the ice slurry for 30 minutes and then centrifuged at 10 000 rpm, 30 minutes, 4° C. The supernatant (S1) was transferred to another 1 liter flask and kept in the ice slurry and the pellet (P1) was resuspended in 3 mL 10 mM Tris HCl pH 7.5. An aliquot of S1 was saved for the tellurite reductase spectrophotometric and gel submersion assays.

4.45g of ammonium sulphate was then added to 35 mL of S1 to a final concentration of 75% w/v, mixed and kept on ice for 30 minutes. The mixture was then centrifuged at 10 000 rpm, 30 minutes, 4° C. The supernatant (S2) was then

transferred to a centrifuge tube and the pellet (P2) was resuspended in 7 ml 10 mM Tris HCl pH 7.5.

The crude cell free extract (CFE), S1, P1, S2 and P2 were transferred into separate dialysis tubing and dialysed against 8 liters (4 liters x 2) of 10 mM Tris HCl pH 7.5 overnight at 4°C. All samples were then filtered through a 0.2 µm filter and aliquots were used to perform the TR activity gel submersion assays. The remaining samples were frozen at –20°C.

2.19.6.2 Purification by ion exchange chromatography (MonoQ) column.

The MonoQ column was prepared by washing with 10 ml sterile and filtered distilled water and equilibrated with 10 ml 10 mM Tris HCl buffer, pH 7. 5. 2 ml of sample was applied to the MonoQ column and proteins were separated in a gradient (0-100 %) of 10 mM Tris HCl containing 1 M NaCl at a rate of 0.5 ml/min. 1 ml fractions were collected in sterile Eppendorf tubes and kept on ice. An FPLC trace was obtained and fractions corresponding to protein peaks on the trace were concentrated in the YM-10 (Centricon) and used for the TR gel assays. The remaining samples were frozen at –20°C.

2.19.6.3 Purification by gel exclusion chromatography (Superdex 200 10/300GL)

The Superdex 200 column was prepared by washing with 30 ml sterile and filtered distilled water and equilibrated with 50 mM sodium phosphate buffer. 200 µl of sample was applied to the Superdex 200 column and eluted with 50 mM sodium phosphate buffer containing 0.15 M NaCl at a rate of 0.5 ml/min. 1ml fractions were collected in sterile Eppendorf tubes and kept on ice. Fractions corresponding to protein peaks on the FPLC trace were concentrated in using a YM-10 (Centricon) and used for the TR gel assays. The remaining samples were frozen at –20°C.

2.19.6.4 Protein concentration using Centricon YM10

500 µl of sample was loaded into a YM-10(Centricon) column and centrifuged at 14000 g for 12 minutes at room temperature. The filtrate (F) was saved and the column was then turned over and spun at 1000 g for 3 minutes which yielded approximately 5 µl retentate (R) that was collected in an Eppendorf tube. Aliquots of the filtrate and retentate were used to perform the TR gel assays and the remaining samples were frozen at −20°C and used in the TR assays.

2.19.6.5 N-terminal sequencing for protein identification
2.19.6.5.1 Electrophoresis and blotting

Identical samples were loaded in triplicate on 7.5 % w/v native-PAGE and separated by electrophoresis. After separation, the gel was cut into 3 identical pieces, each having the same samples. A piece of a gel was used for Coomassie Blue stain, TR activity and electroblotting. As the gel was running, a gel-sized piece of polyvinylidene diflouride PVDF (BioRad Immun-Blot) membrane was placed in 100 % v/v methanol for 1 - 3 seconds. The PVDF membrane was then transferred to dH$_2$O for 1 - 2 mins and to CAPS transfer buffer (2.2.15.2) for 5 − 10 mins. Gel-sized pieces of Whatman 3 mm filter paper were also pre-equilibrated in transfer buffer for 10 mins. One piece of the gel was used to transfer the proteins to the PVDF membrane which was carried out using Bio-Rad Transfer Apparatus. The electroblotting sandwich was assembled according to the manufacturer's instructions as follows:

Top electrode BLACK sandwich plate (cathode)

One white sponge (soaked in transfer buffer)

Three pieces of filter paper (same size as gel soaked in transfer buffer)

Gel

PVDF membrane (wetted with transfer buffer)

Three pieces of filter paper

One white sponge (soaked in transfer buffer)

Bottom electrode WHITE sandwich plate (anode)

The electroblotting apparatus was connected to the power pack and transfer of the polypeptides onto the PVDF membrane of pore size 0.2um (Bio-Rad) was performed in CAPS transfer buffer at 100V for 60 minutes.

After the transfer procedure the PVDF membrane was soaked in dH_2O for 5 min, followed by 5 min soaking in methanol at room temperature. The membrane was stained with 30 ml Coomassie blue stain for 1 min and then destained for 3 x 5 min in 50 % v/v methanol (for 1 min each). The blot was then dried protein side up on clean blotting paper for 1h at room temperature.

2.19.6.5.2   N-terminal sequencing

Proteins of interest were marked clearly and the corresponding protein band on the membrane was carefully excised and sequenced using an ABI 476A sequencer by Dr Arthur Moir (Department of Molecular Biology and Biotechnology, Sheffield University).

2.19.7   Protein overexpression

Clones were made in petBlue-1 in Tuner (DE3)pLacI cells.

2.19.7.1   Large scale growth and induction of expression

A starter culture of Tuner (DE3)pLacI containing recombinant petBlue-1 plasmid was prepared by inoculating 10 ml of TB containing ampicillin (100 µg/ml) in a universal tube. The culture was incubated at 37°C with shaking (250rpm) overnight. 2.5 mL of the starter culture was added to 250 ml fresh TB in a 2 liter flask and incubated with shaking (250rpm) until OD_{600} 1.0 (2-3 hours). A 1ml aliquot of the culture was removed and cells were harvested by centrifugation at 5000 rpm for 10 min. at room temperature. The supernatant was discarded and the pellet (uninduced sample) was frozen at –20°C. The remaining culture was then induced with 1 mM IPTG and incubation continued for 2.5 hours and cells were harvested by centrifugation at 6000 g for 15 min. at 4°C. The supernatant was discarded and the pellet (induced sample) was frozen at –20°C.

were harvested by centrifugation at 6000 g for 15 min. at 4°C. The supernatant was discarded and the pellet (induced sample) was frozen at –20°C.

2.19.7.2 Determination of overexpression – total protein analysis

Both the uninduced and induced cells were thawed and resuspended with 100 µl PBS and the OD_{600} of each sample was determined. The samples were then mixed with 2x SDS sample buffer containing 5.6 % w/v 2-mercaptoethanol to equal final concentrations (OD_{600}). The mixtures were then sonicated, heated for 3 min. at 70°C, cooled for 5 minutes and then centrifuged at 13 000 g for 5min at room temperature. The supernatant was retained for analysis by SDS-PAGE.

2.19.7.3 Analysis of recombinant protein solubility

Induced cells were resuspended in 500 ul Buffer A and 1 µg/ml (final concentration) lysozyme was added. The mixture was incubated for 1 hour at room temperature and sonicated on ice using Sanyo soniprep 150 at setting 10, 3 times (10s on, 10s rest). The suspension was centrifuged at 13 000 rpm for 10 min. at 4°C to remove unbroken cells and the supernatant (soluble fraction) was transferred to a separate tube and filter sterilised (0.45 µM filter). The pellet (insoluble fraction) was resuspended in 500 ul Buffer A containing 8 M urea and vortexed hard. 250 µl sodium phosphate buffer (0.1 M, pH7.2) was added to both the soluble and insoluble fractions. Samples were then mixed with SDS sample buffer and analysed by SDS-PAGE.

2.19.7.4 Protein purification using MonoQ and Superdex 200 columns

The Mono Q and Superdex 200 columns were prepared as in Chapters 2.19.5.2 and 2.19.5.3. An overnight preculture of the clone containing the recombinant plasmid of interest in Tuner cells (*E.coli* Top 10) was prepared and induction with 1mM IPTG was performed (Chapter 2.19.6.1). A cell free extract of the culture was prepared (Chapter 2.19.1.2) and the sample was applied to a MonoQ column and the protein eluted (Chapter 2.19.5.2). Fractions corresponding to protein peaks were collected and aliquots were analysed for TR activity

(Chapters 2.19.4). The fraction with observed TR activity was then applied to a Superdex 200 column and the protein eluted (Chapter 2.19.5.3). Fractions were collected and analysed for TR activity (Chapters 2.19.4).

2.19.7.5   Protein identification by N-terminal sequence

The Superdex fraction showing TR activity (Chapter 2.19.4) was prepared for identification (Chapter 2.19.5.5) using N-terminal sequence.

2.20   Sensitivity assays

2.20.1   Disc diffusion

A 15 mm disc (Whatman) was placed on appropriate agar plates and seeded with *S.aureus*. The stress compound was added immediately to the center of the disc:

1 M methyl viologen	25 µl
1 M H_2O_2	25 µl
1 M tellurite	25 µl
1 M diamide	25 µl

Plates were incubated at 37 °C overnight and inhibition zones measured in mm from the edge of the disc.

2.20.2 H_2O_2 sensitivity liquid assay

Strains were grown in 5 ml chemically defined media (CDM) with the appropriate antibiotic(s) and sulfur source overnight at 37 °C with shaking (250 rpm), then pre-cultured in 5 ml fresh CDM to log phase. Cells were diluted to OD_{600} 0.1 in 1 ml CDM (no antibiotics) and centrifuged at 10,000 rpm for 10 min. Cells were washed twice with PBS and resuspended in 1 ml PBS and 7.5 mM H_2O_2 added. Cells were placed in a heating block set at 37 °C and 50 µl samples were taken at appropriate time points and immediately diluted into 450 µl PBS with 10mg ml^{-1} catalase. 25 µl of 10^{-1} to 10^{-6} dilutions of each strain at each time point were

spotted onto BHI agar plates and incubated at 37 °C overnight. The percentage survival rate was calculated based on the starting CFU ml^{-1}.

CHAPTER THREE

ANALYSIS OF THE ROLE OF GLUTATHIONE IN
STAPHYLOCOCCUS AUREUS

3.1 Introduction

Sulfur is an essential element for life that is required for some amino acids (methionine and cysteine), low mass thiols and other cellular components. A previous study by Lithgow *et al.* (2004) showed that *S.aureus* is able to utilize a variety of compounds as the sole sulfur source including cysteine, cystine, glutathione and thiosulphate. It was also shown that *S.aureus* is not able to use sulphate and sulfite and in fact lacks the gene homologues that are required for the uptake and utilization of these sulfur compounds. Conversely, *S.aureus* possesses genes homologous to those of *B.subtilis* and *E.coli* for the uptake and utilization of various sulfur sources such as cystine, cysteine, thiosulphate and glutathione (Chapter 1.5.2). However, the mechanisms of uptake are as yet undetermined.

Glutathione, the tripeptide γ-glutamylcysteinylglycine, is one of the most common occurring low molecular weight thiols in living organisms (Fuchs and Warner, 1975). In humans, glutathione is synthesized through two ATP-dependent enzymatic reactions catalyzed by γ-glutamylcysteine synthase and glutathione synthethase (Meister and Anderson, 1983). In bacteria, glutathione synthesis is more prevalent amongst gram-negatives but is less common in gram-positive organisms (Fahey *et al.*, 1978). *Escherichia coli* and *Proteus*

vulgaris are able to synthesize glutathione in significant amounts whilst its synthesis in gram-positives is found only in *Streptococcus agalactiae* and *Lactococcus lactis* (Fahey et al 1978). Other organisms such as *Streptococcus mutans* (Sherrill *et al.*, 1998), *B.subtilis*, and *B.cereus* (Fahey, 1978) and *S.aureus* are not able to synthesize glutathione but acquire it from the environment.

Utilization of glutathione in *Escherichia coli* and *Proteus vulgaris* is facilitated by gammaglutamyltranspeptidase (GGT) that performs both hydrolytic and transpeptidation functions (Meister and Anderson, 1983). The GGT from *E.coli* is similar to mammalian GGTs apart from two main differences (Suzuki *et al.*, 2002). It possesses a signal peptide resulting in it being a soluble periplasmic enzyme whereas the mammalian GGts are membrane bound enzymes. In addition, *E.coli* GGT is nonglycosylated whereas mammalian GGT are heterologously glycosylated (Suzuki *et al.*, 2002). The biological roles of GGT include both hydrolysis and transfer of γ-glutamyl amino acids (Chapter 1.5.4; Meister and Anderson, 1983). Glutathione is a substrate for GGT and is degraded to glutamate and γ-cysteinylglycine via hydrolysis of the γ-glutamyl linkage, thereby releasing the amino acids that are taken up and used by the bacterial cell (Suzuki *et al.*, 1993). GGT from *E.coli* K12 can utilize a variety of γ-glutamyl peptides as substrates for the hydrolysis reaction and as donors for the transpeptidation reaction. Inhibition of the enzyme by sulfoxamine, 6-Diazo-5-oxonorleucine (DON) or L-serine-borate in *P.mirabilis* (Nakayama *et al.*, 1984) or

E.coli (Suzuki and Kumagai, 2002) causes leakage of glutathione into the medium.

Immunocytochemical studies and lyzozyme treatment suggest that GGT in *P mirabilis* is localized in the periplasmic space (Nakayama *et al.*, 1984), however, the GGT from *Bacillus* species is extracellular and can be purified from the culture broth (Minami *et al.*, 2003).

The roles of glutathione in mammalian tissues have been widely studied and include maintenance of the redox environment, combating oxidative and thiol stress inducing agents, and detoxification of heavy metals and xenobiotics (Meister and Anderson, 1983). In addition, glutathione serves as a major storage form of cysteine for use as a sulfur source. Extracellular GGT from *Bacillus subtilis* was found to hydrolyse exogenous glutathione resulting in formation of cysteinylglycine that was used as a sulfur source (Minami *et al.*, 2004). *E.coli* utilizes exogenous glutathione, γ-glutamylcysteine and γ-glutamylglycine as a cysteine source and a glycine source (Suzuki *et al.*, 1993). GGT-deficient mutants of *E.coli* were unable to utilize γ-glutamyl peptides as amino acid sources. Glutathione was also shown to be a source of cysteine for growth in *Lactococcus lactis* (Li *et al.*, 2003). However, the authors suggest that the absence of this tripeptide in a wide variety of bacteria indicates that glutathione is not likely to be involved in protein synthesis, amino acid synthesis or amino acid transport.

Glutathione is also involved in the protection of mammalian cells against the oxidative stress that results from oxygen metabolism (Meister and Anderson,

1983). In *Haemophilus influenzae*, glutathione and catalase provide overlapping defence against endogenously generated H_2O_2 (Vergauwen *et al.*, 2003a,b). Glutathione has also been shown to protect cells against thiol stress and other cell damaging agents. In *Streptococcus mutans*, cellular glutathione has been shown to resist diamide, a thiol oxidant (Sherrill and Fahey, 1998). Chesney *et al.* (1996) report the role of bacterial glutathione used as a sacrificial defense against chlorine compounds in *E.coli*. In addition, the absence of glutathione together with trehalose has been shown to increase sensitivity of *E.coli* K12 to the toxicity of mercury and arsenite (Latinwo, 1998). The role of glutathione in many gram-positives however remains elusive, especially in those that do not synthesize glutathione but can transport and concentrate it intracellularly from the environment.

Glutathione uptake and utilization in *S.aureus* is likely facilitated by the presence of genes that encode for the gammaglutamyltranspeptidase (*ggt*, SACOL0188), which has 50% homology with *E.coli* GGT. In this chapter, the putative GGT of *S.aureus* was identified and characterized. The *ggt* gene was found in a locus also encoding a potential glutathione transporter. Mutagenesis studies were used to determine the role of GGT in the use of glutathione as a sulfur source. The role of glutathione in stress resistance in *S.aureus* was also studied.

3.2 Results

3.2.1. Sulfur utilization by *S.aureus* SH1000

3.2.1.1 Utilization of glutathione as sole sulfur source

To verify that *S.aureus* is able to utilize glutathione as sole sulfur source SH1000 was grown in liquid chemically defined media (lacking cysteine) and supplemented with different sulfur sources. *S.aureus* SH1000 was shown to use cysteine, glutathione and thiosulphate but not sulphate as a sole sulfur source (Fig 3.1). All cultures reached stationary phase after approximately 10 hours. Glutathione and cysteine proved the best sulfur sources with yields of 2.43 and 1.7 OD_{600} respectively after 10 hours. Initial apparent growth in the no addition culture was most likely due to residual sulfur within the inoculum.

3.2.1.2 Glutathione requirements for growth of *S.aureus* SH1000

Growth of SH1000 was glutathione concentration dependent when it was supplied as sole sulfur source (Fig. 3.2). A non-limiting concentration was reached at an addition of 50 µM. Possible toxicity was measured by addition of 10 mM glutathione. Even at 10 mM no growth defect was observed (Fig. 3.3).

110
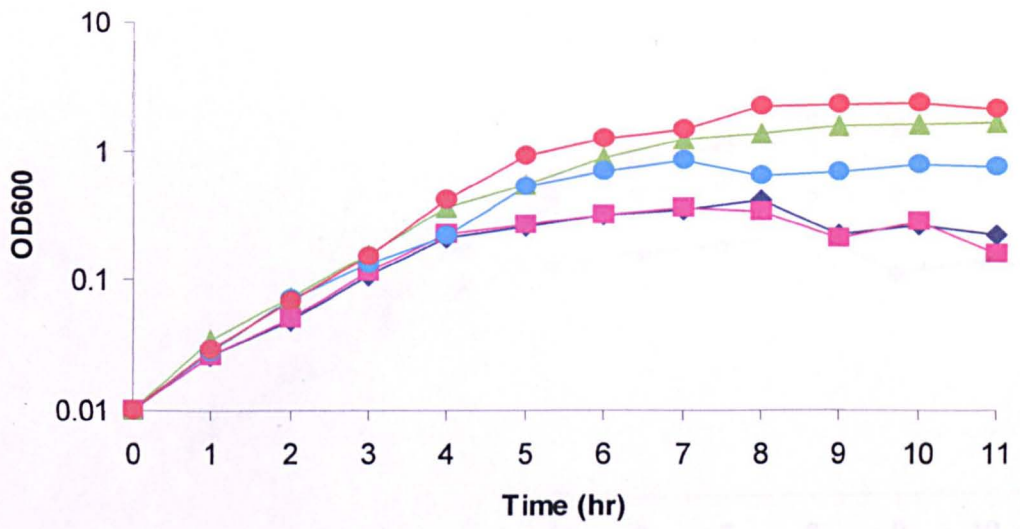
Figure 3.1

Growth curve (OD_{600}) of *S.aureus* SH1000 in chemically defined media (CDM) with 200 µM sulphate (⬛), cysteine (△), thiosulphate (⬤) and glutathione (⬤) or no addition (◆).
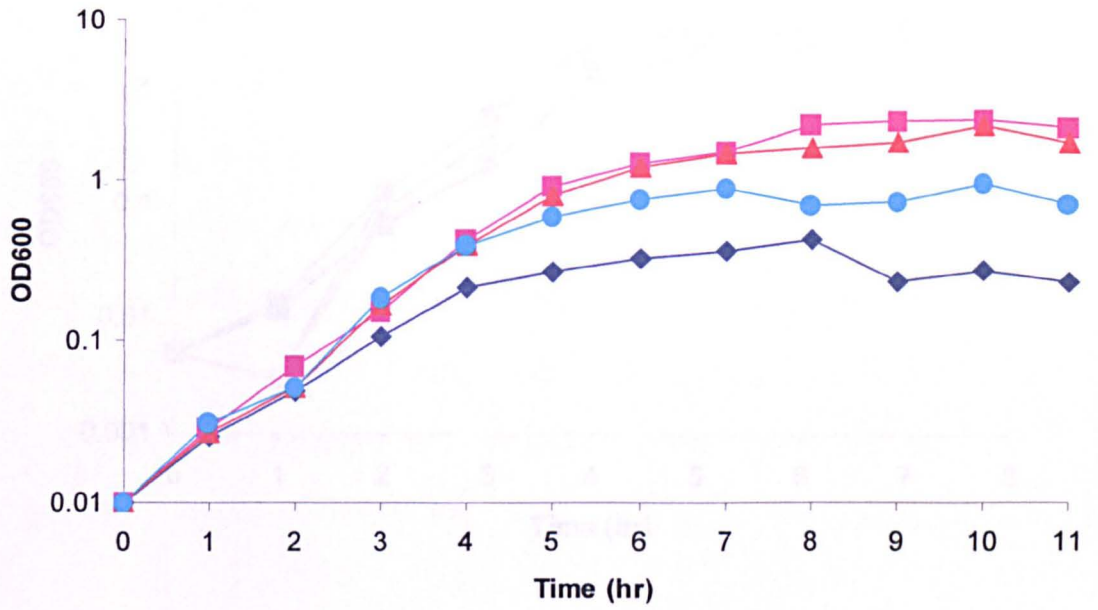
Figure 3.2
Glutathione requirement of *S.aureus* SH1000. SH1000 was grown in CDM supplemented with glutathione at 10 μM (⬤), 50 μM (▲), 200 μM (⬛) and no addition (◆).

112
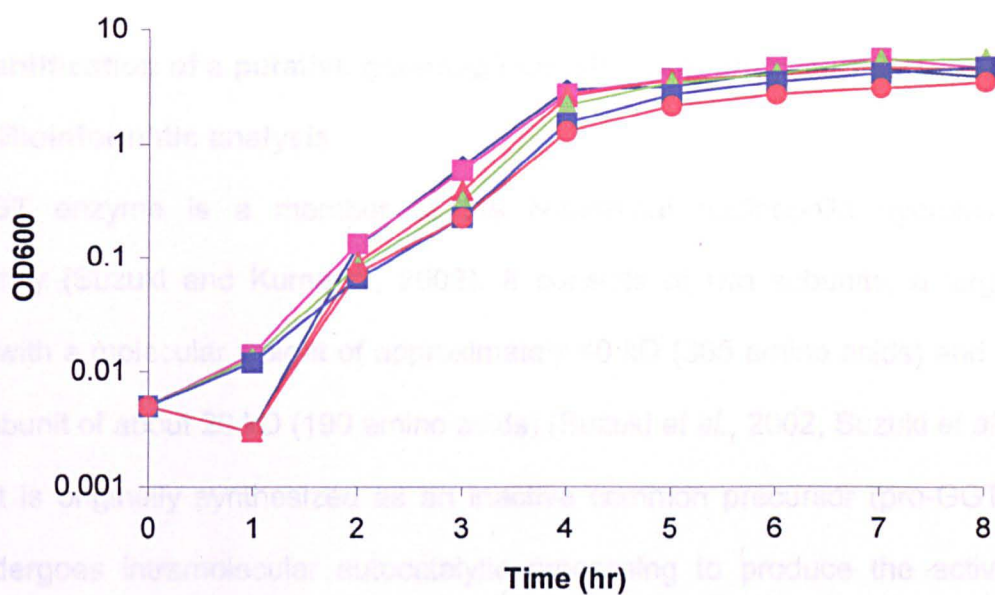
Figure 3.3

Effect of high glutathione levels on growth of *S.aureus* SH1000. SH1000 was grown in CDM with 50 µM cysteine supplemented with glutathione at 50 µM (■), 625µM (▲), 2.5mM (▲), 5.0mM (■), and 10mM (●). Control is CDM with 50µM cysteine (◆).

3.2.2 Identification of a putative gammaglutamyltranspeptidase in *S.aureus*

3.2.2.1 Bioinformatic analysis

The GGT enzyme is a member of the N-terminal nucleophile hydrolase superfamily (Suzuki and Kumagai, 2002). It consists of two subunits, a large subunit with a molecular weight of approximately 40 kD (365 amino acids) and a small subunit of about 20 kD (190 amino acids) (Suzuki *et al.*, 2002, Suzuki *et al.*, 1989). It is originally synthesized as an inactive common precursor (pro-GGT) that undergoes intramolecular autocatalytic processing to produce the active GGT.

Using the *B.subtilis* GGT amino acid sequence as query, a BLAST search was carried out against the *S.aureus* COL genome (www.tigr.org/tigr-scripts/CMR2/CMRGenomes.spl). This revealed a single protein with 36% identity over 545 amino acids to that of *Bacillus subtilis* (Table 3.2). The putative *ggt* gene is present in a possible operon with 3 other genes of which *ggt* is the last (Fig 3.4). The initial 2 genes in this operon (SACOL0185, and SACOL0186) and that running divergently from SACOL0185 (SACOL0184) all encode putative ABC transporter ATP-binding and permease proteins. A gene (SACOL0187) immediately upstream from *ggt* encodes a hypothethical protein (Table 3.1).

114
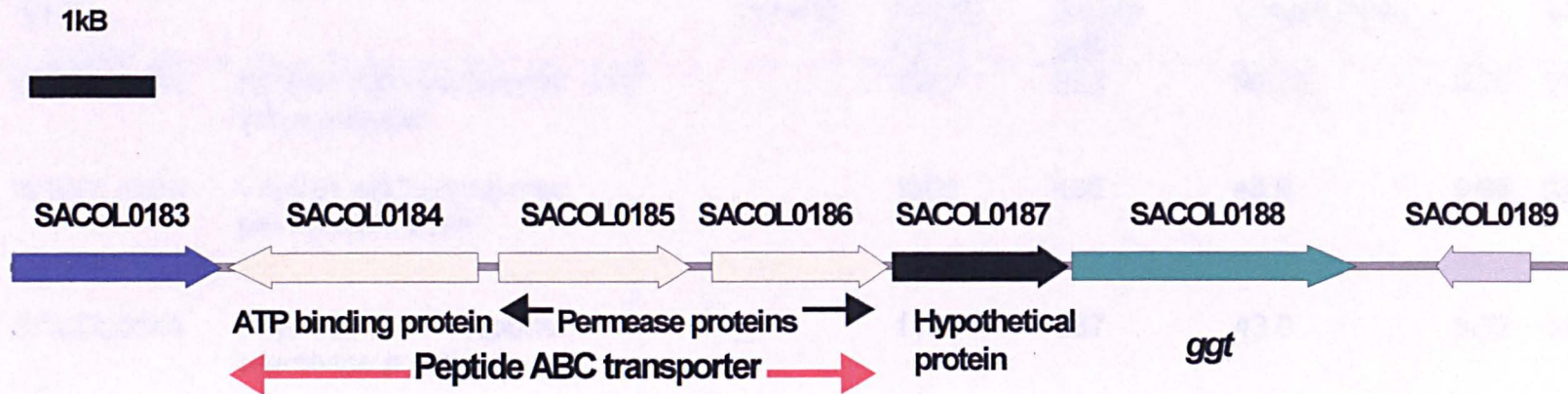
Figure 3.4

Organization of the *ggt* locus in *S. aureus* COL

TIGR Locus Name	Putative Identification	Gene symbol	Gene length (bp)	Protein length (aa)	Molecular weight (kDa)	pI	% GC
SACOL0184	Peptide ABC transporter, ATP binding protein	–	1593	530	59.18	6.25	35.65
SACOL0185	Peptide ABC transporter, permease protein	–	1308	435	48.9	9.95	33.5
SACOL0186	Peptide ABC transporter, permease protein	–	1164	387	43.0	9.72	34.6
SACOL0187	Hypothetical protein	–	1176	591	67.0	9.43	33.3
SACOL0188	gammaglutamyltranspeptidase	*ggt*	2006	668	74.69	4.9	37.61

Table 3.1

Physical information on the five proteins of the putative *ggt* locus of *S.aureus* COL

116

Comprehensive bioinformatics were carried out to determine the relationship of the GGT and the neighboring gene products in the *ggt* locus from *S.aureus* COL with those from other representative gram-positive bacteria. The SIB BLAST Network Service (http://au.expasy.org/cgi-bin/blast.pl) of the Swiss Institute of Bioinformatics was used with the amino acid sequences from *Staphylococcus epidermidis* (ATCC 12228), and *Bacillus subtilis* as query sequences (Table 3.2, Fig 3.5). The GGT from *S.aureus* COL showed significant identity with *B.subtilis* (36% over 545 amino acids) and lower identity with *S.epidermidis* (25% identity over 535 amino acids). Of the three ABC transporter proteins, SACOL0184 showed significantly high identity with both *S.epidermidis* (52% over 259 amino acids) and *B.subtilis* (50% over 265 amino acids). SACOL0185 and SACOL0186 showed higher identity with *B.subtilis* (30-32 identity% over 252-280 amino acids) compared to *S.epidermidis* (25-29% identity over 274-359 amino acids). SACOL0187 showed relatively low identities to both *B.subtilis* (19% identity over 314 amino acids) and *S.epidermidis* (23% over 110 amino acids).

	B.subtilis	*S.epidermidis* ATCC 12228
SACOL0184	BSU1139 50% (265)	SE0678 52% (259)
SACOL0185	BSU1140 30% (252)	SE0680 25% (359)
SACOL0186	BSU1141 32% (280)	SE0681 29% (274)
SACOL0187	BSU1142 19% (314)	SE2093 23% (110)
SACOL0188	BSU1841 36% (545)	SE2089 25% (535)

Table 3.2

Homology of *ggt* locus encoded proteins from *S.aureus* with other gram-positive bacteria. Data are presented as percentage of identities over number of amino acids (shown in brackets).
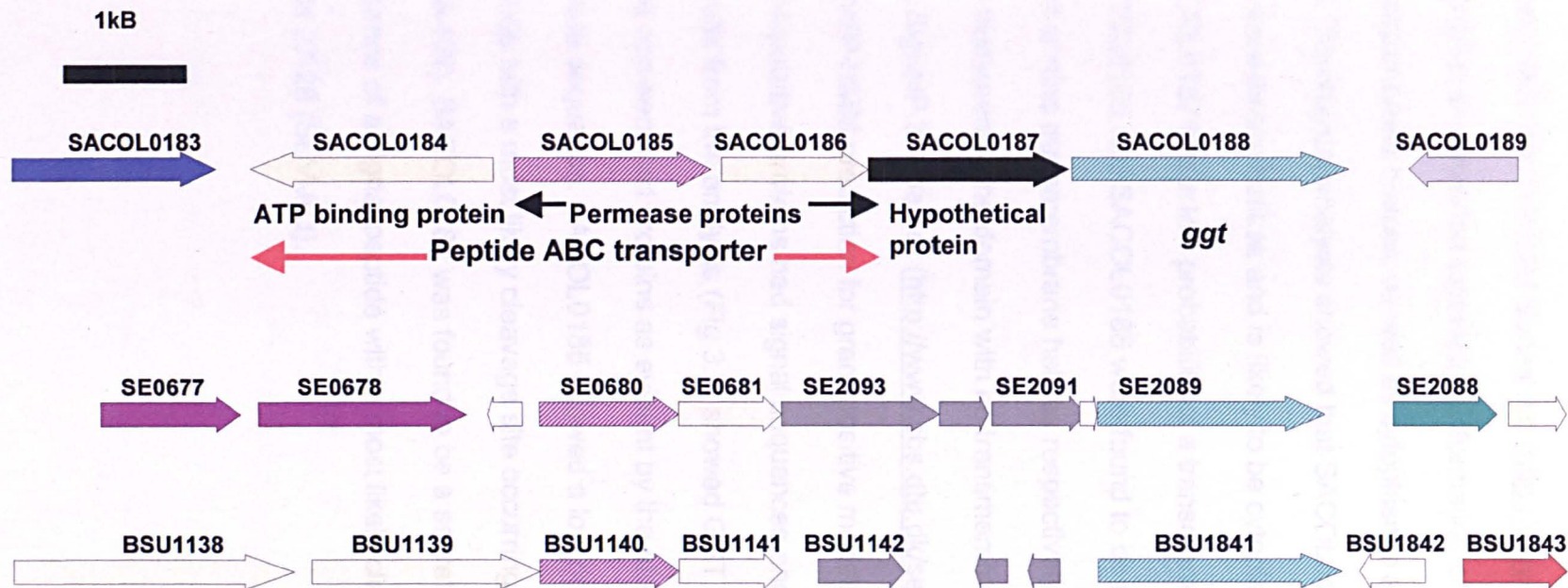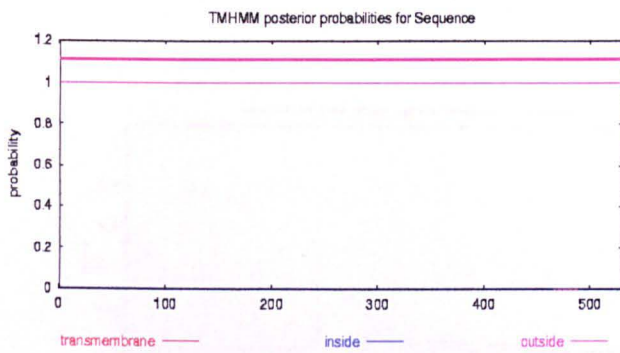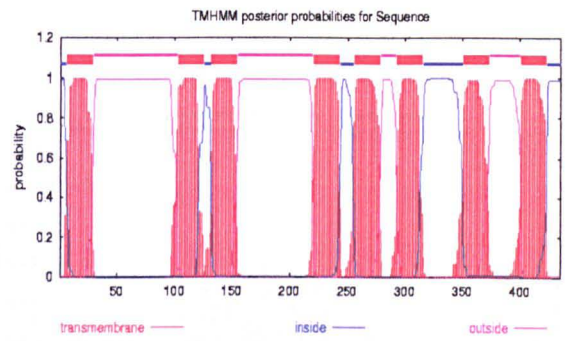
Figure 3.5

Physical map of *ggt* region in *S.aureus* COL (SACOL), *S.epidermidis* (SE), *B. subtilis 168* (BSU) showing regions of identity for *ggt* (▨▨▨) and SACOL0185 (▨▨▨).

The putative subcellular location of the members of the GGT locus was determined. The TmHMM Server 2.0 (http://www.cbs.dtu.dk/services/TMHMM-2.0/) program provided topological information of the proteins including transmembrane helices, as well as cytoplasmic and non-cytoplasmic loops (Fig 3.6). Topological analysis showed that SACOL0184 possesses no transmembrane helices and is likely to be cytoplasmic in location while SACOL0187 has a low probability of a transmembrane domain. Both SACOL0185 and SACOL0186 were found to be membrane proteins, possessing eight or nine transmembrane helices respectively. GGT showed a low probability of a transmembrane domain with no transmembrane helix.

The SignalP 3.0 Server (http://www.cbs.dtu.dk/services/SignalP/) using the SignalP-HMM prediction for gram-positive models was used to investigate if any of the putative proteins had signal sequences and are thus possibly secreted. Results from the analysis (Fig 3.7) showed GGT, SACOL0184, and SACOL0186 to be non-secreted proteins as evident by the absence of a putative signal peptide sequence. SACOL0185 showed a low probability of having a signal peptide with a most likely cleavage site occurring between amino acids 30-31 (FSA-KR). SACOL0187 was found to be a secreted protein as suggested by the presence of a signal peptide with a most likely cleavage site between amino acids 27-28 (SEV-AQ).

SACOL0184

SACOL0185
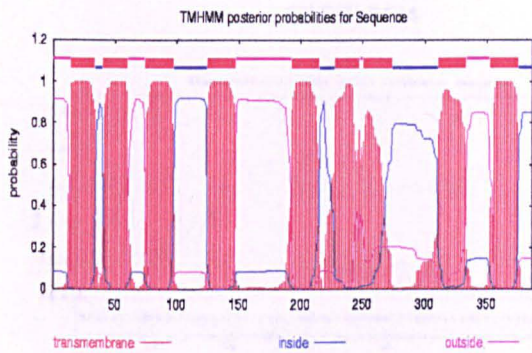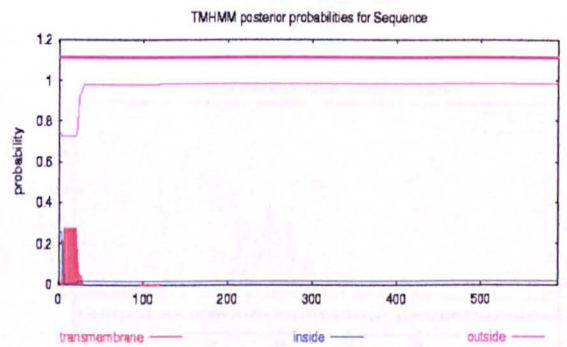
SACOL0186
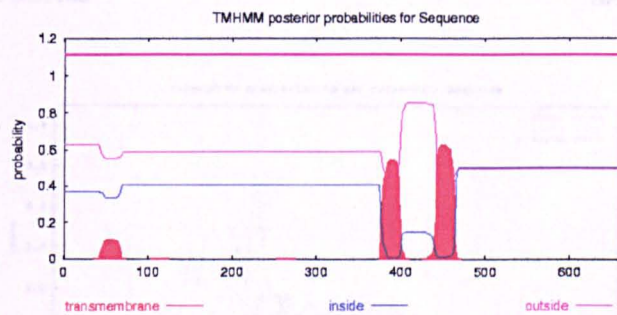
SACOL0187

SACOL0188

Figure 3.6

Membrane topology of the members of the GGT locus in *S.aureus*. Predicted transmembrane regions are shown in red. X-axis of all profiles shows the amino acid residues of the proteins.
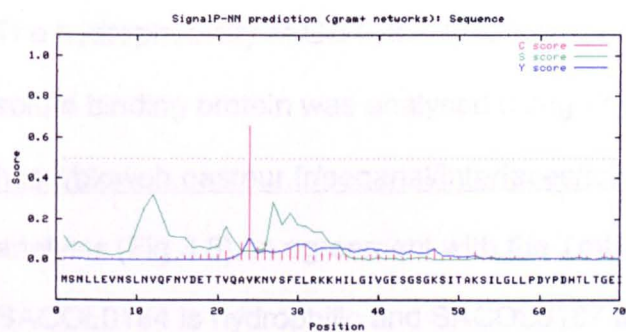
SACOL0184
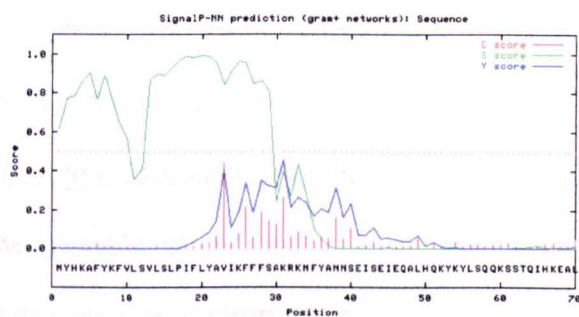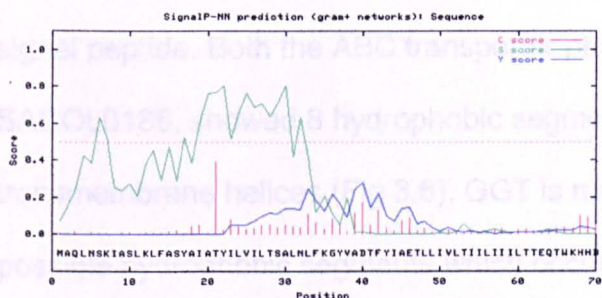
SACOL0185
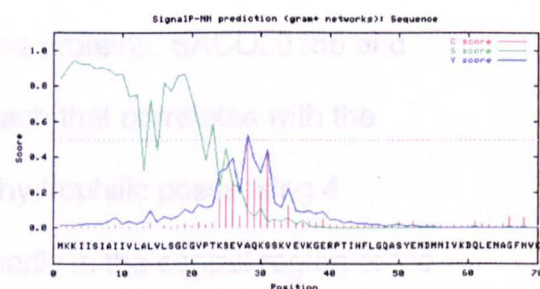
SACOL0186
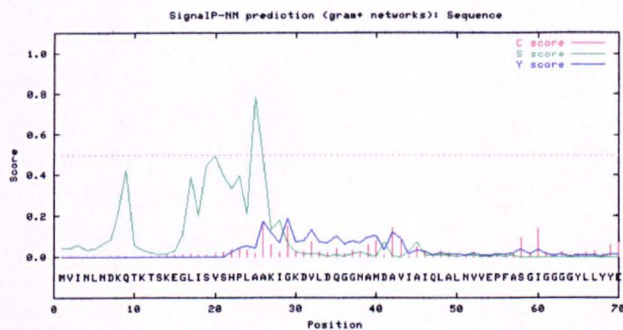
SACOL0187

SACOL0188

Figure 3.7

Signal peptide sequence prediction of the putative GGT locus proteins

(SACOL0184-SACOL0188) *S.aureus* putative cleavage sites are indicated by the

tallest red line. X axis of all profiles shows the amino acid residues.

The hydrophobicity of GGT, the ABC transporter proteins and the hypothetical

solute binding protein was analysed using TopPred II Server at

http://bioweb.pasteur.fr/seqanal/interfaces/toppred.html. Results from this

analysis (Fig 3.8), in agreement with the TmHMM analysis, show that

SACOL0184 is hydrophilic and SACOL0187 to possess one hydrophobic

segment early in the amino acid sequence probably due to the presence of a

signal peptide. Both the ABC transporter permease proteins, SACOL0185 and

SACOL0186, showed 8 hydrophobic segments each that correlates with the

transmembrane helices (Fig 3.6). GGT is mainly hydrophilic possessing 4

possible hydrophobic segments which occur primarily in the central region of the

protein.
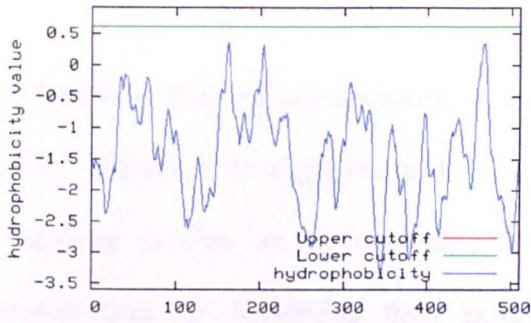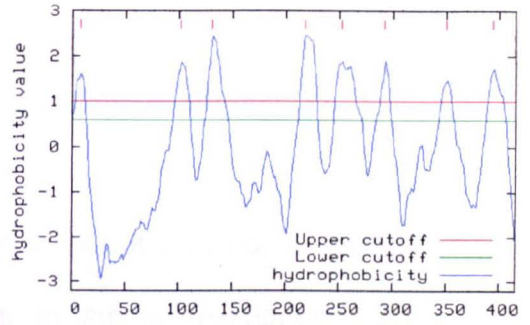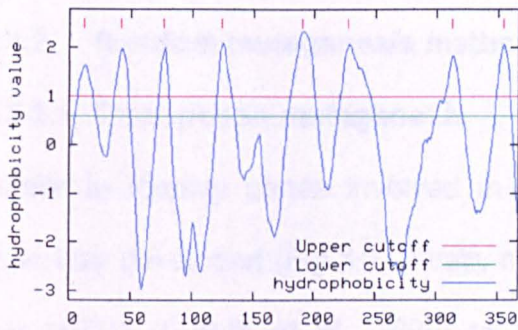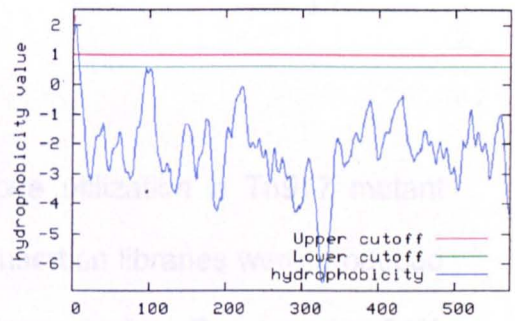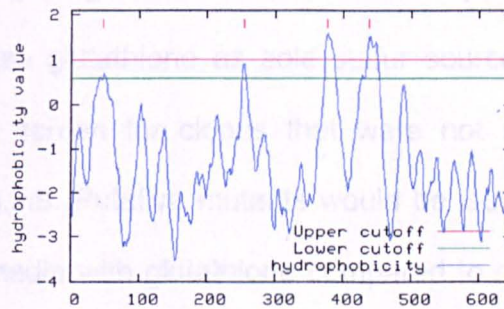
Figure 3.8

Hydrophobicity profiles of the putative GGT locus proteins (SACOL0184-SACOL0188). Hydrophobicity values that cross the upper cutoff (red line) designate a putative membrane spanning region. X axis of all profiles shows the amino acid residues of the proteins.

3.2.3 Identification of components involved in glutathione utilization.

3.2.3.1 Isolation of a *ggt* mutant

To facilitate studies on the mechanism of glutathione uptake and utilization in *S.aureus* and to determine their putative role in stress resistance, genes putatively involved in its utilization/uptake were characterized. This included both random mutagenesis and targeted inactivation approaches.

3.2.3.2 Random mutagenesis method

3.2.3.2.1. Transposon mutagenesis

In order to identify genes involved in glutathione utilization a Tn*917* mutant screen was developed (Fig 3.9). Firstly multiple insertion libraries were produced using pLTV1 (Camilli et *al.*, 1990) as the delivery vector. One gave a 94% insertion rate suitable for screening. Tn insertion mutants were screened to identify clones unable to utilize glutathione as sole sulfur source. The replica plating method was used to screen for clones that were not able to utilize glutathione as depicted in Fig.3.9. Putative mutants would be isolated as those showing reduced growth on media with glutathione compared to cysteine. More than 10,000 colonies were screened to no avail. All clones screened showed comparable growth to SH1000 on CDM agar plates supplemented with only glutathione as the sole sulfur source. Thus this approach did not yield any putative mutants.
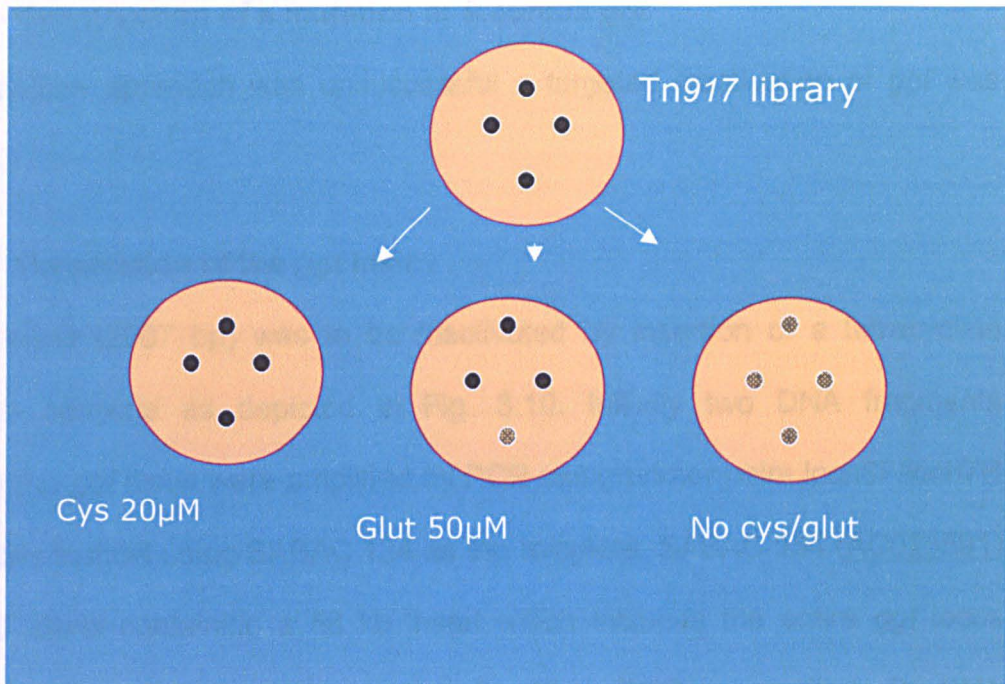
Figure 3.9
Replica plating scheme to identify Tn*917* mutants altered in glutathione utilization. Clones were grown on CDM with 20 µM cysteine before replica plating onto three different media. Clones showing reduced growth specifically on glutathione were expected.

3.2.3.3   Construction of a mutation in *S.aureus ggt*

As the random approach was unsuccessful a targeted inactivation of *ggt* was designed.

3.2.3.3.1 Preparation of the *ggt* insert

The *ggt* gene (2007 bp) was to be inactivated by insertion of a tetracycline resistance cassette as depicted in Fig. 3.10. Initially two DNA fragments spanning the *ggt* locus were amplified by PCR using primer pairs loch8F/loch7R and loch5F/ loch6R using SABAC 134 as the template. SABAC 134 (AC025591) is a BAC clone containing a 58 kb insert which includes the entire *ggt* locus (http://w3.ouhsc.edu/MI/faculty/iandolo.html). The PCR generated 2 DNA fragments called A and B of the predicted sizes of 1249 bp and 1659 bp (Fig.3.11B). The PCR primers had been designed to create novel restriction sites (loch8F: *Eco*RI, loch6R: *Bam*HI, loch5F and loch7R: *Kpn*I). Fragments A and B were separately digested with appropriate restriction enzymes (A *Eco*RI/*Kpn*I, B *Bam*HI/*Kpn*I), cleaned and ligated together. The ligated product was then amplified by PCR using the primers loch8(F) and loch6(R) which yielded fragment AB of 2.9 kb (Fig. 3.11C). AB was then digested with *Kpn*I and separated on a 1% w/v agarose gel. Two bands were observed at the expected band sizes of 1249 bp (A) and 1659 bp (B) thereby verifying the presence of a *Kpn*I site in the middle of the fragment (Fig.3.11D). AB was then digested separately with *Eco*RI and *Bam*HI and each digestion yielded one band when resolved on a 1% w/v agarose gel at approximately 2.9 kb. The double digested

127

AB fragment was then gel extracted and ligated with pMUTIN4 (Vagner *et al.*, 1998) (Fig. 3.12) linearized with *Eco*RI and *Bam*HI to create pMUTggt (Fig.3.13). Plasmid pMUTggt was verified by restriction digest with *Kpn*I revealing a single fragment of 11.5 kb (Fig. 3.13). Plasmid pAZtet which was obtained from Ramlan Mohamad (personal communication) was digested with *Kpn*I to reveal a 1.5 kb *tet* cassette. Gel extracted *tet* cassette was ligated with *Kpn*I cut pMUTggt to give pRMHO1. Plasmid pRMH01 was digested with *Kpn*I which gave bands of 1.5 kb (*tet* cassette) and 11.5 kb (vector + *ggt* insert). (Fig 3.14A). *Bam*HI and *Eco*RI digestions gave 2 fragments of 4.4 kb (*ggt* locus plasmid insert) and 8.6 kb (linearized pMUTIN4) (Fig.3.14B).
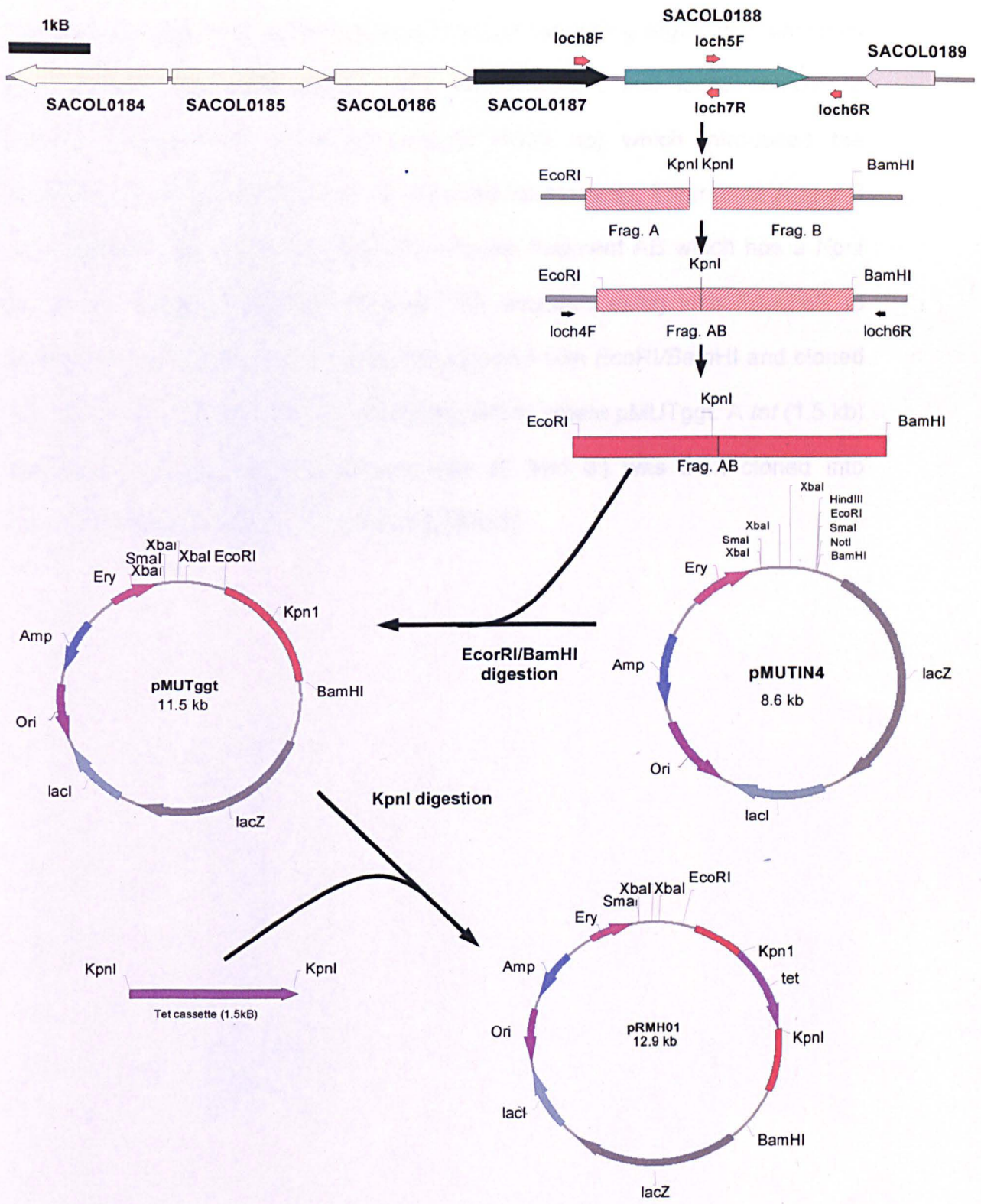
Figure 3.10

Inactivation protocol for *ggt* of *S.aureus*. The *ggt* containing region was amplified from SABAC 134 using primer pairs loch8F/loch6R and loch5F/loch7F to produce fragments A (1249 bp) and B (1659 bp) which introduced the engineered sites *EcoRV/Kpn*I and *Kpn*I/*Bam*HI respectively. Fragments A and B were digested with *Kpn*I and ligated to produce fragment AB which has a *Kpn*I site in the middle. Fragment AB was PCR amplified using loch8F/loch6R to produce the *ggt* insert which was double digested with *EcoRV/Bam*HI and cloned into pMUTIN4 (pre-digested with *EcoRV/Bam*HI) to create pMUTggt. A *tet* (1.5 kb) resistance cassette flanked by *Kpn*I sites (5' and 3') was then cloned into pMUTggt (digested with *Kpn*I) to create pRMH01.
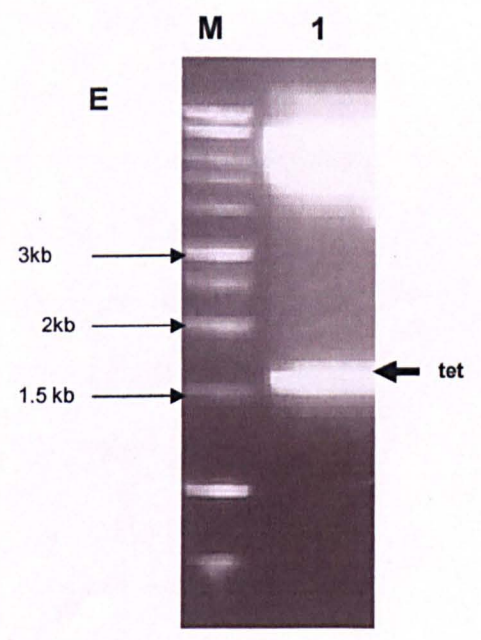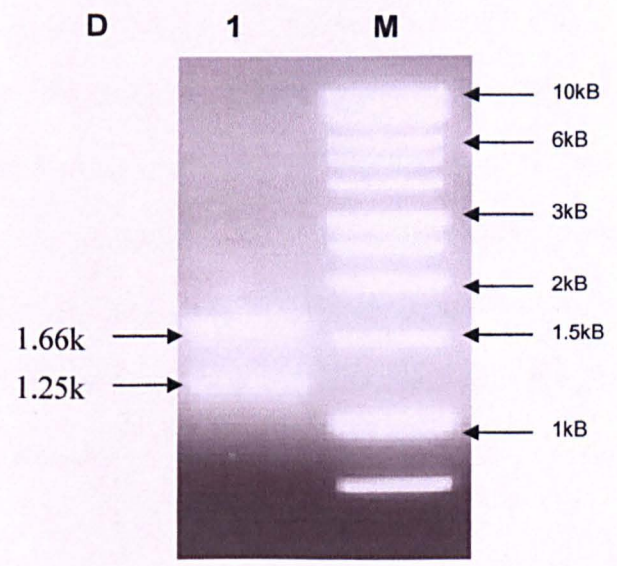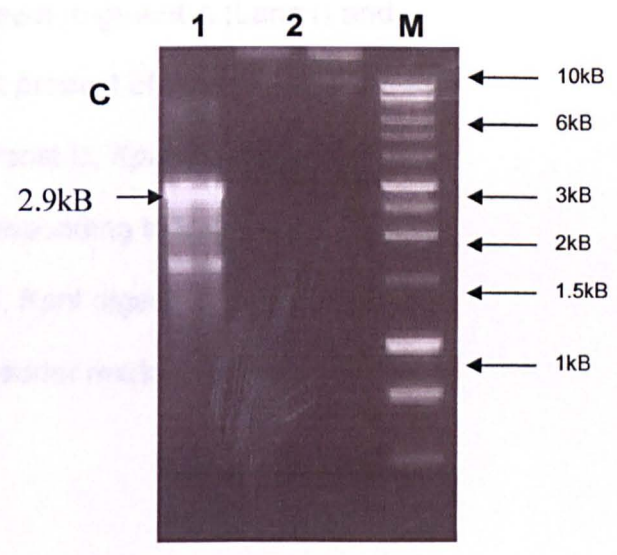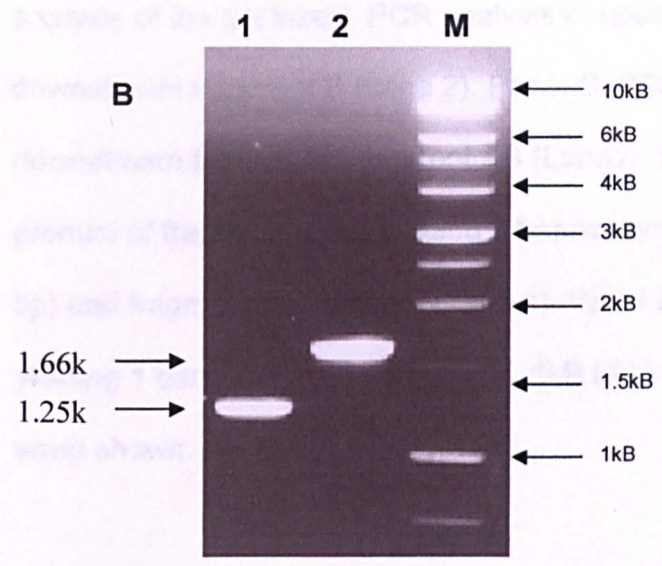
Figure 3.11

Preparation of a *ggt* insert for inactivation of the GGT region. Panel A, Physical

map of the GGT region showing primer sites. Panel B, PCR and restriction digest

analysis of the *ggt* insert. PCR analysis of upstream fragment A (Lane1) and

downstream fragment B (Lane 2). Panel C. PCR product of ligated upstream and

downstream fragments; fragment AB (Lane1). Panel D, *Kpn*I digestion of PCR

product of fragment AB producing 2 bands corresponding to fragment A (1249

bp) and fragment B (1659 bp) (Lane 1). Panel E, *Kpn*I digestion of pAZtet

yielding 1 band at 1.5 kb (lane 1). M, 1kB DNA ladder marker with appropriate

sizes shown.
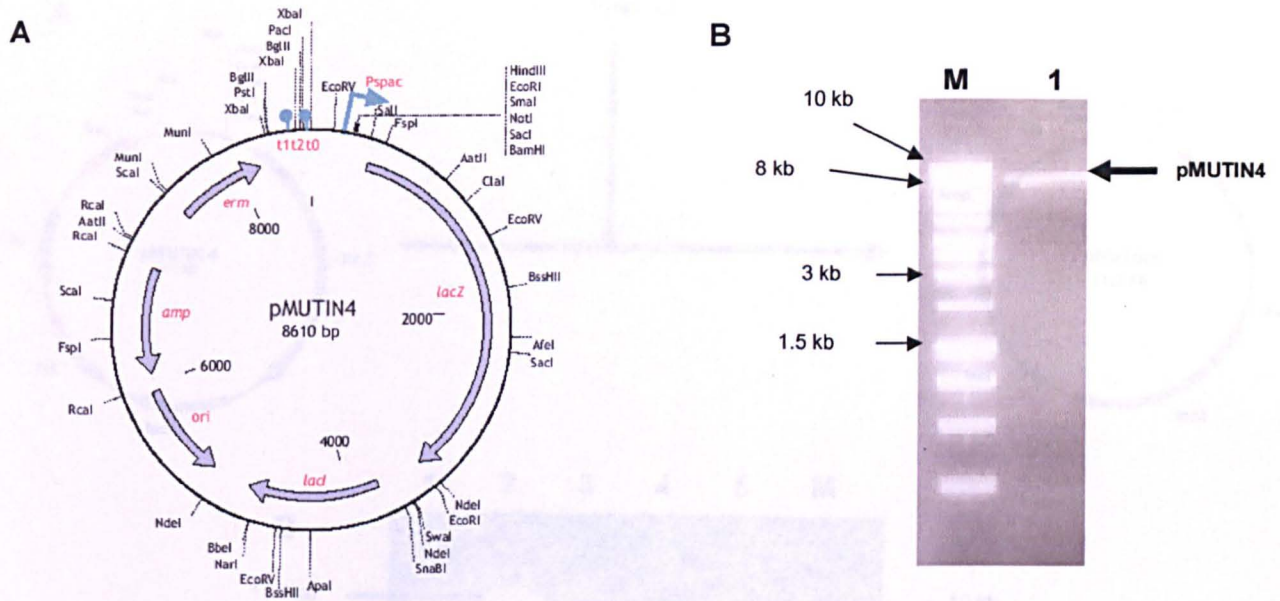
Figure 3.12

Preparation of pMUTIN4 for cloning with *ggt* insert. Panel A, Physical map of pMUTIN4 used for mutagenesis in *S.aureus* (adapted from Vagner *et al.*, 1998). This plasmid vector cannot replicate in *S.aureus* but contains the ColE1 replication sequence (*ori*) and an ampicillin resistance gene (*amp*) for selection in *E.coli*. The erythromycin resistance gene (*erm*) allows for selection in *S.aureus*. The promoterless *lacZ* gene is located downstream from the multiple cloning sites. Panel B, pMUTIN4 was digested with *Bam*HI and *Eco*RI. Lane 1 shows the expected band size of 8.6 kb. M, 1kB DNA ladder marker with appropriate sizes is shown.

133
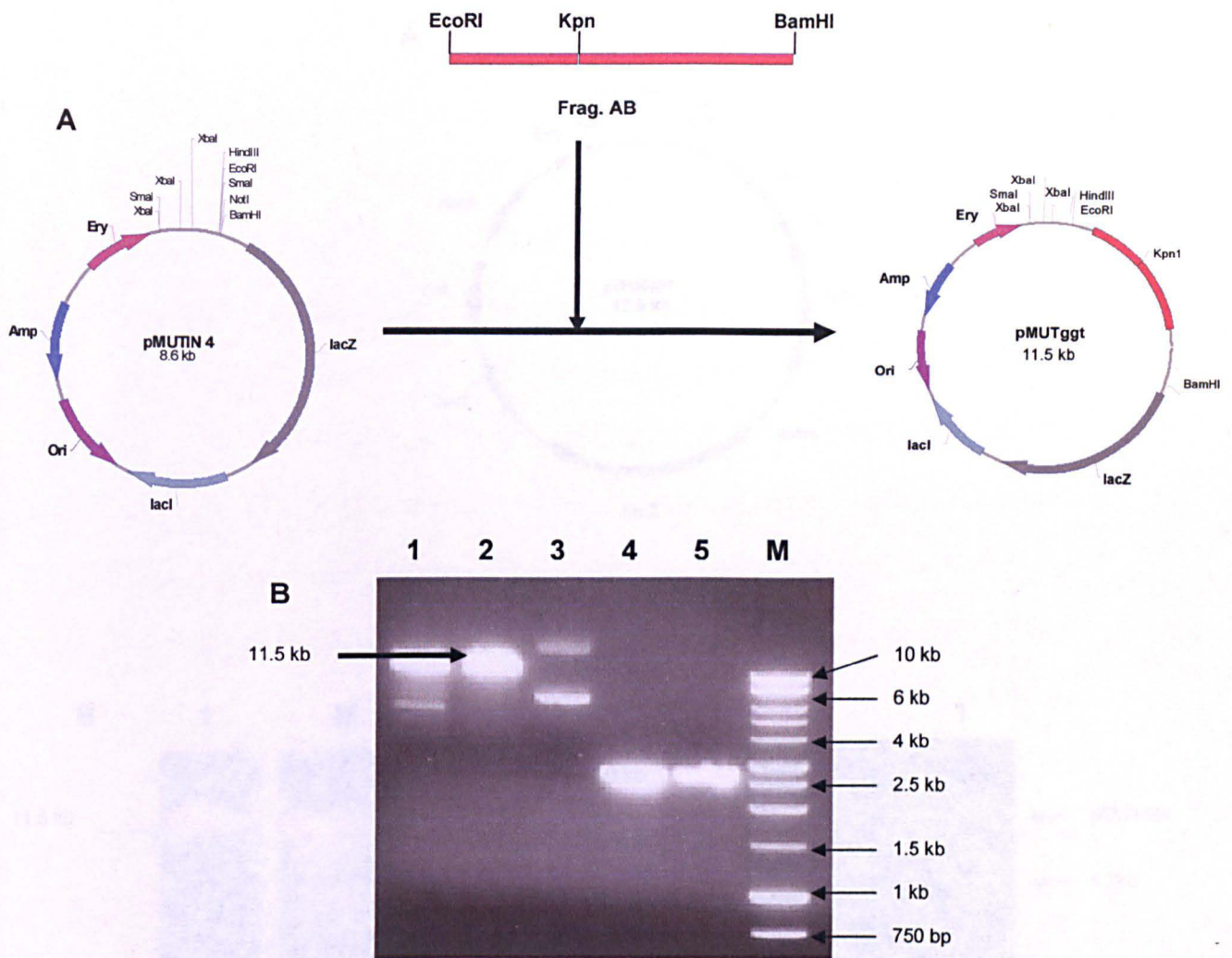
Figure 3.13

Construction of pMUTggt. Panel A, Cloning strategy. Panel B, Restriction digest analysis of five putative pMUTggt clones. pMUTggt plasmid DNA was digested with *Kpn*I (lanes 1,2,3,4,5). Lane 2 shows the expected band size of 11.5 kb and this clone was further used. M, 1kb DNA ladder marker with appropriate sizes is shown.

134
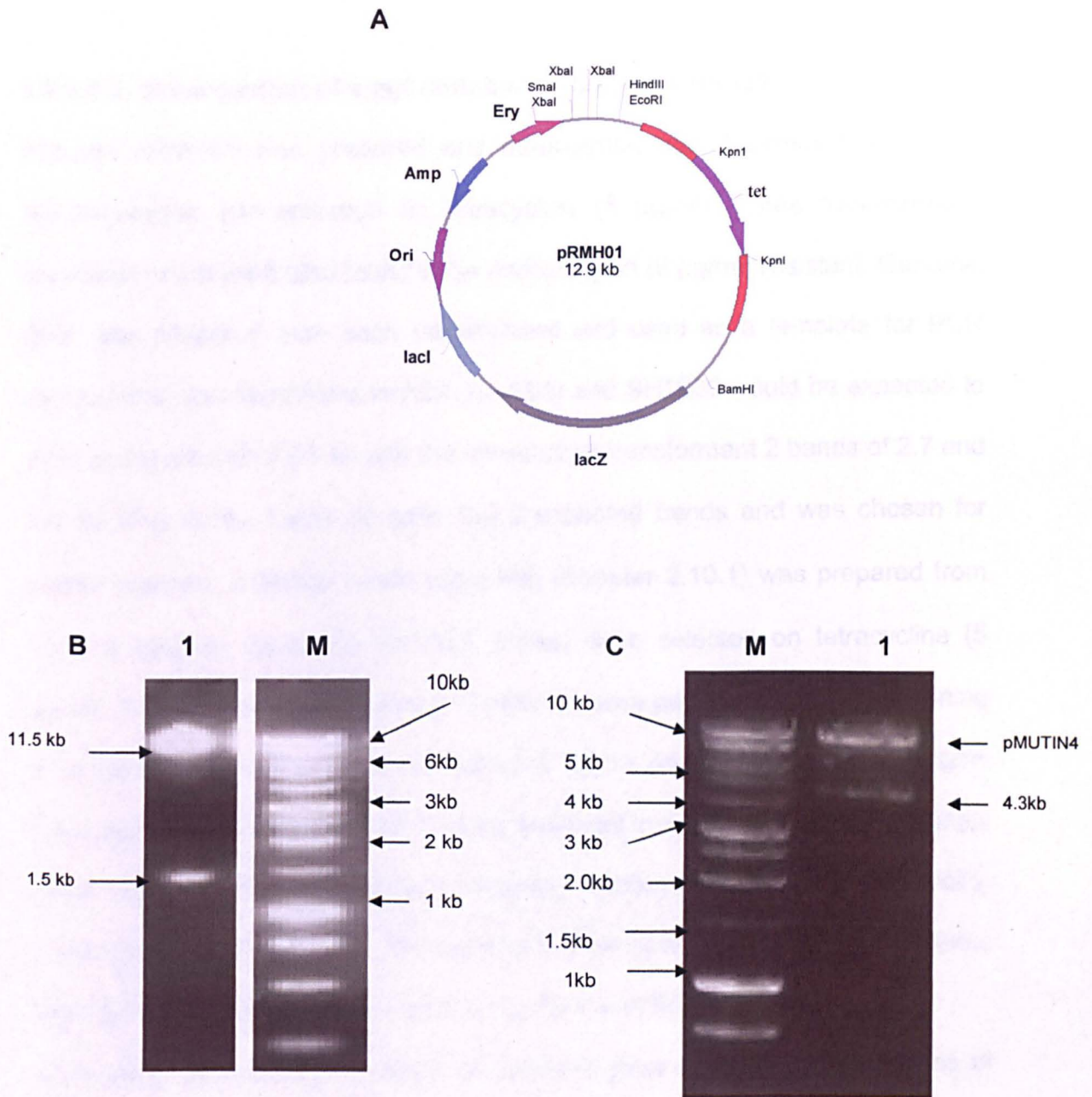
Figure 3.14

Construction of pRMH01. Panel A, Physical map of pRMH01. Panel B, Restriction digest analysis of pRMH01 (Lane 1) digested with *Kpn*I or Panel C, *Bam*HI and *Eco*RI. M, 1 kb DNA ladder marker showing appropriate sizes is shown.

3.2.3.3.2 Construction of a *ggt* mutation in *S.aureus* RN4220

Plasmid pRMH01 was prepared and transformed into *S.aureus* RN4220 by electroporation and selection on tetracycline (5 μg/ml). Three transformants appeared which were also found to be erythromycin (5 μg/ml) resistant. Genomic DNA was prepared from each transformant and used as a template for PCR using primer pair loch8Fand loch6R. RN4220 and SH1000 would be expected to yield a single band of 2.7 kb and the merodiploid transformant 2 bands of 2.7 and 4.3 kb (Fig. 3.18). Clone 3a gave the 2 expected bands and was chosen for further analysis. A phage lysate using θ85 (Chapter 2.10.1) was prepared from 3a and used to transduce SH1000. Clones were selected on tetracycline (5 μg/ml). After 48 hours incubation, 215 colonies were patched onto BHI containing 5 μg/ml tetracycline or BHI containing 5 μg/ml erythromycin and 25 μg/ml lincomycin and incubated at 37°C. After overnight incubation, 15 yellow colonies grew only on the BHI plate containing tetracycline but not containing erythromycin and lincomycin. Transductants were picked for isolation of genomic DNA for verification of the *ggt* mutation by PCR and Southern Blot.

PCR using the primer pair loch8F and loch6R gave a single predicted band of 4.3kB as expected for transductant RMH12(*ggt*) in the SH1000 background indicating the presence of the tet cassette in *ggt* (Fig 3.16).
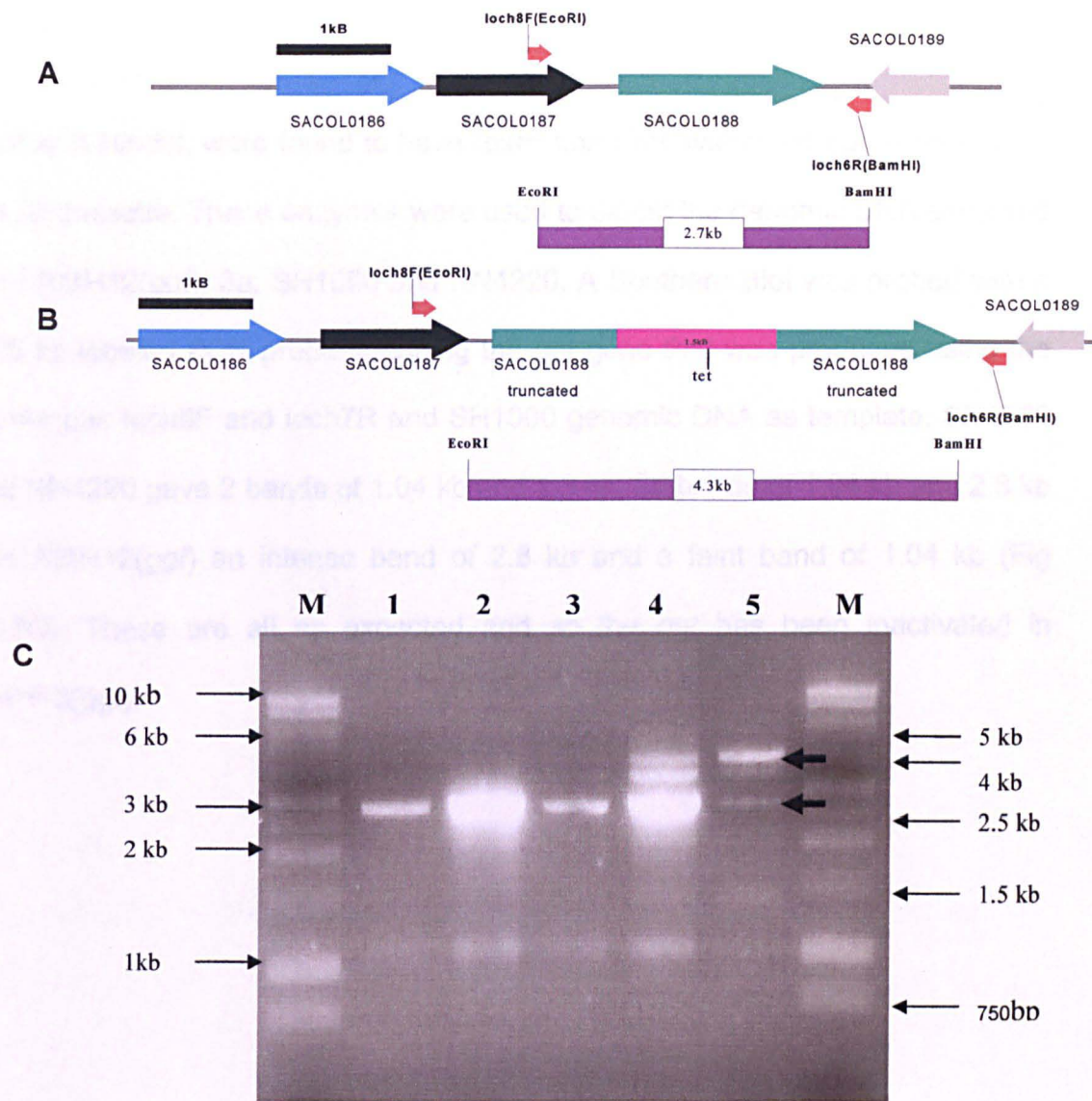
Figure 3.15

Verification of pRMH01 transformants in *S.aureus* RN4220. The *ggt* locus showing the position of the generated PCR products without (Panel A) and with (Panel B) *tet* insertion on genomic DNA using primer pair loch8F/loch6R. PCR products were separated by 1% w/v agarose gel electrophoresis (Panel C). Lane 1, SH1000; lane 2, RN4220; lane 3, transformant 3; lane 4, transformant 3b; lane 5, transformant 3a. M, 1kB DNA ladder marker showing appropriate sizes is shown.

*Xba*I and *Hind*III, were found to have restriction sites within the *ggt* locus but not the *tet* cassette. These enzymes were used to digest the genomic DNA extracted from RMH12(*ggt*), 3a, SH1000 and RN4220. A Southern Blot was probed with a 1.25 kb labeled PCR probe spanning the *ggt* gene that was produced using the primer pair loch8F and loch7R and SH1000 genomic DNA as template. SH1000 and RN4220 gave 2 bands of 1.04 kb and 1.3 kb, 3a bands of 1.04 kb and 2.8 kb and RMH12(*ggt*) an intense band of 2.8 kb and a faint band of 1.04 kb (Fig 3.17C). These are all as expected and so the *ggt* has been inactivated in RMH12(*ggt*).
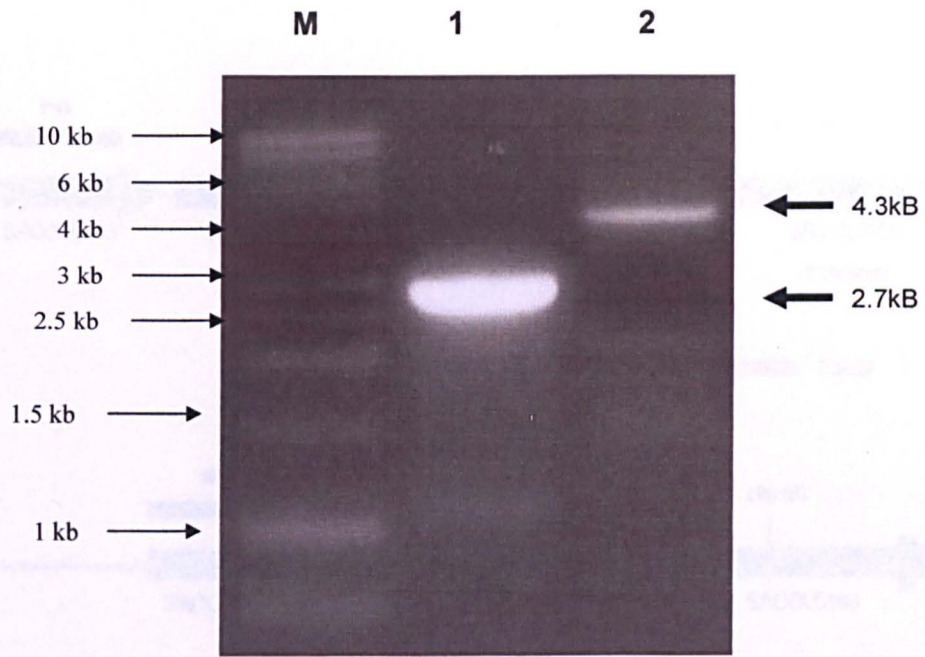
Figure 3.16

PCR verification of the *ggt* mutation in *S.aureus* SH1000 by PCR with primers loch8F and loch6R. Lanes M, DNA markers of sizes shown; 1, SH1000; and 2, RMH12(*ggt*).
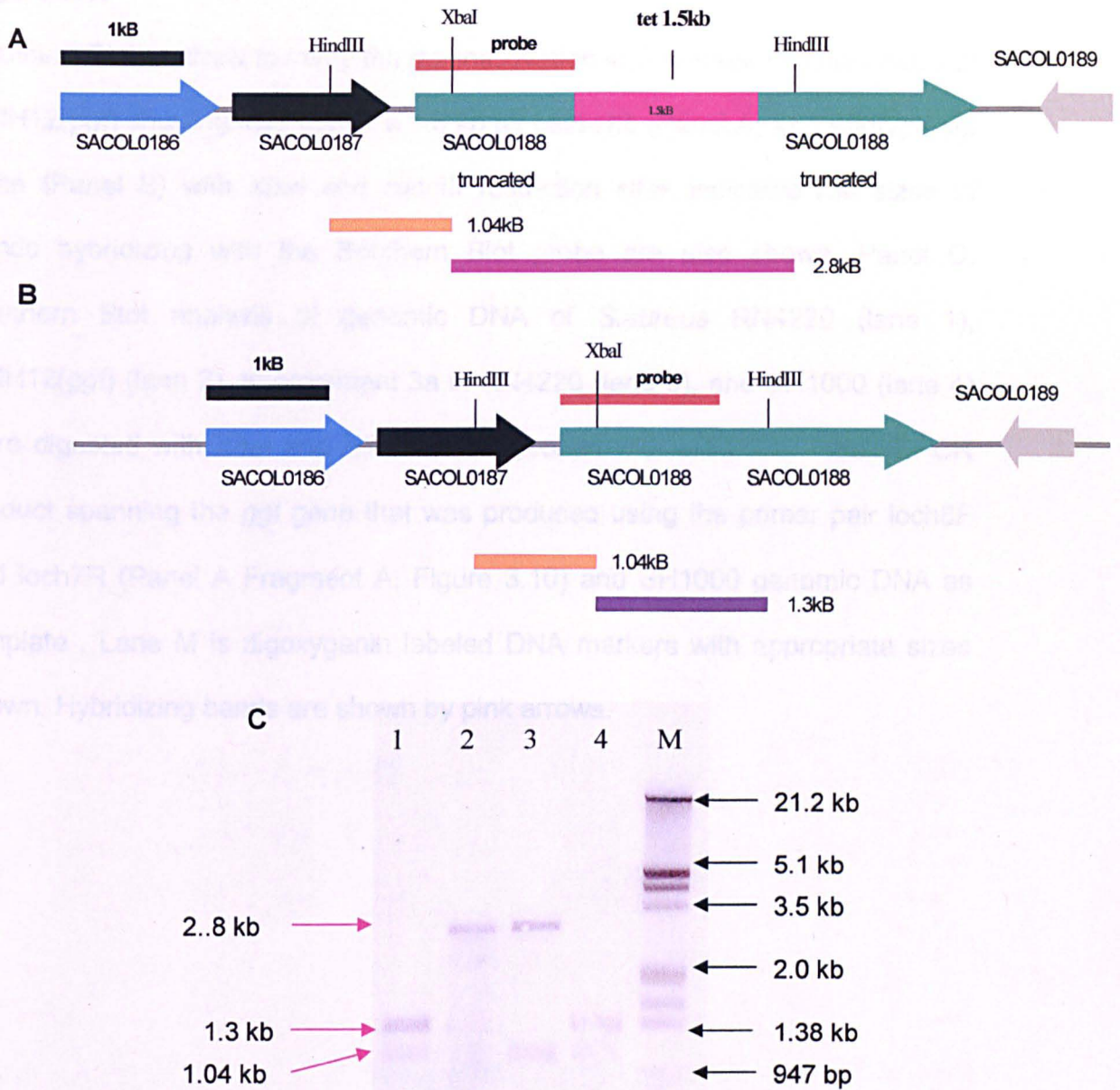
Figure 3.17

Southern Blot analysis to verify the *ggt* inactivation in *S.aureus*. Physical maps of RMH12(*ggt*) showing insertion of a 1.5 kb *tet* cassette (Panel A) and wildtype *ggt* gene (Panel B) with *Xba*I and *Hind*III restriction sites indicated.The sizes of bands hybridizing with the Southern Blot probe are also shown. Panel C, Southern Blot analysis of genomic DNA of *S.aureus* RN4220 (lane 1), RMH12(*ggt*) (lane 2), transformant 3a in RN4220 (lane 3), and SH1000 (lane 4) were digested with *Xba*I and *Hind*III and probed with a 1.25 kb labeled PCR product spanning the *ggt* gene that was produced using the primer pair loch8F and loch7R (Panel A Fragment A, Figure 3.10) and SH1000 genomic DNA as template . Lane M is digoxygenin labeled DNA markers with appropriate sizes shown. Hybridizing bands are shown by pink arrows.

3.2.3.4 Role of *ggt* in glutathione utilization

To test the role of *ggt* in glutathione utilization as sole sulfur source RMH12(*ggt*) was grown in liquid chemically defined media (CDM) (Fig 3.18) lacking cysteine and CDM supplemented with cysteine at concentrations of up to 200 µM and glutathione up to 200 µM. Surprisingly, RMH12(*ggt*) is still able to grow with glutathione as sole sulfur source.

The role of *ggt* was also tested on the ability to form colonies on CDM agar plates (Table 3.3). There was no apparent visible difference in colony size between RMH12(*ggt*) and SH1000 on any of the media. Both strains did not grow without a sulfur source.

CDM agar supplement	SH1000	RMH12(ggt)
Cys50 µM	4mm	4mm
Glut50 µM	1mm	1mm
Glut100 µM	2mm	2mm
Glut150 µM	4mm	4mm

Table 3.3

Role of *ggt* in growth on solid media. RMH12(*ggt*) and *S.aureus* SH1000 were grown on CDM agar plates supplemented with sulfur source as indicated. Colony size (mm) was measured after 24 hours.
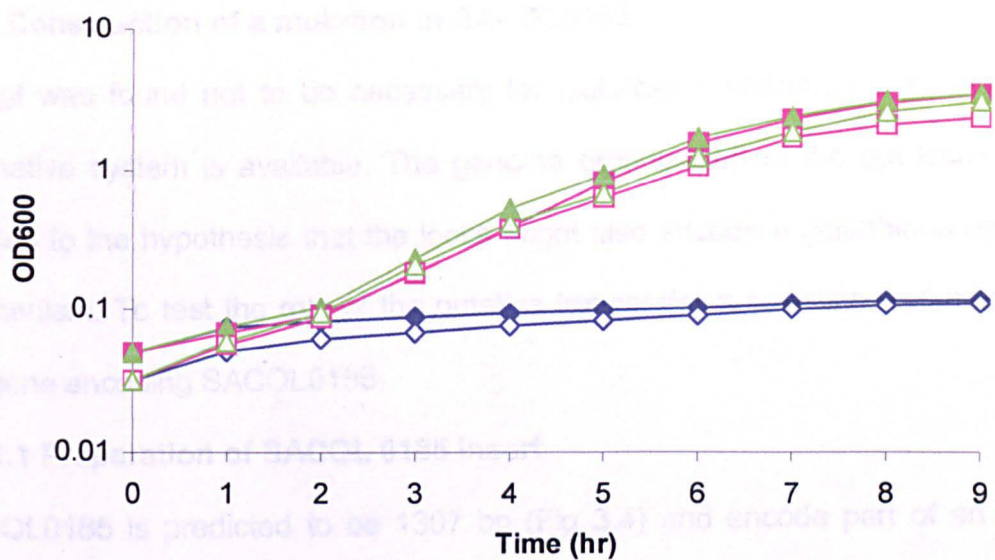
Figure 3.18

Role of *ggt* in utilization of glutathione. *S.aureus* strains SH1000 (closed symbols) and RMH12(*ggt*) (open symbols) were grown in liquid chemically defined media (CDM) with 50 µM cysteine (■ □) or 50 µM glutathione (▲ △). Control is liquid CDM with no sulfur source (◆ ◇).

3.2.4.Construction of a mutation in SACOL0185

As *ggt* was found not to be necessary for glutathione utilization it is likely an alternative system is available. The genome organization of the *ggt* locus (Fig 3.4) led to the hypothesis that the locus might also encode a glutathione uptake mechanism. To test the role of the putative transporter a mutation was made in the gene encoding SACOL0185.

3.2.4.1 Preparation of SACOL 0185 insert

SACOL0185 is predicted to be 1307 bp (Fig 3.4) and encode part of an ABC transporter. SACOL0185 was inactivated by insertional duplication using pMUTIN4. Two primers, loch9F and loch10R, were designed to amplify an internal part of the SACOL0185 gene (Fig.3.19) with engineered *Hind*III and *Bam*HI sites respectively using SH1000 genomic DNA as template. An 886 bp DNA fragment was PCR amplified using *Taq* polymerase and cloned into the pCR 2.1-TOPO vector (Fig 3.20) (Materials and Methods) and transformed into One Shot Top10 chemically competent *E.coli* (Materials and Methods).

Transformants were selected on ampicillin (50 ug/ml) agar with X-gal. White colonies were picked and presence of the 846 bp insert verified by restriction digestion with *Hind*III and *Bam*HI (Fig 3.21A). The insert was prepared by large scale digestion of the recombinant plasmid with *Hind*III and *Bam*HI and gel purification of the insert. Similarly pMUTIN4 was *Hind*III and *Bam*HI digested and gel purified. Insert and vector were ligated and transformed into *E.coli* Top 10
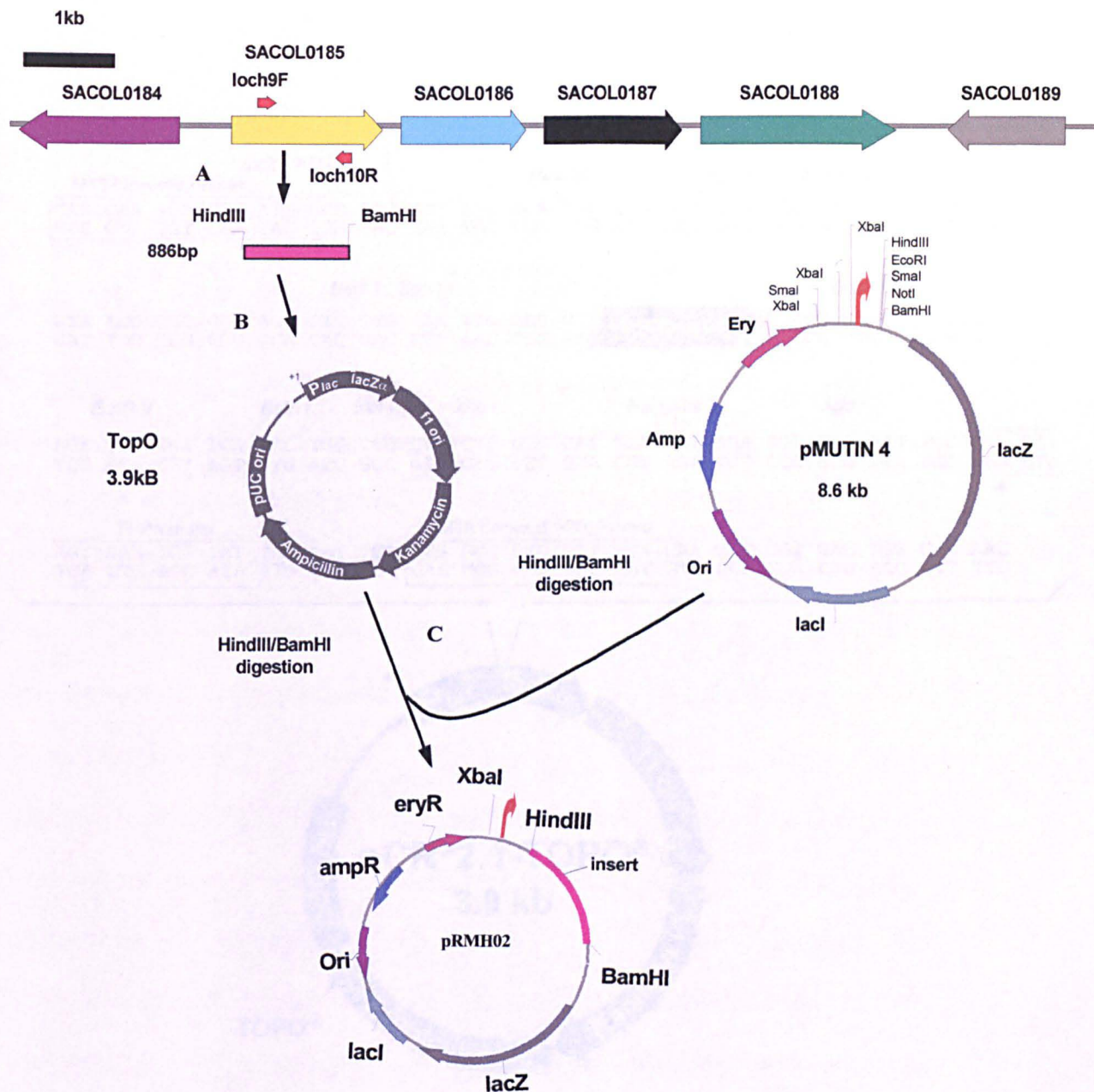
Figure 3.19

Construction of pRMH02. A. PCR of the SACOL0185 gene insert from SH1000 using primer pairs loch9F/loch10R to produce an 886 bp fragment; B. Cloning into TopO Vector C. Digestion with BamHI and HindIII and cloning of the fragment into pMUTIN4 (predigested with HindII/BamHI) creating pRMH02.

```
                    lacZα ATG                          Hind III          Kpn I    Sac I BamHI    Spe I
    M13 Reverse Primer     |                              |                |         |    |         |
    CAG GAA ACA GCT ATG ACC ATG ATT ACG CCA AGC TTG GTA CCG AGC TCG GAT CCA CTA
    GTC CTT TGT CGA TAC TGG TAC TAA TGC GGT TCG AAC CAT GGC TCG AGC CTA GGT GAT


                          BstX I  EcoR I                                    EcoR I
                            |       |                                         |
    GTA ACG GCC GCC AGT GTG CTG GAA TTC GCC CTT  PCR Product  AAG GGC GAA TTC TGC
    CAT TGC CGG CGG TCA CAC GAC CTT AAG CGG GAA             TTC CCG CTT AAG ACG


    EcoR V          BstX I    Not I    Xho I              Nsi I Xba I        Apa I
      |               |        |        |                  |   |             |
    AGA TAT CCA TCA CAC TGG CGG CCG CTC GAG CAT GCA TCT AGA GGG CCC AAT TCG CCC TAT
    TCT ATA GGT AGT GTG ACC GCC GGC GAG CTC GTA CGT AGA TCT CCC GGG TTA AGC GGG ATA
                                                                                  ▲
        T7 Promoter                      M13 Forward (-20) Primer
    AGT GAG TCG TAT TAC AAT TCA CTG GCC GTC GTT TTA CAA CGT CGT GAC TGG GAA AAC
    TCA CTC AGC ATA ATG TTA AGT GAC CGG CAG CAA AAT GTT GCA GCA CTG ACC CTT TTG
```

Figure 3.20

Map of pCR 2.1-TOPO showing the features and sequence surrounding the
TOPO cloning site. The plasmid contains a *lacZα* fragment and carries both the
kanamycin and ampicillin resistance markers. Adapted from TOPO TA Cloning
User Manual, Invitrogen.

146

with selection on ampicillin (50 µg/ml). The presence of the cloned insert in pMUTIN4 was verified by *Bam*HI and *Hind*III digestion revealing the 846bp insert and 8.6kb backbone (Fig. 3.21B). The recombinant plasmid was named pRMH02. Plasmid pRMH02 was transformed into *S.aureus* RN4220 by electroporation and selection on BHI ery lin. Transformants were patched onto BHI ery lin containing X-gal and colonies were found to be blue after overnight growth verifying the presence of *lacZ* on pMUTIN4 as a transcriptional fusion with SACOL0185. One transformant was picked and called RMHcol8.

3.2.4.2   Transduction by θ85 phage into SH1000

Phage transduction using θ85 was used to transfer the pMUTIN4 chromosomal insertion from RMHcol8 to SH1000 using ery/lin selection. Transductants were not blue on X-gal. Genomic DNA from transductant RMHcol11(*SACOL0185*) was purified and the presence of the pMUTIN4 insertion verified by PCR using primer pair loch11F and loch10R (Fig. 3.22). The correct insertion in RMHcol11(*SACOL0185*) was verified by Southern Blot analysis. Genomic DNA was digested *Hind*III or *Bam*HI. Agarose gel separated DNA fragments were blotted and hybridized with the 846bp pRMH02 insert as probe. The expected sizes of hybridizing bands are shown in Fig. 3.23. These are 2.8kB for SH1000 and 2.5kB and 12.7kB for the mutant with *Hind*III digestion and 6.7kB for SH1000 and 4.4kB and 11.3kB for the mutant with *Bam*HI digestion. Bands were all of the expected (Fig 3.24) sizes thus verifying the inactivation of SACOL0185.

147
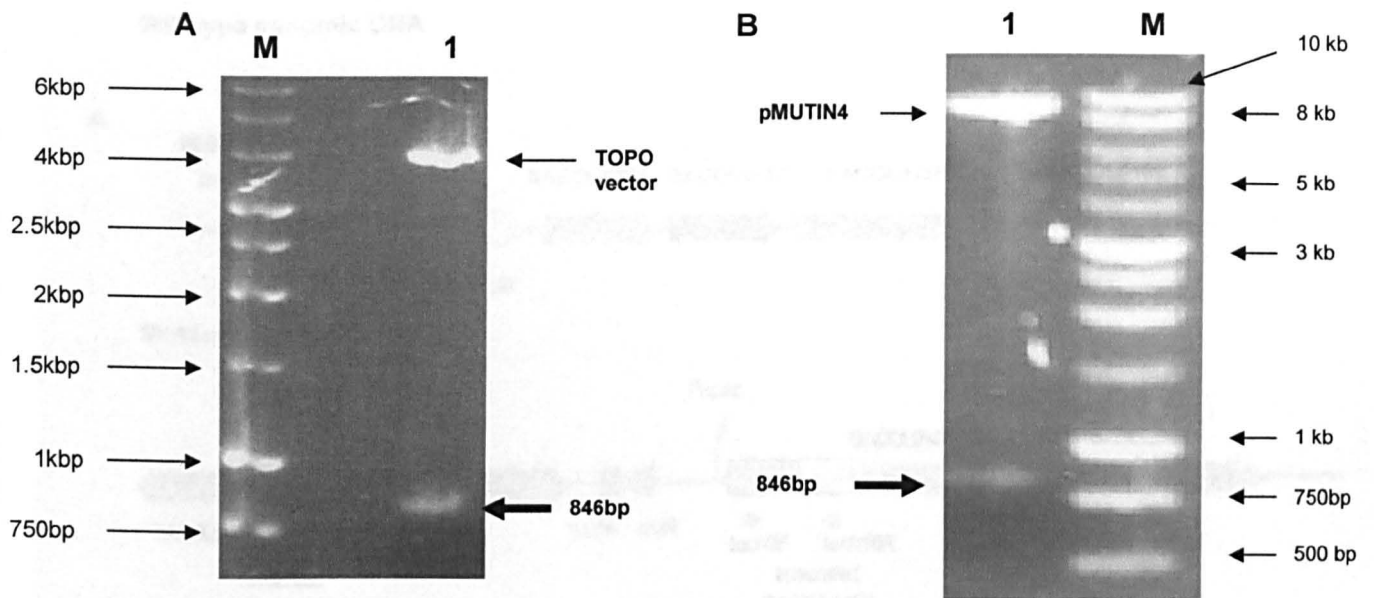
Figure 3.21

Verification of SACOL0185 clones. Lane 1 *Hind*III and *Bam*HI digestions of pTOPOSACOL0185 (Panel A) and pRMH02 (Panel B). M, 1kB DNA ladder marker with appropriate sizes is shown.
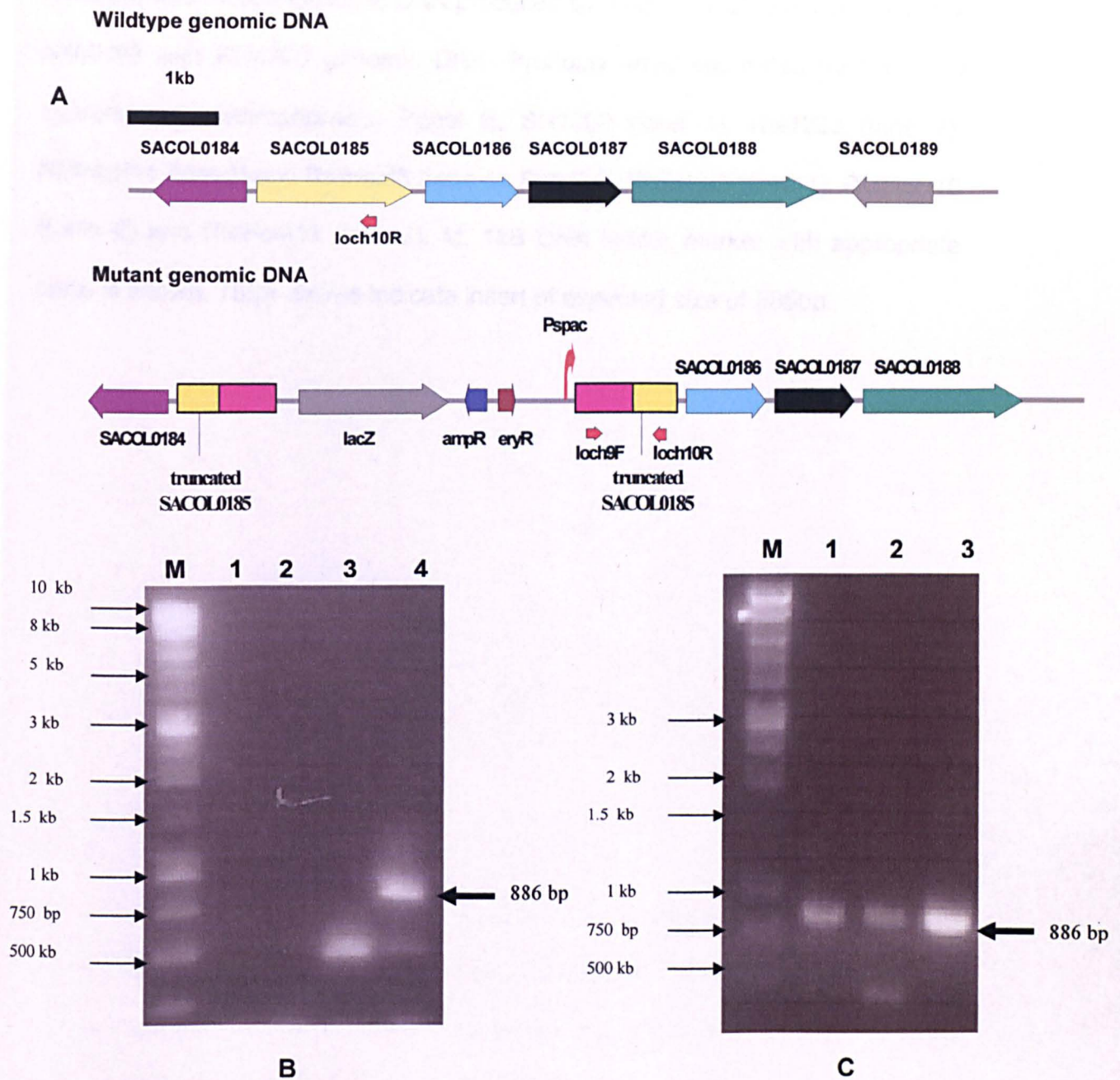
Figure 3.22

Verification by PCR analysis of SACOL0185 inactivation using genomic DNA from RMHcol8, RMHcol7 and RMHcol11 with primers loch11F/loch 10R. Panel A, Physical map of SACOL0185 gene in wildtype genomic DNA (SH1000 and

RN4220) and mutant genomic DNA produced by single homologous crossover of pRMH02 with RN4220 genomic DNA. Products were separated by 1% (w/v) agarose gel electrophoresis. Panel B, SH1000 (lane 1); RN4220 (lane 2); RMHcol11 (lane3) and RMHcol8 (lane 4). Panel C, RMHcol7 (lane 1); RMHcol10 (Lane 2) and RMHcol11 (lane 3). M, 1kB DNA ladder marker with appropriate sizes is shown. Thick arrows indicate insert of expected size of 886bp.
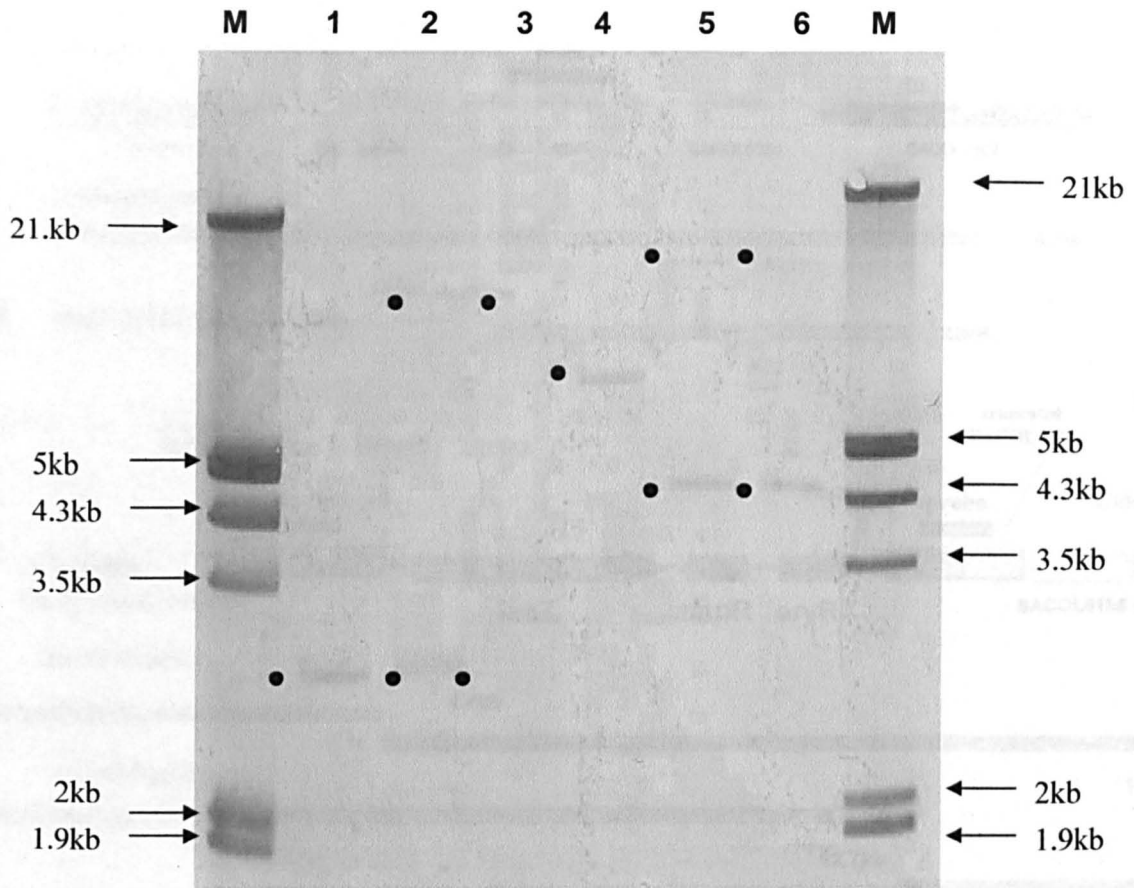
Figure 3.23

Southern Blot verification of SACOL0185 inactivation. Genomic DNA of *S.aureus* SH1000, (lanes 1 and 4), RMHcol7 (lanes 2 and 5), and RMHcol11 (lanes 3 and 6) were digested with *Hind*III (lanes 1-3) or *Bam*HI (lanes 4-6). The probe was the 886bp insert which is a PCR product the internal part of the SACOL0185 gene using primers loch9F and loch10R (Figure 3.19). Lane M is digoxigenin labeled DNA markers with appropriate sizes shown. Hybridizing bands are indicated by black dots on the left of each band.
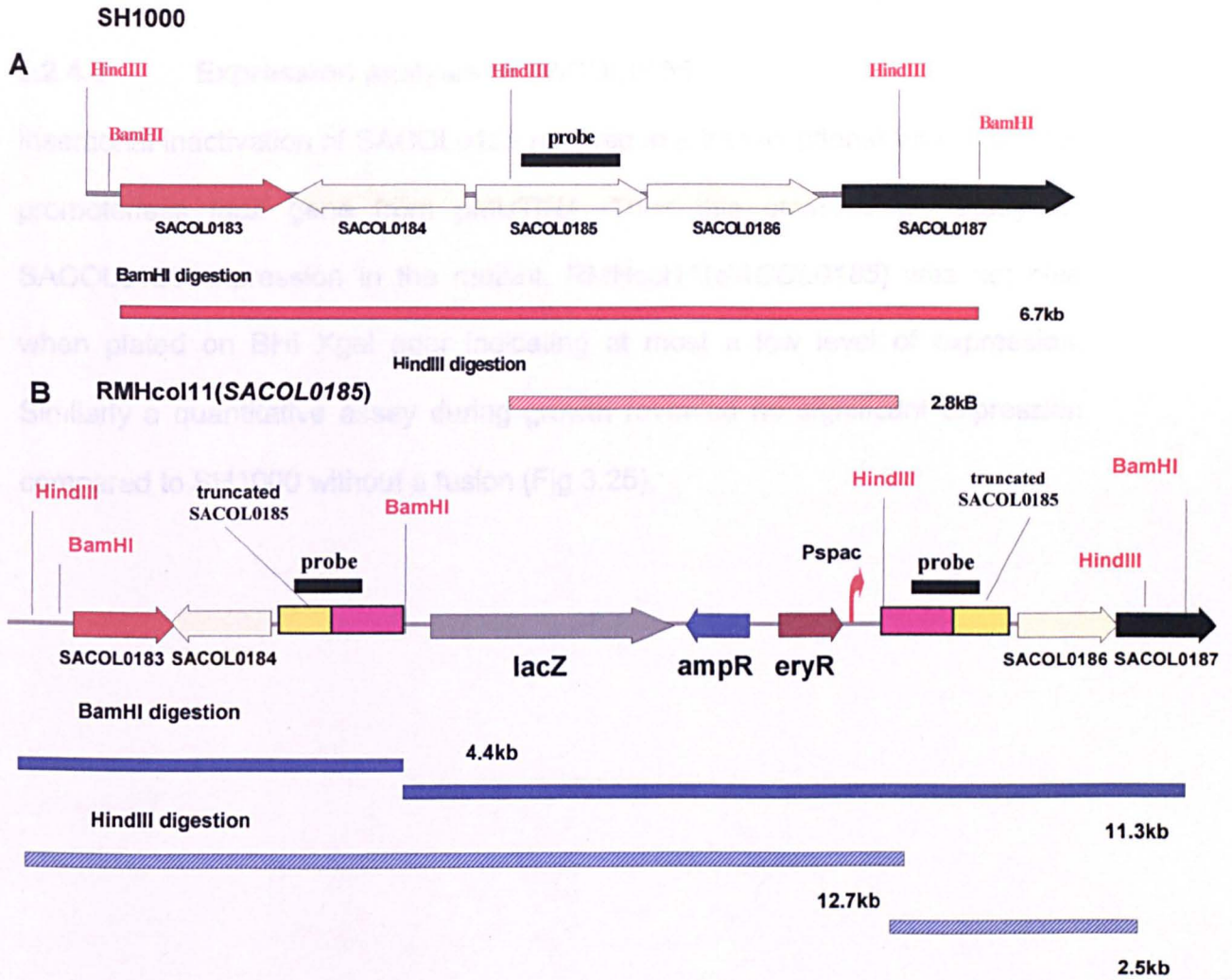
Figure 3.24

Physical map showing SACOL0185 region with restriction sites indicated. Expected hybridizing band fragment sizes from SH1000 (Panel A) digested with BamHI and HindIII are 6.7kB and 2.8kB respectively. RMHcol11(*SACOL0185*) (Panel B) digestion with *Bam*HI is expected to produce fragments of 4.4kB and 11.3kB and with *Hind*III 12.7kB and 2.5kB.Probe binding region is shown.

3.2.4.3   Expression analysis of SACOL0185

Insertional inactivation of SACOL0185 resulted in a transcriptional fusion with the promoterless *lacZ* gene from pMUTIN4. Thus this provided an assay for SACOL0185 expression in the mutant. RMHcol11(*SACOL0185*) was not blue when plated on BHI Xgal agar indicating at most a low level of expression. Similarly a quantitative assay during growth revealed no significant expression compared to SH1000 without a fusion (Fig 3.25).
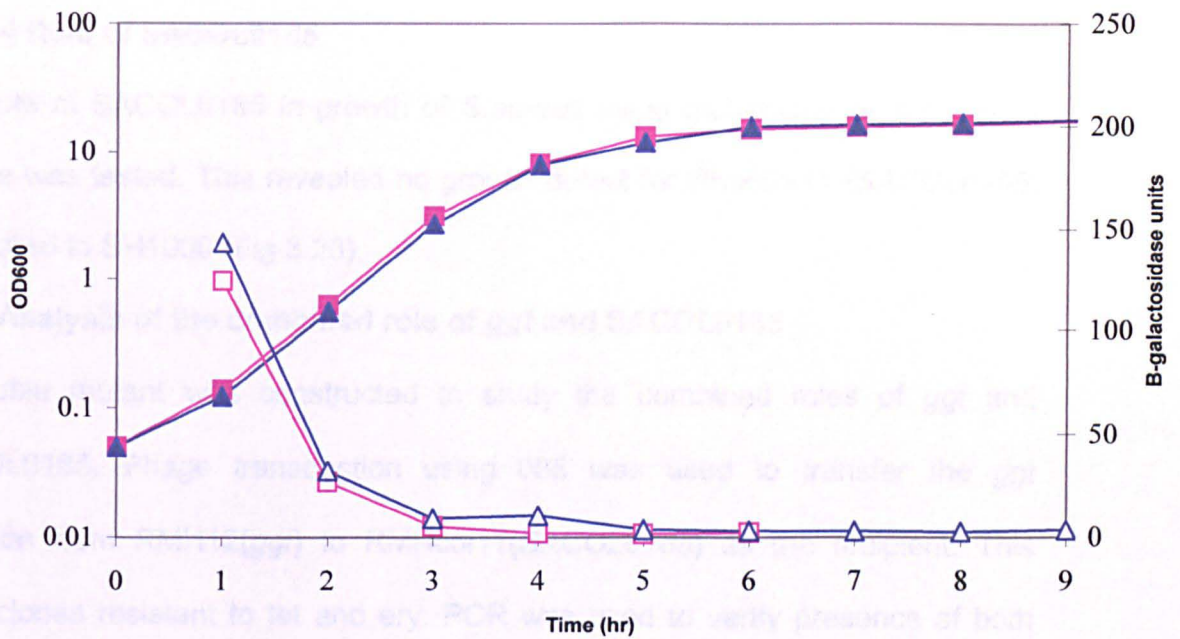
Figure 3.25

Expression of the *SACOL0185::lacZ* fusion in RMHcol11(*SACOL0185*). LacZ activity(△ □) and OD$_{600}$ (▲ ■) were measured for SH1000 (□ ■) and RMHcol11(△ ▲).

3.2.4.4 Role of SACOL0185

The role of SACOL0185 in growth of *S.aureus* using glutathione as sole sulfur source was tested. This revealed no growth defect for RMHcol11 (*SACOL0185*) compared to SH1000 (Fig 3.26).

3.2.5 Analysis of the combined role of *ggt* and SACOL0185

A double mutant was constructed to study the combined roles of *ggt* and SACOL0185. Phage transduction using θ85 was used to transfer the *ggt* mutation from RMH12(*ggt*) to RMHcol11(*SACOL0185*) as the recipient. This gave clones resistant to tet and ery. PCR was used to verify presence of both mutations in one such clone RMH25 (*ggt SACOL0185*). Primer pair loch8F and loch6R was used to amplify the *ggt* insert in the cloned DNA. The expected size for the correct mutation would be 4.3kb (*ggt* insert). Gel electrophoresis of the PCR product revealed a band of the expected size and thus verification of the mutation (Fig 3.27).

3.2.5.1 Combined role of *ggt* and SACOL0185

3.2.5.1.1 Role in glutathione utilization

The combined roles of *ggt* and *SACOL0185* in growth of *S.aureus* using glutathione as sole sulfur source were tested. This revealed no growth defect for RMH25 (*ggt SACOL0185*) compared to SH1000 (Fig.3.28).
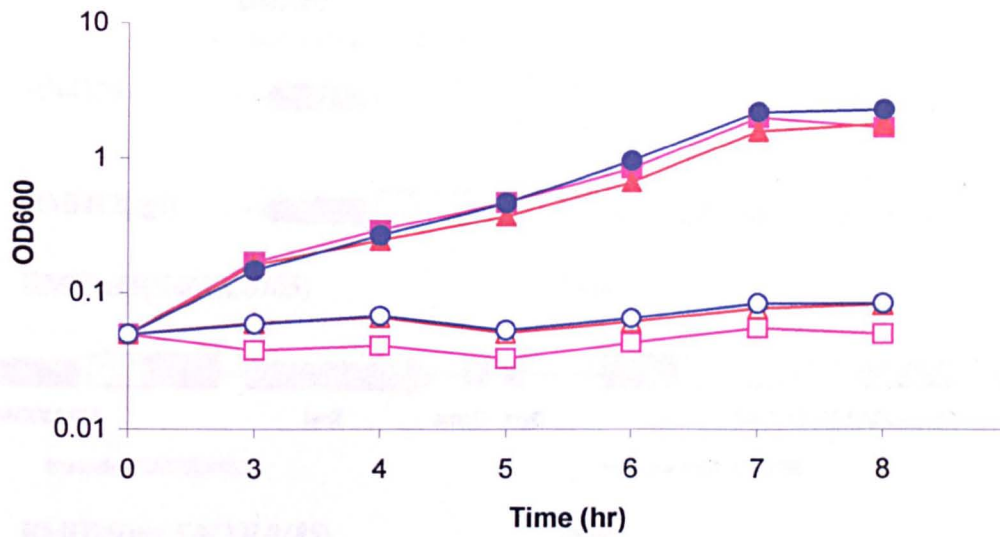
Figure 3.26

Role of *ggt* and *SACOL0185* in growth. Growth curve (OD_{600}) in liquid chemically defined media (CDM) with 50 µM glutathione (filled) and without glutathione (open) of *S.aureus* SH1000 (■ □), RMH12(*ggt*) (▲ △) and RMHcol11(*SACOL185*) (● ○).
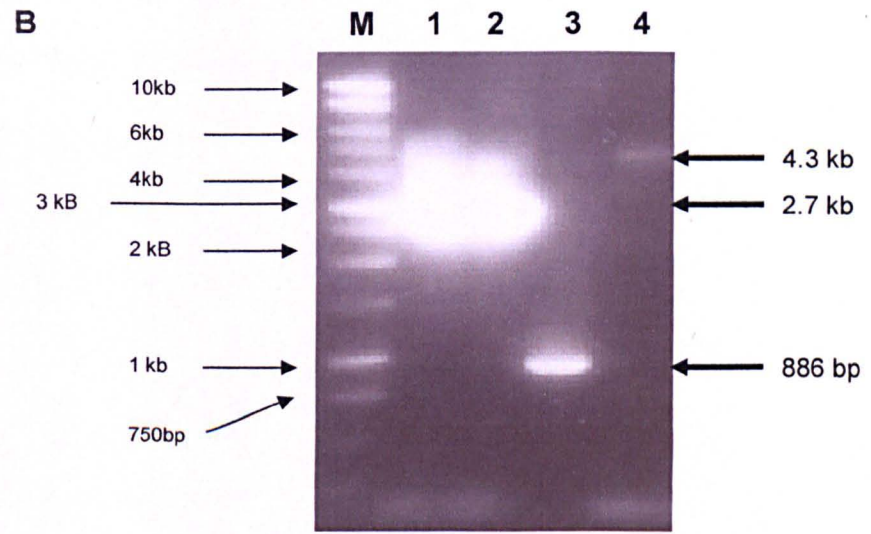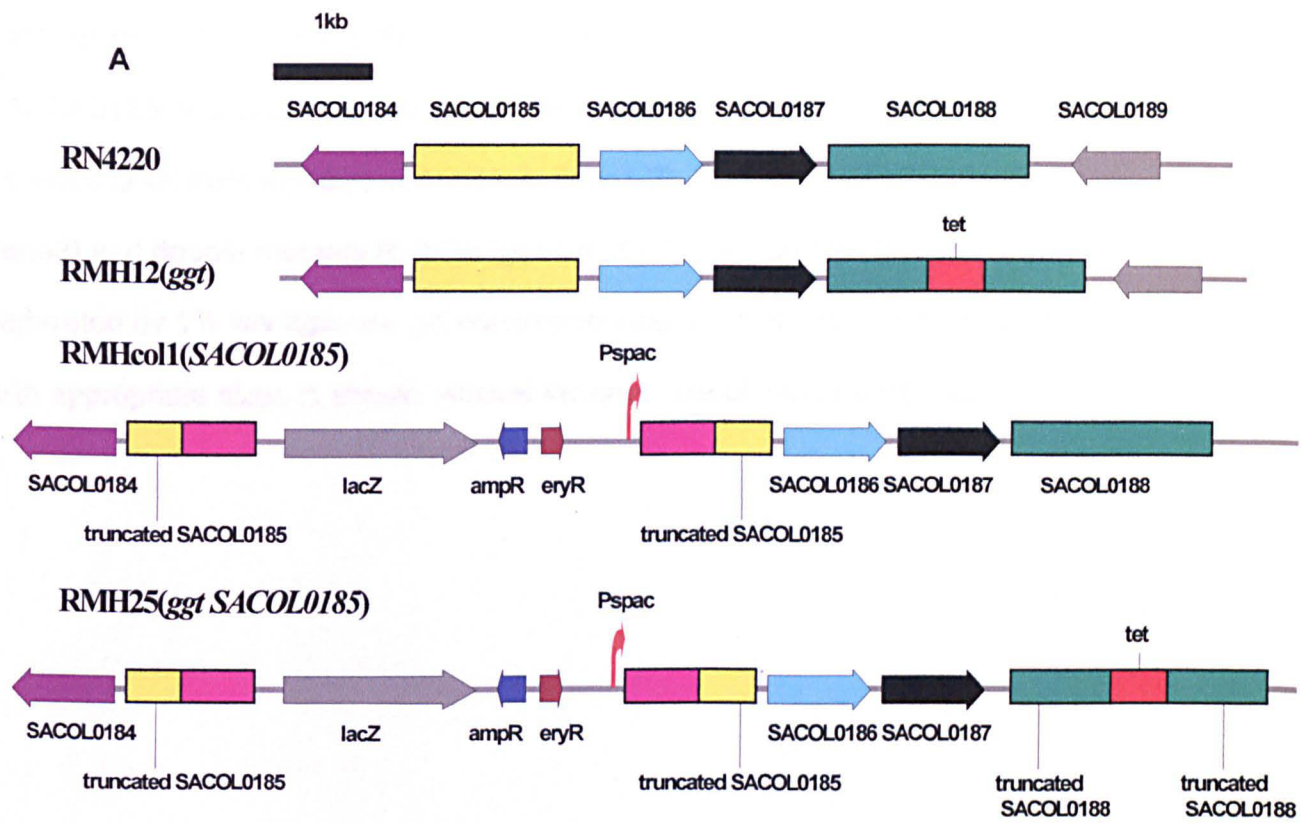
Figure 3.27

Verification of *S.aureus* RMH25. Panel A, Physical map of *ggt* and *SACOL0185*

gene region in RN4220, RMH12(*ggt*) with *tet* insertion in *ggt*,

RMHcol11(*SACOL0185*) with pMUTIN4 insertion in SACOL0185, and

RMH25(*ggt SACOL0185*) with both *tet* insertion in *ggt* and pMUTIN4 insertion in

SACOL0185. Panel B, PCR was performed using primer pair loch8F/loch6R on

genomic DNA from SH1000 as template (lane1-2), RMHcol11(*SACOL0185*)

(lane3) and double mutants RMH25 (*ggt SACOL0185*) (lane4). Products were

separated by 1% w/v agarose gel electrophoresis. M, 1kB DNA ladder marker

with appropriate sizes is shown. Arrows indicate size of PCR fragments.
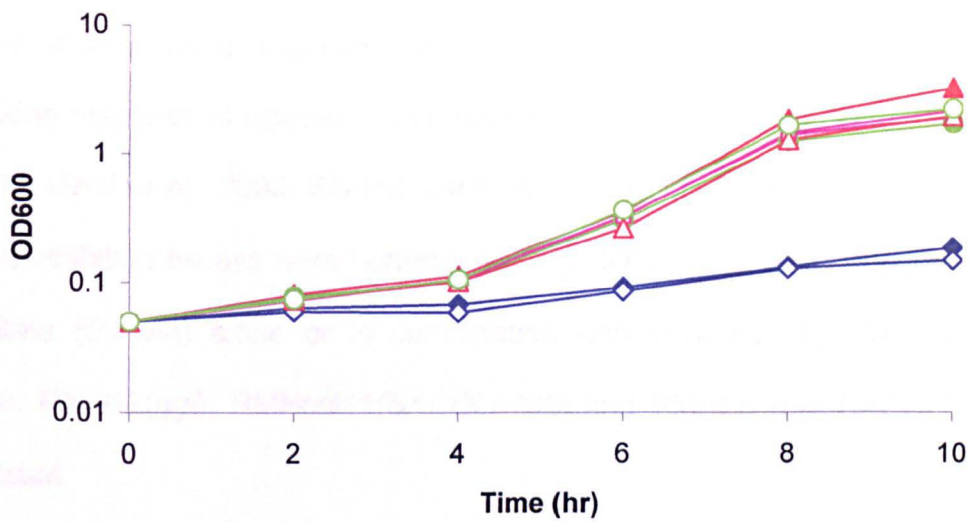
Figure 3.28

Role of *ggt* and SACOL0185 in growth on glutathione. Growth curve (OD_{600}) in liquid chemically defined media (CDM) of *S.aureus* SH1000 (filled symbol) and RMH25 (*ggt SACOL0185*) (open symbol) in 50 µM cysteine (■ □), 50 µM glutathione (▲ △), a combination of 50 µM cysteine and 50 µM glutathione (● ○), and no addition (◆ ◇). ■ □ are hidden behind ▲ △ and ● ○.

3.2.5. Role of *ggt* and SACOL0185 in glutathione associated stress resistance

Previous studies have suggested that low molecular weight thiols such as glutathione may protect against stress induced by various agents (Vergauwen *et al.*, 2003, Uziel *et al.*, 2003, Sherrill and Fahey, 1998, and Hibberd, 1978). Disc diffusion inhibition assays were performed using CDM plates supplemented with glutathione (50 µM) alone or in combination with cysteine (50 µM). Strains SH1000, RMH12(*ggt*), RMHcol11(*SACOL0185*) and RMH25 (*ggt SACOL0185*) were tested.

3.2.6.1 Diamide

The presence of cysteine or glutathione as sulfur source did not significantly affect diamide resistance for any strain. RMH12(*ggt*) showed a significant increase in sensitivity to diamide compared to SH1000 in the presence of glutathione and combination of cysteine and glutathione (Fig 3.29, p = 0.02 and p = 0.005 respectively). RMHcol11(*SACOL0185*) and RMH25 (*ggt SACOL0185*) showed comparable levels of resistance to SH1000.

3.2.6.2 Methyl viologen

RMH12(*ggt*) showed significant increase in sensitivity against 1M methyl viologen in the presence of cysteine or glutathione (p = 0.007, p = 0.03) compared to SH1000 (Fig. 3.30). A slight increase in sensitivity was observed in the presence of a combination of cysteine and glutathione (p = 0.06). RMH25 (*ggt SACOL0185*) showed significant increase in sensitivity in the presence of glutathione and a combination of cysteine and glutathione (p = 0.009, p = 0.01) while RMHcol11 (*SACOL0185*) was only significantly more sensitive in the

presence of a combination of cysteine and glutathione (p = 0.04) compared to SH1000.

3.2.6.3 H_2O_2

Resistance to H_2O_2 was tested using the disc diffusion assay and RMH12(*ggt*) showed a significant increase in sensitivity against 0.1M H_2O_2 in the presence of cysteine (p=0.04) compared to SH1000 (Fig 3.31). RMHcol11(*SACOL0185*) showed significant increase in sensitivity against 0.1M H_2O_2 in the presence of both cysteine and glutathione (p<0.01)).

A liquid H_2O_2 kill assay was also carried out (Fig 3.32). Growth in CDM with glutathione or cysteine did not make a significant difference to H_2O_2 resistance for SH1000. When grown in CDM with glutathione RMH12(*ggt*), RMHcol11(*SACOL0185*) and RMH25(*ggt SACOL0185*) all showed similar H_2O_2 sensitivity with approximately 100-fold drop in viability after 45 minutes. Similar sensitivity was seen for RMHcol11(*SACOL0185*) when grown in CDM with cysteine. However RMH12(*ggt*) and RMH25(*ggt SACOL0185*) were more resistant than SH1000 with 10.3% and 1.4% survivors respectively compared to 0.2% for SH1000 at 45 minutes.
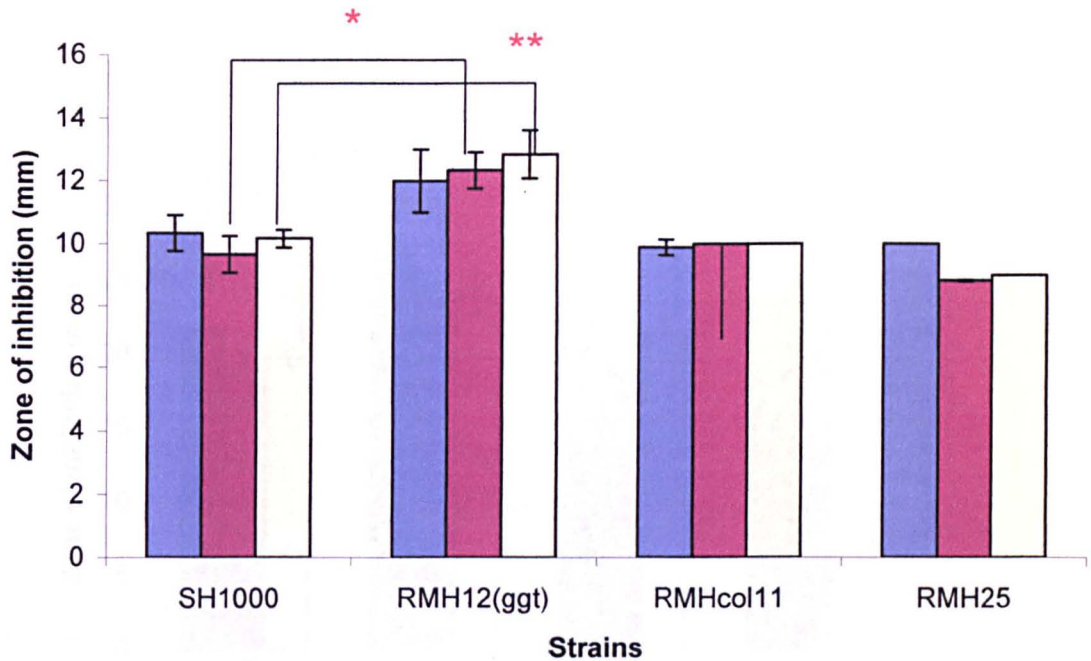
* p = 0.05
** p = 0.005

Figure 3.29

Diamide resistance of *S.aureus* SH1000, RMH12(*ggt*), RMHcol11(*SACOL0185*)

and RMH25(*ggt SACOL0185*) grown on chemically defined media (CDM)

supplemented with 50 μM cysteine (blue bar), 50 μM glutathione (maroon bar) or

50 μM cysteine plus 50 μM glutathione (cream bar) and tested against 1M

diamide. Values shown are means of three separate experiments with standard

deviations shown.
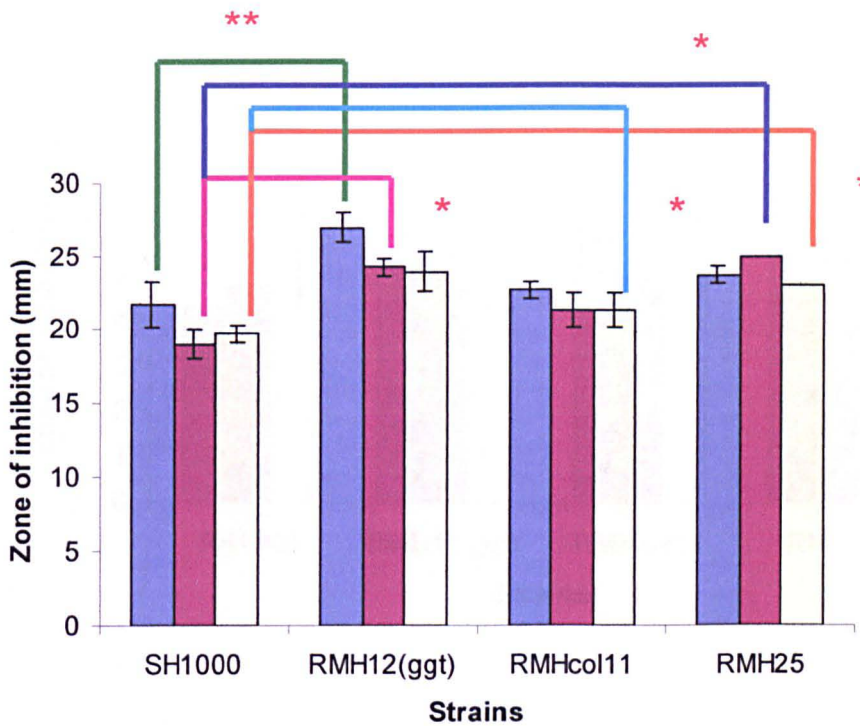
* p = 0.05
** p = 0.005

Figure 3.30

Methyl viologen resistance of *S.aureus* SH1000, RMH12(*ggt*), RMHcol11(*SACOL0185*) and RMH25(*ggt SACOL0185*) were grown on chemically defined media (CDM) supplemented with 50 µM cysteine (blue bar), 50 µM glutathione (maroon bar), or 50 µM cysteine plus 50 µM glutathione (cream bar) and tested against 1M methyl viologen. Values are means of three separate experiments with standard deviations shown.
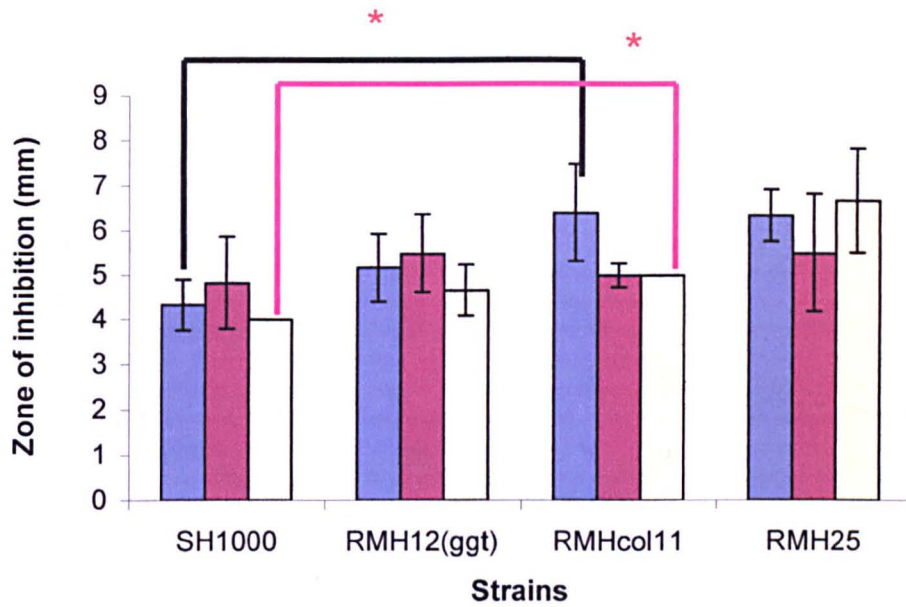
* p = 0.05
** p = 0.005

Figure 3.31

H_2O_2 resistance of *S.aureus* SH1000, RMH12(*ggt*), RMHcol11(*SACOL0185*) and RMH25(*ggt SACOL0185*) were grown on chemically defined media (CDM) supplemented with 50 µM cysteine (blue bar), 50 µM glutathione (maroon bar), or 50 µM cysteine plus 50 µM glutathione (cream bar) and tested against 0.1M H_2O_2. Values are means of three separate experiments with standard deviations shown.
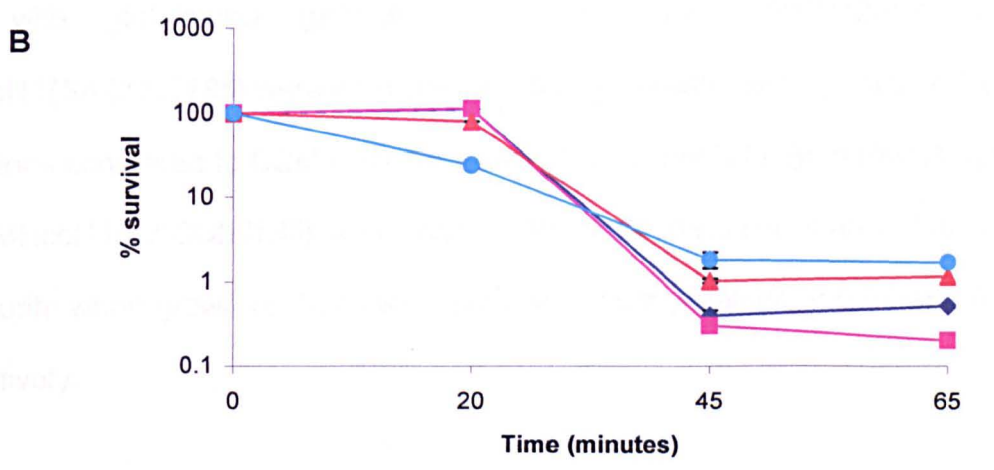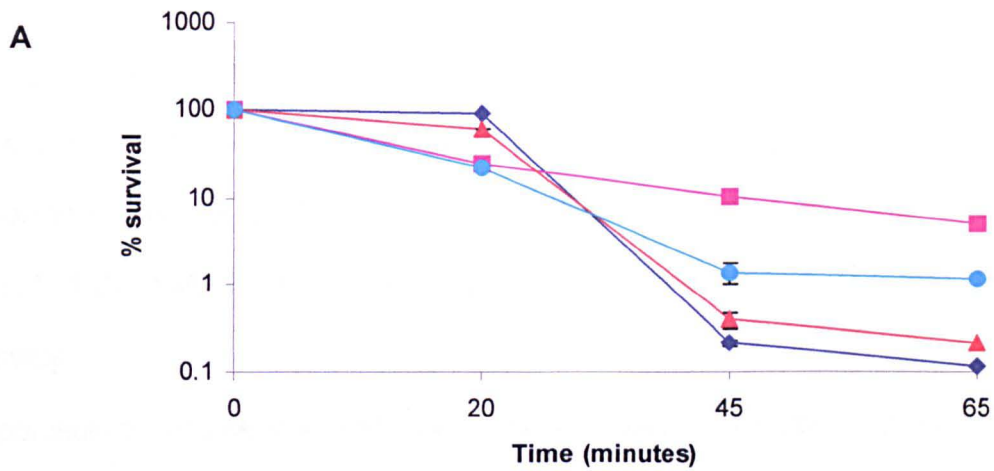
Figure 3.32

Liquid H_2O_2 kill curve *S.aureus* SH1000 (◆), RMH12(*ggt*) (■),

RMHcol11 (*SACOL0185*) (▲) and RMH25 (*ggt SACOL0185*) (●) grown in CDM

with cysteine (Panel A) and glutathione (Panel B) washed and treated with 0.1M

H_2O_2. Values are the means of three independent experiments with standard

deviation shown.

3.2.6.4 Potassium tellurite

Increasing concentrations of glutathione (0.625-10mM) showed a protective effect on SH1000 against 1M K_2TeO_3 (Fig 3.33, 5mM p=0.16; 10mM p =0.03). Protection was greatest at 10 mM and no significant protection was observed at 0.625 mM, 1.25 mM, 2.5 mM, and 5mM with p values of 1, 1, 0.7 and 0.16 respectively.

A 1M potassium tellurite disc diffusion inhibition assay revealed that SH1000 grown on CDM with cysteine was not significantly more sensitive than that on CDM with glutathione (p=0.29) (Fig 3.34). Both RMH12(*ggt*) and RMHcol11(*SACOL0185*) were no more sensitive to tellurite when grown on CDM glutathione compared to CDM cysteine. (p=0.25) and (p=0.27). Both RMH12(*ggt*) and RMHcol11(*SACOL0185*) were significantly more sensitive than SH1000 to 1M tellurite when grown on CDM with glutathione with p values of 0.04 and 0.02 respectively.
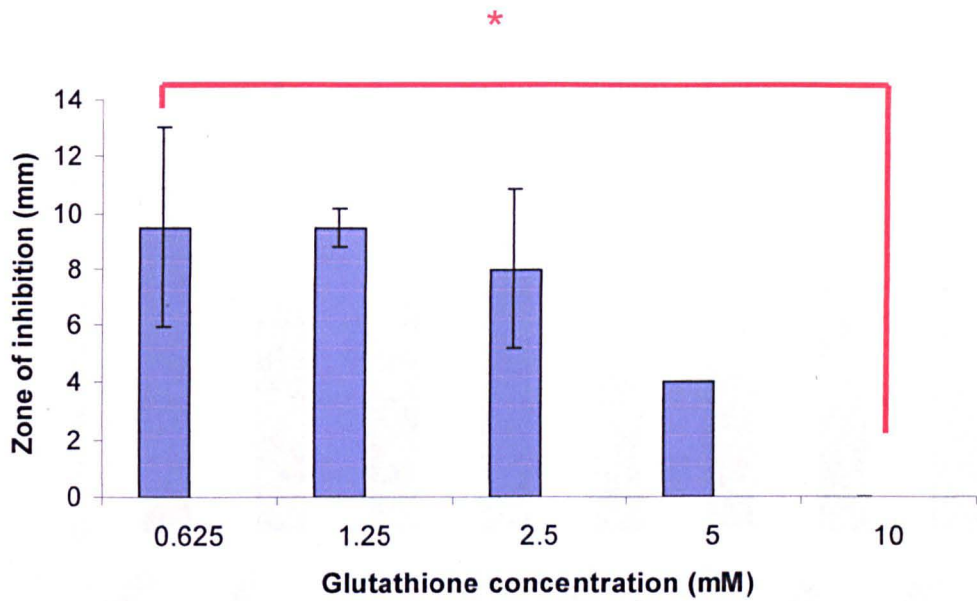
* p = 0.05
** p = 0.005

Figure 3.33

Tellurite resistance of *S.aureus* SH1000 on chemically defined media (CDM) supplemented with glutathione (0.625 mM – 10 mM) and tested against 1M K_2TeO_3. Values shown are the means of two separate experiments.
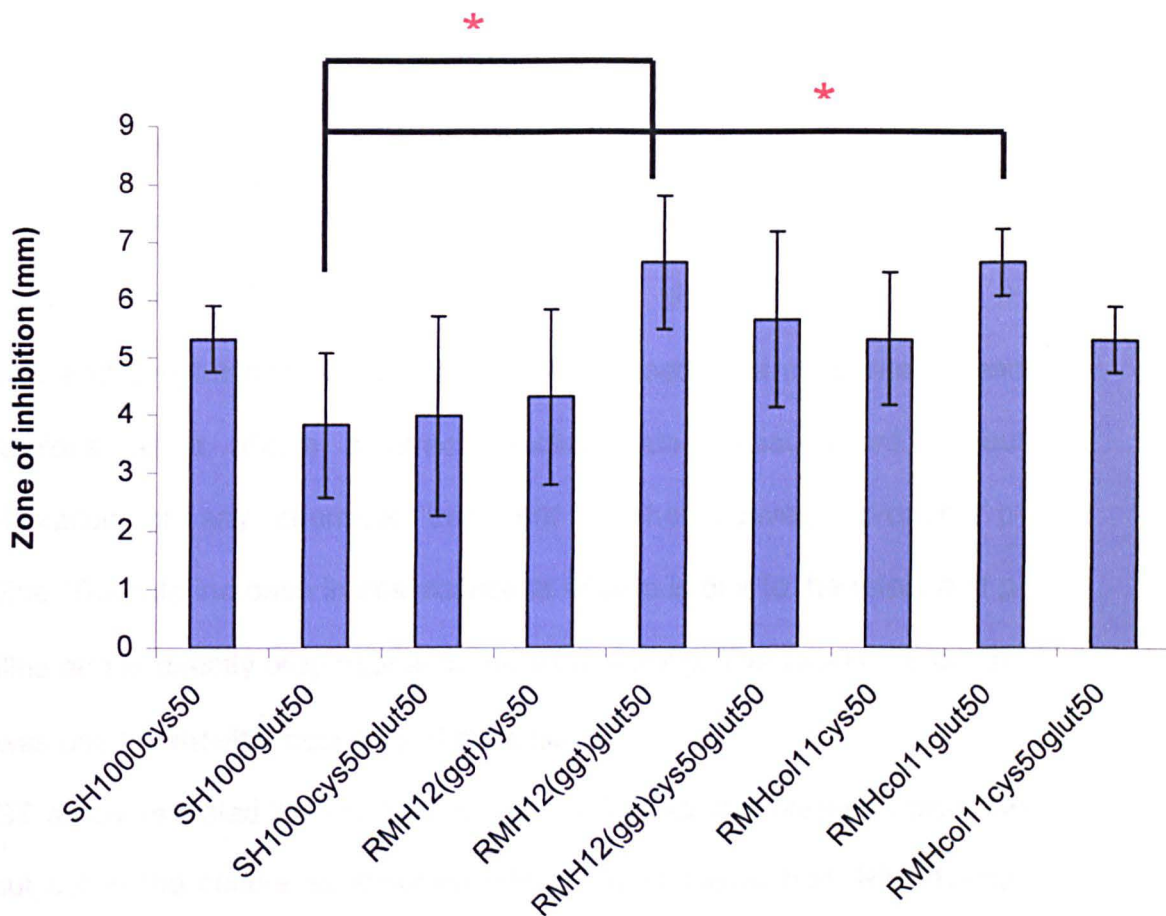
* p = 0.05
** p = 0.005

Figure 3.34

Tellurite resistance disc inhibition assay for *S.aureus* SH1000, RMH12(*ggt*) and RMHcol11(*SACOL0185*) grown on chemically defined media (CDM) supplemented with 50 µM cysteine, 50 µM glutathione.and 50 µM cysteine plus glutathione and tested against 1M K_2TeO_3. Values shown are mean values of three separate experiments.

3.2.7 γ-glutamyltranspeptidase assay (GGT assay).

The GGT assay measures the transfer the γ-glutamyl group from the substrate L-γ-glutamyl-p-nitroanilide (γGPNA) to the acceptor glycylglycine to form p-nitroaniline and L-γ-glutamylglycylglycine. GPNA is used as a substrate instead of glutathione as it allows a direct reaction rate measurement without deproteinization or any chemical treatment of the cleavage product, p-nitroaniline. The rate increase in absorbance at 405nm is due to the release of p-nitroaniline and is directly proportional to the γ-GT activity. The DC-TROL control serum was used to monitor accuracy of the assay.

The GGT assay revealed activity only in the cell free extract prepared from the pellet but not in the culture supernatant (Fig 3.35). However both RMH12(*ggt*) and RMHcol11(*SACOL0185*) had undiminished activity. This suggests a mechanism other than γ-GT activity enables utilization of the substrate and possibly an alternative novel mechanism for the metabolism of glutathione in *S.aureus*.
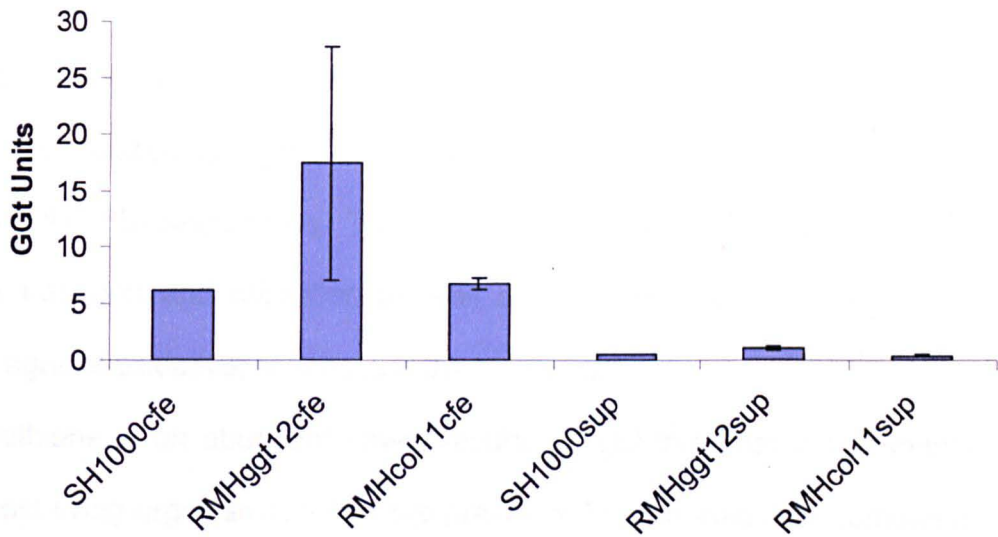
Figure 3.35

GGT specific activity assay of cell free extracts (cfe) and supernatants (sup) from
S.aureus SH1000, RMH12(*ggt*) and RMHcol11(*SACOL0185*) grown in
chemically defined media (CDM) supplemented with 50 µM glutathione. Values
shown are mean values of three independent assays with standard deviation
shown.

3.3   Discussion

This chapter describes a molecular genetic approach to study the role of glutathione as a sulfur source and in stress resistance. Two mutations were created in the putative *ggt* gene and in a putative ABC transporter encoding genes (SACOL0185) respectively. The aim was to elucidate the mechanism of glutathione transport and utilization as well as to determine its physiological function(s) against oxidative, tellurite and thiol stresses.

Glutathione is an abundant low-molecular weight thiol that is commonly found in most living organisms. It is more prevalent in gram-negative compared to gram-positive bacteria (Fahey *et al.*, 1978) and amongst the gram-positives only *Streptococcus agalactiae*, *Streptococcus pyogenes*, *Enterococcus faecalis* and *Lactococcus lactis* synthesize glutathione (Sherrill *et al.*, 1998, Fahey *et al* .,1998, Newton, 1996). Synthesis of glutathione in these organisms is not only species specific but also strain dependent (Sherrill *et al.,* 1998). Glutathione possesses manifold roles, from being a cysteine storage reserve to maintaining cellular redox potential, as well as protective functions against oxidative and thiol stress (Dickinson *et al.*, 2002, Storey, 1996, Meister *et al.,* 1983). *S.aureus* is not able to synthesize glutathione and it does not possess the gene homologues for γ-cysteinylglycine synthetase or gluthathione synthase. However, Lithgow *et al.*, 2004 reported the existence of the gene homologue for *ggt* in *S.aureus* that codes for a putative gammaglutamyltranspeptidase (GGT). GGT catalyzes the transfer of γ-glutamyl residues from γ-glutamyl compounds to amino acids and peptides, as well as the hydrolysis of γ-glutamyl compounds (Kumagai *et al.,*

1989, Meister et al., 1983). GGT has been shown to be involved in the utilization of glutathione as a sulfur source in E.coli K12 (Suzuki et al., 1993), Helicobacter pylori (Shibayama et al., 2007) and Haemophilus influenzae (Vergauwen et al., 2003).

The role of glutathione in S.aureus has not been determined and as it is unable to synthesize glutathione (Fahey et al., 1978), it must acquire it from the host environment. S.aureus has been previously shown to be able to utilize glutathione as the sole sulfur source (Lithgow et al., 2004). In this study it was verified that the S.aureus strain SH1000 was able to catabolize glutathione or thiosulphate as sole sulfur source. Similarly, S.mutans does not synthesize glutathione but is able to import and accumulate significant levels that it rapidly metabolizes indicating that it may serve as a nutrient source (Sherrill et al., 1998). As expected SH1000 was unable to utilize sulphate as a sulfur source and it does not possess gene homologues for utilization of sulphate (Lithgow et al., 2004).

Although the mechanism of glutathione utilization in S.aureus is unknown, the presence of a ggt homolog in S.aureus SH1000 suggests a possible involvement of the GGT enzyme. The ggt mutant (RMH12(ggt)) was made by insertional inactivation using a tetracycline resistance cassette and a glutathione utilization study was performed. Surprisingly, RMH12(ggt) was repeateadly found to be able to utilize glutathione as the sole sulfur source in both the liquid and plate assays (Fig 3.2 and Table 3.1 respectively). This finding is in contrast with other studies performed that have shown GGT to be essential in gluthathione

utilization. Suzuki *et al.*, 1993 reported that a *ggt* derivative of the cysteine auxotroph of *E.coli* K12 was unable to grow on minimal media supplemented with glutathione. In contrast, glutathione was shown to be dispensable for growth in *gshA* mutants that were defective in γ-glutamylcysteine synthethase (Apontoweil, 1975).

RMH12(*ggt*) however did not show the expected phenotype and instead it thrived in minimal media containing only glutathione. Although GGT is deemed responsible for glutathione degradation, it is proposed that in enteric bacteria in addition to degradation by GGT an alternative mechanism for glutathione breakdown and uptake may exist (Suzuki *et al.*, 1984). When GGT of *P.mirabilis* was inhibited by serine-borate, accumulation of cellular gluthathione content was observed before leakage occurred which suggests the intracellular presence of a GSH degradation system like GGT (Nakayama, 1984). Minami *et al.*, 2004 reported that the YwrD protein that shows identity with the amino acid sequence of the GGTs of *E.coli* K12 (31%) and *B.subtilis* (27%) may play a similar role as GGT. However, the authors found that in *Bacillus subtilis* utilization of extracellular glutathione as a sulfur source is mediated by γ-glutamyltranspeptidase and not YwrD. The role of YwrD in glutathione metabolism has not been elucidated.

Similarly, transposon mutagenesis using the Tn*917* transposon did not allow isolation of any mutants that failed to grow in the presence of glutathione as the sole sulfur source. This is likely due to more than one mechanism of glutathione utilization in *S.aureus*.

As RMH12(*ggt*) did not show the expected phenotype, the role of other genes in glutathione metabolism was studied. Since *S.aureus* does not synthesize glutathione (Fahey *et al.*, 1975) and is known to acquire it from the environment (Lithgow *et al.*, 2004), a transport system for glutathione uptake must exist. Similarly, import and accumulation of glutathione from the media has been demonstrated in other gram-positive bacteria that do not synthesize glutathione such as *S.mutans* (Sherrill *et al.*, 1998) and *S.pneumoniae* (Kumaresan *et al.*, 1995).

The uptake of nutrients in bacteria has been often shown to be mediated by solute binding protein-dependent permeases (Higgins, 1992). The bacterial peptide transport systems most characterized generally belong to the large family of ABC transporters (Hagting *et al.*, 1993) of which the oligopeptide transport system (Opp) is a member (Picon *et al.*, 2000). It constitutes one of the most versatile substrate binding transports proteins. OppA for instance is shown to transport peptides of varying residues in *E.coli* and *Lactococcus lactis* (Picon *et al.*, 1999). Glutathione transporters have been identified in bacteria, plants, and in humans (Zhang *et al.*, 2004, Green *et al.*, 1999, Dringen *et al.*, 1998). The *glt* gene which codes for a permease was identified as the transporter for glutathione and GSSG in *S.pneumoniae* (Kumaresan *et al.*, 1995). HGT1 encodes for Hgt1p that is a high affinity glutathione transporter identified in *Saccharomyces cerevisiae* (Bourbouloux *et al.*, 2000). It is a member of novel class of transporters that however does not have a homologue in *E.coli*.

Study of the *ggt* region reveals that three genes directly upstream of *ggt* encode for a putative ABC transporter that was hypothesized to be involved in glutathione uptake. One of the ABC transporter genes, SACOL0185 was targeted for inactivation by pMUTIN4. As well as SACOL0185 inactivation the construct created a *lacZ* transcriptional fusion. The SACOL0185 mutant and a double mutant (*ggt SACOL0185*) were both also able to utilize glutathione as the sole sulfur source. This suggests that neither the ABC transporter permease protein nor GGT are responsible for the utilization of glutathione and that probably in SH1000 an alternative mechanism may exist by which glutathione is utilized. Involvement of YwrD, the GGT homologue, in glutathione utilization is unlikely as *S.aureus* has no direct homologue.

The possible existence of novel mechanism in SH1000 is further emphasized by the findings from the *ggt* activity assay. Both the RMH12(*ggt*) and RMHcol11(*SACOL0185*) were able to hydrolyse the substrate γ-GPNA, an analog of glutathione, indicating the presence of a GGT-like activity. The activity is found in the cytoplasm. Other studies have shown that GGT mediates glutathione utilization by a mechanism other than making its cysteine residue accessible as a sulfur source through hydrolysis. In *Helicobacter pylori* a recent study reports a role of GGT in glutathione metabolism that facilitates glutathione utilization by converting glutathione to glutamate (Shibayama *et al.*, 2007). This is suggested to contribute to the demise of the host cells through depletion of glutathione and glutamine and production of ammonia.

Since accumulation of glutathione has been shown to be unnecessary for growth in standard medium in *S.mutans* (Sherrill, 1998) and *E.coli* (Apontoweil, 1975), it is suggested that the physiological role of glutathione may possibly be as a protectant against oxidative and thiol stress agents. The protective role of glutathione in stress resistance has been documented in many studies involving different stress agents that induce thiol or oxidative stress (Li *et al.*, 2003, Chesney *et al.*, 1996, Riccillo *et al.*, 2000, Hibberd *et al.*, 1978). Diamide is a thiol-oxidizing agent that is reported to rapidly oxidize glutathione (GSH) to GSSG, the oxidized form (Kosower *et al.*, 1969). In addition diamide was shown to oxidize a variety of electron carriers such as reduced lipoate, reduced Coenzyme A, reduced flavin nucleotides ($FMNH_2$ and $FADH_2$) and ferrodoxin as well as NADH and NADPH (O'Brien *et al.*, 1970). The authors suggest that diamide exerts its bacteriostatic effect through formation of mixed disulphides with proteins which may possibly inactivate sulfhydryls that are essential for the activity of key enzymes. In this study, growth of the *ggt* mutant RMH12(*ggt*) was significantly inhibited by the presence of 1M diamide. However, it is less able to overcome the thiol stress caused by the diamide even in the presence of glutathione. In *E.coli* in addition to glutathione, an alternate pathway of diamide reduction is the thioredoxin-thioredoxin reductase system that like glutathione reductase utilizes NADP as a reductant (Hibberd *et al.*, 1978). Growth of the ABC transporter mutant RMHcol11(*SACOL0185*) was not significantly impaired compared to SH1000 indicating that it is still able to acquire glutathione from the media. This further emphasizes that the transporter may not be involved in the

acquisition of glutathione from the environment in *S.aureus* or that glutathione transport in *S.aureus* is accomplished in synergy with other modes of transport yet to be determined.

Glutathione has been shown to be protective against oxidative stress in yeast (Grant *et al.*, 1996, Penninck *et al.*, 2000) and mammalian cells (Storey, 1996). Vergauwen *et al.*, 2003 report that the glutathione-based H_2O_2 removal and catalase provide overlapping defenses against the toxicity of H_2O_2 in *Hemophilus influenzae,* where glutathione was shown to provide primary defence against low micromolar levels of H_2O_2. In addition, glutathione may also be involved in the regulation of catalase activity and is influenced by intracellular concentrations of H_2O_2 (Oktyabrsky *et al.*, 2001).

In this study resistance to methyl viologen (1M) and H_2O_2 (1M), both oxidative stress agents, showed conflicting results. Both RMH12(*ggt*) and RMH25(*ggt SACOL0185*) were more sensitive to stress induced by methyl viologen in the presence of cysteine. However, surprisingly both strains recovered in the presence of glutathione suggesting that *S.aureus* is able to utilize glutathione by a mechanism other than GGT. Both RMH12(*ggt*) and RMH25(*ggt SACOL0185*) showed increased resistance to H_2O_2 in the liquid assay with cysteine but did not exhibit significant growth inhibition in the disc assay. This could possibly be accounted for by the difference in the metabolic states of the cell in the liquid assay and the disc assay. Protection by glutathione against the oxidative stress caused by hydrogen peroxide in *Lactococcus lactis* is shown to be growth dependent as greater protection is observed in cells in

177

stationary rather than logarithmic phase cells (Li *et al.*, 2003). The authors suggest that this growth dependent protection may be attributed to the significant levels of pyruvate that are present in fast-growing and anaerobically grown cells but is depleted in stationary phase cells. Glutathione depleted cells were found to be more susceptible to hydrogen peroxide during stationary phase when the concentration of pyruvate is lowered. Further, the authors suggest that glutathione uptake triggers the glutathione-glutathione peroxidase-glutathione reductase system which protects the cells during stationary phase (Li *et al.*, 2003). Similarly, gluthathione deficient growing cells of *E.coli* exhibited normal resistance to H_2O_2 whereas non-growing cells showed increased susceptibility to H_2O_2 (Oktyabrysky *et al.*, 2001, Chesney *et al.*, 1996, Greenberg *et al.*, 1986). Interestingly, in *S.pyogenes* the GpoA (glutathione peroxidase) mutant exhibited heightened sensitivity to methyl viologen but not to hydrogen peroxide (Brenot *et al.*, 2004). This phenomenon the authors suggest may be attributed to the existence of a complex defense mechanism against oxidative stress involving several overlapping antioxidant systems. Although, *S.aureus* possesses gene homologues of glutathione peroxidase, their role in conjunction with glutathione in response to oxidative stress has not been determined.

The findings from a previous study on tellurite reduction showed that the cysteine synthase homolog (CysM) in *S.aureus* is involved in tellurite resistance (Lithgow *et al.*, 2004). The *cysM* gene conferred higher tellurite resistance and increased glutathione accumulation when transformed into *E.coli* DH5α. In this study a concentration of glutathione of 10 mM was found to significantly protect

SH1000 against tellurite (Fig. 3.33). This suggests that a link exists between glutathione and tellurite resistance in *S.aureus* SH1000 and that protection against tellurite toxicity is glutathione concentration dependent. It further emphasizes the involvement of thiol groups in tellurite resistance as reported by Turner *et al.* (1999). However, as *S.aureus* does not synthesize glutathione it is highly unlikely that it is solely responsible for tellurite resistance. In human tissues, glutathione concentration ranges from 0.1 to 10 mM and it is most concentrated in the liver (up to 10 mM), whereas plasma concentration is approximately 4.5 μM. The high glutathione concentrations in the liver and other tissues may possibly confer some form of protection towards *S.aureus* against other forms of stress as well such as diamide and oxidative stress.

In the disc inhibition assay both RMH12(*ggt*) and RMHcol11(*SACOL0185*) showed comparable sensitivity to tellurite (1M) with the wildtype when grown in the presence of cysteine and black colonies are formed in all three strains. Replacement of cysteine (50 μM) with glutathione (50 μM) as the sulfur source significantly impaired growth of RMH12(*ggt*) (p=0.05) and RMHcol11(*SACOL0185*) (p=0.02) compared to SH1000 in the presence of 1M tellurite.

Glutathione utilization has been shown to be facilitated by the presence of gammaglutamyltranspeptidase (GGT) in many different organisms. *S.aureus* is able to use glutathione as sole sulfur source. However despite inactivation of the gene encoding for GGT and a hypothesized glutathione transporter, glutathione utilization continues and is apparently unaffected. This suggests possibly a novel

179

mechanism of glutathione uptake and utilization in *S.aureus* which remains to be elucidated. In addition, although a link between glutathione and tellurite resistance is established, the exact mechanism by which this occurs is unknown. Elucidation of this mechanism may possibly provide insights on the mechanisms of stress resistance and will require further study.

Summary

- Two insertional mutations were made in genes encoding a putative gammaglutamyltranspeptidase (SACOL0188) and ABC transporter (SACOL0185) to create strains RMH12(*ggt*) and RMHcol11(*SACOL0185*) respectively.

- The two mutations were combined to create RMH25(*ggt SACOL0185*).

- Inactivation of *ggt* and SACOL0185 did not affect the ability to utilize glutathione as sulfur source.

- Glutathione was protective against stress induced by 1M tellurite.

CHAPTER FOUR

ANALYSIS OF THE MOLECULAR BASIS OF TELLURITE RESISTANCE IN *STAPHYLOCOCCUS AUREUS*

4.1 Introduction

In Chapter 3 it was found that the presence of glutathione affected resistance to stress induced by tellurite. Tellurite (TeO_3^{-2}) is a water-soluble oxyanion belonging to the same group on the periodic table as sulfur and selenium. It occurs rarely in the terrestrial environment and is normally found in copper ores and industrial slimes (Taylor, 1999).

Toxicity of the potassium tellurite oxyanion (TeO_3^{-2}) is attributed to its strong oxidizing ability that interferes with cellular processes thus making it potentially able to cause cellular damage resulting in death. In addition, the high toxicity of tellurite may be due to the formation of toxic by-products such as toxic reactive species during tellurite reduction (Taylor, 1999; Trutko *et al.*, 2000). Most bacteria are intrinsically sensitive to tellurite however resistance to tellurite has been demonstrated in several pathogens including *Corynebacterium diphtheriae*, *Staphylococcus aureus*, *Enterococcus fecalis*, *Vibrio cholerae* and verocytotoxigenic *E.coli* O157 (Zadik *et al.*, 1993). *S.aureus* is naturally resistant to high levels of tellurite (K_2TeO_3) with an MIC of 7mM (Lithgow *et al.*, 2004). Resistance occurs via tellurite reduction resulting in black colonies when grown in the presence of this oxyanion. This characteristic is exploited in Baird Parker medium that is used for selective isolation of *S.aureus* (Baird-Parker, 1984).

The exact chemistry of tellurite reduction has yet to be established although several studies have linked tellurite detoxification with intracellular thiol containing groups (Ramirez *et al.*, 2006; Lithgow *et al.*, 2004; Vasquez *et al.*, 2001; Turner *et al.*, 1999). Taylor (1999) suggests that tellurite reduction may occur at the expense of the reduced forms of cellular glutathione and other thiols. Oxidation of these cellular thiols may result in disruption of vital biosynthetic processes resulting in cell death. In addition, tellurite upon reduction to telluride may be incorporated in amino acids in place of sulfur (Toptchieva *et al.*, 2003). Latinwo (1998) states that heavy metal resistance in most microorganisms is afforded by one of several mechanisms comprising efflux mechanisms, transformation to non-toxic forms and sequestration from target molecules.

Detoxification of tellurite occurs by reduction to elemental tellurium that in *Natronococcus occultus* appears as black crystallites within the cytoplasm (Pearion, 1999). Trutko *et al.* (2000) studied tellurite reduction in several species of gram-negative bacteria and found that tellurium crystallites were deposited in either the periplasmic space, on the outer or inner membrane surface or on both surfaces. Studies on tellurite reduction mechanisms reveal that they occur enzymatically (Moscoso *et al.*, 1998; Chiong *et al.*, 1998) via an enzyme that is commonly referred to as tellurite reductase. Interestingly different bacteria have been shown to have varying enzymes responsible for the tellurite-reducing activity and a single species can possess more than one type of activity. In *E.coli* the basal level of tellurite resistance can in part be attributed to inducible membrane associated nitrate reductases (Avazeri *et al.*, 1997) while tellurite

reduction is also correlated with terminal oxidases in strains of *Pseudomonas aeruginosa, Agrobacterium tumefaciens, Erwinia carotovara* and also *E.coli* (Trutko 2000). However, periplasmic nitrate reductases are not responsible for tellurite resistance in *Rhodobacter sphaeroides* (Sabaty 2001). An unidentified membrane-associated flavin-dependent reductase may be responsible for tellurite reduction in *Rhodobacter sphaeroides* 2.4.1. (Moore 1992). Chiong *et al.* (1988) identified three different enzymes in *Thermus thermophilus* that demonstrated tellurite-reducing activity. Similarly, tellurite reduction occurred in cell free extracts of *Bacillus stearothermophilus* V (Moscoso *et al.*, 1998) and *Mycobacterium avium* (Terai *et al.*, 1958). Terminal oxidases (cytochrome c) in the plasma membrane of gram-negative bacteria are shown to reduce tellurite where the location of tellurium crystallite deposits is determined by the active centers of the terminal oxidases (Trutko, 2000). Unlike in *E.coli* where tellurium deposits are periplasmic, tellurium crystals in *N.occultus* are found deposited within the cytoplasm. In this organism, methylation of tellurium is the proposed mechanism of detoxification as evidence by a garlic odour when it is grown in the presence of potassium tellurite (Pearion, 1999).

Tellurite resistance is observed in both gram-positive and gram-negative bacteria. In gram-negative bacteria tellurite resistance is usually encoded by genes that are found on the chromosome or by conjugative plasmids (Sanchez-Romero, 1998). At least 5 tellurite resistance (Te^R) determinants have been identified in gram-negative bacteria that are either plasmid mediated or chromosomally located (Taylor, 1999).

Tellurite resistance determinants (Te^R) chromosomally located are *tehAB* in *E.coli; tmp* in *P.syringae; trgAB* and *cysK* in *R.sphaeroides*. Plasmid-associated mechanisms are *kilAtelAtelB* in RP4 (IncP) and *terZ terA-F* in R478 (IncH12) (Taylor,1999). The tellurite-resistance determinants *tehAtehB* require a reducing environment or electron-reducing equivalents for high levels of tellurite resistance in *E.coli* (Turner, 1995).

Tellurite is found naturally in the terrestrial environment but not in the human host. Thus the high level of resistance seen for *S.aureus* is unlikely to be a virulence determinant *per se* but may be an indicator of resistance to other forms of stress. Taylor (1999) suggests that tellurite reduction may be a secondary effect of a metabolic process. Unveiling the mechanism of tellurite reduction may possibly provide an insight into other mechanisms involved in enabling *S.aureus* to resist and overcome stress in the human host.

In this chapter, two major tellurite reductases in *S.aureus* were identified as thioredoxin reductase (TrxB) and alkylhydroperoxidase subunit F (AhpF). The TrxB protein was overexpressed and purified to facilitate further determination of its potential role in tellurite reduction.

4.2 Results

4.2.1 Tellurite resistance in *S.aureus*

4.2.1.1 Effect of tellurite on colony and culture morphology of *S.aureus* SH1000

As tellurite is reduced to tellurium a gray/black precipitate is formed. This is clearly visualized as black colonies on agar plates or coloration of liquid cultures (Fig.4.1).
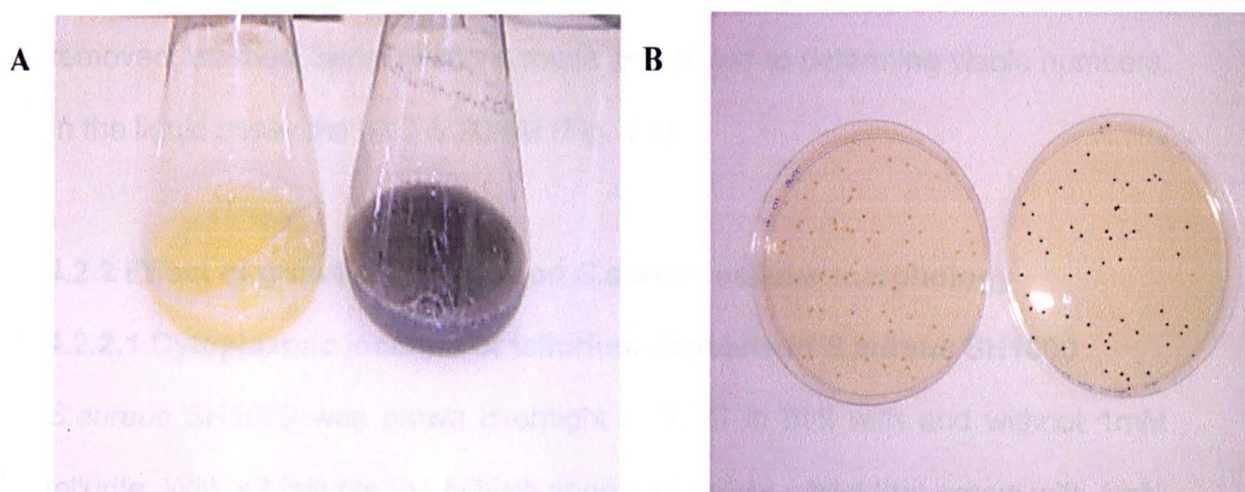
Figure 4.1

Effect of tellurite on culture morphology. *S.aureus* SH1000 grown overnight in BHI broth (A) or BHI plates (B) with (righthand) and without (lefthand) 1mM K_2TeO_3.

4.2.1.2 Minimum inhibitory concentration (MIC) of tellurite for SH1000

4.2.1.2.1 MIC on solid media

S.aureus SH1000 was grown on TSB agar containing different concentrations of potassium tellurite (1-20mM). Serial dilutions of cells from an overnight culture were spotted onto the plates. Figure 4.2 shows the number of colonies at different tellurite dilutions. From this the MIC can be calculated as 5mM.

4.2.1.2.2   MIC on liquid media

SH1000 was inoculated into TSB broth containing potassium tellurite over a range of concentrations (1-20mM). After overnight incubation cells were removed, washed, serial dilutions made and plated to determine viable numbers. In the liquid assay the MIC is 20mM (Fig. 4.3).

4.2.2 Effect of growth in tellurite on S.aureus cellular morphology

4.2.2.1 Cytoplasmic location of tellurium deposits in S.aureus SH1000

S.aureus SH1000 was grown overnight at 37°C in BHI with and without 1mM tellurite. Without tellurite the culture appeared yellow whilst that grown with 1mM K_2TeO_3 was black. Cells were harvested and processed for electron microscopy as described in Materials and Methods (Chapter 2.18.1). Electron micrographs (Fig 4.4A) of cells grown without tellurite showed a generally homogenous cytoplasmic appearance compared the cells grown in 1mM tellurite (Fig 4.4B) which appeared grainy. Tellurium deposits (pink arrows, Fig 4.4B) were clearly

visible within the cytoplasm. In addition, more cell debris was observed reflecting the presence of dead cells.
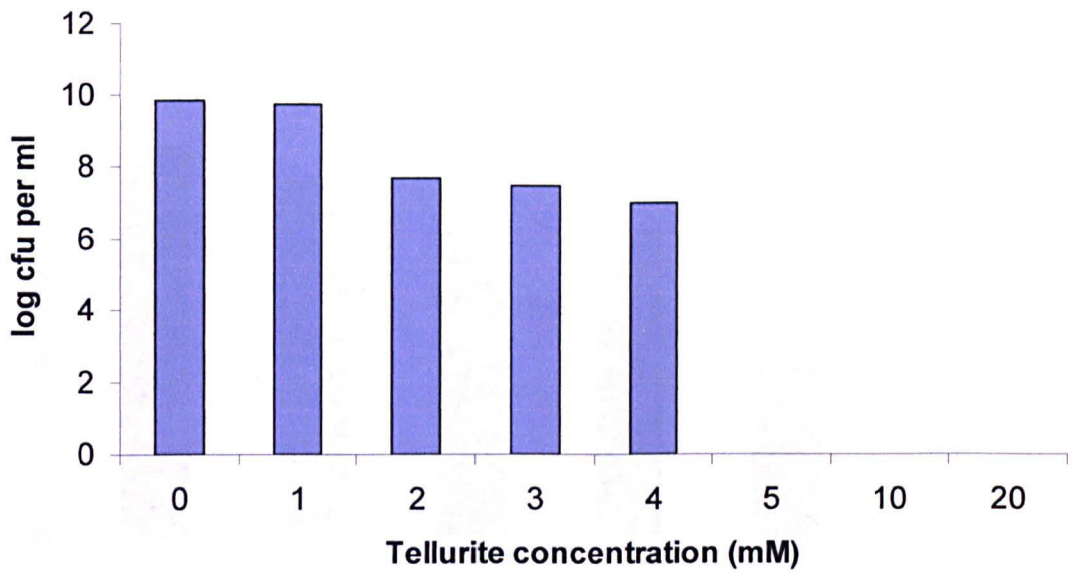
Figure 4.2

MIC of *S.aureus* SH1000 grown on TSB plates containing K_2TeO_3
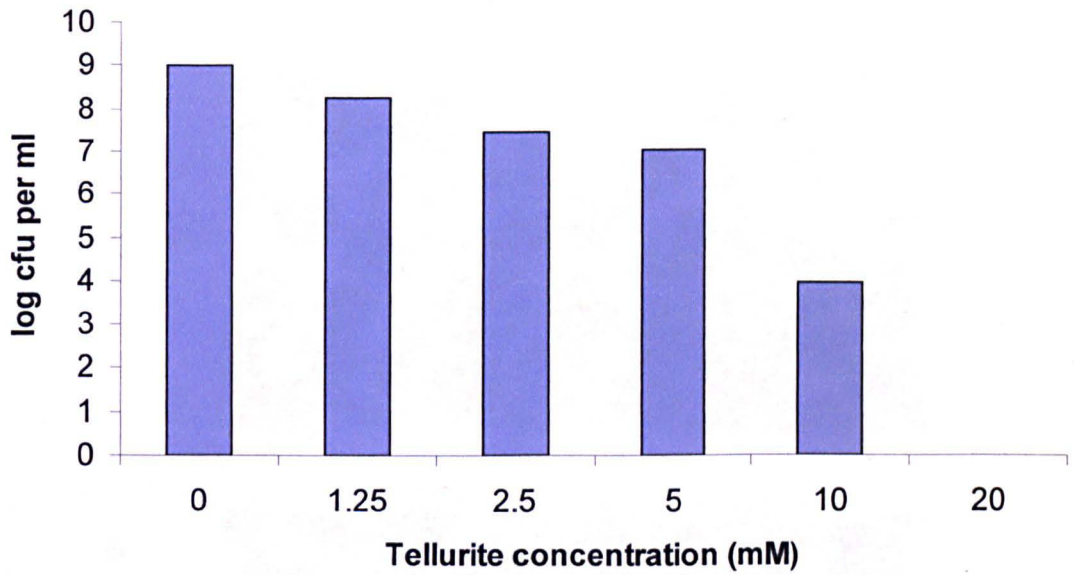
Figure 4.3

MIC of *S.aureus* SH1000 grown in TSB broth containing different concentrations
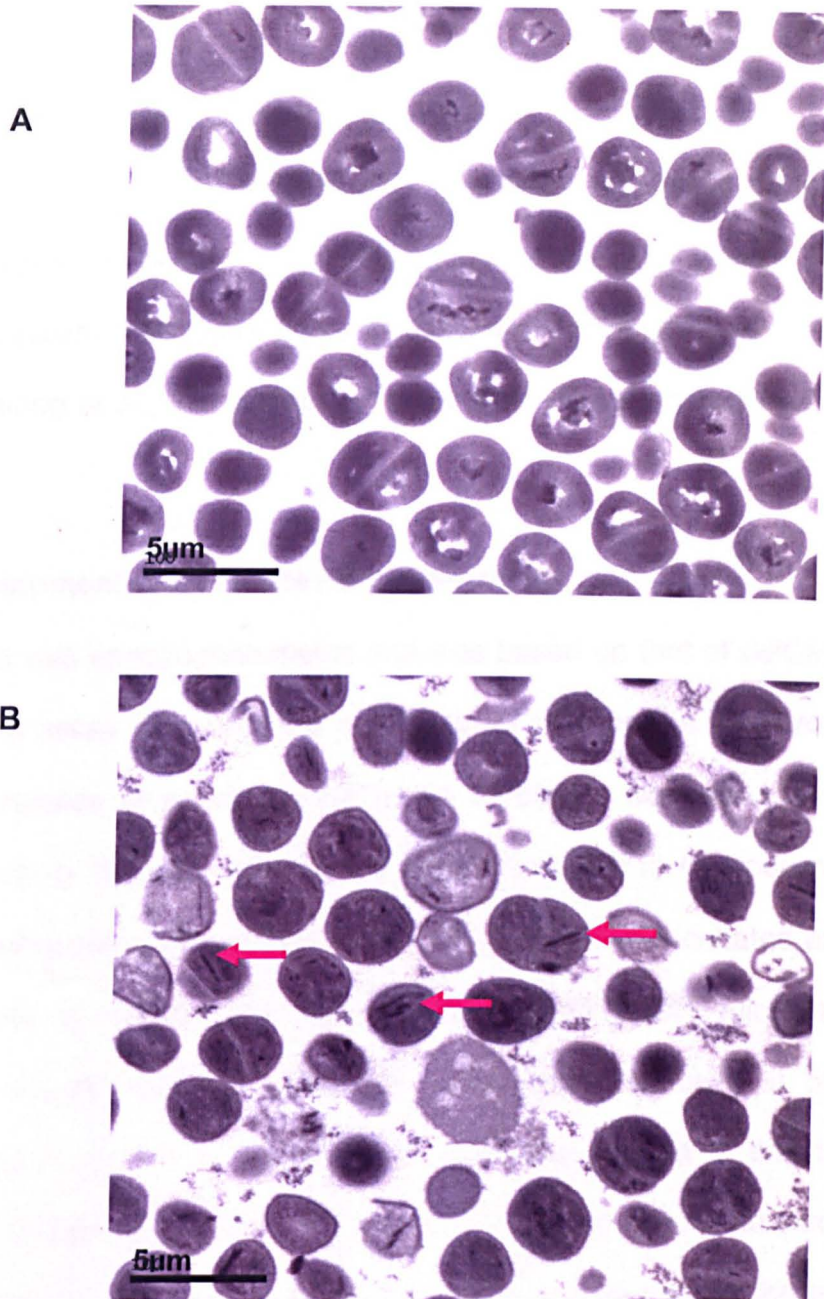
of K_2TeO_3.

Figure 4.4

Electron micrographs of sections of *S.aureus* SH1000 grown in BHI without (A)

or with 1mM K_2TeO_3 (B). Pink arrows indicate tellurium deposits.

4.2.3 Analysis of tellurite reductase (TR) activity.

S.aureus is highly resistant to tellurite and apparently reduces it to tellurium resulting in cytoplasmic crystals. The tellurite reductase (TR) activity is likely found in the cytoplasm. Previous studies (Pearion and Jablonski, 1999; Moscoso et al., 1998; Chiong et al., 1998) have indicated that TR activity requires NADH as a cofactor.

4.2.3.1 Development of a tellurite reductase assay

The assay used was spectrophotometric and was based on that of delCardayre et al., 1998. The assay measures the production of tellurium as an increase in A_{500}. The dependence of activity on NADH as a cofactor was measured (Fig. 4.5). Specific activity (U) was defined as a 0.001 increment in A_{500} per min per mg protein. Freshly prepared cell free extract of SH1000 was incubated at $37^{\circ}C$ with 1mM K_2TeO_3 in the presence and absence of 1mM NADH. Aliquots were removed and tellurite reduction measured spectrophotometrically at 500nm. Tellurite reduction rate in the presence of NADH was highest in the first 30 minutes. In the absence of NADH, tellurite reduction was almost non-existent. For practical reasons, a 15 minutes incubation time was chosen for the tellurite reduction assay since the rate of tellurite reduction at this time is within the linear range.
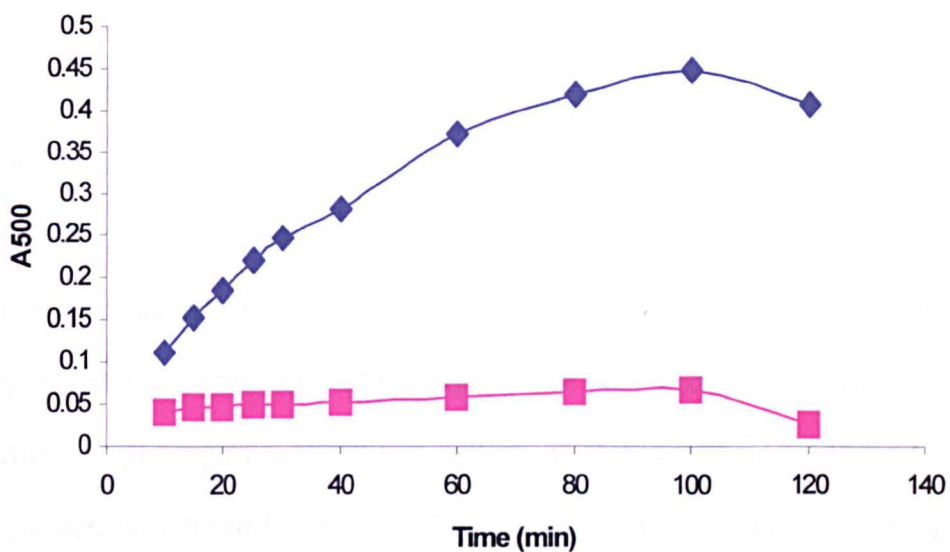
Figure 4.5

Kinetics of tellurite reduction by cell free extract of *S.aureus* SH1000 (0.4 mg protein) with 1mM NADH (◆) and without 1mM NADH (■).

4.2.3.2   Effect of boiling and treatment with Proteinase K on tellurite reduction

It was important to establish that the tellurite reduction process is enzymatic and not due to the presence of low molecular weight thiols. Cell free extract of *S.aureus* SH1000 that was dialyzed against 10mM TrisHCl buffer to remove the low molecular weight thiols, retained tellurite reduction activity (Table 4.1). This activity however, was lost after boiling for 15 minutes or treatment with proteinase K (0.1mg/ml). Moreover activity shows a requirement for NADH for the reduction of tellurite (Table 4.1; Fig 4.5). The rate of tellurite reduction is also dependent on the concentration of 2-mercaptoethanol to maintain a reducing environment. This suggests that tellurite reductase activity in cell free extracts of *S.aureus* SH1000 is enzymatic and not due to low molecular weight thiols.

Sample	% Original Specific Activity (Units)
Undialysed Cell free extract (CFE)	100
Dialysed Cell free extract (dCFE)	79.5
dCFE boiled, 100°C,15min.	0
dCFE + proteinase K, 37°C, 15min	0
No NADH	0
No CFE	0

Table 4.1

Effect of treatments on tellurite reductase activity of *S.aureus* SH1000.

4.2.3.3   Effect of growth phase on tellurite reductase activity

Tellurite activity was determined in CFE of *S.aureus* SH1000 during growth in TSB. Samples were removed during growth in TSB and specific activity of CFE measured after lysostaphin lysis (Fig. 4.6). There was no detectable activity until

193

4 hours after inoculation, which equates to postexponential phase. Activity remains into late stationary phase (27 hours; 22.25 ± 6.83 units).

4.2.3.4 Stability of tellurite reductase activity

4.2.3.4.1 Effect of temperatures on activity

The stability of tellurite reductase was tested by incubating the cell free extract at 4, 25, and 37°C (Fig.4.7). The specific activity of tellurite reduction of the CFE at time zero was used as the benchmark (100% activity). The enzyme activity showed a temperature dependence for stability. At 4°C after 17.5 hours activity had actually increased slightly. However after 24 hours at 37°C all activity had been lost. At 25°C an intermediate loss of activity was observed with 60% activity after 17.5 hours. The tellurite reductase activity is sufficiently stable to allow protein purification to be attempted.

4.2.3.4.2 Effect of NaCl on tellurite reductase activity.

Tellurite reduction was performed on the crude cell free extract from *S.aureus* SH1000 in the presence of NaCl (0.1-0.9M) (Fig 4.8). The specific activity of the CFE without NaCl was used as the benchmark (100% activity). Tellurite reductase was inhibited by increasing NaCl concentration with a >80% inhibition at 0.9M.
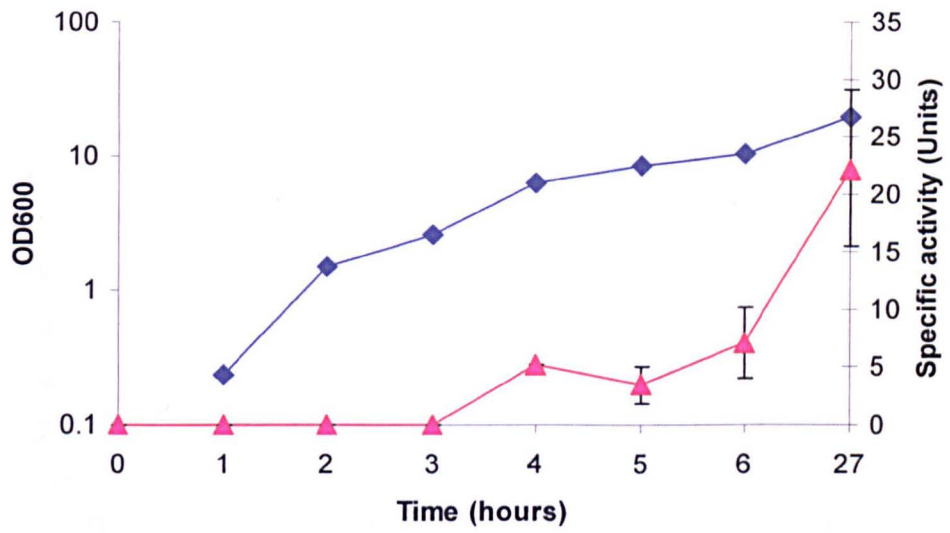
Figure 4.6

Tellurite reductase activity during growth of *S.aureus* SH1000. Cell growth (OD$_{600}$; ◆) and tellurite reductase activity were measured (▲).
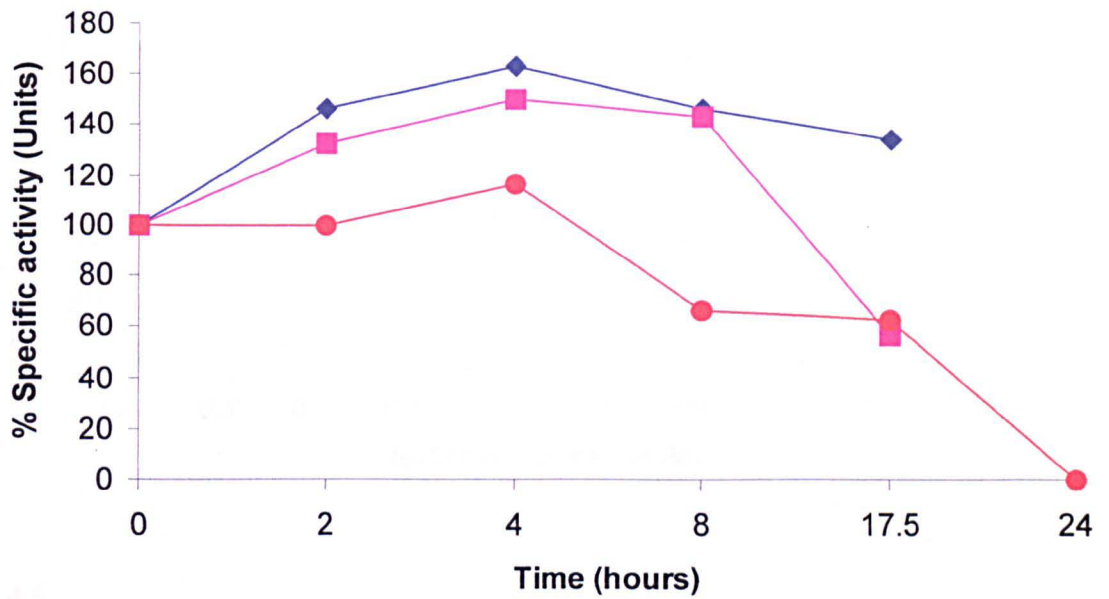
Figure 4.7

Effect of temperature on tellurite reductase activity. CFE of *S.aureus* was stored

at 4°C (◆), 25°C (■) and 37°C (●) and specific activity measured compared

to the T=0 control.
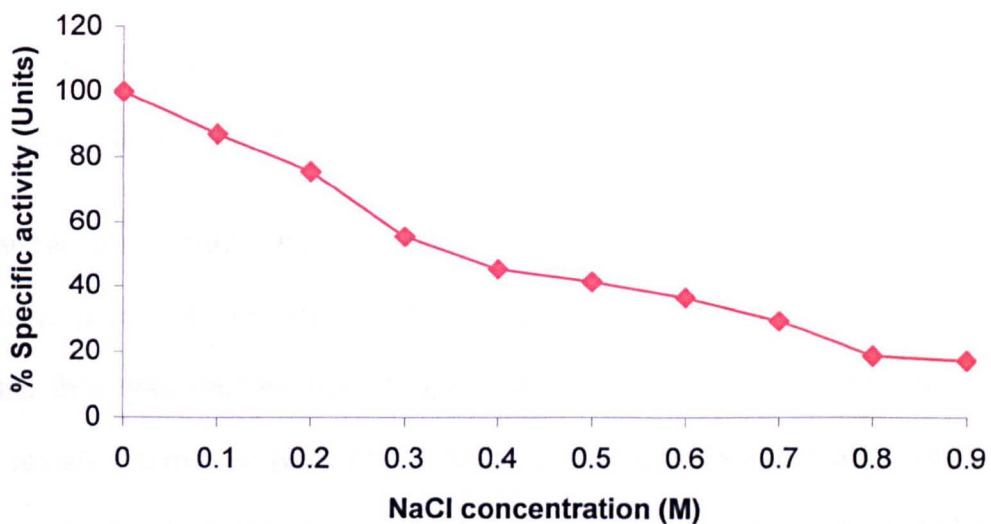
Figure 4.8

Effect of NaCl on tellurite reductase activity. The activity was measured in the presence of increasing concentrations of NaCl.

4.2.4   Molecular analysis of tellurite reductase activity

4.2.4.1 Genetic screen to identify mutants with reduced tellurite reductase activity.

A mariner transposon insertion library was previously constructed (Howard Crossley, personal communication) using the minimariner transposon *Bursa aurealis* that was derived from the Himar1 (mariner) element and carries the ermB resistance marker (Bae *et al.*, 2004). Bursa aurealis was cloned into pTS2, with a temperature-sensitive plasmid replicon (rep_{ts}) and chloramphenicol resistance gene (*cat*) to generate pBursa (Bae *et al.*, 2004) that was used for transposon mutagenesis in *S.aureus*. Dilutions of the transposon insertion library were made in PBS and plated on tryptic soy agar containing 10 µM of K_2TeO_3 and 5µg/ml erythromycin. The concentration of tellurite used in this screening process was determined by plating the transposon library on tryptic soy agar plates containing different concentrations of K_2TeO_3 ranging from 5 µM to 1mM. The lowest concentration of K_2TeO_3 with which *S.aureus* colonies are colored was determined to be 10 µM. At this concentration *S.aureus* produced gray colonies with a darker center compared to those growing on tryptic soy plates without K_2TeO_3 (control). If a mutant lacked tellurite reductase activity the colony would likely show reduced darkening. Only 10 µM K_2TeO_3 was used to prevent any growth inhibition. Approximately 11,600 colonies were screened by this method but no colonies with altered coloration were detected. The lack of success could be due to multiple activities or essentiality of the enzyme.

198

4.2.5   Purification of tellurite reductase

A flow diagram explaining the various steps used to identify tellurite reductase

activity is shown in Fig.4.9. This used both the spectrophotometric assay for

overall activity and zymography using native gels to separate and determine the

number of different activities.

4.2.5.1   Native PAGE tellurite reductase gel submersion assay

In order to visualize the TR activity a zymography assay was used based on that

of Avazeri *et al.* (1997). If TR activity occurred *in situ* in a gel in the presence of

the substrate, insoluble tellurium will be produced resulting in a dark precipitated

band. The dialysed crude cell free extract was separated on 7.5% w/v native

PAGE after which the gel submersion assay was performed (Fig 4.10). Two main

activity bands were observed in close proximity, the upper band (Band 1) that

appears brown while the bottom band (Band 2) appears gray suggesting that at

least two major tellurite reductases are operative in *S.aureus* SH1000. Both

bands were due to tellurite reduction as without the NADH cofactor no bands

were seen.

4.2.5.2   Ammonium sulphate precipitation

In order to concentrate the dialysed CFE, ammonium sulphate precipitation was

used. The crude CFE was subjected to ammonium sulphate (AS) precipitation at

55% w/v. S1 was precipitated using 75% w/v AS to give pellet P2 and

supernatant S2. P1 and P2 were resuspended in 10 Mm Tris HCl Ph 7.5. S1, S2,

P1 and P2 were all dialysed against 10Mm Tris HCl Ph 7.5. All TR activity was

found in the 55% w/v P1 and 75% w/v P2 samples respectively (Fig. 4.11, Table

4.2). P1 and P2 had 2270 and 1840 (Units) of total TR activity respectively (Table 4.2). P2 was chosen for further use. Little or no activity was observed in the supernatants S2 (75% w/v AS).
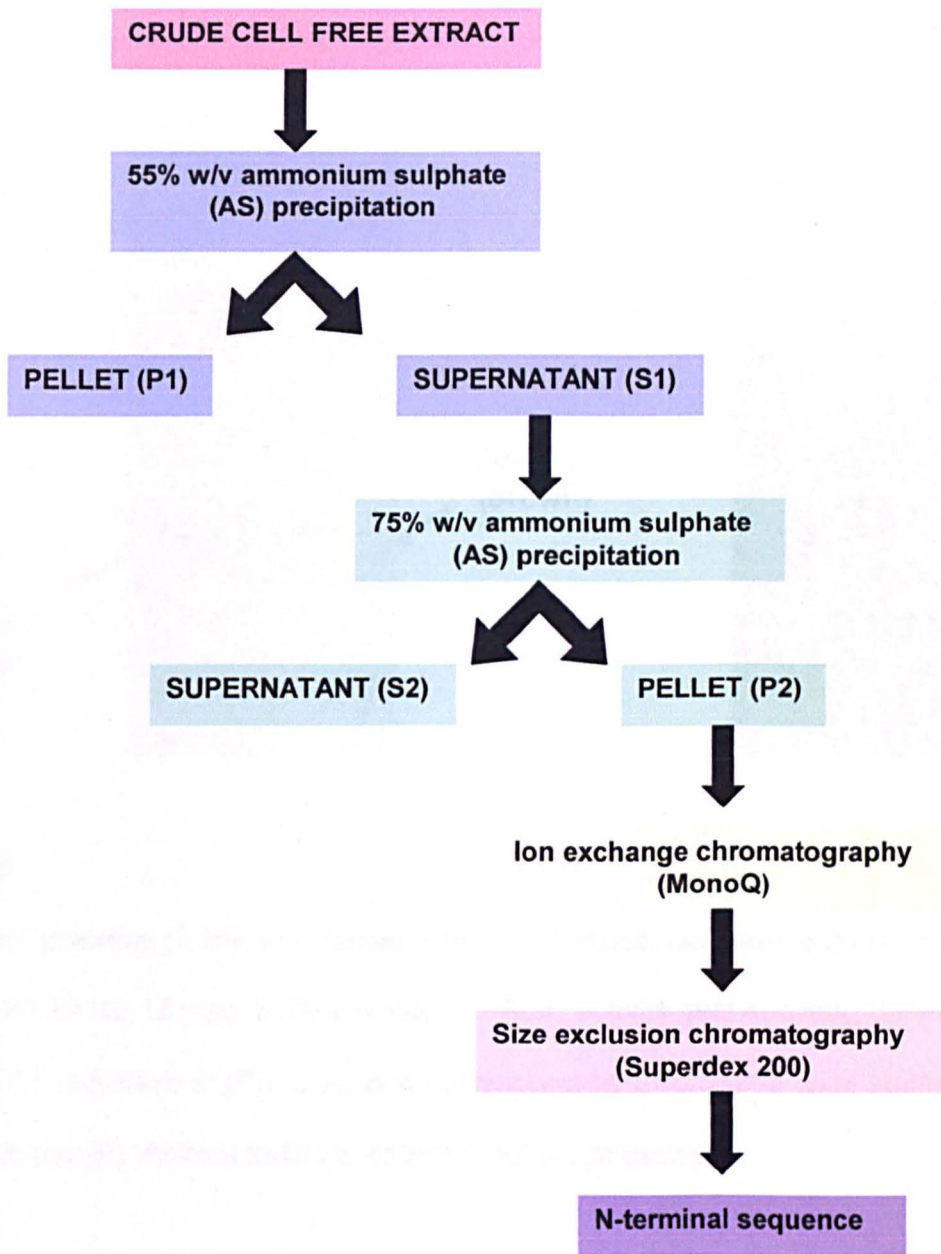
Figure 4.9

Flow diagram illustrating purification steps of tellurite reductase from *S.aureus* SH1000.

A   B

Band 1
(brown)

Band 2
(gray)
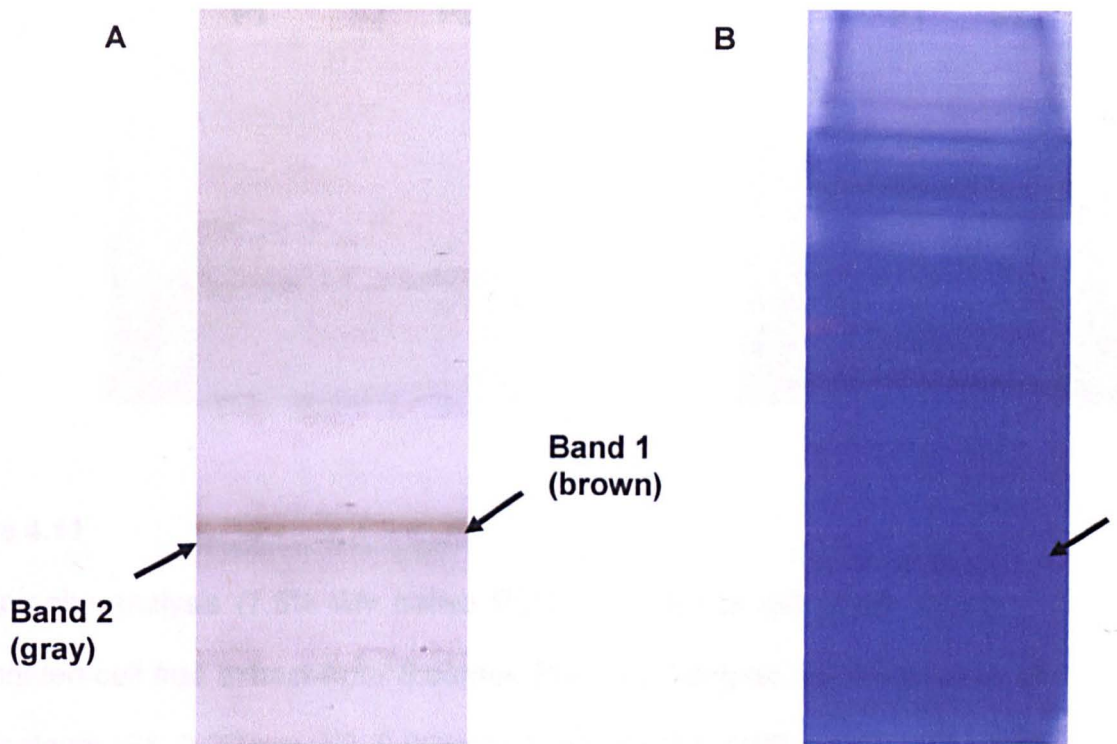
Figure 4.10

Zymography analysis (7.5% w/v native PAGE) of crude cell free extract from *S.aureus* SH1000 (0.13 mg). 7.5% w/v native PAGE activity gels showing tellurite reductase (TR) activities in (Panel A) and corresponding Coomassie Blue stained native PAGE gel (B). Arrows indicate apparent tellurium deposits.
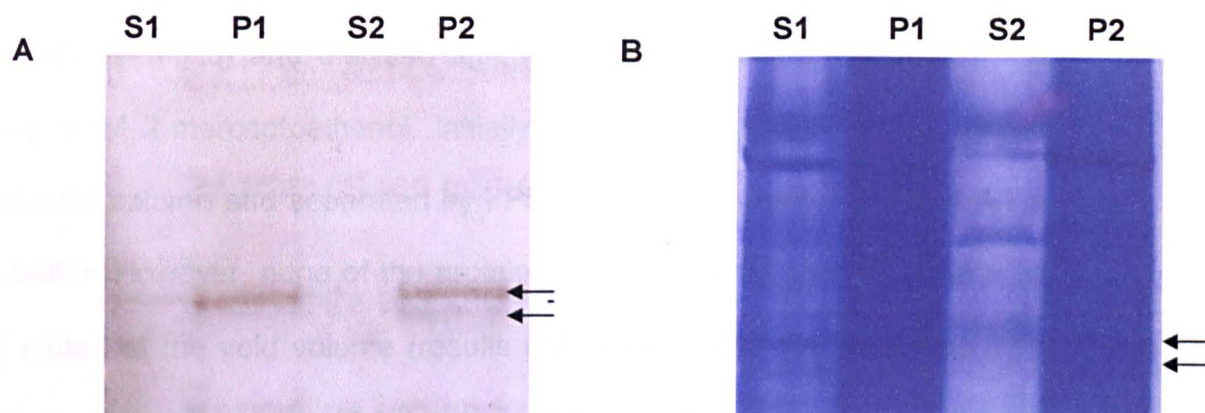
Figure 4.11

Zymography analysis (7.5% w/v native PAGE) of tellurite reductase activity in fractionated cell free extract from *S.aureus* SH1000. Samples were 5 μl each of supernatants (S1, 0.008mg, S2, 0.004mg) or pellets (P1, 0.06 mg; P2, 0.17 mg) of 55% w/v (S1 and P1) and 75% w/v (S2 and P2) ammonium sulphate (AS) precipitation of dialyzed cell free extracts from *S.aureus* SH1000. Panel A, zymogram; Panel B, Coomassie stained protein gel. Arrows indicate tellurium deposits and corresponding regions on Coomassie stained gel.

4.2.5.3 Purification of TR by Ion Exchange Chromatography

The pellet from 75% w/v AS precipitation (P2) was resuspended in 6 ml 10mM TrisHCl buffer (Ph 7.5) and dialysed against 4 liters of 10mM TrisHCl Ph 7.5 containing 1mM 2-mercaptoethanol. Initially, 2 ml of the dialysate was loaded onto a MonoS column and separated by FPLC using a gradient of 0-1M NaCl in starting buffer. However, none of the proteins attached to the MonoS column as all were eluted at the void volume (results not shown). The dialysate was then loaded onto a MonoQ column (2 ml) and separated by FPLC using a gradient of 0-1M NaCl (Fig 4.12). Eluted fractions were resolved on 7.5% w/v native PAGE as in Chapter 2.19.5.2 and analyzed for TR activity (Chapter 2.19.5.4). TR activity was observed in fractions 20, 21 and 22 (Fig.4.12A). The TR activity in fraction 22 is associated with Band 1 (brown band, Fig.4.12A) and fraction 20 with Band 2 (gray band, Fig.4.12B) and thus these can be separated from each other. However the corresponding Coomassie Blue stained gel revealed they are not pure enough to allow identification.

Figure 4.12

Ion exchange chromatogram of AS 75% w/v P2 from *S.aureus* strain SH1000 (66.4 mg loaded). Panel A, Chromatogram of separated proteins. Dashed line shows 0-1M NaCl gradient. Panel B, Zymogram using 7.5% w/v native PAGE showing tellurite reductase activities in eluted fractions 20, 21 and 22 and Panel C, corresponding Coomassie stained protein gel. Arrows indicate tellurium deposits and corresponding regions on Coomassie stained gel. Dark arrows on FPLC trace show fractions containing tellurite reductase activity in Band 1 (22) and Band 2 (20).

4.2.5.4 Purification of TR Band 1 (Brown)

4.2.5.4.1 Size exclusion chromatography

To furthur purify TR Band 1, fraction 22 from the MonoQ separation was loaded onto a Superdex 200 column and separated by FPLC. Fractions 13, 14, 17, 18, 20, 21 and 22 were collected, concentrated using a YM-30 Centricon column, and analyzed by 7.5% w/v native PAGE for TR activity. Fractions 21 and 22 eluted from the Superdex 200 column showed tellurite reduction activities (Fig 4.13A) which corresponded to a single Coomassie Blue stained protein (Fig 4.13B).

4.2.5.4.2 Identification of TR Band 1

Fractions 21 and 22 eluted from the Superdex 200 column were pooled and loaded in triplicate onto a 7.5% w/v native PAGE and separated. The gel was excised into three for TR assay, Commassie Blue staining and electroblot for N-terminal sequence (Fig 4.14). The Band corresponding to Band 1 TR activity was N-terminal sequenced as MLNADLKQQL. A BLAST search of the sequence revealed the TR activity to have 100% identity to alkylhydroperoxidase subunit F (Fig 4.15).
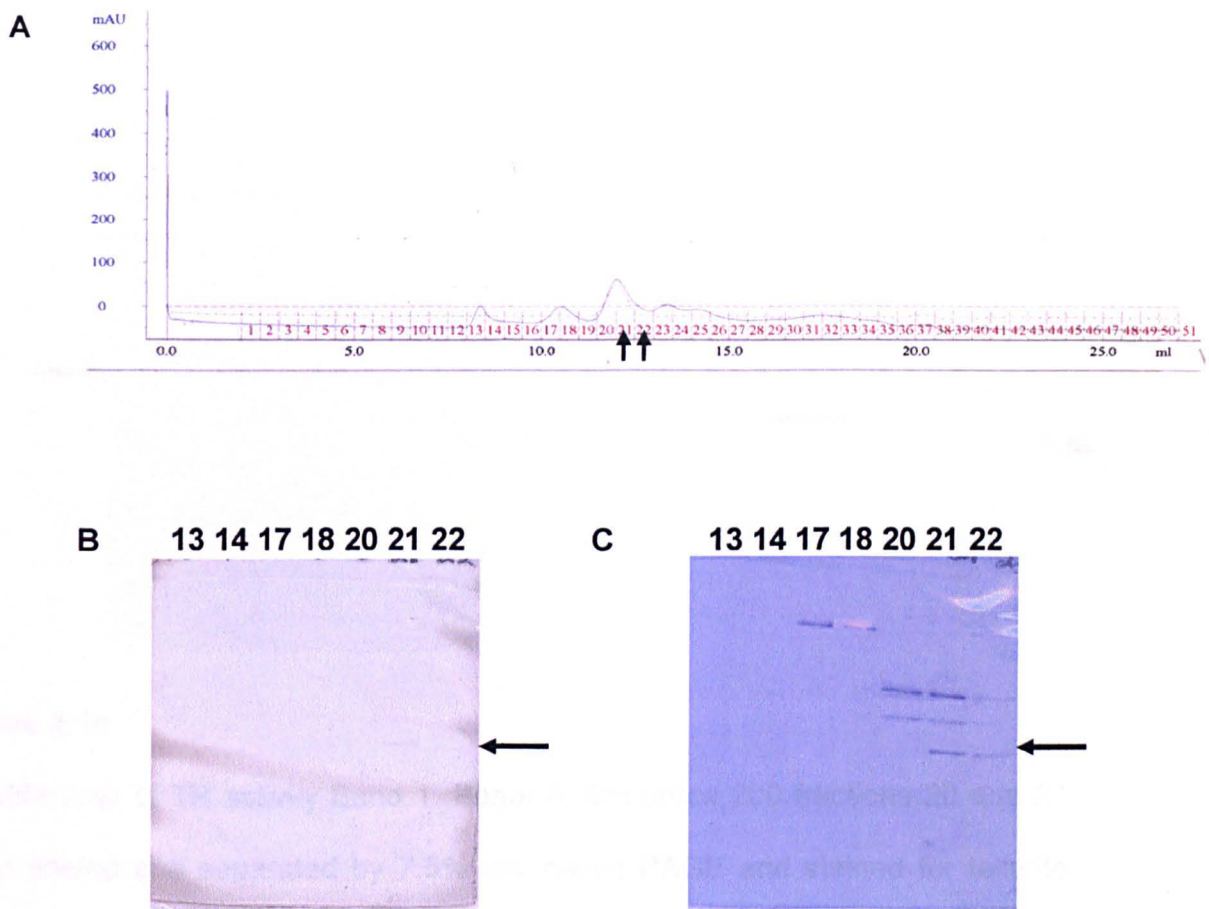
Figure 4.13

Gel filtration purification of tellurite reductase activity Band 1. Panel A, chromatogram of Superdex 200 fractionation; Panel B, zymogram using 7.5% w/v native PAGE showing tellurite reductase activity (arrow), and Panel C corresponding regions on Coomassie stained gel (band corresponding to TR activity highlighted). Dark arrows on FPLC trace show fractions containing tellurite reductase activity.
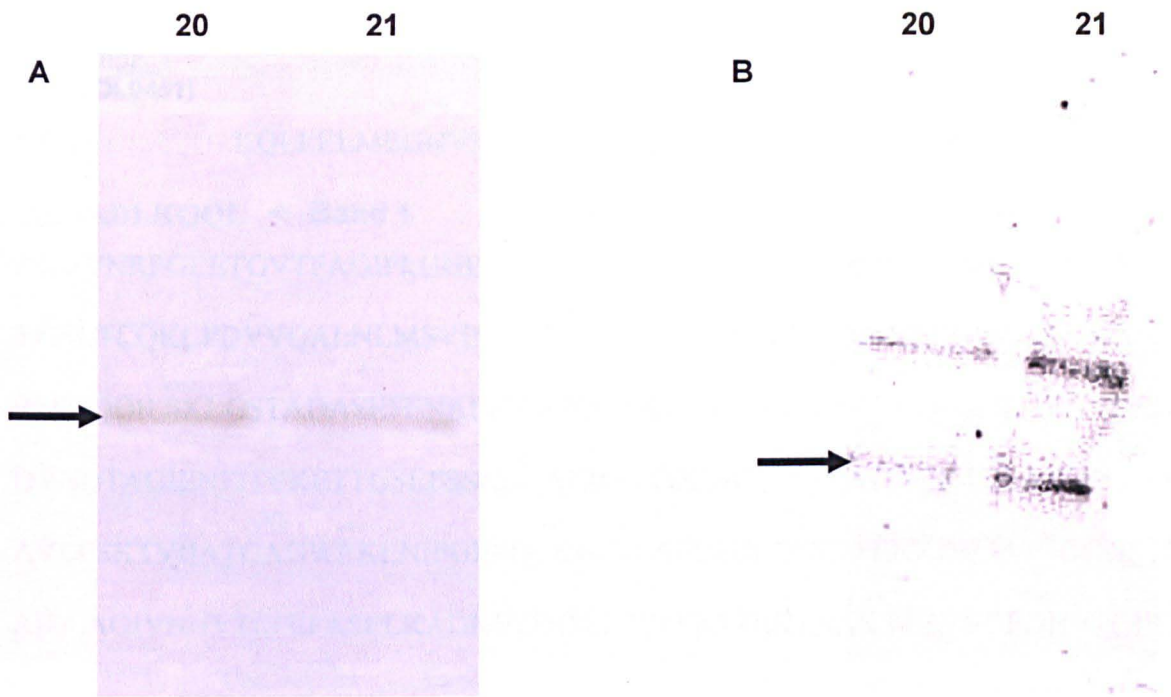
Figure 4.14

Identification of TR activity Band 1. Panel A, Superdex 200 fractions 20 and 21 were pooled and separated by 7.5% w/v native PAGE and stained for tellurite reductase (TR) activity;and Panel B, corresponding regions on Coomassie stained gel (band corresponding to TR activity highlighted). Arrows indicate tellurium deposits and Coomassie stained band identified as alkylhydroperoxidase subunit F (AhpF).

AhpF
(SACOL0451)

MLNADLKQQLKQLLELMEGNVEFVASLGSDDKSKELKDLLTEITDMSPRLSLSEKSLKRT

MLNADLKQQL ← **Band 1**

PSFSVNRPGEETGVTFAGIPLGHEFNSLVLAILQVSGRAPKEKQSIIDQIKKLEGSFHFE

TFISLTCQKCPDVVQALNLMSVINPNITHSMIDGAVFREESENIMAVPAVFLNGEEFGNG

RMTIQDILSKLGSTADASEFENKEPYDVLIVGGGPASGSAAIYTARKGLRTGIVADRIGG

QVNDTAGIENFITVKETTGSEFSSNLAAHIDQYDIDAMTGIRATDIEKTDEAIKVTLENG

AVLESKTVIIATGAGWRKLNIPGEEQLINKGVAFCPHCDGPLFENKDVAVIGGGNSGVEA

AIDLAGIVNHVTLFEFASELKADNVLQDRLRSLSNVDIKTNAKTTEVVGEDHVTGIRYED

Figure 4.15

Identification of TR activity Band 1. The Band 1 N-terminal sequence (blue) is
aligned with AhpF of *S.aureus* COL (red).

4.2.5.5 Purification of TR Band 2 (gray)

4.2.5.5.1 Ion exchange chromatography

After storage at 20°C, the TR activity in fraction 20 eluted from the MonoQ column was lost. A new extract was prepared and a 75% w/v AS cut taken. The resuspended and dialyzed pellet material was separated by MonoQ (as described in Materials and Methods). The separation (Fig 4.16) revealed activity to be in eluted fraction 14 and 15 as shown by zymogram analysis (Fig 4.16).

4.2.5.5.2 Size exclusion chromatography

To furthur purify TR Band 2, fractions 14 and 15 from the MonoQ were pooled and loaded onto a Superdex 200 column and separated by FPLC. Fractions corresponding to the eluted proteins (25, 26, 27, 28, and 29) were collected, concentrated using YM-10 Centricon columns and TR activity determined by zymography. Fractions 26 and 27 from the Superdex 200 elution had TR activity (Fig 4.17A). The corresponding Coomassie stained protein gel (Fig 4.17B) revealed a single prominent band.

4.2.5.5.3 Identification of TR Band 2

Fractions 26 and 27 from the Superdex 200 column were combined and loaded in triplicate onto 7.5% w/v native PAGE and separated. The gel was excised into three for TR assay, Coomassie Blue staining and electroblot for N-terminal sequencing (Fig 4.18). The band corresponding to TR Band 2 had the sequence EIDFDIAIIG. A BLAST search of the sequence revealed 100% identity to thioredoxin reductase (TrxB) (Fig. 4.29).
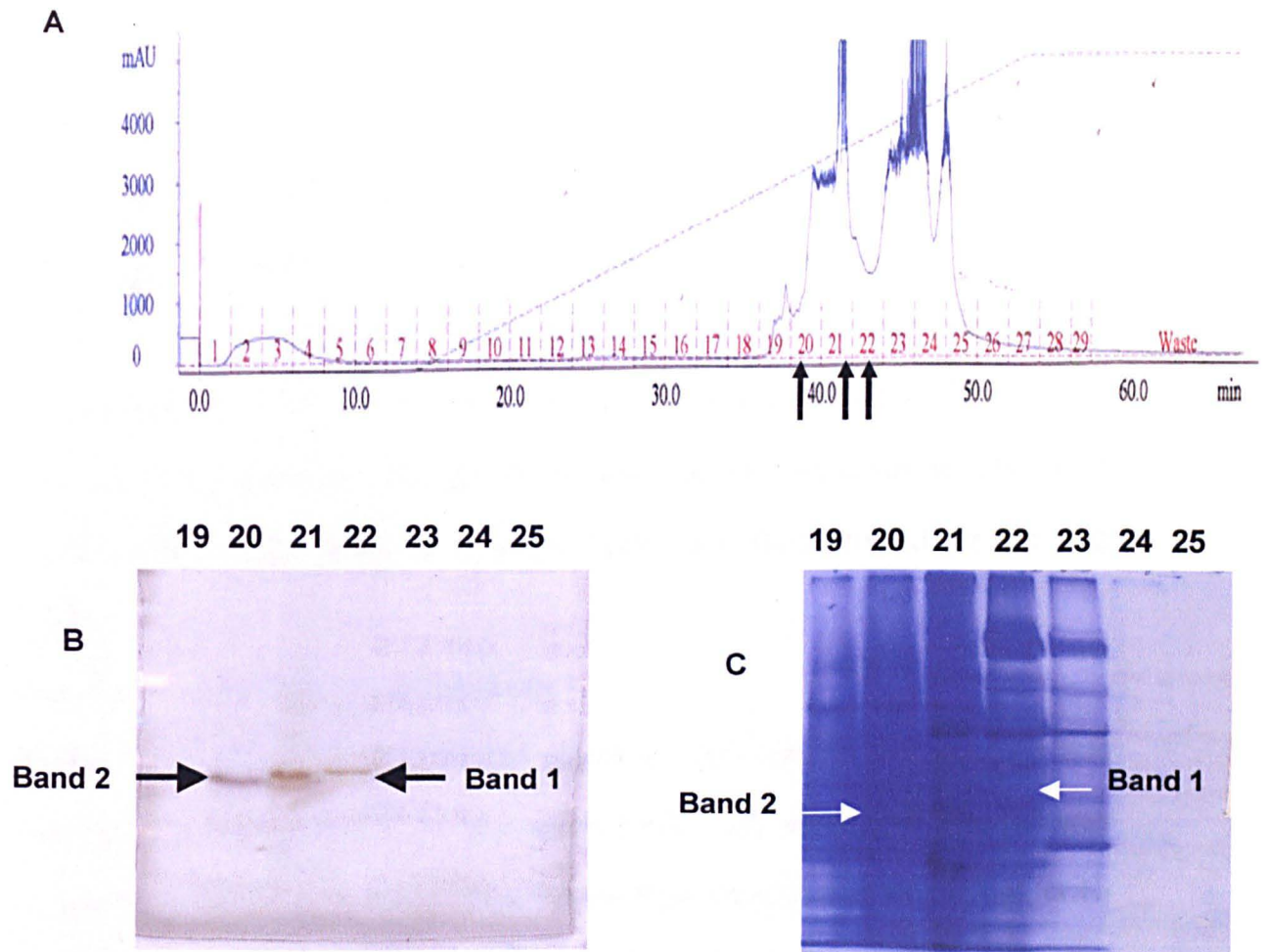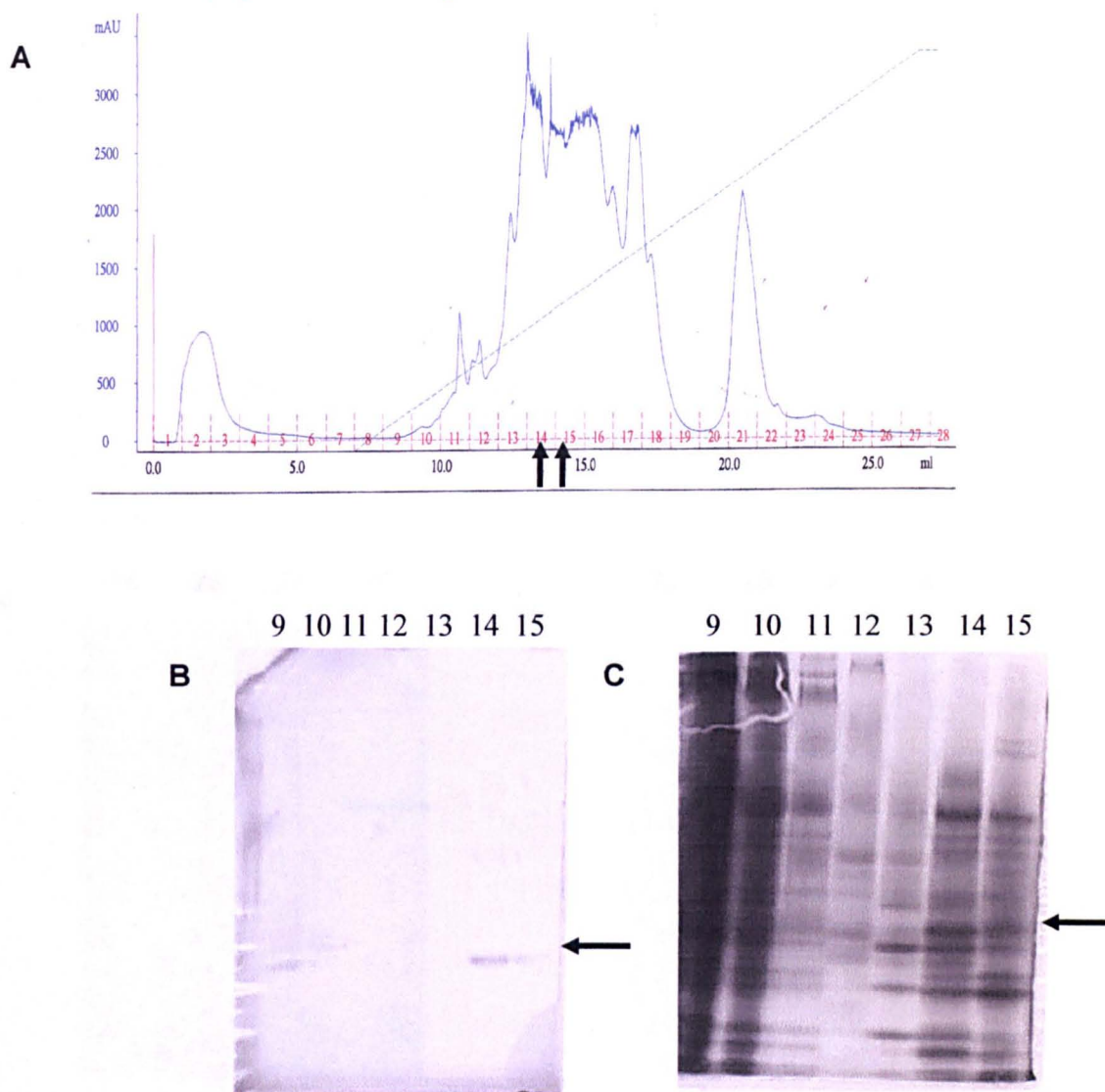
Figure 4.16

Ion exchange chromatography of 75% w/v AS P2 from *S.aureus* strain SH1000 (66.4 mg loaded). Panel A, Chromatogram of separated proteins. Dashed line shows 0-1M NaCl gradient. Panel B, Zymogram using 7.5% w/v native PAGE showing tellurite reductase activities in eluted fractions 14 and 15 and Panel C, corresponding regions on Coomassie stained gel (band corresponding to TR activity highlighted). Arrows indicate tellurium deposits and corresponding regions on Coomassie stained gel. Dark arrows on FPLC trace show fractions containing tellurite reductase activity.
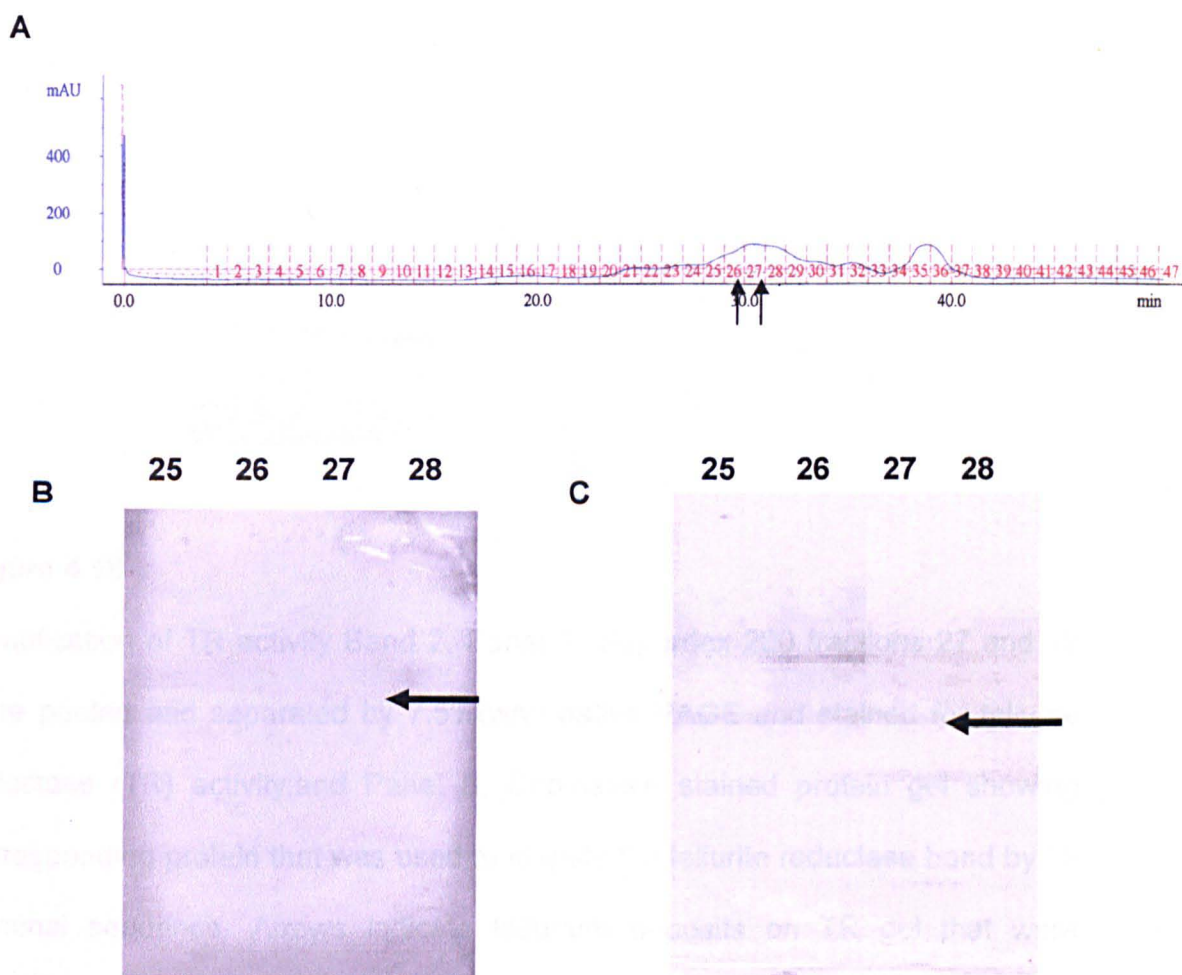
Figure 4.17

Gel filtration purification of tellurite reductase activity Band 2. Panel A, chromatogram of Superdex 200 fractionation; Panel B, zymogram using 7.5% (w/v) native PAGE showing tellurite reductase activity and Panel C corresponding regions on Coomassie stained gel (band corresponding to TR activity highlighted). Arrows indicate tellurium deposits. and corresponding regions on Coomassie stained gel. Dark arrows on FPLC trace show fractions containing tellurite reductase activity.

Figure 4.18

Identification of TR activity Band 2. Panel A, Superdex 200 fractions 27 and 28 were pooled and separated by 7.5%(w/v) native PAGE and stained for tellurite reductase (TR) activity;and Panel B, Coomassie stained protein gel showing corresponding protein that was used to identify the tellurite reductase band by N-terminal sequence. Arrows indicate tellurium deposits on TR gel that were identified as thioredoxin reductase (TrxB).

TrxB
(SACOL0829)

MTEIDFDIAIIGAGPAGMTAAVYASRANLKTVMIERGIPGGQMANTEEVENFPGFEMITG

---- EIDFDIAIIG ⟵ **Band 2**

PDLSTKMFEHAKKFGAVYQYGDIKSVEDKGEYKVINFGNKELTAKAVIIATGAEYKKIG

V

PGEQELGGRGVSYCAVCDGAFFKNKRLFVIGGGDSAVEEGTFLTKFADKVTIVHRRDEL

R

Figure 4.19

Identification of TR activity Band 2. The Band 2 N-terminal sequence (blue) is aligned with the partial sequence of TrxB of *S.aureus* COL (red).

214

4.2.6 Efficiency of TR purification

Table 4.3 shows the overall purification of TR. At each step of the purification stage, the spectrophotometric tellurite reduction assay and the BioRad protein assay were performed. Both these values were used to calculate the specific tellurite reduction activity (units) (Table 4.2). Although fractions 26 and 27 showed visible TR activity bands on the gel assay, activity was not measurable on the spectrophotometric assay.

4.2.7 Verification of TR identity

The *ahpF* gene is the second in an operon with *ahpC* (Bsat *et al.*, 1996). The two gene products encode subunits of alkylhydroperoxidase reductase. The *ahpc* gene has previously been inactivated (Cosgrove *et al.*, 2007), which would not only result in the loss of an essential subunit but the mutation would be polar on *ahpF*. The *ahpCF* operon is under negative regulation by PerR. Thus in a *perR* background there is an increase in expression of the operon. In order to verify that Band 1 of TR activity is due to AhpCF activity, KC041 (*ahpC*) and MHK1(*perR*) mutants were analyzed for TR activity.

4.2.7.1 Preparation of fresh cell free extract of SH1000, KC041 (*ahpC*) and MHK1(*perR*) mutants.

Cell free extracts were prepared and analyzed by 7.5% w/v zymography (Fig 4.20). As can be seen SH1000 has both the brown Band 1 and the gray Band 2. Strain KC041(*ahpC*) has only Band 2 whereas MHK1 (*perR*) has increased Band 1. This verifies the TR Band 1 as being alkylhydroperoxidase reductase as expected.

Separation	Sample	Total Volume (ml)	Total protein (mg)	Total Units	Specific Activity[a] (Units)	% Yield
Crude	CFE	460	2,875	220,800	76.8	100
55% AS	P1	10	110	2270	20.6	1.03
75% AS	P2	6	198	1840	9.29	0.83
MonoQ	Band 2 14 + 15	2	13.6	51	3.75	0.02
	Band 1 17+18	2	12.1	487	40.25	0.22
Superdex 200	26	1	-	-	TR activity not measurable by spectrophotometric assay	-
	27	1	-	-	TR activity not measurable by spectrophotometric assay	-

Table 4.2

Purification of tellurite reductase from *S.aureus* SH1000. CFE was subjected to 55% followed by 75% w/v AS precipitation. Samples were dialysed against 10mM Tris HCl ph 7.5 followed by purification through ion exchange (MonoQ) and gel filtration columns (Superdex 200). After each purification step, 200 µl of samples were used to perform the TR activity and protein assays (BioRad). The data obtained were used to calculate the specific activity (Units) of each sample.
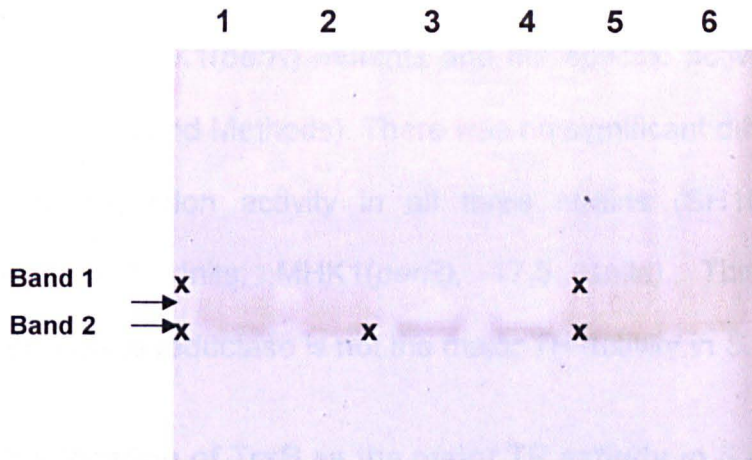
Figure 4.20

Zymography analysis (7.5% w/v native PAGE) of tellurite reductase activity in crude cell free extracts of *S.aureus* SH1000 (Lanes 1 and 2), KC041(*ahpC*) (Lanes 3 and 4), MHK1 (*perR*) (Lanes 5 and 6). Dark crosses indicate tellurium deposits from tellurite reductase activities.

4.2.7.2 Contribution of the alkylhydroperoxidase to total TR activity

The spectrophometric TR assay was used on crude extracts from SH1000, KC041(*ahpC)* and MHK1(*perR*) mutants and the specific activities (Units) were calculated (Materials and Methods). There was no significant difference observed in the tellurite reduction activity in all three strains (SH1000, 18.2 Units; KC041(*ahpC*), 20.3 Units; MHK1(*perR*), 17.5 Units). This suggests that alkylhydroperoxidase reductase is not the major TR activity in *S.aureus*.

4.2.10.4.4 Verification of TrxB as the major TR activity in *S.aureus*

In order to verify the activity of TrxB the TR activity of KC041(*ahpC*) was analyzed. A CFE was concentrated by 75% w/v ammonium sulphate precipitation and separated by MonoQ chromatography (Fig 4.21). Fraction 14 and 15 were pooled and separated by Superdex 200 and concentrated using Y30 columns (Fig 4.22). Eluted fractions 24 and 25 were found to possess TR activity (Fig 4.23) which corresponds to a protein with the N-terminal sequence TEIDFDIA. This matches that found previously (Fig. 4.19) and verified the major TR activity as TrxB.
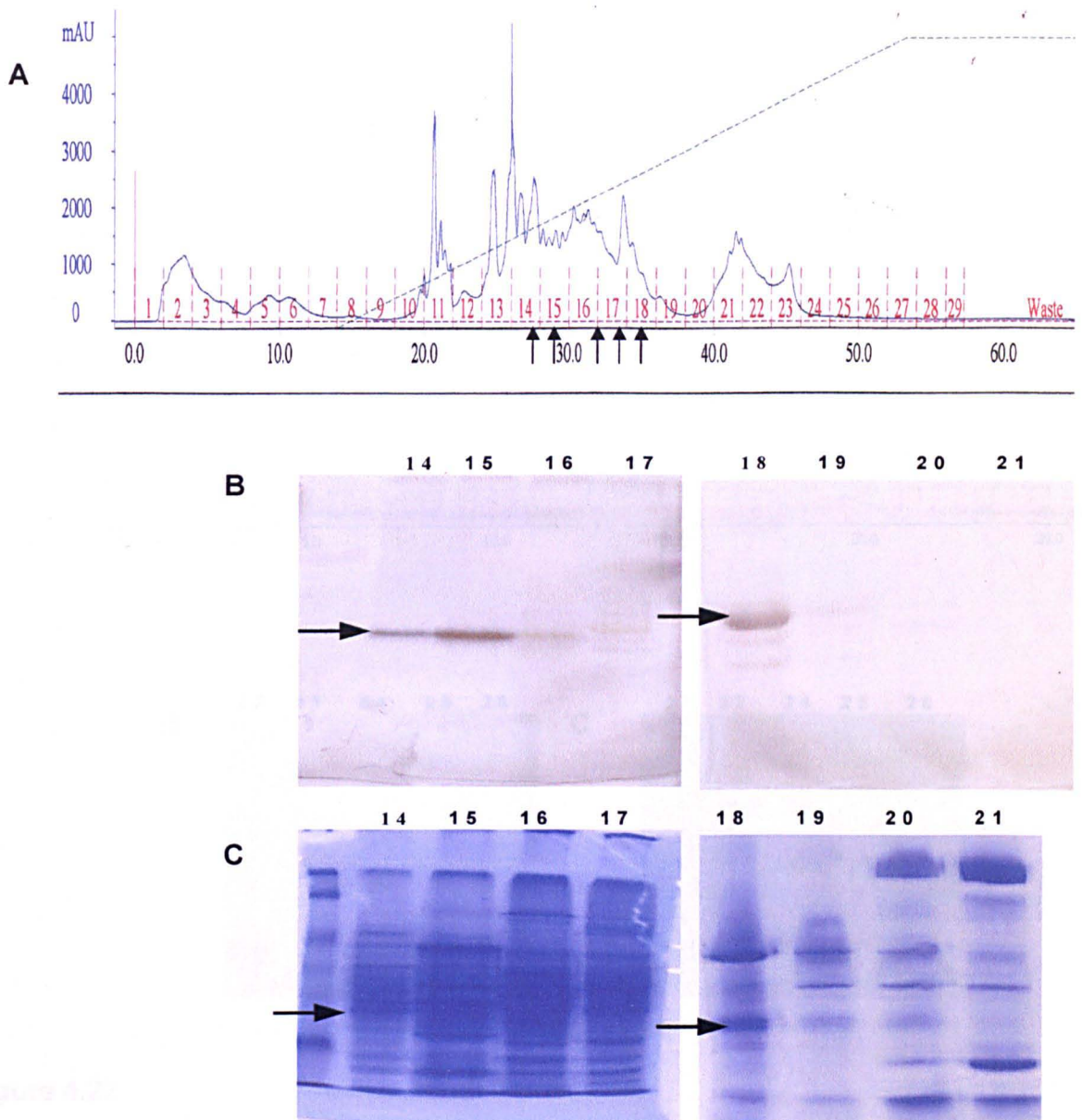
Figure 4.21

Ion exchange chromatography of AS 75% w/v cut P2 from KC041(*ahpC*). Panel A, Chromatogram of separated proteins. Dashed line shows 0-1M NaCl gradient. Panel B, Zymogram using 7.5% w/v native PAGE showing tellurite reductase activities (arrows) in eluted fractions 14,15,16,17 and 18 and Panel C, corresponding Coomassie stained protein gel with arrows showing region of TR activity. Dark arrows on FPLC trace show fractions containing tellurite reductase activity.
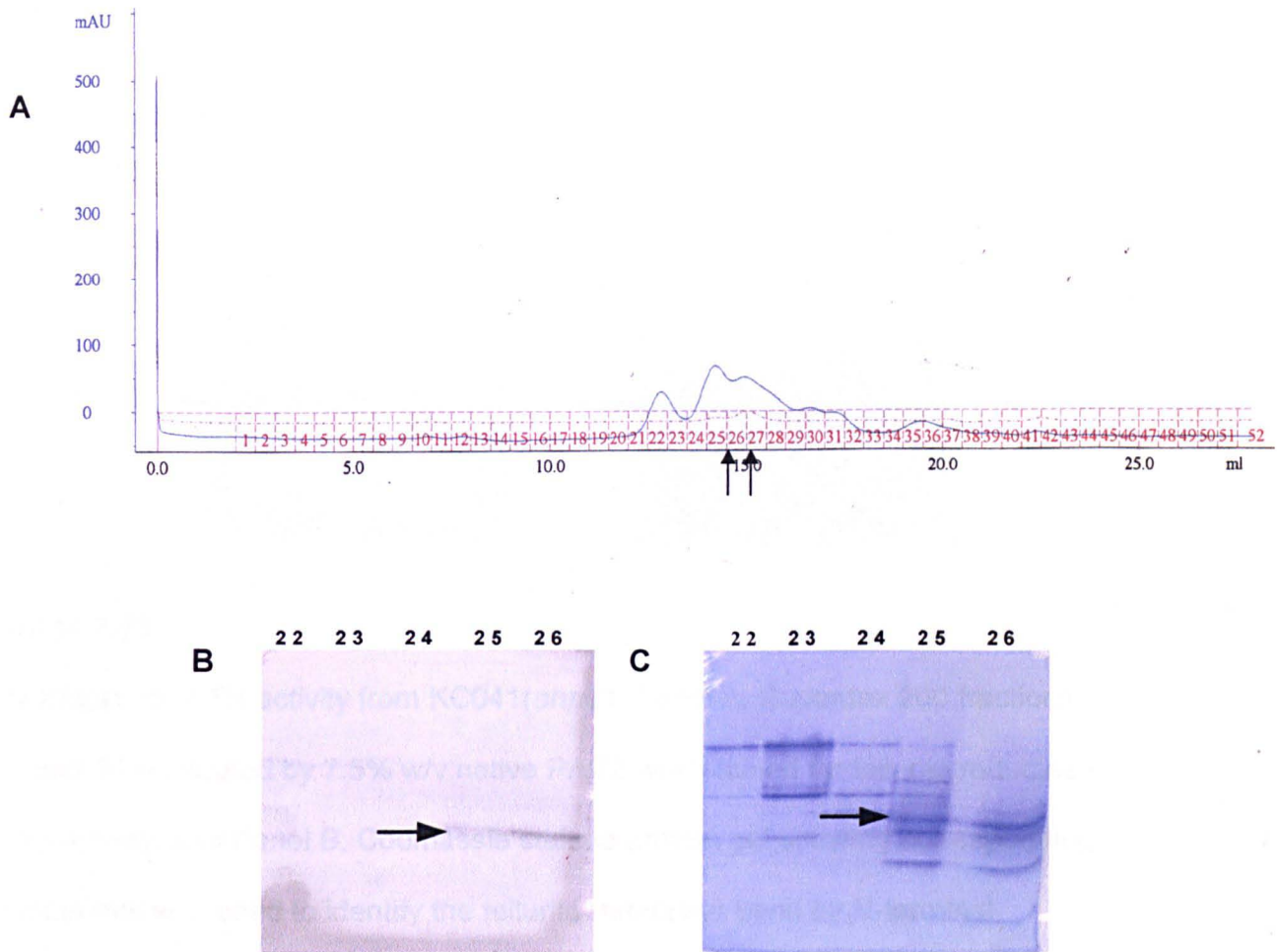
Figure 4.22

Gel filtration purification of tellurite reductase activity from KC041(*ahpC*). Panel A, chromatography of Superdex 200 fractionation; Panel B, zymogram using 7.5% w/v native PAGE showing tellurite reductase activity and Panel C corresponding Coomassie stained protein gel. Arrows indicate tellurium deposits and corresponding region on Coomassie stained gel. Dark arrows on FPLC trace show fractions containing tellurite reductase activity.
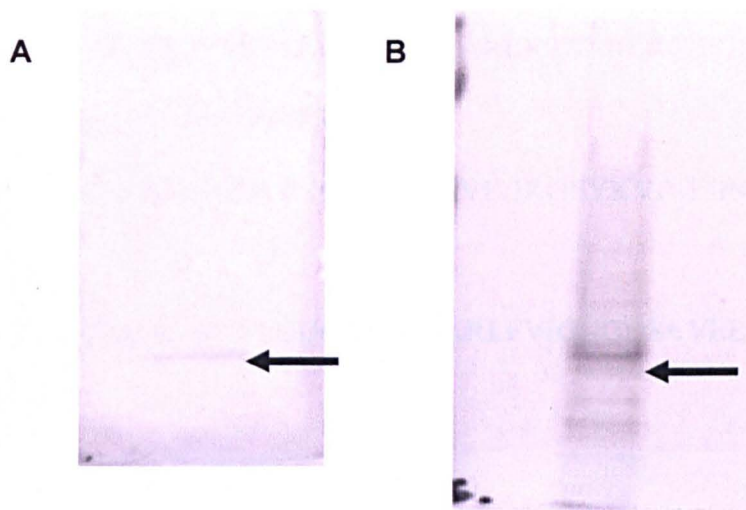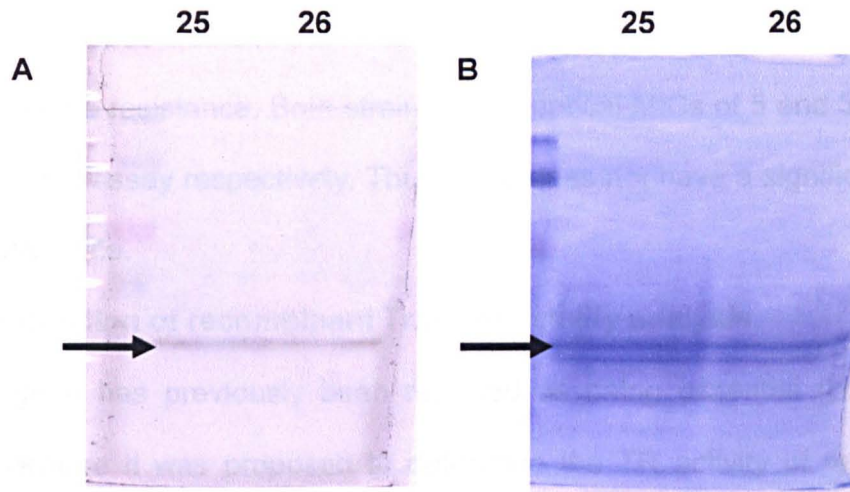
Figure 4.23

Identification of TR activity from KC041(*ahpC*). Panel A, Superdex 200 fractions 25 and 26 separated by 7.5% w/v native PAGE and stained for tellurite reductase (TR) activity; and Panel B, Coomassie stained protein gel showing corresponding protein that was used to identify the tellurite reductase band by N-terminal sequence. Arrows indicate tellurium deposits on TR gel that were identified as thioredoxin reductase (TrxB).

4.2.8 Role of alkylhydroperoxidase reductase in tellurite resistance

The MIC of SH1000 was compared to KC041(*ahpC*) in both the liquid and plate assay of tellurite resistance. Both strains had identical MICs of 5 and 3mm in the plate and liquid assay respectively. Thus *ahpC* does not have a significant role in tellurite resistance.

4.2.9 Production of recombinant TrxB for activity analysis.

The *trxB* gene has previously been reported as being essential (Uziel *et al.*, 2004). Therefore it was proposed to determine the TR activity of recombinant protein. The petBlue vector system (Fig. 4.24) was used for production of recombinant TrxB.

4.2.9.1 Primer design and PCR of the *trxB* gene

The *trxB* gene (936bp) was PCR amplified from SH1000 genomic DNA with *Taq* polymerase using the Extensor Reddymix with primers lochpB1(F) and lochpB1I. The PCR product was resolved on a 1% w/v agarose gel and resulted in one band at the expected size of 936bp (Fig 4.25B). This was then ligated to the petBlue-1 acceptor vector (Materials and Methods) to produce the construct Pbr02 (Fig. 4.25A).
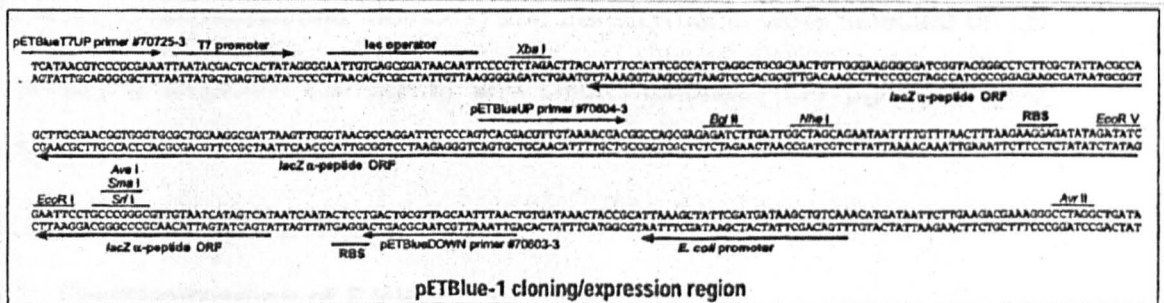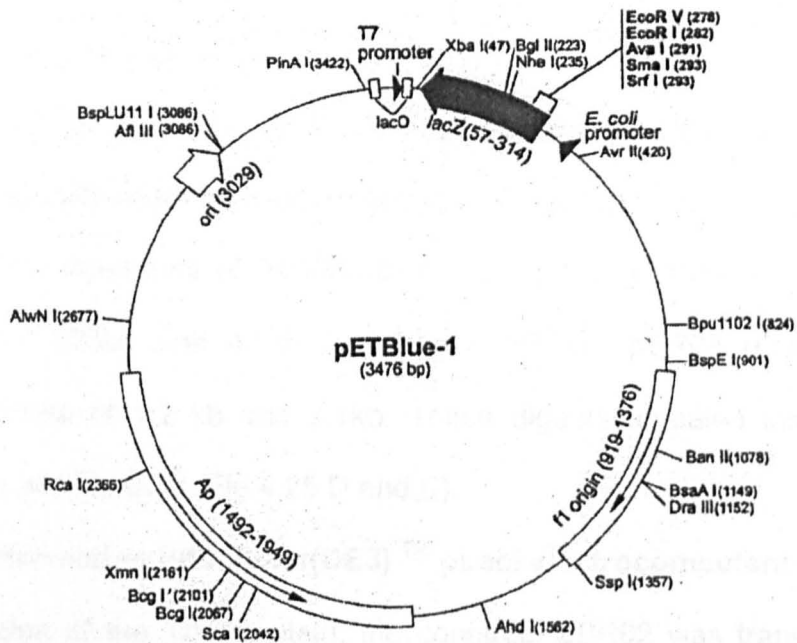
Figure 4.24

Physical map of the pETBLUE-1 vector. The insert is cloned into the EcoR V cloning site located downstream from the *E.coli* ribosome binding site. The *E.coli* promoter mediates blue/white screening, whilst the T7 *lac* promoter that is in the opposed orientation allowing expression of target genes.

223

4.2.9.2 Confirmation of construct with double digestions using XbaI/ BstBI and Xba/EcoRI.

The correct insert in petBlue-1 (pBR02) was verified by PCR with primer IochpB1(F)/IochpB1(R) which showed a band at the expected size of 936bp (Fig. 4.25C). Restriction digestions of *XbaI/BstBI* cut pBR02 (Fig. 4.25D) producing two fragments of 293bp and 4.1kb and *XbaI/EcoRI* cut pBR02 (Fig 4.25E) producing fragments of 1.2 kb and 3.1kb. These digests revealed insert and vector backbone as expected (Fig 4.25 D and E).

4.2.9.3 Transformation into Tuner(DE3) ™ pLacI electrocompetent cells

For overexpression of the TrxB protein, the construct pBR02 was transformed into Tuner cells (Materials and Methods) and transformants were selected on LB agar containing ampicillin (50 µg/ml) and chloramphenicol (34 µg/ml) to give clone RMHt7.

4.2.10 Overexpression of TrxB

4.2.10.1 Overexpression of RMHTrx7 (RMHt7)

Cultures of RMHt7 were grown in Terrific Broth at 37°C until they reached an OD_{600} of 0.08. Then 1mM IPTG was added and incubated for a further 4 hours. 1ml of each of the cultures post induction was sampled, proteins extracted and analyzed by 12.5% w/v SDS PAGE (Fig 4.26). The induced RMHt7 sample produced an intense protein band of approximately 36kDa that corresponds to the size of thioredoxin reductase (TrxB) that is 35.3kDa. This indicates that recombinant thioredoxin reductase (rTrxB) was likely overexpressed.

A

pETBlue-1
[3476 bp]

T7 promoter
PflA I(3423)
BspLU11 I(3086)
Acl II(3086)
ori (50bp)

AlwN I(2677)
Rca I(2366)
Xsp I(1979)
Bsg I(1961)
Bsa I(1940)
Sca I(1840)

Ksp I(1660-1648)

Xba I(47)
lacO
lacZ(57-314)

EcoR V(276)
EcoR I(282)
Nhe I(239)
Ava I(261)
Sma I(263)
Srf I(265)

Bpu1102 I(624)
BsaE I(861)
Som I(1078)
BsaA I(1149)
Drm III(1152)
Bsp I(1357)

E. coli promoter
Aer I(420)

f1 origin (916-1375)

Ahd I(1562)

trxB

lochpB1(F)

lochpB1(R)

936bp

lac operator   lac operator

pUC origin

T7 promoter
lacZ
PstI (339)

trxB

pETBlue-1 trxB
4412 bp

HindIII(1205)
EcoRI (1219)
lacZ
E. coli prom

bla (amp) sequence

f1 origin

B

M   1

10kB

3kB

2kB

1kB

750bp

500bp

250bp

←936bp

C

M   1

10kb

3kb

2kb

1kb
750bp

500bp

250bp

←936bp

D

M   1   2

10kb

6kb

3kb

2kb

1kb

500bp

250bp

←4.1kb

←293bp

E

M   1   2

8kb
5kb

3kb

2kb
1.5kb

1kb

500bp

250bp

Vector
+ insert
←3.1kb

←1.2kb

225

Figure 4.25

PCR and restriction digest analysis of pBR02. Panel A, Construction of pBR02 showing physical map; Panel B, PCR amplification of *trxB* insert from SH1000 using primer pair IochpB1F/IochpB1R separated by 1% w/v agarose gel electrophoresis; Panel C, PCR amplification of *trxB* insert from pBR02 using primer pair IochpB1F/IochpB1R separated by 1% w/v agarose gel electrophoresis; Panel D, 1% w/v agarose gel of *Xbal/BstB*I cut pBR02 (Lanes 1 and 2) producing two fragments of 293bp and 4.1kB; and Panel E, *Xbal/EcoR*I cut pBR02 producing fragments of 1.2kB and 3.1kB. Lane M is DNA ladder with its appropriate sizes shown.

4.2.10.2 Solubility of rTrxB

To determine the solubility of the recombinant TrxB, the cells were fractionated and separated by 12.5% w/v SDS PAGE (Chapter 2.14.5). The TrxB protein appears to be approximately 50% soluble and can be seen in almost equal amounts in lanes 3 and 4 at the expected size of ~ 36 kDa (Fig. 4.26).

4.2.10.3 Confirmation of rTrxB activity

Extracts of *E.coli* pBR02 and *S.aureus* were compared by zymography for TR activity (Fig.4.27B). The Coomassie Blue stained gel (Fig. 4.27A) showed the presence of TrxB in the *E.coli* pBR02 induced sample (lane 1) but not in the uninduced (lane 2) or empty vector (lane 3). The zymogram analysis revealed an identical band corresponding to TR activity in SH1000 and the induced *E.coli* pBR02. The *E.coli* containing the empty vector had no activity. The uninduced *E.coli* pBR02 has slight activity likely due to low level production of TrxB.
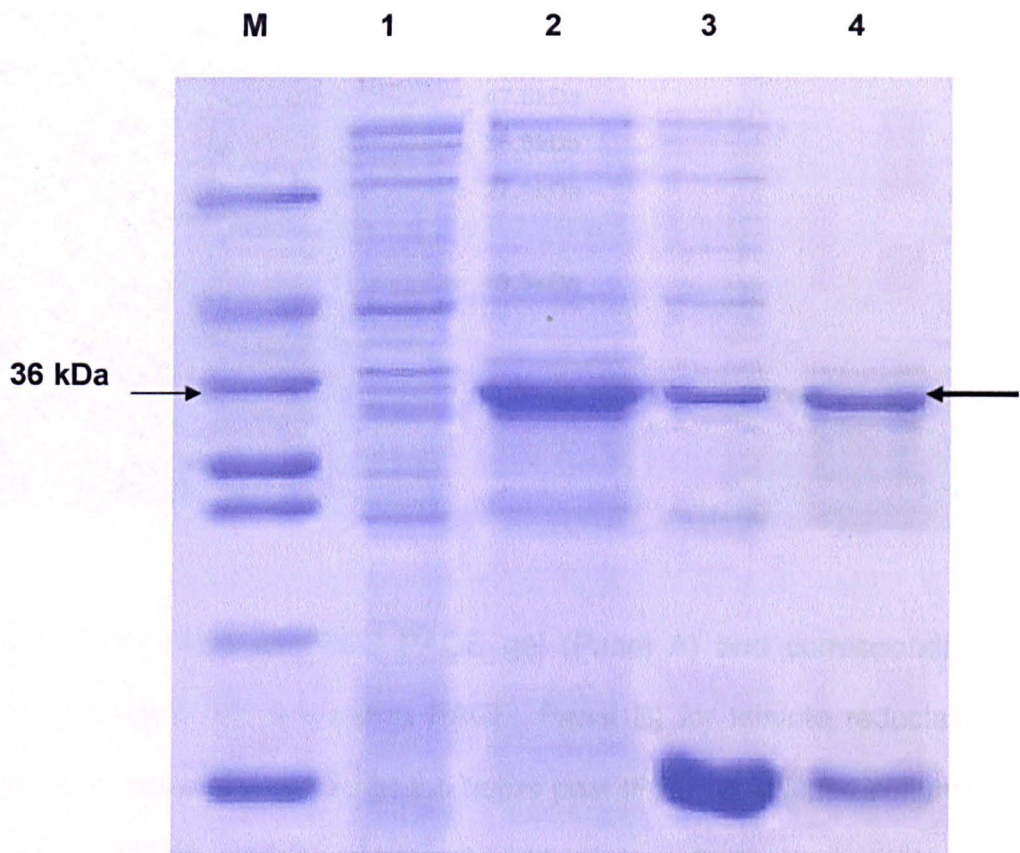
Figure 4.26

Solubility analysis of r-TrxB. Sample from 1.2 OD_{600} units were separated by 12% w/v SDS PAGE. Lane M, low molecular mass marker with the 36 kDa band highlighted; lane 1, uninduced RMHt 7; lane 2, induced RMHt 7; lane 3, soluble material ; lane 4, insoluble material. The TrxB protein appears at about 36 kDa.
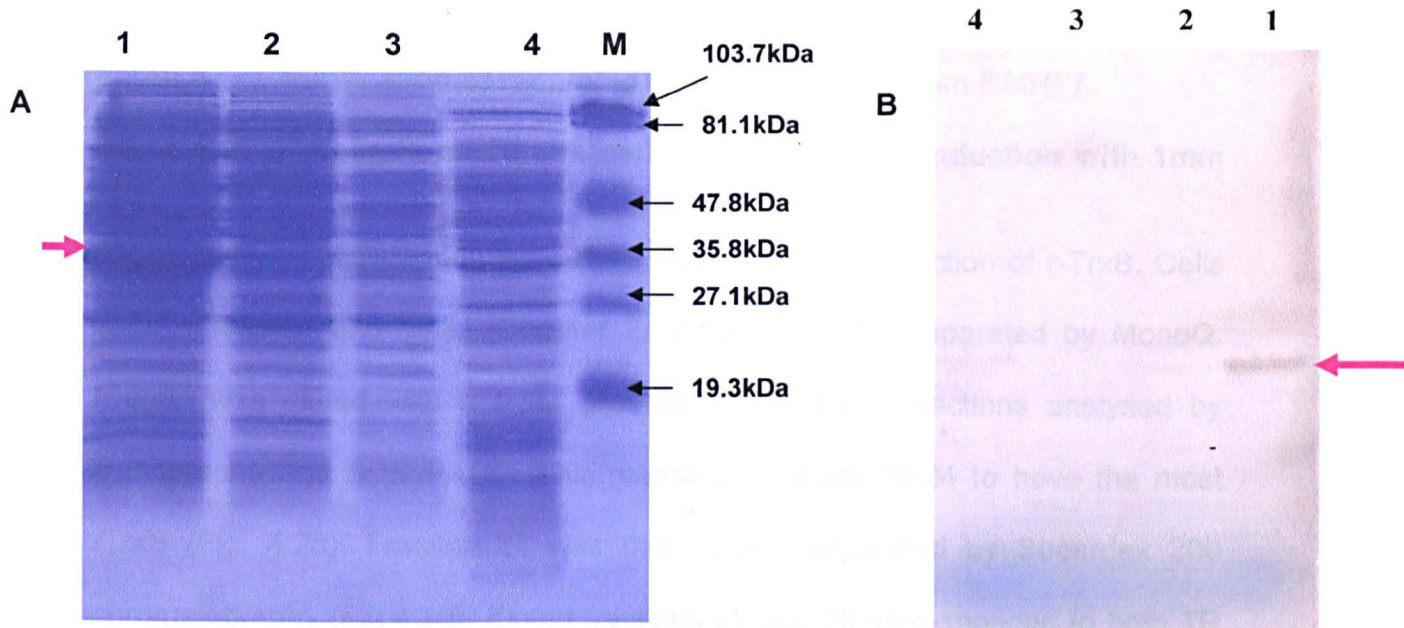
Figure 4.27

TR activity of rTrxB. 12% w/v SDS PAGE gel (Panel A) and corresponding zymography analysis (7.5% w/v native PAGE, Panel B) for tellurite reductase activity. Total protein were analysed at 2.5 hours post IPTG (in induced culture). Lane 1, induced RMHt7; lane 2, uninduced pRMHt7; lane 3, vector (no insert); lane 4, SH1000. Lane M (Panel A) shows low molecular mass protein marker with the corresponding sizes shown on the right. The pink arrows indicates rTrxB protein at ~ 36kDa (Panel A) and TR activity (Panel B).

4.2.10.4 Purification of recombinant TrxB (r-TrxB) from RMHt 7.

4.2.10.4.1 Preparation of fresh cell free extract and induction with 1mm IPTG.

500ml of *E.coli* pBR02 induced culture was used for production of r-TrxB. Cells were harvested and lysed (Chapter 2.19.1.3) and CFE separated by MonoQ. Protein was eluted with a 0-1M gradient of NaCl and fractions analysed by zymography and SDS PAGE. This revealed fractions 20-24 to have the most rTrxB (Fig. 4.28). Fraction 21 was then further separated by Superdex 200 chromatography (Fig 4.29). Eluted fractions 25 and 26 corresponded to both TR activity and a protein of the expected size of 36kDa (Fig 4.30).

4.2.10.4.2 Verification of r-TrxB TR activity.

Fractions 25 and 26 from the Superdex 200 column were pooled and loaded in triplicate onto 7.5% w/v native PAGE and separated (Fig 4.30). The gel was excised into three for zymogram analysis, Coomassie Blue staining and N-terminal sequencing. This revealed a sequence of MTEIDFDIA, which exactly corresponds to that predicted for rTrxB sequence. This identified the tellurite reductase enzyme that is associated with the activity band on 7.5% w/v native PAGE as thioredoxin reductase (TrxB).
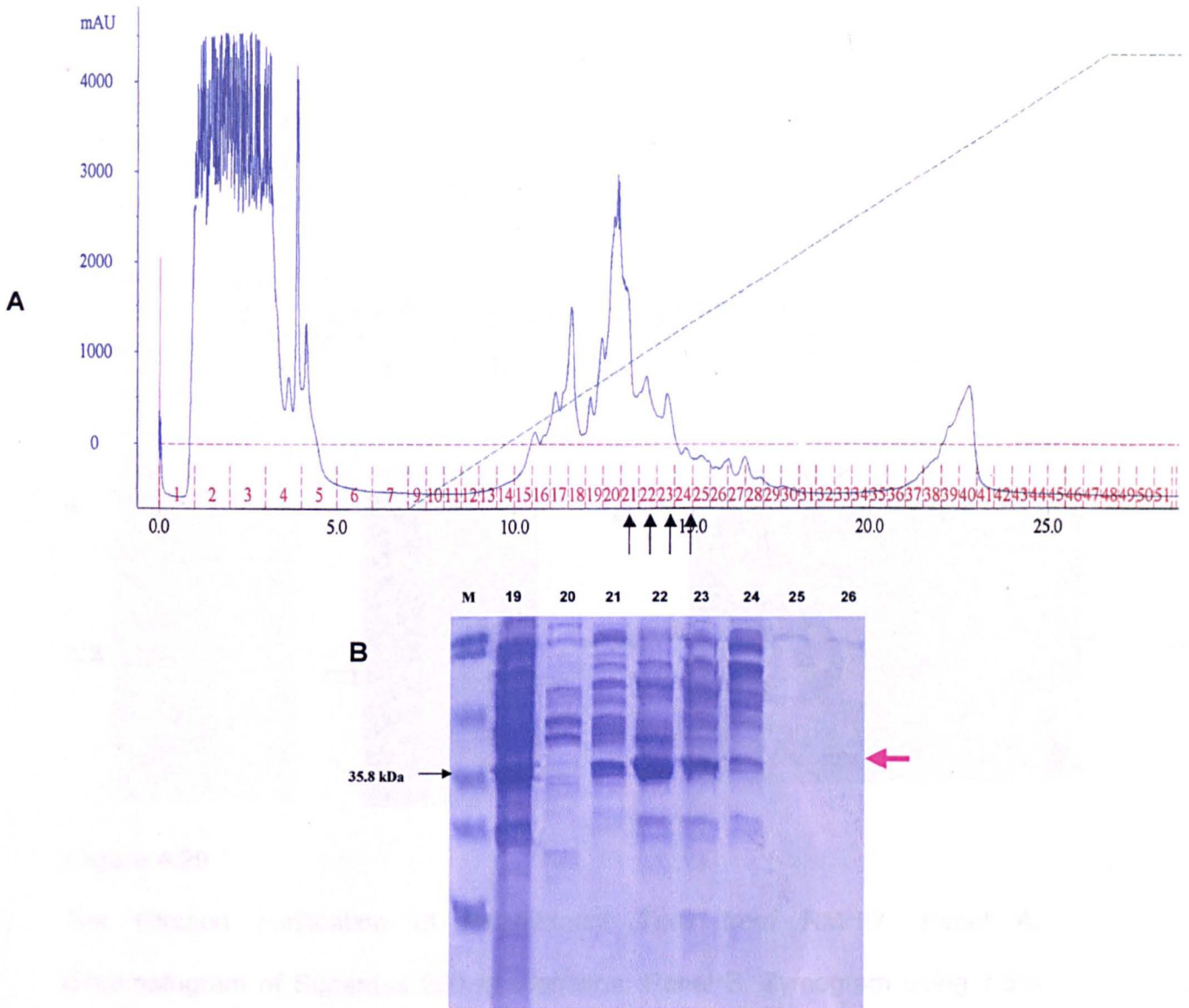
Figure 4.28

Ion exchange chromatography of recombinant TrxB from RMHt7 (74.8 mg loaded). Panel A, Chromatogram of separated proteins. Dashed line shows 0-1M NaCl gradient. Panel B, 12% w/v SDS PAGE gel analysis showing rTrxB eluted in fractions 21, 22, 23 and 24. Lane M (Panel A) shows low molecular mass protein marker with the corresponding sizes shown on the right. The pink arrow indicates rTrxB protein at ~ 36kDa (Panel A). Dark arrows on FPLC trace show fractions containing tellurite reductase activity.
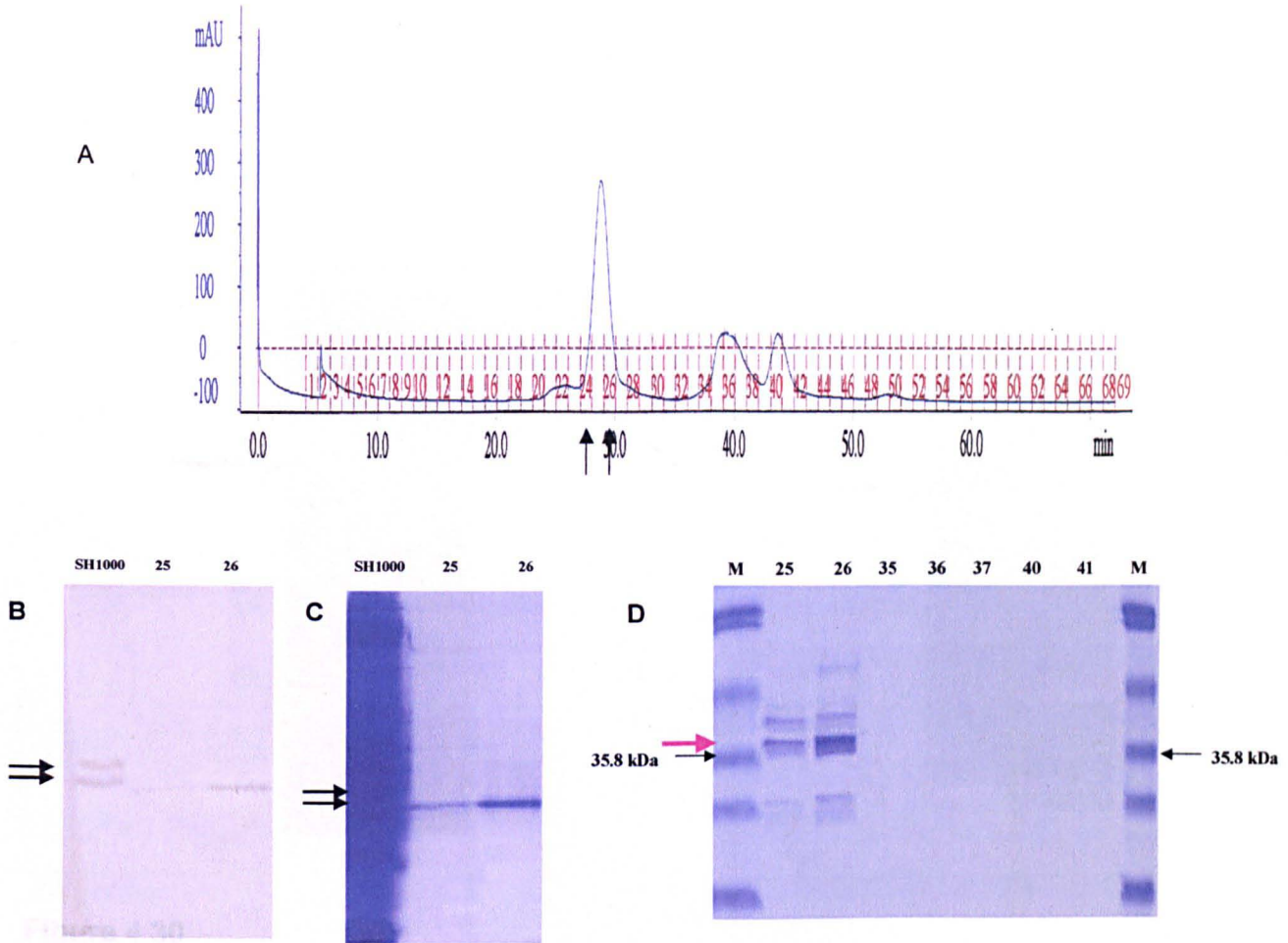
Figure 4.29

Gel filtration purification of recombinant TrxB from RMHt7. Panel A, Chromatogram of Superdex 200 fractionation; Panel B, Zymogram using 7.5% w/v native PAGE showing tellurite reductase activity; Panel C corresponding Coomassie stained protein gel; and Panel D; 12% w/v SDS PAGE gel analysis showing rTrxB eluted in fractions 25 and 26. Lane M (Panel A) shows low molecular mass protein marker with the corresponding sizes shown on the right. The pink arrow indicates rTrxB protein at ~ 36kDa (Panel A). Dark arrows on FPLC trace show fractions containing tellurite reductase activity. Arrows indicate tellurium deposits and corresponding region on Coomassie stained gel. Dark arrows on FPLC trace show fractions containing tellurite reductase activity.
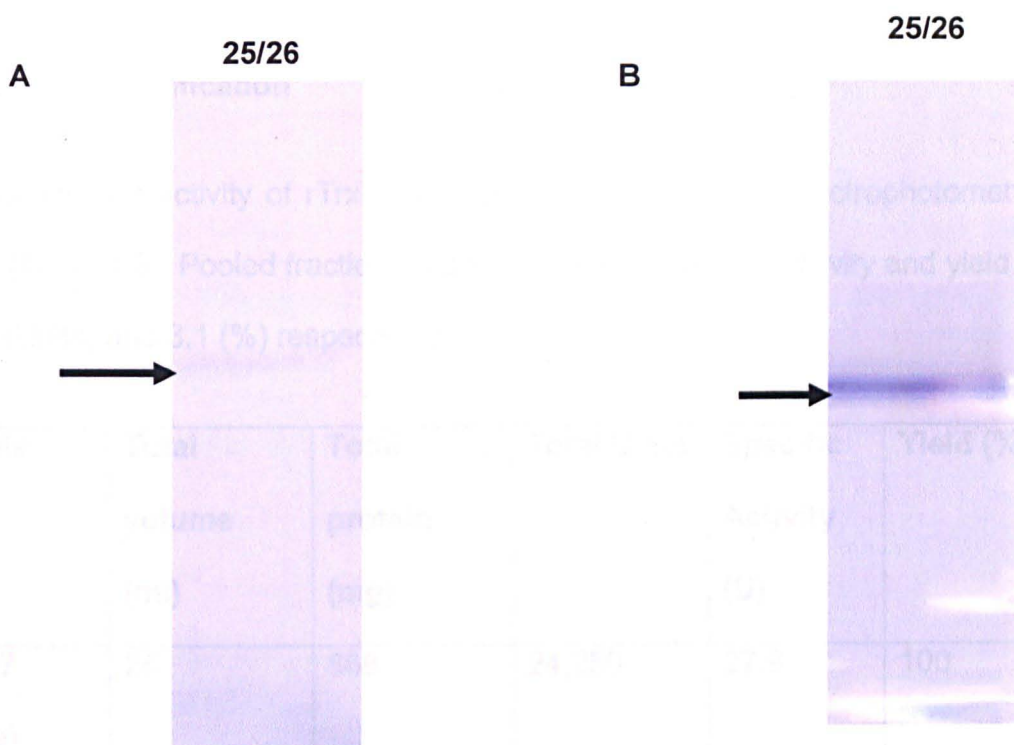
Figure 4.30

Identification of TR activity of r-TrxB. Panel A, Superdex 200 fractions 25 and 26 were pooled and separated by 7.5% w/v native PAGE and stained for tellurite reductase (TR) activity and Panel B, Coomassie stained protein gel showing corresponding protein that was used to identify the tellurite reductase band by N-terminal sequence. Arrows indicate tellurium deposits and Coomassie stained band identified as thioredoxin reductase (*trxB*).

Efficiency of purification

The specific TR activity of rTrxB was determined using the spectrophotometric assay (Table 4.3). Pooled fraction 25 and 26 showed specific activity and yield of 231.2 (Units) and 3.1 (%) respectively.

Sample	Total volume (ml)	Total protein (mg)	Total Units	Specific Activity (U)	Yield (%)
RMHt7 (crude)	25	868	24,250	27.9	100
Superdex 200 fractions 25 and 26	2	3.2	740	231.2	3.1

Table 4.3

Purification of r-TrxB from RMHt7. r-TrxB was purified through a gel filtration (Superdex 200) column. Pooled fractions 25 and 26 from the Superdex 200 were used to perform the TR activity and protein assays (Bradford). The data obtained were used to calculate the specific activity (Units) of each sample.

4.2.15 Enzyme Kinetic Analysis

Purified rTrxB was stored at -20°C. However upon thawing, the protein was found to have lost >80% of activity. The entire purification process was repeated. However the purified enzyme could not be stored in an active state even at -80°C. This prevented in depth kinetic analysis of rTrxB activity.

4.3   Discussion

In this chapter, two tellurite reductases, thioredoxin reductase (TrxB) and alkylhydroperoxidase subunit F (AhpF) were identified in *S.aureus*. TrxB was overexpressed and purified and was shown to be the primary protein involved in tellurite reduction in SH1000. AhpF is a component of the alkylhydroperoxidase AhpCF that shows homology with both thioredoxin (TrxA) and TrxB (Chapter 1 Introduction).

Tellurite is toxic to most microorganisms and before the advent of antibiotics, tellurite was used as an antibacterial agent in the treatment of many diseases (Taylor, 1999). Tellurite resistance is well documented amongst the gram-positive bacteria, a criterion used for isolation of several species including *S.aureus*, *Corynebacterium diphtheriae*, and *Enterococcus faecalis* (Tucker *et al.*, 1961; Tucker *et al.*, 1966). Tellurite is also used in the isolation of several gram-negative pathogens including *E.coli* O157 (Zadik *et al.*, 1993), *Shigella* spp. (Mujibur Rahaman *et al.*, 1986) and *Vibrio cholerae* (Shimada *et al.*, 1990).

Several tellurite resistance determinants (Te^R) have been identified. The presence of these Te^R are well documented in gram negatives as exemplified by *E.coli* (Taylor, 1999) and are either plasmid mediated or coded on the chromosome. *S.aureus* that is reportedly naturally resistant to high levels of tellurite have not been shown to possess any of these known determinants (Taylor 1999). Taylor *et al.* 1994 reported that the *tehAB* genes that code for tellurite resistance in *E.coli* *K12* are not present in *S.aureus*. In this study *S.aureus* SH1000, as expected, showed a high MIC of 5mM.

Tellurite toxicity may be overcomed either by decreasing its uptake, increased efflux or by reducing it to less toxic elemental tellurium (Te^0). However, tellurite is not detoxified by any of of the known mechanisms of heavy metal detoxification such as reduced uptake or increased efflux (Turner, 1994) although the *ars* operon (*arsABC*) which codes for the arsenical ATPase efflux pump may contribute to moderate tellurite resistance in *E.coli* (Turner *et al.*, 1992). Deposited elemental tellurium manifests phenotypically as black colonies when organisms are grown on agar containing tellurite (Taylor, 1999). Most studies show that detoxification of tellurite occurs by its reduction to the non-toxic form tellurium which is commonly seen as black "needlelike" crystals. Tellurium deposits are commonly seen deposited either in the cytoplasm as in *Natronococcus occultus* (Pearion *et al.*, 1999), in the intracytoplasmic membrane as in *Rhodobacter capsulatus* B100 (Borsetti *et al.*, 2003), in the periplasmic space as in *Rhodobacter sphaeroides* (Sabaty 2001) or on membrane surfaces as in *E.coli* (Trutko *et al.*, 2000). In SH1000, cells that are grown in the presence of tellurite turned black and tellurium inclusions were found clearly deposited within its cytoplasm (Fig 4.4). This suggests that the mechanism by which it attains high resistance to tellurite SH1000 is by reducing the damaging effect of tellurite by converting it to the less toxic form, tellurium (Te^0).

In addition, tellurite reduction in SH1000 was found to occur enzymatically with absolute requirement for the reducing power provided by NADH. This tellurite reduction activity is sensitive to boiling and treatment with proteinase K which further emphasizes its enzymatic nature. Also as the cell free extracts

tested for the tellurite reduction activity were exhaustively dialysed, it is highly unlikely that the observed activity was caused by low molecular weight thiols. The activity was also facilitated by the presence of 2-mercaptoethanol that provides a reducing environment for the thiol groups. Similarly, previously studied tellurite reduction in other organisms such as *Bacillus stearothermophilus* V (Moscoso *et al.*, 1998) and *Thermus thermophilus* HB8 (Chiong *et al.*, 1988) have been found to be enzymatic and NADH / NADPH dependent. In the archeon *N.occultus,* tellurite reduction of cell free extracts was shown to be dependent on NADH as well as a reducing environment (Pearion and Jablonski, 1999). Thiol groups are often implicated in this tellurite reduction process (Albeck *et al.*, 1998). Although tellurite is known to be thiol reactive the chemistry involved is unclear. Turner *et al.* (1999) reported that exposure of tellurite-susceptible cells of *E.coli* to tellurite caused a marked reduction in the reduced thiols (RSH) content. In addition, reduced glutathione was shown to be the major initial target of tellurite activity in *E.coli* (Turner *et al.*, 2001). Also *E.coli* with mutations in the genes for disulfide-bond formation (*dsbA* and *dsbB*) are hypersensitive to K_2TeO_3. The presence of tellurite resistance, Te[R], determinants (IncHI, IncHII, IncPα, and *teh*) has been shown to protect *E.coli* from thiol oxidation (loss of RSH content) upon exposure to TeO_3^{2-} (Turner, 1995). In addition, cysteine residues in TehB a tellurite resistance determinant on the *E.coli* chromosome are involved in tellurite substrate recognition and binding which oxidizes the cysteines (Dyllick-Brenzinger, 2000). Further, mutations in the

cysteine, glutathione or thioredoxin biosynthetic pathways were shown to decrease tellurite resistance in the *E.coli tehAB* system.

The *cysK* gene that codes for the enzyme cysteine synthase was found to be a tellurite resistance determinant of *Bacillus stearothermophilus* which conferred tellurite resistance in *E.coli* and *Salmonella typhimurium* LT2 (Vasquez *et al.*, 2001). Disruption of the *cysK* gene in *R.sphaeroides* 2.4.1 resulted in reduced tellurite resistance levels suggesting a link between cysteine biosynthesis and tellurite resistance (O'Gara, 1997).

A study on a cysteine auxotrophic mutant (*cysM*) demonstrated increased sensitivity to tellurite and that tellurite resistance can be linked to survival from oxidative and thiol stress (Lithgow *et al.*, 2004). The *S.aureus cysM* locus increases tellurite resistance in *E.coli* and is involved in stress resistance. However, unlike in *B.subtilis*, *cysM* in *S.aureus* is involved in resistance to diamide and tellurite but not to other stresses such as methyl viologen or hydrogen peroxide. Taylor (1999) suggests that tellurite reduction occurs at the expense of thiol groups, such as glutathione and cysteine. The glutathione studies in this thesis (Chapter 3) suggest that a correlation exists between glutathione and tellurite reduction.

Although the exact chemistry of tellurite reduction is yet unknown, it is apparent from previous studies that it involves some form of oxidation-reduction i.e. electron transfer reaction (Albeck *et al.*, 1998). It is therefore not surprising that the major tellurite reductases characterized from SH1000 in this study were identified as thioredoxin reductase (TrxB) and a related homolog,

alkylhydroperoxidase subunit F, AhpF. Both TrxB and AhpF are oxidoreductases that function to shuttle electrons from NADH/ NADPH to a substrate and possess a redox active disulfide in addition to FAD in their respective active redox centers (Williams, 1995).

The thiol groups (from cysteine residues) of cytoplasmic proteins are kept in the reduced state by specific proteins that maintain a reducing environment. These proteins maintain the oxidation state of the cysteine residues and are therefore responsible in determining the formation of disulphide bonds (Aslund and Beckwith, 1999). Members of the thioredoxin family are oxidoreductases that play a major role in maintenance of the reduced thiol states and include the thioredoxin subfamily and the glutaredoxin subfamily (Ritz and Beckwith, 2001). The disulfide bond oxidoreductases share a common structural characteristic in having the typical active site motif Cys-X-X-Cys (Aslund and Beckwith, 1999) which in thioredoxin is Trp-Cys-Gly-Pro-Cys (Holmgren, 1985). The conserved active site cysteine of *S.aureus* thioredoxin is the key residue for substrate reduction (Roos *et al.*, 2007). In *E.coli*, the thioredoxin subfamily comprises of thioredoxins 1 and 2 (TrxA and TrxC respectively) and thioredoxin reductase (TrxB). The glutaredoxin subfamily is composed of glutaredoxins 1,2 and 3 (GrxA, GrxB and GrxC respectively).

The thioredoxin system is ubiquitous in living organisms and consists of thioredoxin and thioredoxin reductase which are thiol-disulfide oxidoreductases that uses NADPH as reducing power (Arner and Holmgren, 2000). The general enzymatic reactions of this system involves oxidation of thioredoxin (Trx-$(SH)_2$ to

240

a dithiol form (Trx-S$_2$) upon reduction of disulfides (proteins) (Holmgren, 1985). Trx-S$_2$ is in turn reduced by thioredoxin reductase (TxR) to regenerate reduced thioredoxin in the presence of NADPH. In addition, thioredoxin reductase is able to reduce other substrates in the same manner.

Thioredoxin is a thiol-disulfide oxidoreductase that is encoded by *trxA*. The thioredoxin from *E.coli* consists of 108 residues with a molecular weight of approximately 12kD (Holmgren, 1968) and is one the major proteins involved in maintainence of intracellular sulfhydryl status. Being one of the major oxidoreductases, thioredoxin possesses many enzymatic roles associated with maintenance of the thiol redox balance within the cell. Although it has been implicated in several physiological functions, its main roles are in the involvement of protein disulfide reduction and DNA synthesis. In general the main oxidoreductase activity of this enzyme can be categorized into two main roles i.e as electron carriers for important biosynthetic enzymes such as ribonucleotide reductases, methionine sulfoxide reductases and sulfate reductases and as a protectant of cytosolic proteins from aggregation or inactivation via oxidative formation of intra- or inter-molecular disulfide (Arner and Holmgren, 2000). In addition, it plays an important role in cell signaling and defense against oxidative damage and stress by being an electron donor for thioredoxin peroxidases (peroxiredoxins) which catalyzes the reduction of H$_2$O$_2$ (Arner and Holmgren, 2000). In *E.coli*, the thioredoxin and thioredoxin reductase were shown to have chaperone properties by their involvement in protein folding and protein renaturation after stress (Kern *et al.*, 2003).

Thioredoxin reductase (TrxB) is a flavoenzyme that catalyzes the reduction of thioredoxin using the reducing power of NADPH (Lennon *et al.*, 2000). It belongs in the family of pyridine nucleotide-disulfide oxidoreductases which includes glutathione reductase, lipoamide dehydrogenase and other members that characteristically possess a redox active disulfide/dithiol (Arscott *et al.*, 1997). Two classes of thioredoxin reductase exist i.e. the low Mr type (Mr = 35 000 per subunit) that is found in bacteria like *E.coli* and the high Mr type (Mr = 55 000 per subunit) found in higher eukaryotes. In eukaryotic organisms the enzyme is more related to glutathione reductase (Williams *et al.*, 2000). Thioredoxin reductase contains a redox active disulfide in addition to the FAD and the reduction process involves electron transfer from NADPH to the FAD which then transfer the electrons to the disulfide of the active site of the enzyme and finally from the reduced thiols to the disulfide of thioredoxin (Williams, 1995).

The TrxB recombinant protein purified in this study has a molecular mass of less than 35.8 kDa that is consistent with the thioredoxin reductase with a subunit M_R of approximately 35kDa that is isolated from prokaryotes (Uziel *et al.*, 2004). In contrast, human thioredoxin reductase possesses a subunit M_R of 55kDa. In addition, the redox active centre in thioredoxin reductase from *S.aureus* and other prokaryotes is reported to possess the CAT/NC motif whereas that in humans is a hexapeptide with the CVNVGC motif (Uziel *et al.*, 2004). Further, the authors show that exposure to oxidative stress agents such as diamide, menadione and τ-butyl hydoperoxide causes increased transcription of both the *trxA* and *trxB* genes in *S.aureus* resulting in increased disulphide

bond formation. Treatment of *Bacteroides fragilis*, an anaerobe, with diamide, H_2O_2 or exposure to oxygen induced the expression of *trxB* gene (Rocha *et al.*, 2007). In *S.aureus* the thioredoxin system, especially thioredoxin reductase (TrxB) is essential because of the absence of an alternative thiol-redox system (Uziel *et al.*, 2004).

The second tellurite reductase enzyme indentified in this study is AhpF, a member of the peroxiredoxin or alkyl hydroperoxidoreductase (AhpR) family which is closely related to the thioredoxin-thioredoxin reductase system. Together with AhpC, the peroxiredoxins catalyzes an NADH dependent reduction of alkylhydroperoxides. AhpF is a flavoprotein that shows structural similarity to both thioredoxin and thioredoxin reductase (Poole *et al.*, 2000). The C-terminal 60% is similar to the low Mr thioredoxin reductase including the redox-active disulfide located just inside the pyridine nucleotide binding and the N-terminal 40% is a tandem repeat of two thioredoxin-like folds with the redox-active disulfide retained in only one of them (Williams, 2000, Poole *et al.*, 2000). Basically, AhpF shuttles reducing equivalents from NAD(P)H (with a strong preference for NADH) to AhpC, the actual peroxidase and a member of the peroxiredoxin family of thiol peroxidases. The *ahpC* and *ahpF* genes are organized in a two-gene operon, and transcription is PerR controlled (*Bsat et al.*, 1996). The AhpR (AhpCF) system in *E.coli* together with catalases constitute a two-enzyme H_2O_2 scavenging system (Tartaglia *et al.*, 1989).

Although AhpF and TrxB were identified as the major TRs, interestingly, several other minor tellurite activity bands were also observed. These could be

due to other independent activity or modification of TrxB. Previous studies in tellurite sensitive organisms have implicated other oxidoreductases such as the catalase in *Staphylococcus epidermidis* (Calderon *et al.*, 2006) as being the primary enzyme responsible for the tellurite reduction activity. *S.aureus* reportedly (delCardayre *et al.*, 1998) also possesses other oxidoreductases like the Coenzyme A disulfide reductase (CoADR), a ☐immer with identical subunits of M_r 49,000 each. It belongs to the family of the flavin containing pyridine nucleotide-disulfide oxidoreductases and catalyzes the specific reduction of CoA using NADPH. However, it differs from other members of the family in having only a single cysteine in the SFXXC motif in the active site region (delCardayre *et al.*, 1998), instead of the conserved CXXC motif as is present in thioredoxin reductase. It is unknown at this juncture if CoADR is also involved in tellurite reduction although its structure and function is suggestive of its ability to do so. In this study however, it was shown that the major tellurite reductase identified was approximately 35.8 kDa (Fig 4.29) which corresponded to the Mr subunit of thioredoxin reductase (Williams *et al.*, 2000) and not to CoADR.

Tellurite resistance is not a primary characteristic but appears to be product or secondary effect of normal cell functions (Taylor, 1999). Therefore, it may be an effective indicator for resistance to other stressful conditions that may pose a threat to the metabolism and overall survival of the organism in the human host. Taylor (1999) suggests that tellurite can be detoxified through interaction with cellular thiols such as reduced glutathione. The mechanism of interaction between the TrxB, tellurite and glutathione is unknown although the

involvement of thiol groups in the tellurite reduction process is strongly suggested. A previous study showed that thioredoxin and thioredoxin reductase from *E.coli* was able to oxidize NADPH in the presence of selenoglutathione (GS-Se-SG) (Bjornnstedt, 1992). Similarly, tellurium dioxide (TeO_2) has been found to interact rapidly with cysteine (Albeck *et al.*, 1998). The exact role of glutathione in tellurite reduction is unclear, although the presence of the strong electron donating sulfhydryl group on its cysteine moiety suggests a possible involvement in the tellurite reduction process. However, since *S.aureus* does not synthesize glutathione, this compound cannot be solely responsible for tellurite reduction and the high level resistance to tellurite observed in this organism (Lithgow *et al.*, 2004). Thioredoxin/thioredoxin reductase, CoenzymeA reductase and the alkyl hydroperoxidoreductase (AhpCF) are sulfhydryl stabilizing enzymes that constitute the electron-donating components in *S.aureus*. The presence of thiol reactive centers in the thioredoxin and peroxidoreductase proteins is strongly suggestive of their possible involvement in the tellurite reduction process and may perhaps play a role in the high level of tellurite resistance observed in *S.aureus*. The nature of tellurite resistance in *S.aureus* and the possible involvement of glutathione in the tellurite reduction process remains to be elucidated.

Summary

- Two tellurite reductases were identified in *S.aureus* as thioredoxin reductase B (TrxB) and alkylhydroperoxidase subunit F (AhpF).

- TrxB was purified and shown to be the major protein involved in tellurite reduction

- Inactivation of *ahpC* or *perR* did not affect tellurite reductase activity.

CHAPTER FIVE

GENERAL DISCUSSION

S.aureus is a highly versatile and adaptable pathogen that is capable of causing a wide variety of diseases ranging from mild skin infections to serious life threatening bacteremias and endocarditis. It produces several virulence factors such as cell surface proteins that mediate attachment (Foster and Hook, 1998), and extracellular toxins and enzymes (Novick, 2003) that overcome the host defences and allow invasion and persistence. Clearly these flexible and highly adaptive characteristics confer the ability to inhabit a diverse range of niches in the host. The host naturally represents a stressful environment in which in order to survive and proliferate *S.aureus* has developed multiple mechanisms that enable colonization in both an infective (pathogenic) and non-infective (commensal) state. In addition, *S.aureus* has an ability to acquire and exhibit resistance to multiple antibiotics as evidenced by the emergence of vancomycin-resistant MRSA strains.

Both its high adaptive ability and multidrug resistance makes *S.aureus* a successful pathogen that is a problem both as hospital and community acquired infections, in addition to being an economic burden on healthcare systems (Goossens 2005, Lim and Webb, 2005). The emergence of strains that are highly refractive to antibiotics has spurred research into developing novel therapies for prophylactic treatment (vaccine production) and eradication of this organism. The identification of the metabolic functions and their roles in the pathogenicity of

247

S.*aureus* may reveal novel targets that can be used to effectively design strategies aimed at combating this organism.

Previous studies (Lithgow *et al.*, 2004) as well as my work established the role of glutathione as a sulfur source for S.*aureus*. As S.*aureus* does not synthesize glutathione and acquires it from the host, it was hypothesized that the mechanism of utilization of glutathione involved GGT. However, the presence of a novel glutathione utilization mechanism in S.*aureus* is suggested as the organism continues to grow despite disruption of the *ggt* gene (Chapter 3). The mechanism of glutathione utilization in S.*aureus* remains to be elucidated in future work.

The role of glutathione in stress resistance in S.*aureus* remains somewhat obscure. The protective nature of glutathione (GSH) is enabled by the strong electron donating capacity of the thiols that reside on its cysteine moiety. Both the thioredoxin system and glutathione are responsible for maintaining a reduced environment intracellularly to keep protein thiols in their free sulfhydryl state. S.*aureus* however does not synthesize glutathione and relies mostly on the thioredoxin system for maintenance of intracellular thiol balance (Uziel *et al.*, 2004). My work shows that glutathione is associated with stress resistance in S.*aureus*. This has important implications as many *in vitro* experiments are done under conditions without glutathione being present. It is important to measure the role of particular components under conditions that mimic those *in vivo*.

Taylor (1999) suggests that tellurite resistance is a secondary effect of a metabolic function and different tellurite resistance mechanisms are associated

with different organisms (Chapter 4). Elucidation of the tellurite resistance mechanism therefore may provide insight and better understanding of the resistance mechanism(s) in this organism for design of novel antistaphyloccoccal prophylaxis. Previous studies (Avazeri *et al.*, 1997; Chiong *et al.*, 1988; Moscoso *et al.*, 1998; Sabaty, 2001; and Trutko *et al.*, 2000) coupled with my work demonstrate that despite the diverse mechanisms of tellurite resistance, it is commonly associated with the process of electron-transfer with probable involvement of thiol groups. Here I identified both AhpF and TrxB as being capable of tellurite reduction. AhpF and TrxB possess structural homology and both proteins are associated with redox processes. In addition TrxB which is an essential protein in *S.aureus* (Uziel *et al.*, 2004) belongs to the thioredoxin system which is presumably one of the main regulators of thiol-balance in *S.aureus*.

My studies have highlighted the complex interplay between different aspects of *S.aureus* physiology. The interactive web of stress resistance and metabolic capabilities of this organism are a testament to the complex mechanisms that allow *S.aureus* to be such a successful pathogen.

Future Work

The presence of a novel alternative pathway for glutathione utilization in *S.aureus* was suggested in this study. To elucidate the mechanism of this pathway it is necessary to create a mutant that is not able to utilize glutathione and this can hypothethically be achieved by transposon mutagenesis in the *ggt* background. The fate of glutathione in *S.aureus* can also be determined by

analysis of the catabolic products involved in its metabolism. Alternatively protein(s) involved in the utilization of glutathione can be purified, identified and characterized using similar approaches to the tellurite reductase study. In addition, *in vivo* studies will shed light on the roles of *ggt* and putative glutathione ABC transporter in pathogenicity.

In order to determine the role of TrxB in stress resistance it will be necessary to create a conditional lethal mutant. This requires *trxB* to be placed under the control of an inducible promoter. As the level of TrxB is diminished the cells may become specifically more susceptible to tellurite. Tellurite stress might also elicit the expression of genes involved in resistance. This could be followed by transcriptome and proteome studies to identify specific components for further analysis. Genes that are turned on by tellurite at the translational level can be identified along with proteome studies of the modified (oxidized) proteins resulting from tellurite exposure.

REFERENCES

Aarestrup, F.M., Scott, N.L., and Sordillo, L.M. 1994. Ability of *Staphylococcus aureus* coagulase genotypes to resist neutrophil bactericidal activity and phagocytosis. *Infection and Immunity* **62**, 5679-5682.

Abdelnour, A., Arvidson, S., Bremell, T., Ryden, C., and Tarkowski, A. 1993. The accessory gene regulator (agr) controls *Staphylococcus aureus* virulence in a murine arthritis model. Infection and Immunity **61**, 3879-3885.

Albeck, A., Weitman, H., Sredni, B., and Albeck, M. 1998. Tellurium compounds: Selective inhibition of cysteine proteases and model reaction with thiols. Inorg.Chem **37**, 1704-1712.

Apontoweil, A., Berends, W. Isolation and initial characterization of glutathione-deficient mutants of *Escherichia coli* K12. 1975. Biochimica et Biophysica Acta **399**, 10-22.

Armstrong-Buisserat, L., Cole, M.B., and Stewart, G.S. 1995. A homologue to the *Escherichia coli* alkyl hydroperoxide reductase AhpC is induced by by osmotic upshock in *Staphylococcus aureus*. Microbiology **141**, 1655 – 1661.

Arner, E.S.J., Holmgren, A. 2000. Physiological functions of thioredoxin and thioredoxin reductase. Eur. J. Biochem **267**, 6102-6109.

Arvidson, S., and Tegmark, K. 2001. Regulation of virulence determinants in *Staphylococcus aureus*. Int. J. Med. Microbiology **291**, 159-170.

Aslund, F., and Beckwith, J. 1999. The thioredoxin superfamily: Redundancy, specificity and gray-area genomics. Journal of Bacteriology **181**, 1375-1379.

Avazeri, C., Turner, R.J., Pommier, J., Weiner, J.H., Giardano, G., and Vermeglio, A. 1997. Tellurite reductase activity of nitrate reductase is responsible for the basal resistance of *Escherichia coli* to tellurite. Microbiology **143**, 1181-1189.

Baba, T., Bae, T., Schneewind, O., Takeuchi, F., and Hiramatsu, K. 2008. Genome sequence of *Staphylococcus aureus* strain Newman and comparative analysis of staphylococcal genomes: Polymorphism and evolution of two major pathogenecity islands. Journal of Bacteriology **190**, 300 – 310.

Bae, T., Banger, A.K., Wallace, A., Glass, E.M., Aslund, F., Schneewind, O., and Missiakas, D.M. *Staphylococcus aureus* virulence genes identified by *bursa aurealis* mutagenesis and nematode killing. PNAS **101**, 12312-12317.

Baird-Parker, A. C. (1984). Gram-positive cocci. In Bergey's manual of systemic microbiology, pp. 478-489. Edited by J. G. Holt. London: Williams and Wilkins.

Balaban, N., and Rasooly, A. 2000. Review of staphylococcal enterotoxins. International Journal of Food Microbiology **61**, 1 – 10.

Bayer, A., Coulter, S.N., Stover, C.K. and Schwan, W.R.1999. Impact of the high-affinity proline permease gene (putP) on the virulence of *Staphylococcus aureus* in experimental endocarditis. Infection and Immunity **67**, 740 – 744.

Bayer, M.G., Heinrichs, J.H., and Cheung, A.L. 1996. The molecular architecture of the *sar* locus in *Staphylococcus aureus*. Journal of Bacteriology **178**, 4563-4570.

Bebien, M., Kirsch, J., Mejean, V, Vermeglio, A. 2002. Involvement of a putative molybdenum enzyme in the reduction of selenate by *Escherichia coli*. Microbiology **148**, 3865-3872.

Becker, K., Bierbaum, G., von Eiff, C., Engelmann, S., Gotz, F., Hacker, J., Hecker, M., Peters, G., Rosenstein, R., and Ziebuhr, W. 2007. Understanding the physiology and adaptation of staphylococci: A post-genomic approach. International Journal of Medical Microbiology **297**, 483-501.

Beers, M.H., and Berkow, R Bacterial diseases caused by gram-positive cocci. The Merck Manual of Diagnosis and Therapy; 17th Edition. Merck & Company. U.S.A.

Benka, J., Lesnakova, A., Holeckova, K., Ondrusova, A., Wiczmandyova, O., Siadeckova, V., Hvizdak, F., Bartkovjak, M., Seckova, S., Taziarova, M., Huttova, M., Bielova, M., Luzica, R., Karvaj, M., Kovac, M., Bauer, F., Sabo, I., Svabova, V., Findova, L., Bukovinova, P., and Shahum, A. 2007. Neuroinfections due to *Staphylococcus aureus:* an emerging pathogen also in community. Neuro Endocrinol Lett. **28**

Bernheimer, A.W. and Rudy, B. 1986. Interactions between membrane and cytolytic peptides. Biochimica et Biophysica Acta **864**, 123 – 141.

Bhakdi, S., and Tranum-Jensen, J. 1991. Alpha-toxin of *Staphylococcus aureus*. Microbiological Reviews 55, 733 – 751.

Bhalla, A., Aron, D.C., and Donskey, C.J. 2007. *Staphylococcus aureus* intestinal colonization is associated with increased frequency of S.aureus on skin of hospitalized patients. BMS Infectious Diseases **7**: 105.

Bilen, H., Ates, O., Astam, N., Uslu, H., Akcay, G., Baykal, O. 2007. Conjunctival flora in patients with Type 1 and Type 2 diabetes mellitus. Advance in Therapy **24**, 1028 – 1035.

Bjornstedt, M., Kumar, S. Holmgren, A. 1992. Selenoglutathione is a highly efficient oxidant of reduced thioredoxin and a substrate for mammalian thioredoxin reductase. Journal of Biological Chemistry **267**, 8030-8034.

Bocchini, C.E., Hulten, K.G., Mason Jr, E.O., Gonzalez, B.E., Hammerman, W.A. and Kaplan, S.L. 2006. Panton-Valentine leukocidin genes are associated with enhanced inflammatory response and local disease in acute hematogenous *Staphylococcus aureus* osteomyelitis in children. Pediatrics **117**, 433 – 440.

Blevins, J.S., Gillaspy, A.F., Rechtin, T.M., Hurlburt, B.K. and Smeltzer, M.S. 1999. The staphylococcal accessory regulator (sar) represses transcription of the *Staphylococcus aureus* collagen adhesin gene *(cna)* in an *agr*-independent manner. Molecular Microbiology **33**, 317 – 326.

Borghese, R., Borsetti, F., Foladori, P., Ziglio, G., and Zannoni, D. 2004. Effects of the metalloid oxyanion tellurite (TeO_3^{2-}) on growth characteristics of the phototrophic bacterium *Rhodobacter capsulatus*. Applied Environmental Microbiol. **70**, 6595-6602.

Borsetti, F., Borghese, R., Francia, F., Randi, M.R., Fedi, S., and Zannoni. 2003. Reduction of potassium tellurite to elemental tellurium effect on the plasma membrane redox components of the facultative phototroph *Rhodobacter capsulatus*. Protoplasma **221**, 153 -161.

Borup, B., and Ferry, J.G. 2000. O-acetylserine sulfhydrylase from *Methanosarcina thermophila*. Journal of Bacteriology **182**, 45 -50.

Bourbouloux, A., Shahi, P., Chakladar, A., Delrot, S., Bachhawat, A.K. 2000. Hgt1p, a high affinity glutathione transporter from the yeast *Saccharomyces cerevisiae*. Journal of Biological Chemistry **275**,13259 -13265.

Brenot, A., King, K.Y., Janowiak, B., Griffith, O.,and Caparon, M.G. 2004. Contribution of glutathione peroxidase to the virulence of *Streptococcus pyogenes*. Infection and Immunity **72**, 408 - 413.

Bsat, N., Chen, L., and Helmann, J.D. 1996. Mutation of the Bacillus subtilis alkyl hydroperoxide reductase (ahpCF) operon reveals compensatory interactions among hydrogen peroxide stress genes. Journal of Bacteriology **178**, 6579 – 6586.

Calderon, I.L., Arenas, F.A., Perez, J.M., Fuentes, D.E., Araya, M.A., Saavedra, C.P., Tantalean, J.C., Pichuantes, S.E., Youderian, P.A., Vasquez, C.C. 2006. Catalase are NAD(P)H-dependent tellurite reductases. PloS ONE **70**, 1-8.

Camilli, A., Portnoy, D.A., Youngman, P. 1990. Insertional mutagenesis of Listeria monocytogenes with a novel Tn*917* derivative that allows direct cloning of DNA flanking transposon insertions. Journal of Bacteriology **172**, 3738 – 3744.

Cespedes, C., Miller, M., Quagliarello, B., Vavagiakis, P., Klein, R.S., and Lowy, F.D. 2002. Differences between *Staphylococcus aureus* isolates from medical and nonmedical hospital personnel. Journal of Clinical Microbiology **40**, 2594-2597.

Chambers, H.F. 2001. The changing epidemiology of *Staphylococcus aureus*? CDC Emerging Infectious Diseases **7**, 1 – 10.

Chan, P.F., and Foster, S.J.1998a. Role of SarA in virulence determinant production and environmental signal transduction in *Staphylococcus aureus*. Journal of Bacteriology **180**, 6232-6241.

Chan, P.F., and Foster, S.J.1998b. The role of environmental factors in the regulation of virulence-determinant expression in *Staphylococcus aureus* 8325-4. Microbiology **144**, 2469-2479.

Chan, P.F., Foster, S.J., Ingham, E. and Clements, M.O. 1998c. The *Staphylococcus aureus* alternative sigma factor σB controls the environment stress response but not starvation survival or pathogenecity in a mouse abscess model. Journal of Bacteriology **180**, 6082-6089.

Chau, M., and Nelson, J.W. Direct measurement of the equilibrium between glutathione and dithiothreitol by high performance liquid chromatography. FEBS Letters **291**, 296-298.

Cheng, H.M., Aronson, A.I. and Holt, S.C. 1973. Role of glutathione in the morphogenesis of the bacterial spore coat. Journal of Bacteriology **113**, 1134 – 1143.

Chesney, J.A., Eaton, J.W. and Mahoney, J.R. 1996. Bacterial glutathione: a sacrificial defense against chlorine compounds. Journal of Bacteriology **178**, 2131-2135.

Cheung, A.L., and Projan, S.J. 1994. Cloning and sequencing of *sarA* of *Staphylococcus aureus*, a gene required for the expression of *agr*. Journal of Bacteriology **176**, 4168 – 4172.

Cheung, A.L., Chien, Y., and Bayer, A.S. 1999. Hyperproduction of alpha-hemolysin in a *sigB* mutant is associated with elevated SarA expression in *Staphylococcus aureus*. Infection and Immunity **67**, 1331 - 1337.

Cheung, A.L., Bayer, A.S., Zhang, G., Gresham, H. and Xiong, Y. 2004. Regulation of virulence determinants *in vitro* and *in vivo* in *Staphylococcus aureus*. FEMS Immunology and Medical Microbiology **40**, 1-9.

Chien, Y., Manna, A.C., and Cheung, A.L. 1998. SarA level is a determinant of *agr* activation in *Staphylococcus aureus* binds to a conserved motif essential for *sar*-dependent gene regulation. The Journal of Biological Chemistry **272**, 37169 – 37176.

Chien, Y., Manna, A.C., Projan, S.J., and Cheung, A.L. 1999. SarA, a global regulator of virulence determinants in *Staphylococcus aureus*, binds to a conserved motif essential for *sar*-dependent gene regulation. The Journal of Biological Chemistry **272**, 37169 – 37176.

Chiong, M., Gonzalez, E., Barra, R., and Vasquez, C. 1988. Purification and biochemical characterization of tellurite-reducing activities from *Thermus thermophilus* HB8. Journal of Bacteriology **170**, 3269-3273.

Chu, L., Xu, Xiaoping, X., Dong, Z., Capelli, D., and Ebersole, J.L.2003. Role of recombinant γ-glutamyltransferase from *Treponema denticola* in glutathione metabolism. Infection and Immunity **71**, 335-342.

Chuard, C., Lucet, J.C., Rohner, P., Herrmann, M., Auckenthaler, R., Waldvogel, F.A., and Lew, D.P. 1991. Resistance of *Staphylococcus aureus* recovered from infected foreign body *in vivo* to killing by antimicrobials. J Infect Dis. **163**, 1369 – 1373.

Cinel, I. and Dellinger, R.P. 2006. Current treatment of severe sepsis. Current Infectious Disease Report **8**, 1523-1529.

Clarke, S.R., Mohamed, R., Bian, L., Routh, A.F., Kokai-kun, J.F., Mond, J.J., Tarkowski, A., and Foster, S.J. 2007. The *Staphylococcus aureus* surface protein IsdA mediates resistance to innate defenses of human skin. Cell Host & Microbe **1**, 199-212.

Clarke, S.R., Brummell, K.J., Horsburgh, M.J., McDowell, P.W., Mohamed, S.A., Stapleton, M.R., Acevedo, J., Read, R.C., Day, N.P., Peacock, S.J., Mond, J.J., Kokai-kun, J.F.,and Foster, S.J. 2006. Identification of in vivo expressed antigens of *Staphylococcus aureus* and their use in vaccinations for protection against nasal carriage. J. Infect. Dis. **193**, 1098-1108.

255

Clarke, S.R., Wiltshire, M.D. and Foster S.J. 2004. IsdA of *Staphylococcus aureus* is a broad spectrum iron-regulated adhesin. Microbiol **51**, 1509 – 1519.

Clauditz, A., Resch, A., Wieland, K., Peschel, A., and Gotz, F. 2006. Staphyloxanthin plays a role in the fitness of *Staphylococcus aureus* and its ability to cope with oxidative stress. Infection and Immunity **74**, 4950 – 4953.

Clements, M.O., and Foster, S.J. 1998. Starvation recovery of *Staphylococcus aureus* 8325-4. Microbiology **144**, 1755 - 1763.

Clements, M.O., and Foster, S.J. 1999. Stress resistance in *Staphylococcus aureus* . Trends in Microbiology **7**, 458-462.

Clements, M.O., Watson, S.P., and Foster, S.J. 1999. Characterization of the major superoxide dismutase of *Staphylococcus aureus* and its role in starvation survival, stress resistance, and pathogenecity. Journal of Bacteriology **181**, 3898 – 3903.

Clyne, M., de Azavedo, J., Carlson, E., and Arbuthnott, J. 1988. Production of Gamma-hemolysin and lack of production of alpha-hemolysin by *Staphylococcus aureus* strains associated with toxic shock syndrome. Journal of Clinical Microbiology **26**, 535-539.

Collins, L.V., Kristian, S.A., Weidenmaier, C., Faigle, M., van Kessel, K.P.M., van Strijp, J.A.G., Gotz, F., Neumeister, B., and Peschel, A. 2002. *Staphylococcus aureus* strains lacking D-alanine modifications of teichoic acids are highly susceptible to human neutrophil killing and are virulence attenuated in mice. The Journal of Infectious Diseases **186**, 214-219.

Corrigan, R.M., Rigby, D., Handley, P., and Foster, T.J. 2007. The role of *Staphylococcus aureus* surface protein SasG in adherence and biofilm formation. Microbiology **153**, 2435-2446.

Cosgrove, K., Coutts, G, Jonsson, I.,Tarkowski, A., Kokai-Kun, J., Mond, J.J., and Foster, S.J. 2007. Catalase (KatA) and alkyl hydroperoxide reductase (AhpC) have compensatory roles in peroxide stress resistance and are required for survival, persistence, and nasal colonization in *Staphylococcus aureus*. Journal of Bacteriology **189**, 1025-1035.

Coulter, S.N., Schwan, W.R., Ng, E.Y. W., Langhorne, M.H., Ritchie, H.D., Westbrock-Wadman, S., Hufnagle, W.O., Folger, K.R., Bayer, A.S., and Stover, C.K. 1998. *Staphylococcus aureus* genetic loci impacting growth and survival in multiple infection environments. Molecular Microbiology **30**, 393 – 404.

256

Curran, J.P. and Al-Salihi, F.L. 1980. Neonatal staphylococcal scalded skin syndrome: Massive outbreak due to an unusual phage type. Pediatrics **66**, 285 – 290.

Dancer, S.J., Garratt, R., Saidanha, J., Jhoti, H., and Evans, R. 1990. The epidermolytic toxins are serine proteases. FEBS Letters **268**, 129 – 132.

delCardayre, S.B. and Davies, J.E. 1998. *Staphylococcus aureus* Coenzyme A disulfide reductase, a new subfamily of pyridine nucleotide-disulfide oxidoreductase – Sequence, expression and analysis of cdr. Journal of Biological Chemistry **10**, 5752-5757.

delCardayre, S.B., Stock, K.P., Newton, G.L., Fahey, R.C., and Davies, J.E. 1998. Coenzyme A Disulfide Reductase, the Primary Low Molecular Weight Disulfide Reductase from *Staphylococcus aureus* -Purification and Characterization of the Native Enzyme. Journal of Biological Chemistry **273**, 5744-5751.

DeNap, J.C.B., Thomas, J.R. Musk, D.J. and Hergenrother. 2004. Combating drug-resistant bacteria: small molecule mimics of plasmid incompatibility as antiplasmid compounds. J. Am. Chem. Soc. **126**, 15402 – 15404.

Deora, R., Tseng, T., and Misra, T.K. 1997. Alternative transcription factor σ^{SB} of *Staphylococcus aureus*: characterization and role in transcription of the global regulatory locus *sar*. Journal of Bacteriology **179**, 6355 – 6359.

Di Tomaso, G., Fedi, S., Carnevali, M., Manegatti, M., Taddei, C., Zannoni, D. 2002. The membrane bound respiratory chain of *Pseudomonas pseudoalcaligenes* KF707 cell grown in the presence or absence of potassium telluritre. Microbiology **148**, 1699 – 1708.

Dickinson, D.A., and Forman, H.J. 2002. Cellular glutathione and thiols metabolism. Biochemical Pharmacology 64, 1019-1026.

Dickinson, D.A., and Forman, H.J. 2002. Glutathione in defense and signaling. Lessons from a small thiol. Annals of the New York Academy of Sciences **973**, 488-504.

Dossett., J.H., Kronvall, G., Williams Jr, R.C., and Quie, P.G. 1969. Antiphagocytic effects of staphylococcal Protein A. Journal of Immunology **103**, 1405 – 1410.

Dringen, R., Hamprecht, B., Broer, S. 1998. The peptide transporter PepT2 mediated the uptake of the glutathione precursor CysGly in astroglia-rich primary cultures. Journal of Neurochemistry **71**, 388-393.

Dunman, P.M., Murphy, E., Haney, S., Palacios, D., Tucker-Kellogg, G., Wu, S., Brown, E.L., Zagursky, R.J., Shlaes, D., and Projan, S.J. 2001. Transcription profiling-based identification od Staphylococcus aureus genes regulated by the *agr* and/or *sarA* loci. Journal of Bacteriology **183**, 7341-7353.

Dyllick-Brenzinger, M., Liu, M., Winstone, T.L., Taylor, D.E., and Turner, R. 2000. The role of cysteine residues in tellurite resistance mediated by the TehAB determinant. Biochemical and Biophysical Research Communications **277**, 394-400.

Fahey, R.C., Brown, W.C., Adams, W.B., Worsham, M.B. 1978. Occurrence of glutathione in bacteria. Journal of Bacteriology **133**, 1126-1129.

Farr, S.B., and Kogoma, T. 1991. Oxidative stress responses in *Escherichia coli* and *Salmonella typhimurium*. Microbiological reviews **55**, 561 – 585.

Fihman, V., Hannouche, D., Bousson, V., Bardin, T., Liote, F., Raskine, L., Riahi, J., Sanson-Le Pors, M.J., and Bercot, B. 2007. Improved diagnosis specificity in bone and joint infections using molecular techniques. Journal of Infection **55**, 510 – 517.

Fomenko, D.E., and Gladyshev, V.N. 2002. CXXS: Fold-independent redox motif revealed by genome-wide searches for thiol/disulfide oxidoreductase function. Protein Science **11**, 2285-2296.

Fomenko, D.E., and Gladyshev, V.N. 2003. Identity and Functions of CXXC-Derived Motifs. Biochemistry **42**, 11214-11225.

Forsgren, A. 1970. Significnace of Protein A production by *Staphylococci*. Infection and Immunity **2**, 672 – 673.

Foster, T.J., 2005. Immune evasion by staphylococci. Nature Reviews Microbiology **3**, 948 – 958.

Foster, T.J., and Hook, M., 1998. Surface protein adhesins of *Staphylococcus aureus*. Trends in Microbiology **6**, 484 – 488.

Foucaud, C., Kunji, E.R.S., Hagting, A., Richard, J., Konings, W.N., Desmazeaud, M., Poolman, B. 1995. Specificity of peptide transport systems in *Lactococcus lactis*: evidence for a third system which transports hydrophobic di- and tripeptides. Journal of Bacteriology **177**, 4652-4657.

Fournier, B., Klier, A., and Rapoport, G. 2001. The two component ArlS – ArlR is a regulator of virulence gene expression in *Staphylococcus aureus*. Mol. Microbiol **41**, 247 – 261.

Fournier, B., and Hooper, D.C. 2000. A new two-component regulatory system involved in adhesion, autolysis, and extracellular proteolytic activity of *Staphylococcus aureus*. Journal of Bacteriology **182**, 3955-3964.

Fowler, V.G. Jr., Boucher, H.W., Corey, G.R., Abrutyn, E., Karchmer, A.W., Rupp, M.E., Levine, D.P., Chambers, H.F., Tally, F.P., Vigliani, G.A., Cabell, C.H., Link, A.S., DeMeyer, I., Filler, S.G., Zervos, M., Cook, P.,Parsonnet, J., Berstein, J.M., Price, C.S., Forrest, G.N., Fatkenhaeuer, G., Gareca, M., Rehm, ,S.J., Brodt, H.R., Tice, A., Cosgrove, S.E. 2006. Daptomycin vs standard therapy for bacteremia and endocarditis caused by *Staphylococcus aureus*. New England Journal of Medicine **355**, 653-665.

Fuchs, J.A., Warner, H.R. (1975). Isolation of an *Escherichia coli* mutant deficient in glutathione synthesis. Journal of Bacteriology **124**, 140-148.

Fukushima, H., Hoshina, K., and Gomyoda, M. 2000. Selective isolation of *eae*-positive strains of Shiga toxin-producing *Escherichia coli*. Journal of Clinical Microbiology **38**, 1684-1687.

Gemmell, C.G. 1995. Staphylococcal scalded skin syndrome. J. Med Microbiol **43**, 318 – 327.

Gertz, S., Engelmann, S., Schmid, R., Ziebandt, A., Tischer, K., Scharf, C., Hacker, J., and Hecker, M. 2000. Characterization of the σ^B regulon in *Staphylococcus aureus*. Journal of Bacteriology **182**, 6983-6991.

Gharieb, M.M., Gadd, G.M. 2004. Role of glutathione in detoxification of metal(loid)s by *Saccharomyces cerevisiae*. Biometals **17**, 183-188.

Giachino, P., Engelmann, S., and Bischoff, M. 2001. σ^B activity depends on RsbU in *Staphylococcus aureus*. Journal of Bacteriology **183**, 1843-1852.

Giraudo, A.T., Cheung, A.L. and Nagel, R. 1997. The sae locus of *Staphylococcus aureus* controls exoprotein synthesis at the transcriptional level. Arch Microbiol **168**, 53 – 58.

Glauert, A.M. 1974. The high voltage electron microscope in biology. *Journal of Cell Biology* **63**, 717-748.

Goh, S.H., Potter, S., Wood, J.O., Hemmingsen, S.M., Reynolds, R.P. and Chow, A.W. 1996. HSP60 Gene sequences as universal targets for microbial species identification: studies with coagulase-negative staphylococci. Jourmnal of Clinical Microbiology **34**, 818 – 823.

Goossens, H. 2005. European status of resistance in nosocomial infections. International Journal of Experimental and Clinical Chemotherapy **51**, 177 – 181.

Gotz, F. 2004.Staphylococci in colonization and disease: prospective targets for drugs and vaccine. Current Opinion in Microbiology **7**, 477-487.

Grant, C.M., MacIver, F.H., and Dawes, I.W. 1996. Glutathione is an essential metabolite required for resistance to oxidative stress in the yeast *Saccharomyces cerevisiae*. Current Genetic **29**, 511 – 515.

Green, R.M., Seth, A., Connell, N.D. 2000. A peptide permease mutant of Mycobacterium bovis BCG resistant to the toxic pepides glutathione and S-nitrosoglutathione. Infection and Immunity **68**, 429-436.

Greenberg, D.P., Bayer, A.S., Turner, D., and Ward, J.I. 1990. Santibody response to Protein A in patients with *Staphylococcus aureus* bacteremia and endocarditis. Journal of Clinical Microbiology **28**, 458 – 462.

Greenberg, J.T., Demple, B. 1986. Glutathione in *Escherichia coli* is dispensable for resistance to H_2O_2 and gamma radiation. Journal of Bacteriology **168**, 1026-1029.

Gregory, R., Saunders, J.R., and Saunders, V.A. 2007. Rule based modeling of conjugative plasmid transfer and incompatibility. Biosystems **(2007)**, doi: 10.1016/j.biosystems.2007.09.003

Gresham, H.D., Lowrance, J.H., Caver, T.E., Wilson, B.S., Cheung, A.L., and Lindberg, F.P. 2000. Survival of *Staphylococcus aureus* inside neutrophils contributes to infection. Journal of Immunology **164**, 3713- 3722.

Guyer, C.L., Morgan, D.G. and Staros, J.V. 1986. Binding specificity of the periplasmic oligopeptide-binding protein from *Escherichia coli*. Journal of Bacteriology **168**, 775 – 779.

Hagting, A., Kunji, E.R.S., Leenhouts, K.J., Poolman, B., Koning, W.N. 1994. The di- and tripeptide transport protein of *Lactococcus lactis*. A new type of bacterial peptide transporter. Journal of Biological Chemistry **269**, 11391-11399.

Hanigan, M.H., Ricketts, W.A. 1993. Extracellular glutathione is a source of cysteine for cells that express γ-glutamyl transpeptidase. Biochemistry **32**, 6302-6306.

Hanson, A.D., Gage, D.A. and Shachar-Hill, Y. 2000. Plant one-carbon metabolism and its engineering. Trends in Plant Science **5**, 206 – 213.

Hayat, M.A. 1981. *Fixation for electron microscopy*. New York: Academic Press.

Hassan, H.M., and Fridovich, I. 1979. Paraquat and *Escherichia coli*. Mechanism of production of extracellular superoxide radical. The Journal of Biological Chemistry **254**, 10846 – 10852.

Heinrichs, J.H., Bayer, M.G., and Cheung, A.L. 1996. Characterization of the *sar* locus and its interaction with *agr* in *Staphylococcus aureus*. Journal of Bacteriology 178, 418 – 423.

Hibberd, K.A., Berget, P.B., Warner, H.R. and Fuchs, J.A. 1978. Role of glutathione in reversing the deleterious effects of a thiol-oxidizing agent in *Escherichia coli*. Journal of Bacteriology **133**, 1150-1155

Higgins, C.F.1992. ABC transporters: From microorganisms to man. Annu. Rev. Cell. Biol **8**, 67-113.

Hiramatsu, K., Hanaki, H., Ino, T., Yabuta, K., Oguri, T., and Tenover, F.C. 1997. Methicillin-resistant *Staphylococcus aureus* clinical strain with reduced vancomycin susceptibility. Journal Antimicrob Chemother **40**, 135 – 136.

Holmgren, A.1968. Thioredoxin. 6. The amino acid sequence of the protein from *Escherichia coli* B. European J. Biochem **6**, 475-484.

Horsburgh, M.J., Wiltshire, M.D., Crossley, H., Ingham, E., and Foster, S.J. 2004. PheP, a putative amino acid permease of *Staphylococcus aureus* contributes to survival *in vivo* and during starvation. Infection and Immunity **72**, 3073 - 3076.

Horsburgh, M.J., Wharton, S.J., Cox, A.G., Ingham, E., Peacock, S. and Foster, S.J. 2002. MnTR modulates expression of the PerR regulon and superoxide resistance in *Staphylococcus aureus* through control of manganese uptake. Molecular Microbiology **44**, 1269 – 1286.

Horsburgh, M.J., Aish, J., White, I., Shaw, L., Lithgow, J. and Foster, S.J. 2002. SigmaB modulates virulence determinant expression and stress resistance: characterization of a functional *rsbU* strain derived from *Staphylococcus aureus* 8325-4. Journal of Bacteriology **184**, 5457-5467.

Horsburgh, M.J., Clements, M.O., Crossley, H., Ingham, E., and Foster, S.J. 2001. PerR controls oxidative stress resistance and iron storage proteins and is required for virulence in *Staphylococcus aureus*. Molecular Microbiology **44**, 1269 – 1286.

Hryniewicz, M., Sirko, A., Palucha, A., Bock, A., and Hulanicka, D. 1990. Sulfate and thiosulphate transport in *Escherichia coli* K-12: Identification of a gene encoding a novel protein involved in thiosulphate binding. Journal of Bacteriology **172**, 3358-3366.

Hurd, T.R., Filipovska, A., Costa, N.J. Dahm, C.C. and Murphy, M.P. 2005. Disulphide formation on mitochondrial protein thiols. Biochem. Soc. Trans. 33, 1390-1393.

Ikeda, Y., Taniguchi, N. 2005. Gene expression of γ-glutamyltranspeptidase. Methods Enzymology **401**, 408-425.

Izawa, S., Inoue, Y., and Kimura, A. 1996. Importance of catalase in the adaptive response to hydrogen peroxide: analysis of acatalasaemic *Saccahromyces cerevisiae*. Biochemical Pharmacology **55**, 1747 – 1758.

Jarraud, S., Peyrat, M.A., Lim, A.,Tristan, A., Bes, M., Mougel, C., Etienne, J., Vandenesch, F., Bonneville, M., and Lina, G. 2001. *egc*, A highly purified operon of enterotoxin gene, forms a putative nursery of superantigens in *Staphylococcus aureus*. The Journal of Immunology **166**, 669 – 677.

Ji, G., Beavis, R., and Novick, R.P. 1997. Bacterial interference caused by autoinducing peptide variants. Science **276**, 2027 – 2030.

Johnson, L.B., and Saravolatz, L.D. 2005. Community-acquired MRSA: Current Epidemioligy and Management Issues. Infect Med **22**, 16-20.

Jonas, D., Walev, I., Berger, T., Liebetrau, M., Palmer, M., and Bhakdi, S. 1994. Novel path to apoptosis: small transmembrane pores created by Staphylococcal alpha-toxin in T lymphocytes evoke internucleosomal DNA degradation. Infection and Immunity **62**, 1304 – 1312.

Kapral, F.A., Smith, S., and Lal, D. 1992. The esterification of fatty acids by *Staphylococcus aureus* fatty acid modifying enzyme (FAME) and its inhibition by glycerides. J Med Microbiol **37**, 235 – 237.

Karavalos, M.H., Horsburgh, M.J., Ingham, E., and Foster, S.J. 2003. Role and regulation of the superoxide dismutases of *Staphylococcus aureus*. Microbiology **149**, 2749-2758.

Karlsson, A., Saravia-Otten, P., Tegmark, K., Morfeldt, E., and Arvidson, S. 2001. Decreased amount of cell-wall associated Protein A and fibronectin-binding proteins in *Staphylococcus aureus sarA* mutants due to up-regulation of extracellular proteases. Infection and Immunity **69**, 4742 – 4748.

Kern, R., Malki, A., Holmgren, A., Richarme, G. 2003. Chaperone properties of *Escherichia coli* thioredoxin and thioredoxin reductase. Biochem J. **371**, 965 – 972.

Kitabatake, M., So, M.W. Tumbula, D.L., and Soll, D. 2000. Cysteine biosynthesis pathway in the archeon *Methanosarcina barkeri* encoded by acquired bacterial genes? Journal of Bacteriology **182**, 143 – 145.

Kloos, W.E., and Schleifer, K.H. 1975. Simplified scheme for routine identification of human *Staphylococcus* species. Journal of Clinical Microbiology **1**, 82 – 88.

Kloos, W.E., and Wolfshohl, J.F. 1982. Identification of *Staphylococcus* species with the API STAPH-IDENT system. Journal of Clinical Microbiology **16**, 509 - 516.

Kosower, N.S., Kosower, E.M., Wertheim, B. 1969. Diamide, a new reagent for the intracellular oxidation of glutathione to the disulfide. Biochemical and Biophysical Research Communications 37, 593-596.

Kren, B., Parsell, D. Fuchs, J.A. 1988. Isolation and characterization of an *Escherichia coli* K-12 mutant deficient in glutaredoxin. Journal of Bacteriology **170**, 308-315.

Kravitz G.R., Dries, D.J., Peterson,M.L., and Schlievert,P.M. 2005. Bacterial infections and antibiotic resistance. Clin. Infect. Dis. **40**, 941 – 947.

Kreiswirth, B.N., Lofdahl, S., Betley, M.J., O'Reilly, M., and Schlievert, P.M. 1983. The toxic shock syndrome exotoxin structural gene is not detectably transmitted by a prophage. Nature **305**, 709 – 712.

Kumagai, H., Suzuki, H, Shimizu, M., Tochikura, T. 1989. Utilization of the γ-glutamyltranspeptidase reaction for glutathione synthesis. Journal of Biotechnology **9**, 129-138.

Kumaresan, K.R., Springhorn, S.S., Lacks, S.A. 1995. Lethal and mutagenic actions of N-methyl-N'-Nitro-N-Nitrosoguanidine potentiated by oxidized glutathione, a seemingly harmless substance in the cellular environment. Journal of Bacteriology **177**, 3641-3646.

Kwok, A.Y.C., Su, S., Reynolds, R.P., Bay, S.J., Av-Gay, Y., Dovichi, N.J. and Chow, A.W. 1999. Species identification and phylogenetic relationships based on partial HSP60 gene sequences within the genus *Staphylococcus*. **49**, 1181-1192.

Kwok, A.Y.C., and Chow, A.W. 2003. Phylogenetic study of *Staphylococcus* and *Macrococcus* species based on partial *hsp60* gene sequences. International Journal of Systematic and Evolutionary Microbiology **53**, 87-92.

Labandeira-Rey, M., Couzon, F., Boisset, S., Brown, E.L., Bes, M., Benito, Y., Barbu, E.M., Vazquez, V., Hook, M., Etienne, J., Vandenesh, F., and Bowden, G. 2007. *Staphylococcus aureus* Panton-Valentine leukocidin causes necrotizing pneumonia. Science **315**, 1130-1133.

Latinwo, L.M., Donald, C., Ikebiobi, C., and Silver, S.1998. Effects of intracellular glutathione on sensitivity of *Escherichia coli* to mercury and arsenite. Biochemical and Biophysical Research Communications **242**, 67-70.

Lee, J.C. 1998. An experimental vaccine that targets staphylococcal virulence. Trends in Microbiology **6**, 461 – 463.

Leichert, L.I.O., Scharf, C., and Hecker, M. 2003. Global characterization of disulfide stress in *Bacillus subtilis*. Journal of Bacteriology **185**, 1967 – 1975.

Lennon, B.W., Williams Jr., C.H. and Ludwig, M.L. 2000. Twist in catalysis: Alternating conformations of *Escherichia coli* thioredoxin reductase. Science **289**, 1190 – 1194.

Li, R., Moore, M., and King, J. 2003. Investigating the regulation of one-carbon metabolism in *Arabidopsis thaliana*. Plant and Cell Physiology 2003 **44**, 233 – 241.

Li, Y., Hugenholtz, J., Abee, T., and Molenaar, D. 2003. Glutathione protects *Lactococcus lactis* against oxidative stress. Applied and Enviromental Microbiology **69**, 5739-5745.

Lim, S.M., and Webb, S.A.R. 2005. Nosocomial bacterial infections in intensive care units. I: Organisms and mechanisms of antibiotic resistance. Anaesthesia **60**, 887 – 902.

Liochev, S.I., and Fridovich, I.1991. Effects of overproduction of superoxide dismutase on the toxicity of paraquat toward *Escherichia coli*. The Journal of Biological Chemistry **266**, 8747-8750.

Lithgow, J.K., Hayhurst, E.J., Cohen, G., Aharonowitz, Y., and Foster, S.J. 2004. Role of cysteine synthase in *Staphylococcus aureus*. Journal of Bacteriology **186**, 1-12.

Liang, X., Zheng, L., Landwehr, C., Lunsford, D., Holmes, D., and Ji, Y. 2005. Global regulation of gene expression by ArlRS, a two-component signal

transduction regulatory sytem of *Staphylococcus aureus*. Journal of Bacteriology **187**, 5486-5492.

Liu, G.Y. Essex,A., Buchanan, J.T., Datta, V., Hoffman, H.M., Bastian, J.F. Fierer, J., and Nizet, V. 2005. *Staphylococcus aureus* golden pigment impairs neutrophil killing and promotes virulence through its antioxidant activity. Journal of Experimental Medicine **202**, 209-215.

Lowy, F.D. *Staphylococcus aureus* infections. 1998. The New England Journal of Medicine 339, 520-532.

Lu, P., Tsai, J., Chiu, Y., Chang, F., Chen, Y., Hsiao, C. and Siu, L.K. 2007. Methicillin-resistant *Staphylococcus aureus* carriage, infection and transmission in dialysis patients, healthcare workers and their family members. Nephrol Dial Transplant **0**, 1-7.

Mack, D., Riedewald, J., Rohde, H., Magnus, T., Feucht, H.H., Elsner, H.A., Laufs, R., and Rupp, M.E. 1999. Essential functional role of the polysaccharide intercellular adhesin of *Staphylococcus epidermidis* in hemagglutination. Infection and Immunity **67**, 1004 – 1008.

Mack, D., Becker, P., Chatterjee, I., Dobinsky, S., Knobloch, J.K., Peters, G., Rohde, H., and Herrmann, M. 2004. Mechanisms of biofilm formation in *Staphylococcus epidermidis* and *Staphylococcus aureus*: functional molecules, regulatory circuits, and adaptive responses. Int J Med Microbiol **294**, 203 – 212.

Makris, G., Wright, J.D., Ingham, E., and Holland, K.T. 2004. The hyaluronate lyase of *Staphylococcus aureus* – a virulence factor? Microbiology **150**, 2005 – 2013.

Manna, A.C., and Cheung, A.L. 1998. *sarU*, a *sarA* homolog, is repressed by SarT and regulates virulence genes in *Staphylococcus aureus*. Infection and Immunity **71**, 343 – 353.

Mattsson, E., Heying, R., van de Gevel, J.S., Hartung, T., and Beekhuizen, H. 2007. Staphylococcal peptidoglycan initiates an inflammatory response and procoagulant activity in human vascular endothelial cells: a comparison with highly purified lipoteichoic acid and TSST-1 FEMS Immunol Med Microbiol (PMID 18031538)

McAleese, F., Walsh, E.J., Sieprawski, M., Potempa, J., and Foster, T.J. 2001. Loss of clumping factor B fibrinogen binding activity by *Staphylococcus aureus* involves cessation of transcription, shedding and cleavage by metalloprotease. Journal of Biological Chemistry **276**, 29969 – 29978.

McDevitt, D., Francois, P., Vaudaux, P., and Foster, T.J. 1994. Molecular characterization of the clumping factor (fibrinogen receptor) of *Staphylococcus aureus*. Mol, Microbiol **11**, 237 – 248.

Mehrotra, M., Wang, G., and Johnson, W.M. 2000. Multiplex PCR for detection of genes for Staphylococcus aaureus enterotoxins, exfoliative toxins, toxic shock syndrome toxin 1 and methicillin resistance. Journal of Clinical Microbiology **38**, 1032 – 1035.

Mei, J., Nourbakhsh, F., Ford, C.W., and Holden, D.W. 1997. Identification of *Staphylococcus aureus* virulence genes in a murine model of bacteremia using signature-tagged mutagenesis. Molecular Microbiology **26**, 399 – 407.

Meister, A., Anderson, M.E.1983. Glutathione. Annu. Rev. Biochemistry **52**, 711- 760.

Mertz, P.M. Cardenas, T.C., Snyder, R.V., Kinney, M.A., Davis, S.C.,and Piano, L.R. 2007. *Staphylococcus aureus* virulence factors associated with infected skin lesions: influence on the local immune response. Arch. Dermatol **143**, 1259 – 1263.

Menestrina, G., Serra, M.D., Comai, M.,Coraiola, M., Viero, G., Werner, S., Colin, D.A., Monteil, H., and Prevost, G. 2003. Ion channels and bacterial infection: the case of β-barrel pore-forming protein toxins of *Staphylococcus aureus*. FEBS Letters **552**, 54-60.

Messens, J.,Van Molle,Van Molle, I., Vanhaesebrouck, P., Limbourg, M., Van Belle, K., Wahni, K., Martins, J.C., Loris, R., and Wyns, L. How thioredoxin can reduce a buried disulphide bond. 2004. Journal Mol. Biol **339**, 527-537.

Michelet, F., Gueguen, R., Leroy, P., Wellman, M., Nicolas, A., and Siest, G. 1995. Blood and plasma glutathione measured in healthy subjects by HPLC: Relation to sex, aging, biological variables, and life habits. Clin. Chem. **41**,1509-1517.

Miles, F., Voss, L., Segedin, E., and Anderson, B.J. 2005. Review of *Staphylococcus aureus* infections requiring admission to a paediatric intensive care unit. Arch Dis Child **90**, 1274 – 1278.

Minami, H., Suzuki, H.,Kumagai, H. 2004. γ-glutamyltranspeptidase, but not YwrD, is important in utilization of extracellular glutathione as a sulfur source in *Bacillus subtilis*. Journal of Bacteriology **186**, 1213-1214.

Minami, H., Suzuki, H., and Kumagai, H. 2003. Salt-tolerant γ-glutamyltranspeptidase from *Bacillus subtilis* 168 with glutaminase activity. Enzyme and Microbial Technology **32**, 431-438.

266

Minami, H., Suzuki, H., and Kumagai, H. 2003. A mutant *Bacillus subtilis* γ-glutamyltranspeptidase specialized in hydrolysis activity. FEMS Microbiology Letters **224**, 169-173.

Morfeldt, E., Tegmark, K., and Arvidson, S. 1996. Transcriptional control of the agr-dependent virulence gene regulator, RNAIII, in *Staphylococcus aureus*. Mol Microbiol 21, 1227 – 1237.

Mortensen, J.E., Shryock, T.R., and Kapral, F.A. 1992. Modification of bactericidal fatty acids by an enzyme of *Staphylococcus aureus*. J. Med Microbiol **36**, 293 – 298.

Moscoso, H., Saavedra, C., Loyola, C., Pichuantes, S., and Vasquez, C. 1998. Biochemical characterization of tellurite-reducing activities of *Bacillus stearothermophilus V*. Res. Microbiol **149**, 389-397.

Mujibur Rahaman, M., Golam Morshed, M., Sultanal Aziz, K.M., and Munshi, M.M.H. 1986. Improved medium for isolating Shigella. Lancet I, 271-272.

Muller, F., Svardal, A., Aukrust, P., Berge, R.K., Ueland, P.M., and Froland, S.S. 1996. Elevated plasma concentration of reduced homocysteine in patients with human immunodeficiency virus infection. Am. J. Clin. Nutr. **63**, 242-248.

Myolnakis, E., and Calderwood, S.B. 2001. Infective endocarditis in adults. New England Journal of Medicine **345**, 1318 – 1330.

Nakamura, T., Iwahashi, H., and Eguchi, Y.1984. Enzymatic Proof for the Identity of the S-sulfocysteine synthase and Cysteine Synthase B of *Salmonella typhimurium*. Journal of Bacteriology **158**, 1122-1127.

Nakata, K., Inoue, Y., Harada, J., Maeda, N., Watanabe, H., Tano, Y., Shimomura, Y., Harino, S., and Sawa, M. 2000. A high incidence of *Staphylococcus aureus* colonization in the external eyes of patients with atopic dermatitis.Ophthalmology **107**, 2167-2171.

Nakayama, R., Kumagai, H., Tochikura, T. (1984). γ-glutamyltranspeptidase from *Proteus mirabilis*: Localization and activation by phospholipids. Journal of Bacteriology **160**, 1031-1036.

Nakayama, R., Kumagai, H., Tochikura, T. (1984). Purification and properties of γ-glutamyltranspeptidase from *Proteus mirabilis*. Journal of Bacteriology. **160**, 341-346.

Nakayama, R., Kumagai, H., Tochikura, T. (1984). Leakage of glutathione from bacterial cells caused by inhibition of γ-glutamyltranspeptidase. Applied and Environmental Microbiology. **47**, 653-657.

Needham, A.J., Kilbart, M., Crossley, H., Ingham, P.W., and Foster, S.J. 2004. Drosophila melanogaster as a model host for Staphylococcus aureus infection. Microbiology **150**, 2347 - 2355.

Newton, G.L., Arnold, K., Price, M.S., Sherrill, C., Delcardayre, S.B., Aharonowitz, Y.,Cohen, G., Davies, J., Fahey, R.C., Davis, C. 1996. Distribution of thiols in microorganisms: Mycothiol is a major thiol in most actinomycetes. Journal of Bacteriology **178**, 1990-1995.

Newton, G.L., Javor, B. 1985. γ-glutamylcysteine and thiosulfate are the major low-molecular-weight thiols in halobacteria. Journal of Bacteriology **161**, 438-441.

Novick, R.P., Projan, S.J., Kornblum, J., Ross, H.F., Ji, G., Kreiswirth, B., Vandenesch, F., and Moghazeh, S. 1995. The agr P2 operon: an autocatalytic sensory transduction system in Staphylococcus aureus. Mol Gen Genet. **248**, 446 – 458.

Novick, R.P. 2003a. Autoinduction and signal transduction in the regulation of staphylococcal virulence. Molecular Microbiology **48**, 1429-1449.

Novick, R.P. and Jiang, D. 2003b. The staphylococcal saeRS system coordinates environmental signals with agr quorum sensing. Microbiology **149**, 2709-2717.

NiEdhin, D., Perkin, S., Francois, P., Vaudaux, P., Hook, M., and Foster, T.J. 1998. Clumping factor B (ClfB), a new surface-located fibrinogen-binding adhesin of Staphylococcus aureus. Mol. Microbiol **30**, 245 – 257.

Nilsson, I., Hartford, O., Foster, T., and Tarkowski, A. 1999. Alpha-toxin and gamma-toxin jointly promote Staphylococcus aureus virulence in murine septic arthritis. Infection and Immunity **67**, 1045-1049.

O'Brien, R.W., Weitzman, P.D.J., Morris, J.G. 1970. Oxidation of a variety of natural electron donors by the thiol-oxidising agent, diamide. FEBS Letters **10**, 343-345.

O'Callaghan, R.J., Callegan, M.C., Moreau, J.M., Green, L.C., Foster, T.J., Hartford, O.M., Engel, L.S., and Hill, J.M. 1997. Specific roles of alpha-toxin and beta-toxin during Staphylococcus aureus corneal infection. Infection and Immunity **65**, 1571-1578.

Ocana, M.G., Asensi, V., Montes, A.H., Meana, A., Celada, A., and Valle-Garay, E. 2007. Autoregulation mechanism of human neutrophil apoptosis during bacterial infection. Mol. Immunol. doi: 10.1016/j.molimm.2007.10.1013

O'Gara, J.P., Gomelsky, M., and Kaplan, S. 1997. Identification and molecular genetic analysis of multiple loci contributing to high-level tellurite resistance in Rhodobacter sphaeroides 2.4.1. Applied Environmental Microbiology 63, 4713-4720.

Oktyabsrsky, O.N., Smirnova, G.V., and Muzyka, N.G. 2001. Role of glutathione in regulation of Hydroperoxidase I in growing Escherichia coli. Free Radica Biology & Medicine 31, 250 – 255.

Owens, R.A., Hartman, P.E. (1986). Export of glutathione by some widely used Salmonella typhimurium and Escherichia coli strains. Journal of Bacteriology 168, 109 -114.

Palmqvist, N., Foster, T., Fitzgerald, J.R., Josefsson, E., and Tarkowski, A. 2005. Fibronectin-binding proteins and fibrinogen-binding clumping factors play distinct roles in staphylococcal arthritis and systemic inflammation. J. Infect. Dis. 191, 791 -798.

Pan, Y., Ding, D., Li, D., and Chen, S. 2007. Expression and bioactivity analysis of Staphylococcal enterotoxin M and N. Protein expression and purification 56, 286 – 292.

Pasternack, L.B. Littlepage, L.E., Laude Jr., D.A., and Appling, D.R. 1996. 13C NMR analysis of the use of alternative donors to the tetrahydrofolate-dependent one-carbon pools in Saccharomyces cerevisiae. Archives of Biochemistry 326, 158 – 165.

Patti, J.M., Bremmell, T., Krajewska-Pietrasik, D., Abdelnour, D., Tarkowski, A., Ryden, C., and Hook, M. 1994. The Staphylococcus aureus collagen adhesion is a virulence determinant in experiment septic arthritis. Infect Immun 62, 152 – 161.

Pauwels, F., Vergauwen, B.,Vanrobaeys, F., Devreese, B., and Van Beeumen, J. J. 2003. Purification and characterization of a chimeric enzyme from Hemophilus influenzae Rd that exhibits glutathione-dependant peroxidase activity. Journal of Biological Chemistry 278, 16658-16666.

Pearion, C.T., and Jablonski, P.E. 1998. High level intrinsic resistance of Natronococcus occultus to potassium tellurite. FEMS Microbiology Letters 174,19-23.

Penninckx, M. 2000. A short review on the role of glutathione in the response of yeasts to nutritional, environmental, and oxidative stresses. Enzyme and Microbial Technology **26**, 737-742.

Penninckx, M.J., and Elkskens, M.T. 1993. Metabolism and functions of glutathione in microorganisms. Adv. Microb. Physiol. **34**, 239 – 301.

Petersohn, A., Brigulla, M., Haas, S., Hoheisel, J.D., Volker, U., and Hecker, M. 2001. Global analysis of the general stress response of *Bacillus subtilis*. Journal of Bacteriology **183**, 5617 – 5631.

Pericone, C.D., Park, S., Imlay, J.A., and Weiser, J.N. 2003. Factors contributing to hydrogen peroxide resistance in *Streptococcus pneumoniae* include pyruvate oxidase (SpXB) and avoidance of the toxic effects of the Fenton Reaction. Journal of Bacteriology **185**, 6815-6825.

Peterson, P.K., Verhoef, J., Sabath, L.D., and Quie, P.G. 1977. Effect of Protein A on staphylococcal opsonization. Infection and Immunity **15**, 760 – 764.

Picon, A., Kunji, E.R., Lanfermeijer, F.C., Konings, W.N., Poolman, B. 2000. Specificity mutants of the binding protein of the oligopeptide transport system of *Lactococcus lactis*. Journal of Bacteriology **182**, 1600-1608.

Piechowicz, L., Garbacz, K., and Galinski, J. 2007. *Staphylococcus aureus* of phage type 187 isolated from people occurred to be a genes carrier of enterotoxin C and toxic shock syndrome toxin-1 (TSST-1). International Journal of Hygiene and Environmental Health, doi: 10.1016/j.ijheh.2007.06.010.

Poole, L.B., Godzik, A., Nayeem, A. Schmitt, J.D. 2000. AhpF can be dissected into two functional units: Tandem repeats of two thioredoxin-like folds in the N-terminus mediate electron transfer from the thioredoxin reductase-like C-terminus to AhpC. Biochemistry **39**, 6602-6615.

Poole, L.B., Reynolds, C.M., Wood, Z.A., Karplus, P.A., Ellis, H.R., Calzi, M.L. 2000. AhpF and other NADH:peroxiredoxin oxidoreductases homologues of low Mr thioredoxin reductase. Eur. J. Biochem **267**, 6126-6133.

Pragman, A.A., Schlievert, P.M. 2004. Virulence regulation in *Staphylococcus aureus*: the need for in vivo analysis of virulence factor regulation. FEMS Immunology and Medical Microbiology **42**, 147-154.

Prinz, W.A., Aslund, F., Holmgren, A., and Beckwith, J. 1997. The role of the thioredoxin and glutaredoxin pathways in reducing protein disulfide bonds in the *Escherichia coli* cytoplasm. Journal of Biological Chemistry **272**, 15661-15667.

Projan, S.J., Novick, R.P. 1997. The molecular basis of pathogenecity. P 55-81, *In* K. B. Crossley and G.L..Archer (ed.), The staphylococci in human disease. Churchill Livingstone, New York, N.Y.

Rabilloud, T., Heller, M., Gasnier, F., Luche, S., Rey, C., Aebersold, R., Benahmed, M., Louisot, P., and Lunardi, J. Proteomics analysis of cellular response to oxidative stress – Evidence for in vivo overoxidation of peroxiredoxins at their active site. The Journal of Biological Chemistry **277**, 19396-1940.

Prokesova, L., Potuznikova, B., Potempa, J., Zikan, J., Radi, J., Hachova, L., Baran, K., Porwit-Bobr, Z., and John, C. 1992. Cleavage of human immunoglobulins by serine protease from *Staphylococcus aureus*. Immunol Lett. **31**, 259 – 265.

Ramirez, A., Castaneda, M., Xiqui, M.L., Sosa, A., and Baca, B.E. 2006. Identification, cloning and characterization of *cysK*, the gene encoding O-acetylserine (thiol)-lyase from *Azospirillum brasilense*, which is involved in tellurite resistance. FEMS Microbiol Lett **261**, 272-279.

Reynolds, C.M., Meyer, J., Poole L.B. 2002. An NADH-dependent bacterial thioredoxin reductase-like protein in conjunction with a glutaredoxin homologue form a unique peroxiredoxin (AhpC) reducing system in *Clostridium pasteurianum*. Biochemistry **41**, 1990-2001.

Reynolds, C.M., Poole L.B. 2000. Attachment of the N-terminal domain of *Salmonella typhimurium* AhpF to *Escherichia coli* thioredoxin reductase confers AhpC reductase activity but does not affect thioredoxin reductase activity. Biochemistry **39**, 8859-8869.

Rice, K., Peralta, R., Bast, D., de Azavedo, J., and McGavin, M.J. 2001. Description of Staphylococcus serine protease (*ssp*) operon in *Staphylococcus aureus* and nonpolar inactivation of *ssp*-encoded serine protease. Infect. Immun **69**, 159 - 169

Rieber, E., Kosower, N.S.,and Jaffe, E.R. 1968. Reduced nicotinamide adenine dinucleotide and the reduction of oxidized glutathione in human erythrocytes. The Journal of Clinical Investigation **47**, 66-71.

Ritz, D., and Beckwith, J. 1999. Roles of thiol-redox pathways in bacteria. Annu. Rev. Microbiol **55**, 21 – 48.

Ritz, D.,Patel, D.,Doan,B., Zheng, M., Aslund, F., Storz, G., Beckwith, J. 1999. Thioredoxin 2 is involved in the oxidative stress response in *Escherichia coli*. Journal of Biological Chemistry **275**, 2505-2512.

Robards, A. and Wilson, A. (1999). *Procedures in electron microscopy*. John Wiley and Sons.

Rocha, E.R., Tzianaboss, A.O., and Smith C.J. 2007. Thioredoxin reductase is essential for thiol/disulphide redox control and oxidative stress survival of the anaerobe *Bacteroides fragilis*. Journal of Bacteriology **189**, 8015 – 8023.

Rocha. E.R., and Smith C.J. 1999. Role of alkyl hydroperoxide reductase (*ahpCF*) gene in oxidative stress defense of the obligate anaerobe *Bacteroides fragilis*. Journal of Bacteriology **181**, 5701-5710.

Roghmann, M., Taylor, K.L., Gupte, A., Zhan, M., Johnson, J.A., Cross, A., Edelman, R., and Fattom, A.I. 2005. Epidemiology of capsular and surface polysaccharide in *Staphylococcus aureus* infections complicated by bacteremia. Journal of Hospital Infection **59**, 27-32.

Rohde, H., Burdelski, C., Bartscht, K., Hussain, M., Buck, F., Horstkotte, M.A., Knobloch, J. K-M., Hellman, C., Herrmann, M., and Mack, D. 2005. Induction of *Staphylococcus epidermidis* biofilm formation via proteolytic processing of the accumulation-associated protein by staphylococcal and host proteases. Molecular Microbiology **55**, 1883 – 1895.

Roos, G., Garcia-Pino, A., Van belle, K., Brosens, E., Wahni, K., Vandenbussche, G., Wyns, L., Loris, R., and Messens, J. 2007. The conserved active site proline determines the reducing power of *Staphylococcus aureus* thioredoxin. J. Mol. Biol. **368**, 800 – 811.

Russell, M., and Model, P. 1986. The role of thioredoxin in filamentous phage assembly. Journal of Biological Chemistry **261**, 14997 – 15005.

Russell, M., Model, P. and Holmgren, A. 1990. Thioredoxin or glutaredoxin in *Escherichia coli* is essential for sulfate reduction but not for deoxyribonucleotide synthesise. Journal of Bacteriology **172**, 1923 – 1929.

Sabaty, M., Avazeri, C., Pignol, D., and Vermeglio, A. 2001. Characterization of the reduction of selenate and tellurite by nitrate reductases. Applied and Environmental Microbiology **6**, 5122-5126.

Said-Salim, B, Dunman, P.M., McAleese, F.M., Macapagal, D., Murphy, E., McNamara, P.J., Arvidson, S., Foster, T.J., Projan, S.J., and Kreiswirth, B.N.

2003. Global regulation of *Staphylococcus aureus* by Rot. Journal of Bacteriology **185**, 610-619.

Sambrook, J.E., Fritsch, E.F., Maniatis,T. 1989. Molecular Cloning: A Laboratory Manual. Cold Spring Harbor, NY: Cold Spring Harbor Laboratory Press.

Sanchez-Romero, J.M., Diaz-Orejas, R., De Lorenzo, V. 1998. Resistance to tellurite as a selection marker for genetic manipulations of Pseudomonas strains. Applied and Environmental Microbiology **64**, 4040-4046.

Scharf, C., Riethdorf, S., Ernst, H., Engelmann, S., Volker, U., and Hecker, M. 1998. Thioredoxin is an essential protein induced multiple stresses in Bacillus subtilis. Journal of Bacteriology **180**, 1869 – 1877.

Schenk, S., and Laddaga, R.A. 1992. Improve method for electroporation of *Staphylococcus aureus*. FEMS Microbiology Letters **94**, 133-138.

Schmidt, K.A., Manna, A.C., Gill, S., and Cheung, A.L. 2001. SarT, a repressor of α-hemolysin in *Staphylococcus aureus*. Infection and Immunity **69**, 4749 – 4758.

Schwan, W.R., Lehmann, L., and McCormick, J. 2006. Transcriptional activation of the *Staphylococcus aureus putP* gene by low-proline-high osmotic conditions and during infection of murine and human tissues. Infection and Immunity **76**, 399 – 409.

Schwan, W.R., Coulter, S.N., Ng. E.Y.W., Langhorne, M.H., Ritchie, H.D., Brody, L.L., Westbrock-Wadman, S., Bayer, A., Folger, K.R., and Stover, C.K. 1998. Identification and characterization of the PutP proline permease that contributes to in vivo survival of *Staphylococcus aureus* in animal models. Infection and Immunity **66**, 567 – 572.

Scopes, R.K. 1987. Protein Purification Principles and Practice Second Edition. Springer-Verlag. New York.

Seaver, L.C. and Imlay, J.A. 2001. Alkyl hydroperoxide reductase is the primary scavenger of endogenous hydrogen peroxide in *Escherichia coli*. Journal of Bacteriology **183**, 7173 – 7181.

Sen, C.K. 1998. Redox signaling and the emerging therapeutic potential of thiol antioxidants. Biochemical Pharmacology **55**, 1747 – 1758.

Serru, V., Baudin, B., Ziegler, F., David, J., Cals, M., Vaubourdolle, M., and Mario, N. 2001. Quantification of reduced and oxidized glutathione in whole blood samples by capillary electrophoresis. Clinical Chemistry **7**, 1321- 1324.

273

Shaw, L., Golonka, E., Potempa, J., and Foster S.J. 2004. The role and regulation of the extracellular proteases of *Staphylococcus aureus*. Microbiology **150**, 217-228.

Sherrill, C., and Fahey, R.C. 1998. Import and metabolism of glutathione by *Streptococcus mutans*. Journal of Bacteriology **180**, 1454 – 1459.

Shibayama, K., Wachino, J., Arakawa, Y., Saidijam, M., Rurtherford, N.G., Henderson, P.J.F. 2007. Metabolism of glutamine and glutathione via γ-glutamyltranspeptidase and glutamate transport in *Helicobacter pylori*: possible significance in the pathophysiology of the organism. Molecular Microbiology **64**, 396-406.

Shimada, T., Sakazaki, R., Fujimura, S., Niwano, K., Mishina, M., and Takizawa, K. 1990. A new selective, differential agar medium for isolation of *Vibrio cholerae* O1:PMT (polymyxin mannose-tellurite) agar. Jpn. J. Med. Sci. Biol **43**, 37-41.

Schneewind, O., Fowler, A., and Faull, K.F. 1995. Structure of the cell wall anchor of surface proteins in *Staphylococcus aureus*. Science **268**, 103 – 106.

Sievert, D.M., Boulton, M.L., Stolman, G., Johnson, D., Stobierski, M.G., Downes, F.P.,Somsel, P.A., Rudrik, J.T., Brown, W., Hafeez, W., Lundstrom, T., Flanagan, E., Johnson, R., and Chang, S. 2002. *Staphylococcus aureus* resistant to vancomycin –– United States, 2002. MMWR Weekly **51**, 565 – 567.

Somerville, C.R. 2001. An early Arabidopsis demonstration. Resolving aa few issues concerning photorespiration. Plant physiology **125**, 20 – 24.

Srinivasan, A., Dick, J.D. and Perl, T.M. 2002. Vancomycin Resistance in Staphylococci. Clinical Microbiology Reviews **15**, 430-438.

Stalenheim, G., Gotze, O., Cooper, N.R., Sjoquist, J., and Muller-Eberhard, H.J. 1973. Consumption of human complement components by complexex of IgG with Protein A of *Staphylococcus aureus*. Immunochemistry **10**, 501 – 507.

Suprenant, K.A., Bloom, N., Fang, J., and Lushington, G. 2007. The major vault protein is related to the toxic anion resistance protein (TelA) family. Journal of Experimental Biology **210**, 946 – 955.

Storey, K.B. 1996. Oxidative stress: animal adaptations in nature. Brazilian Journal of Medical and Biological Research **29**, 1715-1733.

Suzuki, H., and Kumagai, H. 2002. Autocatalytic processing of γ-glutamyltranspeptidase. J. Biol.Chem **277**, 43536-43543.

Suzuki, H., Hashimoto, W., and Kumagai, H. 1993. *Escherichia coli* K-12 can utilize an exogenous γ-glutamyl peptide as an amino acid source, for which γ-glutamyltranspeptidase is essential. Journal of Bacteriology **175**, 6038-6040.

Suzuki, H., Kumagai, H., Echigo, T., and Tochikura, T. 1989. DNA sequence of *Escherichia coli* K-12 γ - glutamyltranspeptidase gene, *ggt*. Journal of Bacteriology **171**, 5169 – 5172.

Suzuki, H., Kumagai, H., Tochikura, T. 1987. Isolation, Genetic mapping, and characterization *Escherichia coli* K12 mutants lacking γ-glutamyltranspeptidase Journal of Bacteriology **169**, 3926-3931.

Suzuki, H., Kumagai, H., Tochikura, T. 1986. γ-Glutamyltranspeptidase from *Escherichia coli* K12: Purification and Properties Journal of Bacteriology **168**, 1325-1331.

Tam, C., Glass, E.M., Anderson, D.M. and Missiakas, D. Transposon mutagenesis of Bacillus anthracis strain Sterne using Bursa aurealis. Plasmid **56**, 74-77.

Tate, S.S., Grau, E.M., Meister, A.1979. Conversion of glutathione to glutathione disulfide by cell membrane-bound oxidase activity. Proc. Natl. Acad. Sci. USA **76**, 2715-2719.

Tate, S.S., Meister, A.1976. Subunit structure and isozymic forms of γ-glutamyl transpeptidase. Proc. Natl. Acad. Sci. USA **73**, 2599-2603.

Taylor, D.E. 1999. Bacterial tellurite resistance. Trends in Microbiology **7**, 111 –115

Tegmark, K., Karlsson, A., Arvidson, S. 2000. Identification and characterization of SarH1, a new global regulator of virulence gene expression in *Staphylococcus aureus*. Molecular Microbiology **37**, 398–409

Terai, T., Kamahora, T. and Yamamura, Y. 1958. Tellurite reductase from *Mycobacterium avium*. J. Bacteriology **75**, 535 -539

Tolan R.W. Jr, 2007. *Staphylococcus aureus* infections at http://www.emedicine.com/ped/TOPIC2704.HTM.

Tong, V., Teng, X., Chang, T.K.H., and Abbott, F.S. 2005. Valproic Acid II: Effects on oxidative stress, mitochondtial membrane potential, and

cytotoxicity in glutathione-depleted rat hepatocytes. Toxicological Sciences **86**, 436-443.

Toptchieva, A., Sisson, G., Bryden, L.J., Taylor, D.E., and Hoffman, P.S. 2003. An inducible tellurite- resistance operon in *Proteus mirabilis*. Microbiology **149**, 1285 –1295.

Tristan, A., Ferry, T., Durand, G., Dauwalder, O., Bes, M., Lina, G., Vandenesch, F., and Etienne, J. 2007. Virulence determinants in community and hospital methicillin –resistant *Staphylococcus aureus*. Journal of Hospital Infection **65**, 105 – 109.

Trutko, S.M., Akimenko, V.K., Suzina, N.E., Asinimova, L.A., Shiyapnikov, M.G., Baskunov, B.P., Duda, V.I., Boronin, A.M. 2000. Involvement of the respiratory chain of gram-negative bacteria in the reduction of tellurite. Arch Micobiol **173**, 178 -186.

Tucker, F.L., Walper, J.F., Appleman, M.D., and Donohue, J. 1961. Complete reduction of tellurite to pure tellurium metal by microorganisms. Journal of Bacteriology **83**, 1313 – 1314.

Tsang, M.L., and Weatherbee, J.A. 1981. Thioredoxin, glutaredoxin, and thioredoxin reductase from cultured HeLa cells. Proc. Natl. Acad. Sci. USA **78**, 7478 – 7482.

Tucker, F.L., Thomas, J.W., Appleman, M.D., Goodman, S.H., and Donohue, J. 1966. X-ray diffraction studies on metal deposition in Group D streptococci. Journal of Bacteriology **92**, 1311 – 1314.

Turner, R.J., Aharonowitz, Y., Weiner, J.H., and Taylor, D.E. 2001. Glutathione is a target in tellurite toxicity and is protected by tellurite resistance determinants in *Escherichia coli*. Can. J. Microbiol. **47**, 33 – 40.

Turner, R.J., Weiner, J.H. and Taylor, D.E.1999. Tellurite-mediated thiol oxidation in *Escherichia coli*. Microbiology **145**, 2549 -2557.

Turner, R.J., Taylor, D.E., and Weiner, J.H. 1997. Expression of *Escherichia coli* TehA gives resistance to antiseptics and disinfectants similar to that conferred by multidrug resistance efflux pumps. Antimicrobial Agents and Chemotherapy **41**, 440 - 444.

Turner, R.J., Weiner, J.H. and Taylor, D.E. 1995. Neither reduced uptake nor increased efflux is encoded by tellurite resistance determinants expressed in *Escherichia coli*. Can.J. Microbiology **41**, 92-98.

Turner, R.J., Weiner, J.H. and Taylor, D.E. 1995. The tellurite-resistance determinants tehAtehB and klaAklaBtelB have different biochemical requirements. Microbiology **141**, 3133-3140.

Tynkkynen, S., Buist, G., Kunji, E., Kok, J., Poolman, B., Venema, G., and Haandrikman, A. 1993. Genetic and biochemical characterization of the oligopeptide transport system of *Lactococcus lactis*. Journal of Bacteriology **175**, 7523 – 7532.

Uziel, O., Borovok, I., Schreiber, R., Cohen, G., and Aharonowitz, Y. 2004. Transcriptional regulation of the *Staphylococcus aureus* thioredoxin and thioredoxin reductase genes in response to oxygen and disulfide stress. Journal of Bacteriology **186**, 326 – 334

Vagner, V., Dervyn, E., Ehrlich, S.D. 1998. A vector for systematic gene inactivation in *Bacillus subtilis*. Microbiology **144**, 3097-3104.

Vasquez, C.C., Saavedra, C.P., Loyola, C.A., Araya, M.A. and Pichuantes, S. 2001. The product of the cysK gene of *Bacillus stearothermophilus* V mediates potassium tellurite resistance in *Escherichia coli*. Current Microbiology **43**, 418-423.

Vellapan, N., Sblattero, D., Chasteen, L., Pavlik, P., and Bradbury, R.M. 2007. Methods Plasmids incompatibility: more compatible than previously thought? Plasmid Engineering, Design & Selection **20**, 309 – 313.

Verdier, I., Durand, G., Bes, M., Taylor, K.L., Lina, G., Vandenesch, F., Fattom, A.I., and Etienne, J. 2007. Identification of the capsular polysaccharides in *Staphylococcus aureus* clinical isolates by PCR and agglutination tests. Journal of Clinical Microbiology **45**, 725-729.

Vergauwen, B., Pauwels, F., Vaneechoutte, M., and Beeumen, J.V. 2003A. Exogenous glutathione completes the defense against oxidative stress in *Hemophilus influenzae*. Journal of Bacteriology **185**, 1572-1581

Vergauwen, B., Pauwels, F., and Beeumen, J.V. 2003B. Glutathione and catalase provide overlapping defenses for protection against respiration-generated hydrogen peroxide in *Hemophilus influenzae*. Journal of Bacteriology **185**, 5555 – 5562

Vido, K., Diemer, H., Dorsselaer, A.V., Leize, E., Juillard, V., Gruss, A., Gaudu, P. 2005. Roles of thioredoxin reductase during the aerobic life of *Lactococcus lactis*. Journal of Bacteriology **187**, 601-610.

Vijayarankul, U., Nadakavukaren, M.J., de Jonge, B.L.M., Wilkinson, B.J., and Jayaswal. R.K. 1995. Increased cell size and shortened peptidoglycan in

terpeptide bridge of NaCl-stresses *Staphylococcus aureus* and their *reversal* by glycine betaine. Journal of Bacteriology **177,** 5116 – 5121.

Watson, S.P., Antonio, M., and Foster, S.J. 1998a. Isolation and characterization of *Staphylococcus aureus* starvation-induced, stationary-phase mutants defective in survival or recovery. Microbiology **144,** 3159 – 3169.

Watson, S.P., Clements, M.O., and Foster, S.J. 1998b. Characterization of the starvation-survival response of *Staphylococcus aureus*. Journal of Bacteriology **180,** 1750 – 1758.

Watts, A., Ke, D., Wang, Q., Pillay, A., Nicholson-Weller, A., and Lee, J.C. 2005. *Staphylococcus aureus* strains that express serotype 5 or serotype 8 capsular polysaccharides differ in virulence. Infect Immun. **73,** 3502-3511.

Wengender, P.A., and Miller, K.J. 1995. Identification of a PutP proline permease gene homolog from *Staphylococcus aureus* by expression cloning of the high-affinity proline transport system in *Escherichia coli*. Applied and Environmental Microbiology **61,** 252 – 259.

Wilkinson, B. J. (1997). Biology. In *The* Staphylococci in human disease. New York: Churchill Livingstone

Williams Jr., C.H. 2000. Thioredoxin - thioredoxin reductase – a system that has come of age. Eur. J. Biochem **267,** 6101-6101

Williams Jr., C.H. 1995. Mechanism and structure of thioredoxin reductase from *Escherichia coli*. FASEB Journal **9,** 1267 – 1276

Williams, C.H., Arscott, L.D., Muller, S., Lennon, B.W., Ludwig, M.L., Wang, P., Veine, D.M., Becker, K., Schirmer, R.H. 2000. Thioredoxin reductase two modes of catalysis have evolved. Eur. J. Biochem **267,** 6110-6117.

Williams, R.J. Nair, S.P., Henderson, B., Holland, K.T., and Ward, J.M. 2002. Expression of the *S.aureus hysA* gene in *S.carnosus* from a modified *E.coli*-staphylococcal shuttle vector. Plasmid **47,** 241-245.

Xu, K., Strauch, M.A. 1996. Identification, sequence, and expression of the gene encoding γ-glutamyltranspeptidase in *Bacillus subtilis*. Journal of Bacteriology **178,** 4319-4322.

Yamaguchi, K., Yamaguchi, M., and Tomizawa, J. 1982. Incompatibility plasmids containing the replication origin of the *Escherichia coli* chromosome. Proc. Natl. Acad. Sci. USA **79,** 5347 – 5351.

Yamasaki, O., Kaneko, J., Morizane, S., Akiyama, H., Arata, J., Narita, S., Chiba, J., Kamio, Y, and Iwatsuki, K., 2005. The association between *Staphylococcus aureus* strains carrying Panton-Valentine leukocidin genes and the development of deep-seated follicular infection. Clin. Infect. Dis **40**, 381 – 385.

Yarwood, J.M., McCormick, J.K., and Schlievert, P.M. 2001. Identification of a novel two-component regulatory system that acts in global regulation of virulence factors of *Staphylococcus aureus*. Journal of Bacteriology **183**, 1113 –1123.

Zadik, P.M., Chapman, P.A., Siddons, C.A. 1993. Use of tellurite for the selection of verocytotoxigenic *Escherichia coli* O157. J. Med. Micobiol **39**, 155-158.

Zhang, M.Y., Bourbouloux, A., Cagnac, O., Srikanth, C.V., Rentsch, D., Bachhawat, A.K. and Delrot, S. 2004. A novel family of transporters mediating the transport of glutathione derivatives in plants. Plant physiology **134**, 482-491.

Zheng, S., Yumei, F., and Chen, A. 2007. De novo synthesis of glutathione is a prerequisite for curcumin to inhibit hepatic stellate cell (HSC) activation. Free Radical Biology & Medicine **43**, 444-453.

Zheng, M., Aslund, F.,and Storz, G. 1998. Activation of the OxyR transcription factor by reversible disulfide bond formation. Science, **279**, 1718-1721.

Ziebandt, A., Weber, H., Rudolph, J., Schmid, R., Hoper, D., Engelmann, S., and Hacker, M. 2001. Extracellular proteins of *Staphylococcus aureus* and the role of SarA and σ^B. Proteomics **1**, 480-493.